Western University
Scholarship@Western

Digitized Theses | Digitized Special Collections

1986

Vibration Behaviour Of In-plane Loaded Thin Rectangular Plates With Initial Geometrical Imperfections

Sinniah Ilanko

Follow this and additional works at: https://ir.lib.uwo.ca/digitizedtheses

Recommended Citation
Ilanko, Sinniah, "Vibration Behaviour Of In-plane Loaded Thin Rectangular Plates With Initial Geometrical Imperfections" (1986). *Digitized Theses*. 1497.
https://ir.lib.uwo.ca/digitizedtheses/1497

This Dissertation is brought to you for free and open access by the Digitized Special Collections at Scholarship@Western. It has been accepted for inclusion in Digitized Theses by an authorized administrator of Scholarship@Western. For more information, please contact tadam@uwo.ca, wlswadmin@uwo.ca.

The author of this thesis has granted The University of Western Ontario a non-exclusive license to reproduce and distribute copies of this thesis to users of Western Libraries. Copyright remains with the author.

Electronic theses and dissertations available in The University of Western Ontario's institutional repository (Scholarship@Western) are solely for the purpose of private study and research. They may not be copied or reproduced, except as permitted by copyright laws, without written authority of the copyright owner. Any commercial use or publication is strictly prohibited.

The original copyright license attesting to these terms and signed by the author of this thesis may be found in the original print version of the thesis, held by Western Libraries.

The thesis approval page signed by the examining committee may also be found in the original print version of the thesis held in Western Libraries.

Please contact Western Libraries for further information:
E-mail: libadmin@uwo.ca
Telephone: (519) 661-2111 Ext. 84796
Web site: http://www.lib.uwo.ca/

National Library of Canada | Bibliothèque nationale du Canada

Canadian Theses Service | Services des thèses canadiennes

Ottawa, Canada
K1A 0N4

CANADIAN THESES | THÈSES CANADIENNES

NOTICE

The quality of this microfiche is heavily dependent upon the quality of the original thesis submitted for microfilming. Every effort has been made to ensure the highest quality of reproduction possible.

If pages are missing, contact the university which granted the degree.

Some pages may have indistinct print especially if the original pages were typed with a poor typewriter ribbon or if the university sent us an inferior photocopy.

Previously copyrighted materials (journal articles, published tests, etc.) are not filmed.

Reproduction in full or in part of this film is governed by the Canadian Copyright Act, R.S.C. 1970, c. C-30.

AVIS

La qualité de cette microfiche dépend grandement de la qualité de la thèse soumise au microfilmage. Nous avons tout fait pour assurer une qualité supérieure de reproduction.

S'il manque des pages, veuillez communiquer avec l'université qui a conféré le grade.

La qualité d'impression de certaines pages peut laisser à désirer, surtout si les pages originales ont été dactylographiées à l'aide d'un ruban usé ou si l'université nous a fait parvenir une photocopie de qualité inférieure.

Les documents qui font déjà l'objet d'un droit d'auteur (articles de revue, examens publiés, etc.) ne sont pas microfilmés.

La reproduction, même partielle, de ce microfilm est soumise à la Loi canadienne sur le droit d'auteur, SRC 1970, c. C-30.

THIS DISSERTATION HAS BEEN MICROFILMED EXACTLY AS RECEIVED

LA THÈSE A ÉTÉ MICROFILMÉE TELLE QUE NOUS L'AVONS REÇUE

NL-339 (r. 86/06)

Canada

VIBRATION BEHAVIOUR OF IN-PLANE LOADED THIN RECTANGULAR PLATES WITH INITIAL GEOMETRICAL IMPERFECTIONS

by

Sinniah Ilanko
Faculty of Engineering Science

Submitted in partial fulfillment
of the requirements for the degree of
Doctor of Philosophy

Faculty of Graduate Studies
The University of Western Ontario
London, Ontario
November, 1985

© Sinniah Ilanko 1985

Permission has been granted to the National Library of Canada to microfilm this thesis and to lend or sell copies of the film.

L'autorisation a été accordée à la Bibliothèque nationale du Canada de microfilmer cette thèse et de prêter ou de vendre des exemplaires du film.

The author (copyright owner) has reserved other publication rights, and neither the thesis nor extensive extracts from it may be printed or otherwise reproduced without his/her written permission.

L'auteur (titulaire du droit d'auteur) se réserve les autres droits de publication; ni la thèse ni de longs extraits de celle-ci ne doivent être imprimés ou autrement reproduits sans son autorisation écrite.

ISBN 0-315-29467-1

ABSTRACT

The effect of in-plane loading on the natural frequencies of simply supported thin rectangular plates with initial geometrical imperfection is investigated theoretically and experimentally. It is shown that the natural frequencies depend on applied in-plane load, initial geometrical imperfection and the in-plane boundary conditions.

In the theoretical analysis, the natural frequencies, out-of-plane static displacements and in-plane stress distribution are calculated using the Rayleigh-Ritz minimization technique. A concept of 'connection coefficients' has been used to reduce the computational work. In this concept, the relationship between the out-of-plane and in-plane displacement coefficients are first determined by solving the equations resulting from the minimization of the total potential energy with respect to the in-plane displacement coefficients. This relationship is then substituted into the equations obtained by minimizing the total potential energy with respect to the out-of-plane displacement coefficients.

In the experimental side of the work, tests were carried out on several thin (thickness ranging from 0.56 mm to 1.15 mm) mild steel plates (300 mm x 250 mm). Uniaxial

in-plane loading was applied through two 'V' grooved edge beams. The other two edges were supported between two rows of ball bearings placed in 'V' grooves, carefully adjusted to minimize the friction along these edges.

The agreement between the measured and calculated values of natural frequencies, out-of-plane central displacements and static strain distribution is very good. An interesting observation from the result is that a simple approximate linear relationship between a load-frequency parameter (involving the fundamental natural frequency and the state of in-plane stress) and the square of the central deflection is obtained. Further experimental and theoretical work in this field is strongly recommended.

ACKNOWLEDGEMENTS

It is the pleasure of the author to acknowledge the aid he received from several individuals and organizations without which the completion of this work would have been impossible.

The author wishes to express his heartfelt gratitude to his supervisor, Professor S.M. Dickinson for his constant guidance and encouragement throughout the course of this work. He has also painstakingly corrected and refined the manuscript of this thesis.

The author wishes also to thank Messrs. Harry Cook, R. Bruce Campbell and David Woytowich for making the testing rig, and Messrs. Ric Shermerluk and Kendrick Allen for their assistance in placing the strain gauges on a plate specimen. Acknowledgements are also due to Ms. Joanne Lemon and Ms. Linda McGugan for their meticulous typing and to Mr. Subba Reddy for preparing the photographs. The financial assistance of the Canadian National Research Council is gratefully acknowledged. Thanks are also due to the authorities of the University of Peradeniya for granting a study leave.

TABLE OF CONTENTS

NOMENCLATURE

The following is a list of the main symbols used in this thesis. Other symbols are defined as they appear in the text.

a	Dimension of a plate in x-direction
A	Cross-sectional area of a beam
$A_{i,j}, B_{i,j}$	Static displacement coefficients
$\bar{A}_{i,j}, \bar{B}_{i,j}$	Dynamic displacement coefficients
b	Dimension of a plate in y-direction
D	Plate rigidity defined by $D = Eh^3/12(1-.^2)$
E	Young's modulus
F	Airy stress function for the static analysis
$\bar{F}$	Airy stress function for the dynamic analysis
$f_{ui}(x), f_{vi}(x)$	Shape functions (ith) in x direction for the static displacements in x,y directions
$\bar{f}_{ui}(x), \bar{f}_{vi}(x)$	Shape functions (ith) in x direction for the dynamic displacements in x,y directions
$g_{uj}(y), g_{vj}(y)$	Shape functions (jth) in y direction for the static displacements in x,y directions
$\bar{g}_{uj}(y), \bar{g}_{vj}(y)$	Shape functions (jth) in y direction for the dynamic displacements in x,y directions
[G]	Dynamic connection coefficients matrix
[H]	Static connection coefficients matrix
h	Thickness of a plate

$H_{i,j}$ or H	Dynamic out-of-plane displacement coefficients
i	Integer
I	Second moment of area of a beam
I	Also used as an integer in Chapter 3
j,k	Integers
k_1,k_2,k_e	Stiffness factor
L	Length of a beam
L	Also used as an integer in Chapter 3
ℓ,m	Integers
$\bar{m}$	Mass density
n,N,p	Integers
P	Static axial load
P'	Dynamic axial force
P_E	Euler load
P_x	In-plane load along x-direction
q,r,s	Integers
t	Time
$\bar{T}$	Kinetic energy
u,v,u_s,v_s	Static in-plane displacements along x-y directions
u_d,v_d,w	Dynamic displacements in x,y,z directions measured from the equilibrium position
$\bar{U},\bar{V}$	Strain energy, potential energy due to static loading
U,V	Strain energy, potential energy due to the vibration

x, y, z	Cartesian co-ordinates
$z(x,y)$	Static out-of-plane deflection of a plate measured from the plane of the supports
$z_o(x,y)$	Initial out-of-plane imperfection
$Z_{i,j}$ or $\{Z\}$	Static out-of-plane displacement coefficients
$Z_{o_{i,j}}$	Fourier coefficients in the out-of-plane initial imperfection
$\varepsilon_x, \varepsilon_y, \gamma_{xy}$	In-plane strains due to static loading
$\bar{\varepsilon}_x, \bar{\varepsilon}_y, \bar{\gamma}_{xy}$ or $\varepsilon'_x, \varepsilon'_y, \gamma'_{xy}$	In-plane strains due to vibration
[illegible]$_c$	Central displacement of a plate
[illegible]	Load ratio
[illegible]	Frequency ratio
[illegible]	Deflection parameter
[illegible]$_o$	Non-dimensional initial imperfection at the centre
$\sigma_x, \sigma_y, \tau_{xy}$	Static in-plane stresses
$\bar{\sigma}_x, \bar{\sigma}_y, \bar{\tau}_{xy}$	Dynamic in-plane stresses
ν	Poisson's ratio
$\omega_{i,j}$	Natural frequency corresponding to (i,j) mode
$\Omega_{i,j}$	Theoretical natural frequency of an unstressed flat plate corresponding to (i,j) mode

CHAPTER 1

INTRODUCTION

1.1 INTRODUCTORY REMARKS

A considerable amount of work has been done on the practically important problem of the vibration of rectangular plates subject to in-plane loads. A preponderance of this work has dealt with plates having a uniform in-plane stress distribution, although numerous studies have included the effect of in-plane stresses which vary over the area of the plate. Almost all of the studies to date have been of a theoretical nature and have been concerned with plates which vibrate about the perfectly flat state. In practice, plates cannot be perfectly flat and, so called, geometric imperfection (curvature) must exist. Any initial curvature in an unstressed plate can be significantly magnified when the plate is subjected to compressive in-plane loads. Experimental work conducted by a minority of researchers has shown this to be the case for very slight initial curvatures and the resulting effect upon the natural frequencies of the plates, when compressively loaded, is very significant, causing the behaviour of the plate to deviate drastically from that predicted using flat plate theory. Very recently, theoretical studies have suggested similar behaviour but, to date, no adequate agreement has been achieved between theoretically predicted and experimentally obtained natural frequencies of rectangular plates having initial geometric imperfection and in-plane loaded in compression; nor have the experimental studies accommodated in-plane loads substantially beyond the first buckling load. Such a study is the subject of the present thesis.

1.2 PRESENT STATE OF STUDIES ON THE VIBRATION BEHAVIOUR OF IN-PLANE LOADED RECTANGULAR PLATES

The basic theory of vibration of unstressed plates was laid down by Lord Rayleigh [1,2], and the initial solutions were obtained by Timoshenko [3]. A comprehensive literature survey in a NASA special publication by Leissa [4] reveals that very little work had been done on the free vibration of in-plane loaded rectangular plates prior to the time it was published (1969). Since then, there have been a number of papers on this problem. Dickinson et al. [5-11] published results for natural frequencies of flat rectangular plates under various in-plane stress distributions and boundary conditions, using analytical and numerical methods. An exact procedure applicable to certain boundary conditions, using a complex stiffness matrix has been developed by Wittrick and

Williams [12,13]. A finite strip method of analysis was proposed by Dawe and Morris [14] for the vibration of circularly curved plate assemblies subjected to membrane stresses. The effect of curvature magnification due to the stresses was not considered. Application of Galerkin's method to the vibration of in-plane stressed flat plates was illustrated in a publication by Laura and Romanelli [15]. Other references on this subject and other complicating effects on plate vibration can be found in two of the papers by Leissa [16,17].

As mentioned, a complicating factor in the vibration analyses of in-plane stressed plates is the presence of geometrical imperfections (deviation from flatness). Experimental results reported by Phillips and Jubb [18] show that the frequencies of essentially unstressed clamped curved plates increase with distortion. Their results indicate a linear relationship to exist between the square of the fundamental natural frequency and the square of the central distortion. This observation was compared with the theoretical results for spherically curved plates published by Reissner [19].

Experimental results for the natural frequencies of in-plane loaded plates appear to have been first reported by Lurie [20]. Measured values of natural frequencies were found to be higher than those computed by using the classical theory for flat plates. The plot of the square of the frequency against load deviated from the theoretical straight line. The discrepancy was attributed to the presence of initial geometrical imperfections. This argument was based on some earlier theoretical work carried out by Massonnet [21] for imperfect circular plates. An experimental investigation on the vibration of box columns (assembly of four rectangular plates) under in-plane loading was reported by Jubb, Phillips and Becker [22]. In this case, the agreement between the observed and predicted (based on the flat plate theory) values of the natural frequencies were very good until close to the buckling load. The frequencies first reduced with in-plane compressive load, but took a sharp turn near the buckling load and began to increase. This was explained as being the influence of distortion which lead to an increase in stiffness resulting from the membrane action.

An experimental study conducted at the University of Manchester, U.K., on rectangular plates with simply supported and clamped (one edge) boundary conditions indicated a deviation in the natural frequencies at high loadings [23,24], as earlier reported by Lurie. The effect of non-uniformity in the in-plane stress distribution was investigated using a finite difference approach. The strain distribution and displacement pattern were also measured along with the natural frequencies. It was found that the non-uniformity in the stress distribution contributed to the discrepancy between the measured and calculated values, but a substantial part of the discrepancy remained.

Hui and Leissa [25] published the results of a theoretical study on the vibration of in-plane stressed rectangular plates with initial geometrical imperfection. This appears to be the first theoretical publication on this problem. The Von Kármán's large deflection equations and the linear shell vibration equations were solved using Galerkin's method. Airy stress functions were used in the compatibility and equilibrium equations. These functions were chosen to satisfy the compatibility equation exactly for any one out-of-plane displacement (or vibration) mode. This method is directly applicable to certain in-plane boundary conditions and simply supported out-of-plane boundary conditions. It was assumed that the flexural vibration modes are decoupled and are similar to the static buckling modes. Consideration of several vibration modes and buckling modes can change the results for large values of displacements as will be shown in Chapter 5 of the present thesis.

To the author's knowledge, no experimental work had been reported on the vibration behaviour of plates subject to in-plane loadings substantially higher than the lowest buckling load. The experimental results published so far have not been quantitatively compared with appropriate theoretical results.

The first part of the title problem is the calculation of static displacement and stresses due to the applied in-plane load. The equilibrium approach has been the popular method for post buckling analysis. Surprisingly, the number of publications on experimental studies appear to be very limited. Yamaki [26,27,28] and Coan [29] reported some experimental and theoretical results for the displacement and stress distribution of plates under large in-plane loadings (up to about three times the lowest critical load). Maximum central displacements were about three times the plate thickness at maximum applied load. The agreement between the experimental and theoretical results was good.

An approximate solution for the post buckling problem of plates with edges elastically restrained (against rotation) was published by Bhattacharya [30]. The energy method has been employed for post buckling analysis using Airy stress functions [31]. This procedure may be difficult to apply for practical boundary conditions (where in-plane displacements are partially restrained) such as in the case of an experimental study since the displacements at the boundaries have to be calculated by integrating the stress functions.

1.3 THE SCOPE OF PRESENT WORK

The object of this project is to investigate the influence of in-plane loading, on the natural frequencies of simply supported rectangular plates. The effect of membrane stiffness on the frequencies and the rate of growth of out-of-plane displacements is studied theoretically and experimentally. The membrane stiffness at loadings lower than the lowest critical load is caused by the presence of initial geometrical imperfections (curvature) which are amplified by the application of load. (From here onwards, in-plane static load will be referred to as 'load'.) It should be mentioned however, that at loads above the lowest buckling load, even a plate that was perfectly flat prior to the loading can develop membrane stiffness. This is due to the fact that at such loads, a stable equilibrium state associated with out-of-plane displacements is possible. Effect of non-uniformity in the in-plane stress distribution is also taken into account.

In the theoretical analysis, the Rayleigh-Ritz method is used to calculate the deflections, stress distribution and natural frequencies. The in-plane and out-of-plane displacements are expressed as the summation of a series of the products of 'shape functions' and corresponding 'displacement coefficients'. Total potential energy is expressed in terms of these displacement coefficients which can be determined by solving the equations resulting from the minimization of the potential energy.

As far as the author is aware, the application of the energy method for vibration or post buckling problems of rectangular plates with undetermined in-plane displacement coefficients has not been reported in the literature. Despite the lack of information on the merits and demerits of this method, it was decided to use this approach because of a significant advantage in its applicability to the experimental problem. Using this approach, the shape function for the in-plane displacements do not have to satisfy the natural boundary conditions. This permits certain modifications in the mathematical modelling, such as allowing for the effect of the flexibility of the testing frame and the inertia of the loading head. As explained later, such modifications can be done very simply when using the energy method with undetermined displacement coefficients.

The task of solving the non-linear post buckling analysis with undetermined displacement coefficients in all three cartesian directions appeared to be very difficult initially. However, the introduction of a concept of connection coefficients significantly reduced the computational effort. This concept is explained in the next chapter, where a simpler, related, beam problem is used to illustrate its applicability. Of particular importance in the use of the energy method is the choice of appropriate shape functions as these significantly affect the accuracy of the results and the rapidity of convergence. This too is illustrated using the simpler beam problem.

The application of the Rayleigh-Ritz method to the post buckling and vibration analysis of initially curved plates is described in Chapter 3.

To establish some confidence in the analytical approach used, results were computed for stress free curved plates having certain standard boundary conditions and are compared with results from a finite element package program in Chapter 5.

An equilibrium approach, using Galerkin's method, was developed initially and used to investigate the influence of membrane stretching on the frequencies of plates with in-plane free and shear diaphragm boundary conditions. It was recognized that although this approach was attractive for such plates, it could not be adapted readily to suit boundary conditions likely to be met in experimentation. Hence, the use of this approach was not pursued but, for completeness, the analysis is given in Appendix A, and some numerical results are presented in Chapter 5.

In the experimental work, the natural frequencies of several rectangular plates under uniaxial in-plane loading were measured. The maximum applied load was well above the lowest critical load in most cases and in one case more than four times as large. At each increment of loading, the fundamental natural frequency and central deflection of the plate were measured. At certain values of load, the deflections at several points on the plate were measured. In one case, the strain distribution in the plate was measured with electric resistance strain gauges. For most of the plates tested, the second natural frequency was also measured. Due to the difficulties in measuring the amplitude of the static deflection corresponding to the second mode, and the computational problems in introducing the anti-symmetrical displacement shapes (the computer program was written for a fully symmetrical shape), the theoretical values of the second natural frequency were not calculated. However, the experimental results are reported in Appendix B.

The experimental procedure is explained in Chapter 4 and the results are compared with the theoretical values in Chapter 5.

One interesting outcome of this study is an approximate linear relationship between the square of the central deflection and a frequency-load parameter, defined by the sum of the square of the non-dimensional natural frequency and the ratio of applied load to critical load. The probability of existence of such an exact linear relationship appears to be mathematically remote. However, the theoretical and experimental results do indicate an approximately linear relationship for the plates tested.

For a simply supported curved beam, a linear relationship between the frequency-load parameter and the square of the central deflection has been established analytically [32]. This is also illustrated in a simpler way in Chapter 2. An attempt has been made in Appendix C to show why an approximately linear relationship for plates may exist. If this relationship is valid generally, it may prove to be very useful in the prediction of the natural frequencies of curved plates (such as aircraft panels) when the shape of the plates and the stress level are known. Alternatively, if the frequencies and the shape are known, the level of stress could be estimated. It is hoped that future work in this area will lead to more definite conclusions.

CHAPTER 2

INTRODUCTORY ANALYSIS

2.1 INTRODUCTORY REMARKS

Before tackling the description of the analysis of the plate problem, it is considered desirable to treat the simpler, but related, problem of the vibration of a slightly curved beam, subject to axial load. This will serve to introduce the concepts used in the plate analysis and permit a direct comparison with 'exact' results. First, the 'exact' analysis using the equilibrium method is given, followed by the approximate Rayleigh-Ritz method, where the concept of 'connection coefficients' is introduced, and which permits a study of the effect of using different 'admissible' shape functions. Additionally, the effect of unequal, partial axial restraint, analogous to that encountered in the plate experiments, is illustrated, showing that, at least for the beam, the unequal restraint can be replaced by an equivalent equal restraint. This will be an approximation in the case of the plate problem but is a very useful simplification, without which the symmetry of the problem is destroyed.

2.2 VIBRATION ANALYSIS OF AN AXIALLY LOADED SIMPLY SUPPORTED CURVED BEAM USING AN (EXACT) EQUILIBRIUM METHOD

Consider the vibration of a simply supported beam with an initial curvature in the form of a half sine wave subjected to an axial load P as shown in Figure 2.2.1.

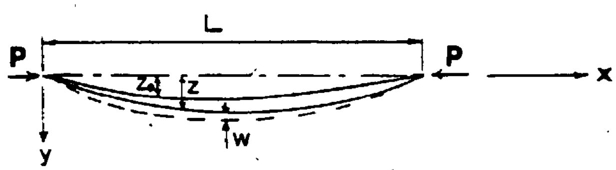

Figure 2.2.1

Let the initial shape of the beam z_o be given by $z_o(x) = Z_o \operatorname{Sin}(\frac{\pi x}{L})$.

It is well known [33] that the deflection under load P will then be given by

$$z(x) = Z \operatorname{Sin}(\frac{\pi x}{L}),$$

where $Z = Z_o/(1-P/P_E)$, in which P_E is the Euler load or the lowest buckling load of the beam.

Let w(x) be the dynamic displacement at the time of maximum positive excursion, measured from the static equilibrium position z(x). Assuming the motion of the beam to be simple harmonic, the beam vibration equations given in Appendix D are as follows:

$$EI \frac{\partial^4 w}{\partial x^4} + P \frac{\partial^2 w}{\partial x^2} - P' \frac{\partial^2 z}{\partial x^2} - m\omega^2 w = 0 \qquad (2.2.1)$$

and

$$P' = EA\left(\frac{\partial u}{\partial x} + \frac{\partial w}{\partial x} \cdot \frac{\partial z}{\partial x}\right), \qquad (2.2.2)$$

where $u(x)$ is the axial displacement.

Neglecting the axial inertia of the beam,

$$\frac{\partial P'}{\partial x} = 0 . \qquad (2.2.3)$$

This means $w = H \operatorname{Sin}(\frac{\pi x}{L})$ is a non-trivial solution of equations (2.2.1) and (2.2.2) where H is an undetermined displacement coefficient.

From equation (2.2.2),

$$\frac{\partial u}{\partial x} = \frac{P'}{EA} - \frac{\partial w}{\partial x} \cdot \frac{\partial z}{\partial x}$$

$$= \frac{P'}{EA} - \frac{\pi^2 ZH}{L^2} \operatorname{Cos}^2\left(\frac{\pi x}{L}\right)$$

$$= \frac{P'}{EA} - \frac{\pi^2 ZH}{2L^2} \left(\operatorname{Cos}\left(\frac{2\pi x}{L}\right) + 1\right)$$

$$u = \frac{P' x}{EA} - \frac{\pi ZH}{4L} \operatorname{Sin}\left(\frac{2\pi x}{L}\right) - \frac{\pi^2 ZH}{2L^2} x + c , \qquad (2.2.4)$$

where c is an integration constant and depends on the axial end conditions. The solution will be obtained for some simple axial boundary conditions as described below.

Case 1. Both Ends Axially Restrained (After the application of the static load).

$$\text{at } x = 0,\ u = 0 \text{ gives } c = 0.$$

$$\text{at } x = L,\ u = 0 \text{ gives } \frac{P'L}{EA} = \pi^2 \frac{ZHL}{2L^2}$$

$$\text{or } \frac{P'}{EA} = \frac{\pi^2 ZH}{2L^2} . \qquad (2.2.5)$$

Substituting these in equation (2.2.4) gives,

$$u = \frac{-\pi ZH}{4L} \sin\left(\frac{2\pi x}{L}\right) . \qquad (2.2.6)$$

Substituting equations (2.2.5) and (2.2.6) into equation (2.2.1) yields

$$\left[EI\left(\frac{\pi}{L}\right)^4 - P\left(\frac{\pi}{L}\right)^2 - m\omega^2\right]w + EA\,\frac{\pi^2}{2L^2}\,ZH\left(\frac{\pi}{L}\right)^2 z = 0.$$

Since $H \cdot z = Z \cdot w$, this becomes

$$\left[EI\left(\frac{\pi}{L}\right)^4 - P\left(\frac{\pi}{L}\right)^2 - m\omega^2 + EA\left(\frac{\pi}{L}\right)^4 \frac{Z^2}{2}\right]w = 0 .$$

Dividing by $\frac{\pi^4 EI}{L^4}$ gives

$$\left(1 - \frac{P}{P_E} - \frac{\omega^2}{\Omega^2} + \frac{1}{2}\,\frac{Z^2}{k^2}\right)w = 0 ,$$

where $P_E = \pi^2 \frac{EI}{L^2}$ (Euler Load),

$\Omega = \frac{\pi^2}{L^2}\sqrt{EI/m}$ (Fundamental natural frequency of a straight simply supported beam without axial load),

$k = \sqrt{I/A}$ (Radius of gyration about the axis of bending).

For non-trivial solution of w,

$$1 - \frac{P}{P_E} - \frac{\omega^2}{\Omega^2} + \frac{1}{2}\frac{Z^2}{k^2} = 0$$

or

$$\omega^2 = \Omega^2\left(1 - \frac{P}{P_E} + \frac{1}{2}\frac{Z^2}{k^2}\right) . \qquad (2.2.7)$$

This simple formula gives the natural frequency of an axially loaded simply supported curved beam. A more general form of this equation can be found in a publication by Plaut and Johnson [32]. If both ends are free to move axially, it can be shown that the curvature will have no influence in the natural frequency as explained in the following paragraphs.

Case 2. Both Ends Free to Move Axially

Figure 2.2.2

In this case, $P' = 0$.

Equation (2.2.1) reduces to that of a straight beam and the fundamental natural frequency will be given by

$$\omega^2 = \Omega^2(1-P/P_E) . \qquad (2.2.8)$$

Substituting $P' = 0$ in equation (2.2.4) gives

$$u = c - \frac{\pi^2 ZHx}{2L^2} - \frac{ZH}{4L}\sin\left(\frac{2\pi x}{L}\right) .$$

The constant of integration c, in this case is undetermined. This is understandable since a free rigid body motion along the axis is permissible. However, for comparing with an approximate solution, let us assume that the motion is symmetrical about the centre of the beam.

At $x = L/2$, $u = 0$ gives $c = \frac{\pi^2 ZH}{4L}$,

$$u = \frac{\pi^2 ZH}{2L^2}\left(\frac{L}{2} - x\right) - \frac{\pi}{4L} \cdot ZH \sin\left(\frac{2\pi x}{L}\right) . \qquad (2.2.9)$$

Another type of boundary condition that is likely to be found in practice is partially restrained motion of the ends. During the conduct of the experiments, on the plates, it was recognized that the top and bottom edges of the plate were actually partially restrained. Therefore, it is useful to study the vibration behaviour of a curved beam with partially restrained boundaries.

Case 3. Both Ends Partially Restrained Axially

Figure 2.2.3

Let the axial displacements at $x = 0$ and $x = L$ be δ_1 and δ_2 respectively. If the axial stiffnesses at the ends are $\bar{k}_1$, $\bar{k}_2$ then

$$\delta_1 = P'/\bar{k}_1 \quad , \quad \delta_2 = -P'/\bar{k}_2 \quad .$$

At $x = 0$, $u = \delta_1 = \dfrac{P'}{\bar{k}_1} = c$.

At $x = L$, $u = \delta_2 = \dfrac{-P'}{\bar{k}_2} = c + \dfrac{P'L}{EA} - \dfrac{\pi^2 ZH}{2L}$

$$= \frac{P'}{\bar{k}_1} + \frac{P'L}{EA} - \frac{\pi^2 ZH}{2L} \ .$$

From this,

$$P' = \frac{\pi^2 ZH}{2L} \Big/ \left[\frac{L}{EA} + \frac{1}{\bar{k}_1} + \frac{1}{\bar{k}_2}\right] \ .$$

Expressing the stiffnesses in a non-dimensional form,

i.e. $k_1 = \dfrac{\bar{k}_1 L}{EA}$, $k_2 = \dfrac{\bar{k}_2 L}{EA}$,

$$P' = \pi^2 \frac{EA \ ZH}{2L^2} \Big/ \left(1 + \frac{1}{k_1} + \frac{1}{k_2}\right)$$

$$= \pi^2 \frac{EA \ ZH \ k_1 k_2}{2L^2 (k_1 k_2 + k_1 + k_2)} \ . \qquad (2.2.10)$$

Substituting this in equation (2.2.1) gives,

$$\frac{\omega^2}{\Omega^2} = 1 - \frac{P}{P_E} + \frac{1}{2} \frac{Z^2}{k^2} \left(\frac{k_1 k_2}{k_1 k_2 + k_1 + k_2}\right) \ . \qquad (2.2.11)$$

<u>Equivalent Equal Springs</u>

Note that the same frequencies will be obtained if two springs of equal stiffness k_e are placed at the ends such that,

$$\frac{k_e^2}{k_e^2+2k_e} = \frac{k_1k_2}{(k_1+k_2+k_1k_2)} .$$

i.e. $k_e^2(k_1k_2+k_1+k_2) = k_1k_2(k_e^2+2k_e)$

$$k_e^2(k_1+k_2) = k_1k_2 \cdot 2k_e$$

$$k_e = \frac{2k_1k_2}{(k_1+k_2)} . \qquad (2.2.12)$$

If $k_1 >> k_2$,

$$k_e = \frac{2k_2}{(1+k_2/k_1)} \simeq 2k_2 . \qquad (2.2.13)$$

This means for a beam with one end axially fully restrained, the frequency can be calculated by applying twice the value of the other end stiffness on each side. The two systems shown in Figure 2.2.4 will have the same fundamental natural frequency.

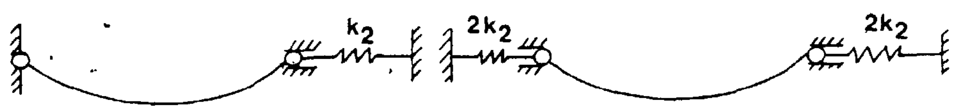

Figure 2.2.4

If an equivalent equal stiffness is to be used, equation (2.2.11) simplifies to

$$\frac{\omega^2}{\Omega^2} = 1 - \frac{P}{P_E} + \frac{1}{2}\frac{Z^2}{k^2}\left(\frac{k_e}{2+k_e}\right) . \qquad (2.2.14)$$

Note that if $k_e=0$, equation (2.2.14) reduces to equation (2.2.8) and if $k_e \to \infty$ it reduces to equation (2.2.7).

2.3 APPROXIMATE ANALYSIS OF THE VIBRATION OF A CURVED BEAM USING THE RAYLEIGH-RITZ METHOD

Figure 2.3.1

The problem treated in section 2.2 is solved using the Rayleigh-Ritz approach in this section (2.3). A concept of 'connection coefficients' is introduced to reduce the computational effort in calculating the frequencies. The accuracy of the solution depends on the choice of shape functions for the axial displacement. This is demonstrated by comparing the results for two different shape functions with the 'exact' results obtained in the previous section.

The maximum total potential energy of the beam during vibration is given by

$$\bar{U} = \frac{1}{2}\int_{x=0}^{L} [EA(\frac{\partial u}{\partial x} + \frac{\partial w}{\partial x}\cdot\frac{\partial z}{\partial x})^2 + EI(\frac{\partial^2 w}{\partial x^2})^2 - P(\frac{\partial w}{\partial x})^2]dx . \quad (2.3.1)$$

Maximum kinetic energy $\bar{T} = \frac{m\omega^2}{2}\int_{x=0}^{L} w^2 dx$. (2.3.2)

Let $w = H_1 \cdot \text{Sin}(\frac{\pi x}{L}) + H_2 \text{ Sin}(\frac{3\pi x}{L})$

and $u = B_1 f_1(x) + B_2 f_2(x)$,

where $f_1(x)$, $f_2(x)$ are the shape functions for axial displacement and B_1, B_2 are the undetermined axial displacement coefficients, then

$$\frac{\partial u}{\partial x} = B_1\left(\frac{\partial f_1}{\partial x}\right) + B_2\left(\frac{\partial f_2}{\partial x}\right) ,$$

$$\frac{\partial w}{\partial x} \cdot \frac{\partial z}{\partial x} = \frac{\pi^2}{L^2} Z \operatorname{Cos}\left(\frac{\pi x}{L}\right)\left(H_1 \operatorname{Cos}\left(\frac{\pi x}{L}\right) + 3H_2 \operatorname{Cos}\left(\frac{3\pi x}{L}\right)\right)$$

$$= \left(\frac{\pi}{L}\right)^2 Z\left[\frac{H_1}{2}\left(\operatorname{Cos}\left(\frac{2\pi x}{L}\right)+1\right) + \frac{3H_2}{2}\left(\operatorname{Cos}\left(\frac{4\pi x}{L}\right) + \operatorname{Cos}\left(\frac{2\pi x}{L}\right)\right)\right],$$

$$\frac{\partial^2 w}{\partial x^2} = -\left(\frac{\pi}{L}\right)^2 \left[H_1 \operatorname{Sin}\left(\frac{\pi x}{L}\right) + 9H_2 \operatorname{Sin}\left(\frac{3\pi x}{L}\right)\right] ,$$

and $$\frac{\partial w}{\partial x} = \frac{\pi}{L} \left[H_1 \operatorname{Cos}\left(\frac{\pi x}{L}\right) + 3H_2 \operatorname{Cos}\left(\frac{3\pi x}{L}\right)\right] .$$

Substitution into equation (2.3.1) gives

$$\overline{U} = \frac{EA}{2} \int_{x=0}^{L} \left[B_1 \frac{\partial f_1}{\partial x} + B_2 \frac{\partial f_2}{\partial x} + \frac{\pi^2 Z}{2L^2}\left(H_1\left(1+\operatorname{Cos}\left(\frac{2\pi x}{L}\right)\right) + 3H_2\left(\operatorname{Cos}\left(\frac{2\pi x}{L}\right) + \operatorname{Cos}\left(\frac{4\pi x}{L}\right)\right)\right)\right]^2$$

$$dx + \frac{EI}{2} \int_{x=0}^{L} \left(\frac{\pi}{L}\right)^4 \left(H_1 \operatorname{Sin}\left(\frac{\pi x}{L}\right) + 9H_2 \operatorname{Sin}\left(\frac{3\pi x}{L}\right)\right)^2 dx$$

$$- \frac{P}{2}\left(\frac{\pi}{L}\right)^2 \int_{x=0}^{L} \left(H_1 \operatorname{Cos}\left(\frac{\pi x}{L}\right) + 3H_2 \operatorname{Cos}\left(\frac{3\pi x}{L}\right)\right)^2 dx$$

or

$$\overline{U} = \frac{EA}{2} \int_{x=0}^{L} \left\{ \left[B_1 \frac{\partial f_1}{\partial x} + B_2 \frac{\partial f_2}{\partial x}\right]^2 + \left[B_1 \frac{\partial f_1}{\partial x} + B_2 \frac{\partial f_2}{\partial x}\right] \frac{\pi^2 Z}{L^2}\right.$$

$$\left[H_1\left(1+\operatorname{Cos}\left(\frac{2\pi x}{L}\right)\right) + 3H_2\left(\operatorname{Cos}\left(\frac{2\pi x}{L}\right) + \operatorname{Cos}\left(\frac{4\pi x}{L}\right)\right)\right]$$

$$+ \left(\frac{\pi}{L}\right)^4 \frac{Z^2}{4} \left[H_1^2\left(1+\cos^2\left(\frac{2\pi x}{L}\right)+2\cos\left(\frac{2\pi x}{L}\right)\right)+9H_2^2\left(\cos^2\left(\frac{2\pi x}{L}\right)\right.\right.$$

$$+ \cos^2\left(\frac{4\pi x}{L}\right) + 2\cos\left(\frac{2\pi x}{L}\right)\cos\left(\frac{4\pi x}{L}\right)\Big) + 6H_1H_2\Big(\cos\left(\frac{2\pi x}{L}\right)$$

$$\left.\left. + \cos\left(\frac{4\pi x}{L}\right) + \cos^2\left(\frac{2\pi x}{L}\right) + \cos\left(\frac{2\pi x}{L}\right)\cos\left(\frac{4\pi x}{L}\right)\right)\right]\Big\}dx$$

$$+ \frac{EI}{2}\left(\frac{\pi}{L}\right)^4\left(H_1^2\left(\frac{L}{2}\right)+81H_2^2\left(\frac{L}{2}\right)\right) - \frac{P}{2}\left(\frac{\pi}{L}\right)^2\left(H_1^2\left(\frac{L}{2}\right)+9H_2^2\left(\frac{L}{2}\right)\right) ,$$

which reduces to

$$\overline{U} = \frac{EA}{2}\int_{x=0}^{L} \Big\{\left[B_1 \frac{\partial f_1}{\partial x} + B_2 \frac{\partial f_2}{\partial x}\right]^2 + \left[B_1 \frac{\partial f_1}{\partial x} + B_2 \frac{\partial f_2}{\partial x}\right]\left(\frac{\pi}{L}\right)^2 \cdot$$

$$Z\left[H_1\left(1+\cos\left(\frac{2\pi x}{L}\right)\right) + 3H_2\left(\cos\left(\frac{2\pi x}{L}\right)+\cos\left(\frac{4\pi x}{L}\right)\right)\right]\Big\}dx$$

$$+ \frac{EA}{2}\left(\frac{\pi}{L}\right)^4 \frac{Z^2}{4}\left[H_1^2\left(\frac{3L}{2}\right) + 9H_2^2\left(\frac{2L}{2}\right) + 6H_1H_2\left(\frac{L}{2}\right)\right]$$

$$+ \left(\frac{\pi}{L}\right)^4 \frac{EI}{2}\left(\frac{L}{2}\right)\left(H_1^2+81H_2^2\right) - \left(\frac{\pi}{L}\right)^2 \frac{P}{2}\left(\frac{L}{2}\right)\left(H_1^2+9H_2^2\right) . \qquad (2.3.3)$$

Also, the kinetic energy expression becomes

$$\overline{T} = \frac{m\omega^2}{2}\int_{x=0}^{L}\left[H_1 \sin\left(\frac{\pi x}{L}\right) + H_2 \sin\left(\frac{3\pi x}{L}\right)\right]^2 dx$$

$$= \frac{m\omega^2}{2}\left(\frac{L}{2}\right)\left[H_1^2 + H_2^2\right] . \qquad (2.3.4)$$

Using the Rayleigh-Ritz method,

$$\frac{\partial \overline{U}}{\partial B_1} - \frac{\partial \overline{T}}{\partial B_1} = 0 , \qquad (2.3.5)$$

$$\frac{\partial \overline{U}}{\partial B_2} - \frac{\partial \overline{T}}{\partial B_2} = 0 , \qquad (2.3.6)$$

$$\frac{\partial \bar{U}}{\partial H_1} - \frac{\partial \bar{T}}{\partial H_1} = 0 \;, \qquad (2.3.7)$$

$$\frac{\bar{U}}{H_2} - \frac{\bar{T}}{H_2} = 0 \;, \qquad (2.3.8)$$

$\bar{T}$ contains the unknown frequency ω. These eigenvalue equations can be solved simultaneously to calculate the eigenvalue ω and the eigenvector B_1, B_2, H_1 and H_2. In the case of a curved plate, the undetermined coefficients in all three cartesian co-ordinate directions must be calculated by solving the minimization equations. A considerable saving in the computational effort can be achieved by the introduction of a concept of 'connection coefficients'.

In this method, the relationship between the axial (in-plane in the case of a curved plate) and transverse (out-of-plane in the case of a plate) displacement coefficients are first determined by solving the equations resulting from the minimization of the total potential energy with respect to the axial (in-plane for plates) displacement coefficients for unit values of the transverse (out-of-plane for plates) displacement coefficients. This relationship, which is expressed as a matrix called the 'connection coefficient matrix', does not depend on the magnitude of the displacement coefficients and can be conveniently substituted into the set of equations resulting from the minimization of the total potential energy with respect to each transverse (out-of-plane for plates) displacement coefficient. These equations can then be solved simultaneously for the frequencies (eigenvalues) and transverse displacement coefficients (eigenvectors).

A similar idea has been employed by Coan [29] and Yamaki [26] in post buckling analysis of rectangular plates where the coefficients for Airy stress functions are expressed as functions of out-of-plane displacement coefficients.

In the beam problem, equations (2.3.5) and (2.3.6) can be first solved for unit values of H_1, H_2 to calculate the connection coefficients. The results can be substituted in equations (2.3.7) and (2.3.8). These two equations can then be solved for ω and the transverse vibration mode (H_1,H_2). In the current example, the problem of solving four eigenvalue equations is reduced to that of solving two eigenvalue equations. The reduction in the size of this problem may not appear to be significant to justify the lengthy calculation of connection coefficients. However, for a more complicated case (such as a plate) the use of connection coefficients can result in substantial saving of computational effort by reducing the number of eigenvalue equations for the vibration problem and the number of non-linear equations for the post buckling analysis. The method will be illustrated by applying it to solve equations (2.3.5) to (2.3.8).

The first step is to solve equations (2.3.5) and (2.3.6) in terms of H_1 and H_2 as follows.

$$\frac{\partial \overline{T}}{\partial B_1} = 0 \ .$$

Therefore,

$$\frac{\partial \overline{U}}{\partial B_1} = EA \int_{x=0}^{L} \{B_1 (\frac{\partial f_1}{\partial x})^2 + B_2 \frac{\partial f_1}{\partial x} \cdot \frac{\partial f_2}{\partial x} + (\frac{\pi}{L})^2 \, z \, \frac{\partial f_1}{\partial x}$$

$$[H_1 (1+\text{Cos}(\frac{2\pi x}{L})) + 3H_2 (\text{Cos}(\frac{2\pi x}{L}) + \text{Cos}(\frac{4\pi x}{L}))]\}dx = 0 .$$

This can be written as,

$$S_{1,1} \times B_1 + S_{1,2} \times B_2 = X_{1,1} \times H_1 + X_{1,2} \times H_2 \ , \qquad (2.3.9)$$

where

$$S_{1,1} = \int_{x=0}^{L} (\frac{\partial f_1}{\partial x})^2 dx, \qquad (2.3.9a)$$

$$S_{1,2} = \int_{x=0}^{L} \frac{\partial f_1}{\partial x} \cdot \frac{\partial f_2}{\partial x} \, dx, \qquad (2.3.9b)$$

$$X_{1,1} = -(\frac{\pi}{L})^2 \, \frac{z}{2} \int_{x=0}^{L} \frac{\partial f_1}{\partial x} (1+\text{Cos}(\frac{2\pi x}{L}))dx, \qquad (2.3.9c)$$

and

$$X_{1,2} = -3(\frac{\pi}{L})^2 \, \frac{z}{2} \int_{x=0}^{L} \frac{\partial f_1}{\partial x} [\text{Cos}(\frac{2\pi x}{L}) + \text{Cos}(\frac{4\pi x}{L})]dx \ . \qquad (2.3.9d)$$

Similarly, $\frac{\partial \overline{U}}{\partial B_2} = 0$ can be written as

$$S_{2,1} \times B_1 + S_{2,2} \times B_2 = X_{2,1} \times H_1 + X_{2,2} \times H_2 , \qquad (2.3.10)$$

where

$$S_{2,1} = S_{1,2} \ , \qquad (2.3.10a)$$

$$S_{2,2} = \int_{x=0}^{L} \left(\frac{\partial f_2}{\partial x}\right)^2 dx\ , \tag{2.3.10b}$$

$$X_{2,1} = -\left(\frac{\pi}{L}\right)^2 \frac{Z}{2} \int_{x=0}^{L} \frac{\partial f_2}{\partial x}\left(1+\mathrm{Cos}\left(\frac{2\pi x}{L}\right)\right) dx, \tag{2.3.10c}$$

and $$X_{2,2} = -3\left(\frac{\pi}{L}\right)^2 \frac{Z}{2} \int_{x=0}^{L} \frac{\partial f_2}{\partial x}\left[\mathrm{Cos}\left(\frac{2\pi x}{L}\right) + \mathrm{Cos}\left(\frac{4\pi x}{L}\right)\right] dx\ . \tag{2.3.10d}$$

In matrix form equations (2.3.9) and (2.3.10) can be written as

$$\begin{bmatrix} S_{1,1} & S_{1,2} \\ S_{2,1} & S_{2,2} \end{bmatrix} \begin{Bmatrix} B_1 \\ B_2 \end{Bmatrix} = \begin{bmatrix} X_{1,1} & X_{1,2} \\ X_{2,1} & X_{2,2} \end{bmatrix} \begin{Bmatrix} H_1 \\ H_2 \end{Bmatrix}\ . \tag{2.3.11}$$

The solution proceeds as follows:

First, the following two sets of equations are solved.

$$\begin{bmatrix} S_{1,1} & S_{1,2} \\ S_{2,1} & S_{2,2} \end{bmatrix} \begin{Bmatrix} B'_{1,1} \\ B'_{2,1} \end{Bmatrix} = \begin{Bmatrix} X_{1,1} \\ X_{2,1} \end{Bmatrix} \tag{2.3.12}$$

$$\begin{bmatrix} S_{1,1} & S_{1,2} \\ S_{2,1} & S_{2,2} \end{bmatrix} \begin{Bmatrix} B'_{1,2} \\ B'_{2,2} \end{Bmatrix} = \begin{Bmatrix} X_{1,2} \\ X_{2,2} \end{Bmatrix} \tag{2.3.13}$$

Hence,

$$\begin{Bmatrix} B_1 \\ B_2 \end{Bmatrix} = \begin{bmatrix} B'_{1,1} & B'_{1,2} \\ B'_{2,1} & B'_{2,2} \end{bmatrix} \begin{Bmatrix} H_1 \\ H_2 \end{Bmatrix}\ . \tag{2.3.14}$$

The coefficients $B'_{i,j}$ are called 'connection coefficients' since they relate the axial displacement coefficients to the transverse displacement coefficients. Note that the calculation of connection coefficients does not require the calculation of the transverse displacement coefficients. Having calculated the connection coefficients, the frequencies and modeshapes can be found as follows:

Substituting equations (2.3.3) and (2.3.4) in equation (2.3.7) gives

$$\frac{EA}{2}\ [(\frac{\pi}{L})^4\ \frac{Z^2}{4}\ (\frac{L}{2})\ [6H_1+6H_2]\ +\ \int_{x=0}^{L}\ (1+\mathrm{Cos}(\frac{2\pi x}{L}))\ (\frac{\pi}{L})^2 Z(B_1\ \frac{\partial f_1}{\partial x}$$

$$+\ B_2\ \frac{\partial f_2}{\partial x})\, dx]\ +\ \frac{EI}{2}(\frac{\pi}{L})^4(\frac{L}{2})\, 2H_1\ -\ (\frac{\pi}{L})^2\ \frac{P}{4}\ \cdot\ 2H_1\cdot\ L$$

$$-\ \frac{m\omega^2 L}{2}\ H_1\ =\ 0\ .$$

i.e.
$$H_1\{\frac{6EA\ \pi^4 Z^2}{16L^3}\ +\ \frac{\pi^4 EI}{2L^3}\ -\ \frac{\pi^2 P}{2L}\}\ +\ \frac{6\pi^4 EAZ^2}{16L^3}\ H_2$$

$$-\ EA(X_{1,1}{}^{\times}B_1\ +\ X_{2,1}{}^{\times}B_2)\ -\ \frac{\bar{m}\omega^2 L}{2}\ H_1\ =\ 0.$$

Substituting $B_1 = B'_{1,1}\ H_1 + B'_{1,2}\ H_2$ from equation (2.3.14) into this gives

$$H_1[\frac{3EA\pi^4 Z^2}{8L^3}\ +\ \frac{\pi^4 EI}{2L^3}\ -\ \frac{\pi^2 P}{2L}]\ +\ \frac{3\pi^4 EAZ^2}{8L^3}\ H_2$$

$$-\ EA[X_{1,1}\ B'_{1,1}\ H_1\ +\ X_{2,1}\ B'_{2,1}\ H_1$$

$$+\ X_{1,1}\ B'_{1,2}\ H_2\ +\ X_{2,1}\ B'_{2,2}\ H_2]\ -\ \frac{\bar{m}\omega^2 L}{2}\ H_1\ =\ 0.$$

This can be written as

$$\bar{S}_{1,1} H_1 + \bar{S}_{1,2} H_2 - \frac{\bar{m}\omega^2 L}{2} H_1 = 0 \,, \qquad (2.3.15)$$

where

$$\bar{S}_{1,1} = \frac{3EA\pi^4 Z^2}{8L^3} + \frac{\pi^4 EI}{2L^3} - \frac{\pi^2 P}{2L} - EA(X_{1,1} B'_{1,1} + X_{2,1} B'_{2,1}) \qquad (2.3.15a)$$

and

$$\bar{S}_{1,2} = \frac{3EA\pi^4 Z^2}{8L^3} - EA(X_{1,1} B'_{1,2} + X_{2,1} B'_{2,2}) \,. \qquad (2.3.15b)$$

Similarly, equation (2.3.8) can be transformed into

$$\bar{S}_{2,1} H_1 + \bar{S}_{2,2} H_2 - \frac{\bar{m}\omega^2 L}{2} H_2 = 0 \,, \qquad (2.3.16)$$

where

$$\bar{S}_{2,1} = \frac{3\pi^4 EAZ^2}{8L^3} - EA(X_{1,2} B'_{1,1} + X_{2,2} B'_{2,1}) \qquad (2.3.16a)$$

and

$$\bar{S}_{2,2} = \frac{9\pi^4 EAZ^2}{4L^3} + \frac{81\pi^4 EI}{2L^3} - \frac{9\pi^2 P}{2L}$$

$$- EA(X_{1,2} B'_{1,2} + X_{2,2} B'_{2,2}) \,. \qquad (2.3.16b)$$

The natural frequencies can be found by solving the eigenvalue equations

$$\begin{bmatrix} \bar{S}_{1,1} & \bar{S}_{1,2} \\ \bar{S}_{2,1} & \bar{S}_{2,2} \end{bmatrix} \begin{Bmatrix} H_1 \\ H_2 \end{Bmatrix} - \frac{\bar{m}\omega^2 L}{2} \begin{bmatrix} 1 & 0 \\ 0 & 1 \end{bmatrix} \begin{Bmatrix} H_1 \\ H_2 \end{Bmatrix} = 0 \,. \qquad (2.3.17)$$

In this simple case this reduces to

$$(\bar{S}_{1,1} - \frac{\bar{m}\omega^2 L}{2})(\bar{S}_{2,2} - \frac{\bar{m}\omega^2 L}{2}) - \bar{S}_{1,2}\bar{S}_{2,1} = 0 \; . \qquad (2.3.17a)$$

It is worth noting that the substitution for axial displacement coefficients should be done after the minimization. The Rayleigh-Ritz method requires that each displacement coefficient must be treated as independent during minimization.

This procedure is illustrated in the following examples. The importance of the choice of shape functions for the axial displacement is also demonstrated in these examples. The choice of shape functions for the in-plane displacements of the curved plate will be explained in Chapter 3.

Example 1

Consider the vibration of the curved beam for axially restrained end conditions with the following shapes:

$$w = H_1 \mathrm{Sin}(\frac{\pi x}{L}) \; , \; u = B_1 \mathrm{Sin}(\frac{2\pi x}{L}) \; .$$

(These functions are the same as those found in the exact analysis.)

The equations in the preceding pages can be used with $H_2 = 0$, $B_2 = 0$, $f_2 = 0$ and $f_1 = \mathrm{Sin}(\frac{2\pi x}{L})$.

$$S_{1,1} = \int_{x=0}^{L} (\frac{\partial f_1}{\partial x})^2 dx = \frac{2\pi^2}{L} \; , \; S_{1,2}=S_{2,1}=S_{2,2}=0 .$$

$$X_{1,1} = -\left(\frac{\pi}{L}\right)^2 \frac{Z}{2} \int_{x=0}^{L} \left(\frac{2\pi}{L}\right) \cos\left(\frac{2\pi x}{L}\right) \left[1+\cos\left(\frac{2\pi x}{L}\right)\right] dx$$

$$= -\frac{\pi^3 Z}{2L^2} ,$$

$$X_{1,2} = -\frac{3\pi^2 Z}{2L^2} \int_{x=0}^{L} \left[\cos\left(\frac{2\pi x}{L}\right) + \cos\left(\frac{4\pi x}{L}\right)\right] \left(\frac{2\pi}{L}\right) \cos\left(\frac{2\pi x}{L}\right) dx$$

$$= -\frac{3\pi^3 Z}{2L^2} ,$$

$$B'_{1,1} = X_{1,1}/S_{1,1} = -\frac{Z\pi}{4L} ,$$

$$\bar{S}_{1,1} = \frac{3EA\pi^4 Z^2}{8L^3} + \frac{\pi^4 EI}{2L^3} - \frac{\pi^2 P}{2L} + \frac{\pi Z}{4L}\left(-\frac{\pi^3 Z}{2L^2}\right) EA$$

$$= \frac{\pi^4 EAZ^2}{4L^3} + \frac{\pi^4 EI}{2L^3} - \frac{\pi^2 P}{2L} .$$

Hence,

$$\frac{\bar{m}\omega^2 L}{2} = \frac{\pi^4}{2L^3} \left(\frac{EAZ^2}{2} + EI - \frac{PL^2}{\pi^2}\right) .$$

i.e. $$\frac{\bar{m}\omega^2 L^4}{EI\pi^4} = 1 + \frac{AZ^2}{2I} - \frac{P}{P_E} ,$$

or $$\frac{\omega^2}{\Omega^2} = \left(1 - \frac{P}{P_E} + \frac{Z^2}{2k^2}\right) .$$

This is the correct exact result.

Example 2

To illustrate the importance of the choice of shape functions, the problem in example 1 can be solved with the following alternative shape functions.

$$w = H_1 \mathrm{Sin}(\frac{\pi x}{L}) + H_2 \mathrm{Sin}(\frac{3\pi x}{L}) \ ,$$

$$u = B_1 \ f_1(x) \ , \text{ where } f_1(x) = \mathrm{Cos}(\frac{\pi x}{L}) + \frac{2x}{L} - 1 \ .$$

This new function $f_1(x)$ also satisfies the forced boundary conditions that the axial displacements at the ends are zero, which is a requirement for the application of the Rayleigh-Ritz method.

$$\frac{\partial f_1}{\partial x} = -\frac{\pi}{L} \sin(\frac{\pi x}{L}) + \frac{2}{L} \ ,$$

$$S_{1,1} = \int_{x=0}^{L} (\frac{\partial f_1}{\partial x})^2 dx = \int_{x=0}^{L} (\frac{4}{L^2} + (\frac{\pi}{L})^2 \sin^2(\frac{\pi x}{L})$$

$$- \frac{4\pi}{L^2} \sin(\frac{\pi x}{L}))\,dx$$

$$= (\pi^2 - 8)/2L,$$

$$X_{1,1} = -(\frac{\pi}{L})^2 \frac{Z}{2} \int_{x=0}^{L} [\frac{2}{L} - \frac{\pi}{L} \sin(\frac{\pi x}{L})][1 + \cos(\frac{2\pi x}{L})]dx$$

$$= \frac{\pi^2 Z}{3L^2} \ ,$$

$$X_{1,2} = \int_{x=0}^{L} [\cos(\frac{2\pi x}{L}) + \cos(\frac{4\pi x}{L})][\frac{2}{L} - \frac{\pi}{L} \sin(\frac{\pi x}{L})](-\frac{3\pi^2 Z}{2L^2})\,dx$$

$$= \frac{6\pi^3 Z}{5L^2} \ ,$$

$$B'_{1,1} = X_{1,1}/S_{1,1} = \frac{\pi^2 Z}{3L^2} \frac{2L}{(\pi^2 - 8)}$$

$$= \frac{2\pi^2 Z}{3L(\pi^2 - 8)} \ ,$$

$$B'_{1,2} = X_{1,2}/S_{1,1} = \frac{6\pi^3 Z}{5L^2}\,\frac{2L}{(\pi^2-8)}$$

$$= \frac{12\pi^3 Z}{5L(\pi^2-8)} ,$$

$$\bar{S}_{1,1} = \frac{3EA\pi^4 Z^2}{8L^3} + \frac{\pi^4 EI}{2L^3} - \frac{\pi^2 P}{2L} - EA\,\frac{2\pi^2 Z}{3L(\pi^2-8)}\,\frac{\pi^2 Z}{3L^2} ,$$

$$\bar{S}_{1,2} = \frac{3\pi^4 EAZ^2}{8L^3} - EA\,\frac{12\pi^3 Z}{5L(\pi^2-8)}\,\frac{\pi^2 Z}{3L^2} ,$$

$$\bar{S}_{2,1} = \frac{3\pi^4 EAZ^2}{8L^3} - \frac{2\pi^2 Z}{3L(\pi^2-8)}\,\frac{6\pi^3 Z}{5L^2} ,$$

$$\bar{S}_{2,2} = \frac{9\pi^4 EAZ^2}{4L^3} + 81\,\frac{\pi^4 EI}{2L^3} - \frac{9\pi^2 P}{2L} - EA\,\frac{12\pi^3 Z}{5L(\pi^2-8)}\,\frac{6\pi^3}{5L^2} .$$

Substituting these into equation (2.3.17a) and dividing by $(\pi^4 EI/2L^3)^2$ yields

$$[1 - \frac{P}{P_E} + \frac{Z^2}{k^2}(\frac{3}{4} - \frac{4}{9(\pi^2-8)} - \frac{\omega^2}{\Omega^2}][81 - \frac{9P}{P_E} + \frac{Z^2}{k^2}(\frac{9}{2} - \frac{144}{25(\pi^2-8)}) - \frac{\omega^2}{\Omega^2}]$$

$$- [\frac{Z^2}{k^2}(\frac{3}{4} - \frac{8}{5(\pi^2-8)})]^2 = 0 . \qquad (2.3.18)$$

Let $\lambda^2 = \frac{\omega^2}{\Omega^2}$, $\rho = \hat{P}/P_E$ and $\phi^2 = \frac{Z^2}{k^2}$,

then

$$(1-\lambda^2-\rho+.512\ \phi^2)(81-9\rho-\lambda^2+1.419\ \phi^2)-.1058^2\ \phi^4 = 0. \qquad (2.3.18a)$$

One term solution gives $\lambda^2 = 1-\rho+.512\ \phi^2$.

The exact solution is $\lambda^2 = 1-\rho+.5\ \phi^2$.

The two term solution is given by the following equation

$$\lambda^4 - \lambda^2(82-10\rho+1.931\phi^2)+(1-\rho+.512\phi^2)(81-9\rho+1.419\phi^2)$$

$$- .1058^2\phi^4 = 0,$$

from which

$$\lambda^2 = \frac{41-5\rho+.9657\phi^2 \mp \sqrt{(41-5\rho+.9657\phi^2)^2}}{-(1-\rho+.512\phi^2)(81-9\rho+1.419\phi^2)+.1058^2\phi^4} .$$

It is interesting to note the variation of λ^2 with ϕ^2.

$$\underset{\phi\to\infty}{\text{Limit}} \frac{\partial\lambda^2}{\partial\phi^2} = .9657 \mp \frac{1}{2} \frac{(2\times.9657^2\phi^2-2\times1.4191\times.5123+2\times.1058^2)}{\sqrt{.9657^2 - 1.4191 \times .512 + .1058^2}}$$

$$= .5 .$$

This example illustrates an interesting point. The approximate solution for a curved beam vibration may exhibit a non-linear relationship between the square of the non-dimensional fundamental frequency and the square of the central deflection, although an exact linear relationship exists.

The application of the Rayleigh-Ritz method for the curved plate problem is explained in Chapter 3.

CHAPTER 3

THEORETICAL ANALYSIS OF THE PLATE PROBLEM

3.1 INTRODUCTORY REMARKS

This chapter consists of the theoretical derivations associated with the application of the Rayleigh-Ritz method to the post buckling and vibration analysis of simply supported curved rectangular plates. Application of the Rayleigh-Ritz method to the post buckling analysis is discussed in section 3.2. The derivation of the formulae that are necessary to calculate the static displacements and in-plane stress distribution is given in this section. Under applied in-plane loading, the plate can vibrate freely about its equilibrium state. Having calculated the deflected shape and stresses under the applied load, the natural frequencies can be calculated by using the Rayleigh-Ritz method. This procedure is explained in section 3.3. A brief discussion on the choice of shape functions can be found in section 3.4. Some notes on a computer program which was developed to obtain numerical values for the natural frequencies, displacements and stress distribution of practical plates using the analysis explained in this chapter are given in section 3.5.

3.2 APPLICATION OF THE RAYLEIGH-RITZ METHOD TO THE POST BUCKLING ANALYSIS OF SIMPLY SUPPORTED RECTANGULAR PLATES

This section deals with the application of the Rayleigh-Ritz method to calculate the static displacements and in-plane stresses due to an applied in-plane load.

Consider the equilibrium of a rectangular plate, subject to uniaxial load P_x, applied at two points on the edges x=o and x=a, through two edge beams as shown in Figure 3.2.1.

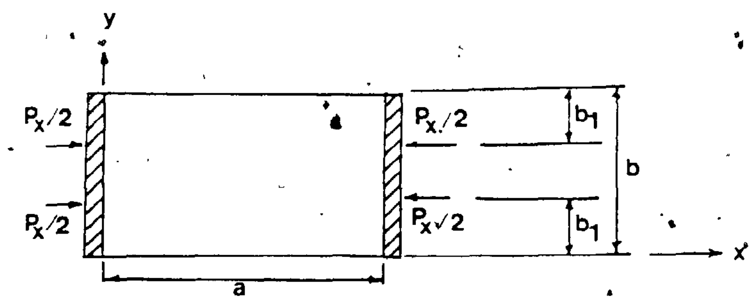

Figure 3.2.1.

For a plate simply supported along all four edges, the initial out-of-plane displacement (initial imperfection) can be expressed as a Fourier series.

$$z_o = \sum_i \sum_j z_{o_{i,j}} \sin\left(\frac{\alpha_i x}{a}\right) \sin\left(\frac{\alpha_j y}{b}\right) \quad i,j=1,2,3\ldots \qquad (3.2.1)$$

where for displacements symmetrical about the axes x=a/2, y=b/2, $\alpha_i = (2i-1)\pi$.

The displacement z at a load P_x can also be given by a Fourier series,

$$z = \sum_i \sum_j Z_{i,j} \operatorname{Sin}(\frac{\alpha_i x}{a}) \operatorname{Sin}(\frac{\alpha_j y}{b}) . \qquad (3.2.2)$$

It is assumed that the plate is initially stress free. Let the in-plane displacements along x,y directions be u_s, v_s respectively.

u_s and v_s are expressed as the sum of a series of the products of in-plane displacement coefficients and the corresponding shape functions as given by the following equations:

$$u_s = \sum_i \sum_j A_{i,j} f_{ui}(x) \, g_{uj}(y) , \qquad (3.2.3)$$

$$v_s = \sum_i \sum_j B_{i,j} f_{vi}(x) \, g_{vj}(y) . \qquad (3.2.4)$$

The shape functions f_{ui}, g_{uj}, f_{vi} and g_{vj} must satisfy the geometric boundary conditions as will be explained in section 3.4.

The total potential energy of the plate and the edge beams consists of the following components:

(a) Strain Energy due to bending of the plate given by [31],

$$\bar{U}_{be} = \frac{Eh^3}{24(1-\nu^2)} \int_{x=0}^{a} \int_{y=0}^{b} \{ [\frac{\partial^2 (z-z_o)}{\partial x^2} + \frac{\partial^2 (z-z_o)}{\partial y^2}]^2$$

$$-2(1-\nu) [\frac{\partial^2 (z-z_o)}{\partial x^2} \frac{\partial^2 (z-z_o)}{\partial y^2} - (\frac{\partial^2 (z-z_o)}{\partial x \partial y})^2] \} dx \, dy . \qquad (3.2.5a)$$

(b) Strain Energy due to the stretching of the middle surface given by [31],

$$\bar{U}_{str} = \frac{Eh}{2(1-\nu^2)} \int_{x=o}^{a} \int_{y=o}^{b} [\varepsilon_x^2 + \varepsilon_y^2 + 2\nu\varepsilon_x\varepsilon_y + \frac{(1-\nu)}{2}\gamma_{xy}^2] dxdy, \tag{3.2.5b}$$

where the middle surface strains are related to the derivatives of displacements as follows:

$$\left.\begin{aligned}
\varepsilon_x &= \frac{\partial u_s}{\partial x} + \frac{1}{2}(\frac{\partial z}{\partial x})^2 - \frac{1}{2}(\frac{\partial z_o}{\partial x})^2 \\
\varepsilon_y &= \frac{\partial v_s}{\partial y} + \frac{1}{2}(\frac{\partial z}{\partial y})^2 - \frac{1}{2}(\frac{\partial z_o}{\partial y})^2 \\
\gamma_{xy} &= \frac{\partial u_s}{\partial y} + \frac{\partial v_s}{\partial x} + \frac{\partial z}{\partial x}.\frac{\partial z}{\partial y} - \frac{\partial z_o}{\partial x}.\frac{\partial z_o}{\partial y}.
\end{aligned}\right\} \tag{3.2.5c}$$

Substituting equations (3.2.5c) into equation (3.2.5b) gives

$$\begin{aligned}
\bar{u}_{str} = \frac{Eh}{2(1-\nu^2)} \int_{x=o}^{a} \int_{y=o}^{b} \{ & [\frac{\partial u_s}{\partial x} + \frac{1}{2}(\frac{\partial z}{\partial x})^2 - \frac{1}{2}(\frac{\partial z_o}{\partial x})^2]^2 \\
& + [\frac{\partial v_s}{\partial y} + \frac{1}{2}(\frac{\partial z}{\partial y})^2 - \frac{1}{2}(\frac{\partial z_o}{\partial y})^2]^2 \\
& + 2\nu [\frac{\partial u_s}{\partial x} + \frac{1}{2}(\frac{\partial z}{\partial x})^2 - \frac{1}{2}(\frac{\partial z_o}{\partial x})^2] [\frac{\partial v_s}{\partial y} + \frac{1}{2}(\frac{\partial z}{\partial y})^2 - (\frac{\partial z_o}{\partial y})^2] \\
& + (\frac{1-\nu}{2}) [\frac{\partial u_s}{\partial y} + \frac{\partial v_s}{\partial x} + \frac{\partial z}{\partial x}.\frac{\partial z}{\partial y} - \frac{\partial z_o}{\partial x}.\frac{\partial z_o}{\partial y}]^2 \} dx\,dy.
\end{aligned} \tag{3.2.5d}$$

(c) Change in the potential energy due to the movement of the load P_x is given by

$$\bar{V}_{LOAD} = - P_x \{ u_s \Big|_{x=o,\, y=b1} - u_s \Big|_{x=a,\, y=b1} \} . \quad (3.2.5e)$$

(d) Strain Energy due to the bending of the edge beam is given by

$$\bar{U}_{beam} = (\frac{EI}{2})_{beam} \int_{y=o}^{b} [(\frac{\partial^2 u_s}{\partial y^2})^2 \Big|_{x=o} + (\frac{\partial^2 u_s}{\partial y^2}) \Big|_{x=a}] dy . \quad (3.2.5f)$$

Total potential energy of the deflected plate and the edge beam is given by

$$\bar{V}_T = \bar{U}_{be} + \bar{U}_{str} + \bar{V}_{LOAD} + \bar{U}_{beam} . \quad (3.2.6)$$

Using the Rayleigh-Ritz method,

$$\{\frac{\partial \bar{V}_T}{A_{i,j}}\} = 0 , \quad (3.2.7)$$

$$\{\frac{\partial \bar{V}_T}{B_{i,j}}\} = 0 , \quad (3.2.8)$$

$$\{\frac{\partial \bar{V}_T}{\partial Z_{i,j}}\} = 0 . \quad (3.2.9)$$

<u>Calculation of Connection Coefficients</u>

Substituting equations (3.2.5a), (3.2.5d), (3.2.5e), (3.2.5f) and (3.2.6) into equation (3.2.7) and, noting that only functions of u_s will yield non-zero terms for $\frac{\partial \bar{V}_T}{\partial A_{i,j}}$, leads to

$$\frac{Eh}{2(1-\nu^2)} \frac{\partial}{\partial A_{i,j}} \int_{x=o}^{a} \int_{y=o}^{b} \{ (\frac{\partial u_s}{\partial x})^2 + \frac{\partial u_s}{\partial x}[(\frac{\partial z}{\partial x})^2 - (\frac{\partial z_o}{\partial x})^2]$$

$$+ 2\nu \frac{\partial u_s}{\partial x} \frac{\partial v_s}{\partial y} + \nu \frac{\partial u_s}{\partial x}[(\frac{\partial z}{\partial y})^2 - (\frac{\partial z_o}{\partial y})^2] + (\frac{1-\nu}{2}) (\frac{\partial u_s}{\partial y})^2$$

$$+ (1-\nu)\frac{\partial u_s}{\partial y} \frac{\partial v_s}{\partial x} + (1-\nu)\frac{\partial u_s}{\partial y}[\frac{\partial z}{\partial x} \frac{\partial z}{\partial y} - \frac{\partial z_o}{\partial x} \frac{\partial z_o}{\partial y}] \} dx\, dy$$

$$- P_x \frac{\partial}{\partial A_{i,j}} \{ u_s \Big|_{x=o, y=bl} - u_s \Big|_{x=a, y=bl} \}$$

$$+ (\frac{EI}{2})_{beam} \frac{\partial}{\partial A_{i,j}} \int_{y=o}^{b} [(\frac{\partial^2 u_s}{\partial y^2})^2 \Big|_{x=o} + (\frac{\partial^2 u_s}{\partial y^2}) \Big|_{x=a}] dy = 0$$

This can be rearranged to give

$$\frac{1}{2} \frac{\partial}{\partial A_{i,j}} \int_{x=o}^{a} \int_{y=o}^{b} \{ (\frac{\partial u_s}{\partial x})^2 + (\frac{1-\nu}{2}) (\frac{\partial u_s}{\partial y})^2$$

$$+ \frac{\partial u_s}{\partial x}[((\frac{\partial z}{\partial x})^2 - (\frac{\partial z_o}{\partial x})^2) + \nu ((\frac{\partial z}{\partial y})^2 - (\frac{\partial z_o}{\partial y})^2)]$$

$$+ 2\nu \frac{\partial u_s}{\partial x} \frac{\partial v_s}{\partial y} + (1-\nu)\frac{\partial u_s}{\partial y} \frac{\partial v_s}{\partial x}$$

$$+ (1-\nu)\frac{\partial u_s}{\partial y}[\frac{\partial z}{\partial x} \frac{\partial z}{\partial y} - \frac{\partial z_o}{\partial x} \frac{\partial z_o}{\partial y}] \} dx\, dy$$

$$- P_x \frac{(1-\nu^2)}{Eh} \frac{\partial}{\partial A_{i,j}} [u_s \Big|_{x=o, y=bl} - u_s \Big|_{x=a, y=bl}]$$

$$+ (\frac{EI}{2})_{beam} \frac{(1-\nu^2)}{(Eh)_{plate}} \frac{\partial}{\partial A_{i,j}} \int_{y=o}^{b} [(\frac{\partial^2 u_s}{\partial y^2})^2 \Big|_{x=o}$$

$$+ (\frac{\partial^2 u_s}{\partial y^2}) \Big|_{x=a}] dy = 0 . \qquad (3.2.10)$$

The following treats the various parts of this expression separately. Using equation (3.2.3),

$$\left(\frac{\partial u_s}{\partial x}\right)^2 + \left(\frac{1-\nu}{2}\right)\left(\frac{\partial u_s}{\partial y}\right)^2 = \left(\sum_i \sum_j A_{i,j} \frac{\partial f_{ui}}{\partial x} g_{uj}\right)^2$$

$$+ \left(\frac{1-\nu}{2}\right)\left(\sum_i \sum_j A_{i,j} f_{ui} \frac{\partial g_{uj}}{\partial y}\right)^2 ,$$

thus $\frac{1}{2} \frac{\partial}{\partial A_{i,j}} \left[\left(\frac{\partial u_s}{\partial x}\right)^2 + \left(\frac{1-\nu}{2}\right)\left(\frac{\partial u_s}{\partial y}\right)^2\right]$

$$= \int_{x=o}^{a} \int_{y=o}^{b} \Big\{ \frac{\partial f_{ui}}{\partial x} g_{uj} \sum_k \sum_\ell A_{k,\ell} \left(\frac{\partial f_{uk}}{\partial x} g_{u\ell}\right)$$

$$+ \left(\frac{1-\nu}{2}\right) f_{ui} \frac{\partial g_{uj}}{\partial y} \sum_k \sum_\ell A_{k,\ell} \left(f_{uk} \frac{\partial g_{u\ell}}{\partial y}\right) \Big\} dx\, dy$$

$$= \left\{\sum_k \sum_\ell A_{k,\ell}\, R1_{i,j,k,\ell}\right\} , \qquad (3.2.11a)$$

where $R1_{i,j,k,\ell} = \left[\int_{x=o}^{a} \frac{\partial f_{ui}}{\partial x} \frac{\partial f_{uk}}{\partial x} dx \int_{y=o}^{b} g_{uj}\, g_{u\ell}\, dy\right]$.

$$+ \left(\frac{1-\nu}{2}\right)\left[\int_{x=o}^{a} f_{ui}\, f_{uk}\, dx \int_{y=o}^{b} \frac{\partial g_{uj}}{\partial y} \frac{\partial g_{u\ell}}{\partial y} dy\right] . \qquad (3.2.11b)$$

Using equations (3.2.1) to (3.2.3) it can be shown that

$$\frac{1}{2} \frac{\partial}{\partial A_{i,j}} \int_{x=o}^{a} \int_{y=o}^{b} \left\{ \frac{\partial u_s}{\partial x} \left\{ \left[\left(\frac{\partial z}{\partial x}\right)^2 - \left(\frac{\partial z_o}{\partial x}\right)^2\right] + \nu\left[\left(\frac{\partial z}{\partial y}\right)^2 - \left(\frac{\partial z_o}{\partial y}\right)^2\right]\right\}\right.$$

$$\left. + (1-\nu) \frac{\partial u_s}{\partial y}\left(\frac{\partial z}{\partial x} \frac{\partial z}{\partial y} - \frac{\partial z_o}{\partial x} \frac{\partial z_o}{\partial y}\right)\right\} dx\, dy$$

$$= \left\{\sum_p \sum_q \sum_r \sum_s (Z_{p,q}\, Z_{r,s} - Z_{op,q}\, Z_{or,s}) R2_{i,j,p,q,r,s}\right\} ,$$

(3.2.12a)

where $R2_{i,j,p,q,r,s}$,

$$= \int_{x=o}^{a} \int_{y=o}^{b} \{ \frac{\partial f_{ui}}{\partial x} g_{uj} [\frac{\alpha_p \beta_r}{a^2} \cos(\frac{\alpha_p x}{a}) \cos(\frac{\beta_r x}{a}) \sin(\frac{\alpha_q y}{a}) \sin(\frac{\beta_s y}{b})$$

$$+ \nu \frac{\alpha_q \beta_s}{b^2} \sin(\frac{\alpha_p x}{a}) \sin(\frac{\beta_r x}{a}) \cos(\frac{\alpha_q y}{b}) \cos(\frac{\beta_s y}{b})]$$

$$+ (\frac{1-\nu}{2}) f_{ui} \frac{\partial g_{uj}}{\partial y} [\frac{\alpha_p \beta_s}{ab} \cos(\frac{\alpha_p x}{a}) \sin(\frac{\beta_r x}{a}) \sin(\frac{\alpha_q y}{b}) \cos(\frac{\beta_s y}{b})$$

$$+ \frac{\alpha_q \beta_r}{ab} \sin(\frac{\alpha_p x}{a}) \cos(\frac{\beta_r x}{a}) \cos(\frac{\alpha_q y}{b}) \sin(\frac{\beta_s y}{b})] \} dx\, dy, \tag{3.2.12b}$$

in which, for symmetrical shapes,

$$\alpha_p = (2p-1)\pi, \ \beta_r = (2r-1)\pi, \ \alpha_q = (2q-1)\pi, \ \beta_s = (2s-1)\pi. \tag{3.2.12c}$$

Also,

$$\frac{P_x(1-\nu^2)}{Eh} \frac{\partial}{\partial A_{i,j}} [u_s \Big|_{x=o,y=bl} - u_s \Big|_{x=a,y=bl}]$$

$$= \{ - \frac{P_x(1-\nu^2)}{Eh} R3_{i,j} \} \tag{3.2.13a}$$

where $R3_{i,j} = [f_{ui}(o) - f_{ui}(a)]\, g_{uj}(bl)$ (3.2.13b)

and

$$(\frac{EI}{2})_{beam} \frac{(1-\nu^2)}{(Eh)_{plate}} \frac{\partial}{\partial A_{i,j}} \int_{y=o}^{b} [(\frac{\partial^2 u_s}{\partial y^2})^2 \Big|_{x=o} + (\frac{\partial^2 u_s}{\partial y^2})^2 \Big|_{x=a}] dy$$

$$= K_{beam} \{ \sum_k \sum_\ell A_{k,\ell}\, R4_{i,j,k,\ell} \}, \tag{3.2.14a}$$

where

$$R4_{i,j,k,\ell} = [(f_{ui}\ f_{uk})\Big|_{x=o} + (f_{ui}\ f_{uk})\Big|_{x=a}] \int_{y=o}^{b} \frac{\partial^2 g_{uj}}{\partial y^2} \frac{\partial^2 g_{u\ell}}{\partial y^2}\, dy$$

$$= [f_{ui}(o)\ f_{uk}(o) + f_{ui}(a)\ f_{uk}(a)] \int_{y=o}^{b} \frac{\partial^2 g_{uj}}{\partial y^2} \frac{\partial^2 g_{u\ell}}{\partial y^2}\, dy$$

(3.2.14b)

and $K_{beam} = (EI)_{beam} (\frac{1-\nu^2}{Eh})_{plate}$ (3.2.14c)

Finally, using equations (3.2.3) and (3.2.4) it can be shown that,

$$\frac{\partial}{\partial A_{i,j}} \frac{1}{2} \int_{x=o}^{a} \int_{y=o}^{b} [2\nu \frac{\partial u_s}{\partial x} \frac{\partial v_s}{\partial y} + (1-\nu) \frac{\partial u_s}{\partial y} \frac{\partial v_s}{\partial x}] dx\ dy$$

$$= \{\sum_m \sum_n B_{m,n} R5_{i,j,m,n}\}, \qquad (3.2.15a)$$

where $R5_{i,j,m,n} = \int_{x=o}^{a} \int_{y=o}^{b} \{\nu \frac{\partial f_{ui}}{\partial x} f_{vm}\ g_{uj} \frac{\partial g_{vn}}{\partial y}$

$$+ (\frac{(1-\nu)}{2}\ f_{ui} \frac{\partial f_{vm}}{\partial x} \frac{\partial g_{uj}}{\partial y}\ g_{vn}\} dx\ dy\ . \qquad (3.2.15b)$$

Substituting equations (3.2.11a), (3.2.12a), (3.2.13a), (3.2.14a) and (3.2.15a) into equation (3.2.10) gives,

$$\{\sum_k \sum_\ell A_{k,\ell} (R1_{i,j,k,\ell} + R4_{i,j,k,\ell}) + \sum_m \sum_n B_{m,n}\ R5_{i,j,m,n}$$

$$+ \sum_p \sum_q \sum_r \sum_s (Z_{p,q}\ Z_{r,s} - Z_{op,q}\ Z_{or,s}) R2_{i,j,p,q,r,s}$$

$$- P_x\ R3_{i,j}\ \} = 0. \qquad (3.2.16)$$

For different values of i and j this will result in different equations. The total number of equations will be equal to the total number of in-plane shapes taken for u_s. This set of equations represents an approximation to the equation of equilibrium in the x-direction. The same operations in the y-direction will result in the following type of equations:

$$\{\sum_k \sum_\ell R4_{i,j,k,\ell} A_{k,\ell} + \sum_m \sum_n B_{m,n} S1_{i,j,m,n} + \sum_p \sum_q \sum_r \sum_s (Z_{p,q} Z_{r,s} - Z_{op,q} Z_{or,s}) S2_{i,j,p,q,r,s}\} = 0, \quad (3.2.17)$$

where

$$S1_{i,j,m,n} = \int_{x=o}^{a} \int_{y=o}^{b} [f_{vi} f_{vm} \frac{\partial g_{vj}}{\partial y} \frac{\partial g_{vn}}{\partial y} + \frac{(1-\nu)}{2} \frac{\partial f_{vi}}{\partial x} \frac{\partial f_m}{\partial x} g_{vj} g_{vn}] dx\, dy \quad (3.2.18a)$$

$$S2_{i,j,p,q,r,s} = \int_{x=o}^{a} \int_{y=o}^{b} [(\frac{\alpha_q \beta_s}{b^2}) \sin(\frac{\alpha_p x}{a}) \sin(\frac{\beta_r x}{a}) \cos(\frac{\alpha_q y}{b}) \times \cos(\frac{\beta_s y}{b}) + \nu(\frac{\alpha_p \beta_r}{a^2}) \cos(\frac{\alpha_p x}{a}) \cos(\frac{\beta_r x}{a}) \sin(\frac{\alpha_q y}{b}) \times \sin(\frac{\beta_s y}{b})] f_{vi} \frac{\partial g_{vj}}{\partial y} dx\, dy$$
$$+ \int_{x=o}^{a} \int_{y=o}^{b} (\frac{1-\nu}{2}) \cdot \frac{\partial f_{vi}}{\partial x} g_{vj} [(\frac{\alpha_p \beta_s}{ab}) \cos(\frac{\alpha_p x}{a}) \sin(\frac{\beta_r x}{a}) \times \sin(\frac{\alpha_q y}{b}) \cos(\frac{\beta_s y}{b}) + (\frac{\alpha_q \beta_r}{ab}) \sin(\frac{\alpha_p x}{a}) \cos(\frac{\beta_r x}{a}) \cos(\frac{\alpha_q y}{b}) \cos(\frac{\beta_s y}{b})] dx\, dy. \quad (3.2.18b)$$

Equations (3.2.16) and (3.2.17) can be used to calculate the relationship between the in-plane and out-of-plane displacement coefficients. Since these equations are linear in $A_{k,\ell}$ and $B_{m,n}$ the solution can be obtained as follows:

Let $A'_{k,\ell}$ and $B'_{k,\ell}$ be the solutions of,

$$\{\sum_k \sum_\ell A'_{k,\ell}(R1_{i,j,k,\ell} + R4_{i,j,k,\ell}) + \sum_m \sum_n B'_{m,n}(R5_{i,j,m,n})\} = -\{R3_{i,j}\} \quad (3.2.19a)$$

and $$\{\sum_k \sum_\ell A'_{k,\ell}(R4_{i,j,k,\ell}) + \sum_m \sum_n B'_{m,n}(S1_{i,j,m,n})\} = \{o\}. \quad (3.2.19b)$$

Also, let $A''_{k,\ell,p,q,r,s}$ and $B''_{m,n,p,q,r,s}$ be the solutions of,

$$\{\sum_k \sum_\ell A''_{i,j,p,q,r,s}(R1_{i,j,k,\ell} + R4_{i,j,k,\ell}) + \sum_m \sum_n B''_{m,n,p,q,r,s}(R5_{i,j,m,n})\} = -\{R3_{i,j,p,q,r,s}\} \quad (3.2.19c)$$

and $$\{\sum_k \sum_\ell A''_{i,j,p,q,r,s}(R4_{i,j,k,\ell}) + \sum_m \sum_n B''_{m,n,p,q,r,s}(S1_{i,j,m,n})\} = -\{S2_{i,j,p,q,r,s}\}. \quad (3.2.19d)$$

Then from linear algebra,

$$\{A_{i,j}\} = \{P_x A'_{i,j}\} + \{\sum_p \sum_q \sum_r \sum_s (Z_{p,q} Z_{r,s} - Zo_{p,q} Zo_{r,s}) A''_{i,j,p,q,r,s}\} \quad (3.2.20a)$$

and $$\{B_{i,j}\} = \{P_x B'_{i,j}\} + \{\sum_p \sum_q \sum_r \sum_s (Z_{p,q} Z_{r,s} - Zo_{p,q} Zo_{r,s}) B''_{i,j,p,q,r,s}\}. \quad (3.2.20b)$$

Equations (3.2.19a) → (3.2.19d) can be solved using Gaussian elimination. The resulting values of $A''_{i,j,p,q,r,s}$ and

$B''_{i,j,p,q,r,s}$ are the connection coefficients which relate the in-plane displacement coefficients to the various products of out-of-plane displacement coefficients. $A'_{i,j}$ and $B'_{i,j}$ give the in-plane displacement coefficients due to the displacement of the applied in-plane load and can be considered as a special set of connection coefficients resulting from the change in the position of the applied load.

At this stage it becomes necessary to introduce the following definitions and matrix notations.

Definitions:

N_{ux} : The maximum number of shape functions for f_u

N_{uy} : The maximum number of shape functions for g_u

N_{vx} : The maximum number of shape functions for f_v

N_{vy} : The maximum number of shape function for g_v

p_m : The maximum number of out-of-plane displacement shapes in x direction

q_m : The maximum number of out-of-plane displacement shapes in y direction

I_p : A position indicator for $Z_{p,q}$ defined by $I_p = q + (p-1)q_m$

I_r : A position indicator for $Z_{r,s}$ defined by $I_r = s + (r-1)q_m$

I_{pq} : The total number of shapes in the out-of-plane displacement series given by $I_{pq} = p_m \times q_m$

L : A position indicator for the connection coefficients defined as $L = 1 + I_r + (I_p - 1) I_{pq} - I_p (I_p - 1)/2$

$\hat{L}$: Maximum value of L; $\hat{L} = 1 + I_{pq}^2 - I_{pq}(I_{pq} - 1)/2$

(The use of L and $\hat{L}$ will be explained later)

N_u : Total number of shapes in the series for u_s and is given by $N_u = N_{ux} \times N_{uy}$

N_v : Total number of shapes in the series for v_s and is given by $N_v = N_{vx} \times N_{vy}$

N_n : Total number of in-plane displacement coefficients and is given by $N_n = N_u + N_v$

The left hand side of the set of equations (3.2.16) and (3.2.17) can be written in matrix form.

i.e. L.H.S. of equations (3.2.16) and (3.2.17) = [SZ]{C}

(3.2.21)

where $C(I) = A_{i,j}$ for $I \leq N_u$,

in which $I = j + (i-1) N_{uy}$, (3.2.21a)

$C(I) = B_{i,j}$ for $I > N_u$

in which, $I = N_u + j + (i-1) N_{vy}$, (3.2.21b)

$SZ(I,J) = (R1_{i,j,k,\ell} + R4_{i,j,k,\ell})$ for $I \leq N_u$ and $J \leq N_u$

in which, $I = j + (i-1) N_{uy}$

and $J = \ell + (k-1) N_{uy}$, (3.2.21c)

$$SZ(I,J) = R2_{i,j,m,n} \quad \text{for } I \le N_u \text{ and } J > N_u ,$$

$$\text{in which } I = j + (i-1)N_{uy}$$

$$\text{and } J = N_u + n + (m-1)N_{vy} , \qquad (3.2.21d)$$

$$SZ(I,J) = R2_{i,j,k,\ell} \quad \text{for } I > N_u \text{ and } J \le N_u ,$$

$$\text{in which } J = \ell + (k-1)N_{uy}$$

$$\text{and } I = N_u + j + (i-1)N_{vy} , \qquad (3.2.21e)$$

and

$$SZ(I,J) = S1_{i,j,m,n} \quad \text{for } I > N_u \text{ and } J > N_u ,$$

$$\text{in which } J = N_u + n + (m-1)N_{vy}$$

$$\text{and } I = N_u + j + (i-1)N_{vy} . \qquad (3.2.21f)$$

Equations (3.2.16) and (3.2.17) cannot be solved at this stage since the out-of-plane displacement coefficients are yet to be determined. However, equations (3.2.19a) to (3.2.19d) can be solved as follows:

Let the connection coefficient matrix be [H], such that H(I,L) gives the displacement coefficient C(I) for a unit value of either the load P_x (if L = 1) or for a product of two out-of-plane displacement coefficients of unit magnitude, the identities of which are indicated by a connection index L as explained below.

$$L = 1 + I_r + (I_p - 1) I_{pq} - I_p (I_p - 1)/2 .$$

L = 1 corresponds to the contribution from displacement of the load.

i.e. $H(I,1) = A'_{i,j}$ for $I \leq N_u$,

where $I = j + (i-1)N_{uy}$, (3.2.22a)

$H(I,1) = B'_{i,j}$ for $I > N_u$

where $I = N_u + j + (i-1)N_{vy}$. (3.2.22b)

If L > 1, L indicates the out-of-plane displacement coefficients that are considered. This can be explained through an example as follows:

Example:

Consider two shape functions in each direction (x,y) for z. The displacement coefficients involved are,

$$z_{1,1},\ z_{1,2},\ z_{2,1},\ z_{2,2}\ .$$

$$p_m = q_m = 2\ ,$$

$$I_{pq} = 4.$$

Using the definition of position indictors, the displacement coefficients can be written as

$$z_{1,1} = Z(1),\quad z_{1,2} = Z(2),\quad z_{2,1} = Z(3),\quad z_{2,2} = Z(4)\ .$$

The following ten combinations of products are then possible.

Z(1) Z(1)	Z(1) Z(2)	Z(1) Z(3)	Z(1) Z(4)
	Z(2) Z(2)	Z(2) Z(3)	Z(2) Z(4)
		Z(3) Z(3)	Z(3) Z(4)
			Z(4) Z(4)

It can be checked by substitution that the positions of these products are given by the connection index L as follows:

2	3	4	5
	6	7	8
		9	10
			11

For example, consider the position of Z(2) Z(4)

$$I_p = 2, \quad I_r = 4 \quad \text{gives, } L = 1 + 4 + (2-1)4 - 2(2-1)/2$$
$$= 8.$$

Therefore, the in-plane displacement coefficients due to the change in the product of two out-of-plane displacement coefficients (having unit value) is given by the matrix [H] where for L > 1,

$$H(I,L) = A''_{i,j,p,q,r,s} \quad \text{for } I \leq N_u,$$

$$\text{in which } I = j + (i-1)N_{uy}, \tag{3.2.22c}$$

$$H(I,L) = B''_{i,j,p,q,r,s}, \quad \text{for } I > N_u,$$

$$\text{in which } I = N_u + j + (i-1)N_{uy}. \tag{3.2.22d}$$

From equations (3.2.20a), (3.2.20b), (3.2.21a) and (3.2.21b) it follows that,

$$C(I) = H(I,1)\,P_x + \sum_{L=2}^{\hat{L}} H(I,L) \times (Z_{p,q}\, Z_{r,s} - Zo_{p,q}\, Zo_{r,s}). \tag{3.2.23}$$

Furthermore, the R.H.S. of equations (3.2.19a) to (3.2.19d) can be written as

R.H.S. of equations (3.2.19a) to (3.2.19d) = [ZB],

(3.2.24a)

where

$$\left.\begin{array}{l} ZB(I,1) = -R5_{i,j} \text{ for } I \leq N_u, \text{ in which } I = j+(i-1)N_{uy} \\ ZB(I,1) = 0.0 \quad \text{ for } I > N_u, \text{ in which } I = N_u+j+(i-1)N_{uy} \end{array}\right\}$$

(3.2.24b)

and

$$\left.\begin{array}{l} ZB(I,L) = -R3_{i,j,p,q,r,s} \\ \text{for } I \leq N_u, \text{ in which } I = j+(i-1)N_{uy} \\ ZB(I,L) = -S3_{i,j,p,q,r,s} \\ \text{for } I > N_u, \text{ in which } I = N_u + j + (i-1)N_{uy} \end{array}\right\} \quad (3.2.24c)$$

Hence,

$$[SZ][H] = [ZB] . \quad (3.2.25)$$

The unknowns in [H] can be found by Gaussian elimination for each value of L.

i.e. [SZ]{H(L1)} = {ZB(L1)} (for L = L1) can be solved for any value of L1. The reduction of [SZ] to a triangular matrix needs to be done only once. A special Gaussian elimination procedure was written for this purpose.

The in-plane displacement coefficients {C} can be found after calculating the out-of-plane displacement coefficients as described below.

Calculation of Out-of-plane Displacement Coefficients

The solution of equation (3.2.9) is obtained using a modified version of Newton-Raphson's method [34] as described below. The idea is demonstrated through a simple example in Appendix E.

$\{\frac{\partial \overline{V}_T}{\partial Z_{i,j}}\} = \{o\}$ is found when

$$[\frac{d}{dZ_{r,s}}(\frac{\partial \overline{V}_T}{\partial Z_{i,j}})]\{\Delta Z_{r,s}\} = -\{\frac{\partial \overline{V}_T}{\partial Z_{i,j}}\}, \qquad (3.2.26)$$

as $\{\Delta Z_{r,s}\} \to \{o\}$ is satisfied.

After calculating $\{(\frac{\partial \overline{V}_T}{\partial Z_{i,j}})\}$ in terms of $A_{i,j}$, $B_{i,j}$ and $Z_{i,j}$, the relationship between the in-plane and out-of-plane displacement coefficients can be substituted in equation (3.2.26). However, at this stage, the in-plane displacement coefficients should be treated as dependent variables, since the relationship between these and the out-of-plane coefficients is used. The following distinctions must be clearly made.

All displacement coefficients are treated as independent variables when applying the Rayleigh-Ritz method to <u>form</u> equations (3.2.7), (3.2.8) and (3.2.9). When <u>solving</u> equations (3.2.9), the relationship between the in-plane and out-of-plane displacement coefficients is used and therefore the in-plane displacement coefficients are treated as dependent variables, giving

$$\frac{d}{dZ_{r,s}}\left\{\frac{\partial \overline{V}_T}{\partial Z_{i,j}}\right\} = \left\{\frac{\partial^2 \overline{V}_T}{\partial Z_{r,s}\partial Z_{i,j}}\right\} + \sum_k \sum_\ell \left\{\frac{\partial^2 \overline{V}_T}{\partial A_{k,\ell}\partial Z_{i,j}} \cdot \frac{d\,A_{k,\ell}}{d\,Z_{r,s}}\right\}$$

$$+ \sum_m \sum_n \left\{\frac{\partial^2 \overline{V}_T}{\partial B_{m,n}\partial Z_{i,j}} \frac{d\,B_{m,n}}{d\,Z_{r,s}}\right\} . \qquad (3.2.27)$$

Hence the required equation

$$\left[\frac{\partial^2 \overline{V}_T}{\partial Z_{r,s}\partial Z_{i,j}} + \left\{\frac{\partial^2 \overline{V}_T}{\partial A_{k,\ell}\partial Z_{i,j}}\right\}^T \left\{\frac{d\,A_{k,\ell}}{d\,Z_{r,s}}\right\}\right.$$

$$\left. + \left\{\frac{\partial^2 \overline{V}_T}{\partial B_{m,n}\partial Z_{i,j}}\right\}^T \left\{\frac{d\,B_{m,n}}{d\,Z_{r,s}}\right\}\right] \{\Delta Z_{r,s}\} = - \left\{\frac{\partial \overline{V}_T}{\partial Z_{i,j}}\right\} . \qquad (3.2.28)$$

Using equations (2.2.21a) and (2.2.21b) this can be written as

$$\left[\frac{\partial^2 \overline{V}_T}{\partial Z_{r,s}\partial Z_{i,j}} + \left\{\frac{\partial^2 \overline{V}_T}{\partial C(I)\partial Z_{i,j}}\right\}^T \left\{\frac{d\,C(I)}{d\,Z_{r,s}}\right\}\right] \{\Delta Z_{r,s}\}$$

$$= - \left\{\frac{\partial \overline{V}_T}{\partial Z_{i,j}}\right\} \qquad (3.2.28a)$$

This is the matrix iteration equation.

Terms in the derivatives of $\overline{V}_T$ can be evaluated successively until all values of $\Delta Z_{r,s}$ become very small. After each iteration, the values of $Z_{i,j}$ are corrected by adding $\Delta Z_{r,s}$ calculated by solving equation (3.2.28a) using Gaussian elimination.

Using equation (3.2.6) and noting that $\bar{V}_{LOAD}$ and $\bar{U}_{beam}$ do not depend on $Z_{i,j}$, the following equation is obtained

$$\frac{\partial \bar{V}_T}{\partial Z_{i,j}} = \frac{\partial \bar{U}_{be}}{\partial Z_{i,j}} + \frac{\partial \bar{U}_{str}}{\partial Z_{i,j}} . \qquad (3.2.29)$$

The term $\frac{\partial \bar{U}_{be}}{\partial Z_{i,j}} = \frac{Eh^3}{24(1-\nu^2)}[(\frac{\alpha_i}{a})^2 + (\frac{\alpha_j}{b})^2]^2 \frac{ab}{4}(Z_{i,j} - Z_{oi,j}) \times 2$

$$= \frac{Eh^3}{24(1-\nu^2)} G_1 , \qquad (3.2.30)$$

where

$$G_1 = \frac{ab}{2}(Z_{i,j} - Z_{o\, i,j}).[(\frac{\alpha_i}{a})^2 + (\frac{\alpha_j}{b})^2]^2 , \qquad (3.2.30a)$$

in which
$$\left.\begin{aligned} \alpha_i &= (2i-1)\pi \\ \alpha_j &= (2j-1)\pi \end{aligned}\right\} \qquad (3.2.30b)$$

It can be shown that,

$$\frac{\partial \bar{U}_{str}}{\partial Z_{i,j}} = \frac{Eh}{(1-\nu^2)} \sum_{m=2}^{10} G_m \qquad (3.2.31)$$

G_2 to G_{10} can be obtained as follows:

$$G_2 = \frac{\partial}{\partial Z_{i,j}} \frac{1}{8} \int_{x=o}^{a} \int_{y=o}^{b} [(\frac{\partial z}{\partial x})^4 + (\frac{\partial z}{\partial y})^4] \, dx \, dy$$

$$= \frac{1}{8} \int_{x=o}^{a} \int_{y=o}^{b} [4(\frac{\partial z}{\partial x})^3 \frac{\partial}{\partial Z_{i,j}}(\frac{\partial z}{\partial x}) + 4(\frac{\partial z}{\partial y})^3 \frac{\partial}{\partial Z_{i,j}}(\frac{\partial z}{\partial y})] dx \, dy$$

$$= \frac{1}{2} \sum_r \sum_s \sum_p \sum_q \sum_k \sum_\ell (Z_{p,q} Z_{r,s} Z_{k,\ell}) \Omega_2 , \qquad (3.2.32)$$

where

$$Q_2 = \left(\frac{\alpha_i \beta_r \gamma_p \phi_k}{a^4}\right) \int_{x=o}^{a} \cos\left(\frac{\alpha_i x}{a}\right) \cos\left(\frac{\beta_r x}{a}\right) \cos\left(\frac{\gamma_p x}{a}\right) \cos\left(\frac{\phi_k x}{a}\right) dx \times$$

$$\int_{y=o}^{b} \sin\left(\frac{\alpha_j y}{b}\right) \sin\left(\frac{\beta_s y}{b}\right) \sin\left(\frac{\gamma_q y}{b}\right) \sin\left(\frac{\phi_\ell y}{b}\right) dy \; +$$

$$\left(\alpha_j \frac{\beta_s \gamma_q}{b^4} \phi_\ell\right) \int_{x=o}^{a} \sin\left(\frac{\alpha_i x}{a}\right) \sin\left(\frac{\beta_r x}{a}\right) \sin\left(\frac{\gamma_p x}{a}\right) \sin\left(\frac{\phi_k x}{a}\right) dx \times$$

$$\int_{y=o}^{b} \cos\left(\frac{\alpha_j y}{b}\right) \cos\left(\frac{\beta_s y}{b}\right) \cos\left(\frac{\gamma_q y}{b}\right) \cos\left(\frac{\phi_\ell y}{b}\right) dy \qquad (3.2.32a)$$

in which

$$\left.\begin{array}{ll} \alpha_i = (2i-1)\pi, & \alpha_j = (2j-1)\pi, \\ \beta_r = (2r-1)\pi, & \beta_s = (2s-1)\pi \\ \gamma_p = (2p-1)\pi, & \gamma_q = (2q-1)\pi \\ \phi_k = (2k-1)\pi, & \phi_\ell = (2\ell-1)\pi. \end{array}\right\} \qquad (3.2.32b)$$

(The definition of these angles α_i to ϕ_ℓ applies to all the following equations in section 3.2.)

$$G_3 = \frac{\partial}{\partial Z_{i,j}} \frac{1}{4} \int_{x=o}^{a} \int_{y=o}^{b} \left(\frac{\partial z}{\partial x}\right)^2 \left(\frac{\partial z}{\partial y}\right)^2 dx\, dy$$

$$= \frac{1}{2} \int_{x=o}^{a} \int_{y=o}^{b} \left(\frac{\partial z}{\partial x}\right) \left(\frac{\partial z}{\partial y}\right)^2 \frac{\partial}{\partial Z_{i,j}} \left(\frac{\partial z}{\partial x}\right) dx\, dy$$

$$+ \frac{1}{2} \int_{x=o}^{a} \int_{y=o}^{b} \left(\frac{\partial z}{\partial y}\right) \left(\frac{\partial z}{\partial x}\right)^2 \frac{\partial}{\partial Z_{i,j}} \left(\frac{\partial z}{\partial y}\right) dx\, dy$$

$$= \frac{1}{2} \sum_r \sum_s \sum_p \sum_q \sum_k \sum_\ell (Z_{p,q} Z_{r,s} Z_{k,\ell}) \times Q_3 \qquad (3.2.33)$$

where

$$Q_3 = (\alpha_i \frac{\beta_r \gamma_q}{a^2 b^2} \phi_\ell) \int_{x=o}^{a} \cos(\frac{\alpha_i x}{a}) \cos(\frac{\beta_r x}{a}) \sin(\frac{\gamma_p x}{a}) \sin(\frac{\phi_k x}{a}) dx$$

$$\int_{y=o}^{b} \sin(\frac{\alpha_j y}{b}) \sin(\frac{\beta_s y}{b}) \cos(\frac{\gamma_q y}{b}) \cos(\frac{\phi_\ell y}{b}) dy +$$

$$(\alpha_j \frac{\beta_s \gamma_p}{a^2 b^2} \phi_k) \int_{x=o}^{a} \sin(\frac{\alpha_i x}{a}) \sin(\frac{\beta_r x}{a}) \cos(\frac{\gamma_p x}{a}) \cos(\frac{\phi_k x}{a}) dx$$

$$\int_{y=o}^{b} \cos(\frac{\alpha_j y}{b}) \cos(\frac{\beta_s y}{b}) \sin(\frac{\gamma_q y}{b}) \sin(\frac{\phi_\ell y}{b}) dy . \qquad (3.2.33a)$$

$$G_4 = \frac{\partial}{\partial Z_{i,j}} (-\frac{1}{4}) \int_{x=o}^{a} \int_{y=o}^{b} [(\frac{\partial z}{\partial x})^2 (\frac{\partial z_o}{\partial x})^2 + (\frac{\partial z}{\partial y})^2 (\frac{\partial z_o}{\partial y})^2] dx\ dy$$

$$= -\frac{1}{4} \int_{x=o}^{a} \int_{y=o}^{b} [2 (\frac{\partial z}{\partial x}) (\frac{\partial z_o}{\partial x}) \frac{\partial}{\partial Z_{i,j}} (\frac{\partial z}{\partial x}) + 2 (\frac{\partial z}{\partial y}) (\frac{\partial z_o}{\partial y})^2$$

$$\frac{\partial}{\partial Z_{i,j}} (\frac{\partial z}{\partial y})] dx\ dy = -\frac{1}{2} \sum_r \sum_s \sum_p \sum_q \sum_k \sum_\ell (Z_{r,s}\ Z_{o_{p,q}}\ Z_{o_{k,\ell}}) \cdot Q_2 .$$

(3.2.34)

$$G_5 = \frac{\partial}{\partial Z_{i,j}} (\frac{-\nu}{4}) \int_{x=o}^{a} \int_{y=o}^{b} [(\frac{\partial z}{\partial x})^2 (\frac{\partial z_o}{\partial y})^2 + (\frac{\partial z}{\partial y})^2 (\frac{\partial z_o}{\partial x})^2] dx\ dy$$

$$= \frac{-\nu}{4} \int_{x=o}^{a} \int_{y=o}^{b} [2 (\frac{\partial z}{\partial x}) (\frac{\partial z_o}{\partial y})^2 \frac{\partial}{\partial Z_{i,j}} (\frac{\partial z}{\partial x}) + 2 (\frac{\partial z}{\partial y}) (\frac{\partial z_o}{\partial y})^2$$

$$\frac{\partial}{\partial Z_{i,j}} (\frac{\partial z}{\partial y})] dx\ dy = -\frac{\nu}{2} \sum_r \sum_s \sum_p \sum_q \sum_k \sum_\ell (Z_{r,s}\ Z_{o_{p,q}}\ Z_{o_{k,\ell}}) \times Q_3 .$$

(3.2.35)

$$G_6 = -\frac{(1-\nu)}{2} \frac{\partial}{\partial Z_{i,j}} \int_{x=o}^{a} \int_{y=o}^{b} \frac{\partial z}{\partial x} \frac{\partial z}{\partial y} \frac{\partial z_o}{\partial x} \frac{\partial z_o}{\partial y} dx\, dy$$

$$= -\frac{(1-\nu)}{2} \int_{x=o}^{a} \int_{y=o}^{b} [(\frac{\partial}{\partial Z_{i,j}}(\frac{\partial z}{\partial x}))\frac{\partial z}{\partial y} \frac{\partial z_o}{\partial x} \frac{\partial z_o}{\partial y}$$

$$+ (\frac{\partial}{\partial Z_{i,j}}(\frac{\partial z}{\partial y})) \frac{\partial z}{\partial x} \frac{\partial z_o}{\partial x} \frac{\partial z_o}{\partial y}] dx\, dy$$

$$= -\frac{(1-\nu)}{2} \sum_r \sum_s \sum_p \sum_q \sum_k \sum_\ell (Z_{r,s}\ Z_{op,q}\ Z_{k,\ell}) \times Q_4, \tag{3.2.36}$$

where

$$Q_4 = (\alpha_i \frac{\beta_s \gamma_p}{a^2 b^2} \phi_\ell) \int_{x=o}^{a} \cos(\frac{\alpha_i x}{a}) \sin(\frac{\beta_r x}{a}) \cos(\frac{\gamma_p x}{a}) \sin(\frac{\phi_k x}{a}) dx$$

$$\int_{y=o}^{b} \sin(\frac{\alpha_j y}{b}) \cos(\frac{\beta_s y}{b}) \sin(\frac{\gamma_q y}{b}) \cos(\frac{\phi_\ell y}{b}) dy$$

$$+ (\alpha_i \frac{\beta_r \gamma_q}{a^2 b^2} \phi_k) \int_{x=o}^{a} \sin(\frac{\alpha_i x}{a}) \cos(\frac{\beta_r x}{a}) \sin(\frac{\gamma_p x}{a}) \cos(\frac{\phi_k x}{a}) dx$$

$$\int_{y=o}^{b} \cos(\frac{\alpha_j y}{b}) \cos(\frac{\gamma_q y}{b}) \sin(\frac{\beta_s y}{b}) \sin(\frac{\phi_\ell y}{b}) dy \;. \tag{3.2.36a}$$

$$G_7 = \frac{1}{2} \frac{\partial}{\partial Z_{i,j}} \int_{x=o}^{a} \int_{y=o}^{b} \frac{\partial u_s}{\partial x} [(\frac{\partial z}{\partial x})^2 + \nu(\frac{\partial z}{\partial y})^2] dx\, dy$$

$$= \int_{x=o}^{a} \int_{y=o}^{b} [\frac{\partial u_s}{\partial x} \frac{\partial z}{\partial x} \frac{\partial}{\partial Z_{i,j}} (\frac{\partial z}{\partial x})$$

$$+ \nu \frac{\partial u_s}{\partial x} \frac{\partial z}{\partial y} \frac{\partial}{\partial Z_{i,j}} (\frac{\partial z}{\partial y})] dx\, dy$$

$$= \sum_r \sum_s Z_{r,s} [\int_{x=o}^{a} \int_{y=o}^{b} \frac{\partial u_s}{\partial x} (\frac{\alpha_i \beta_r}{a^2}) \cos(\frac{\alpha_i x}{a}) \cos(\frac{\beta_r x}{a})$$

$$\sin(\frac{\alpha_j y}{b}) \sin(\frac{\beta_s y}{b}) dx\, dy + \nu \int_{x=o}^{a} \int_{y=o}^{b} (\frac{\alpha_j \beta_s}{b^2}) \sin(\frac{\alpha_i x}{a}) \sin(\frac{\beta_r x}{a})$$

$$\cos(\frac{\alpha_j y}{b}) \cos(\frac{\beta_s y}{b}) dx\ dy],$$

but, $\frac{\partial u_s}{\partial x} = \sum_{I=1}^{N_u} C(I) \frac{\partial f_{uk}}{\partial x} g_{u\ell}$,

where $I = \ell + (k-1)\ N_{uy}$,

therefore $G_7 = \sum_r \sum_s \sum_{I=1}^{N_u} Z_{r,s} \times C(I) \times Q_5$, (3.2.37)

where $$Q_5 = (\frac{\alpha_i \beta_r}{a^2}) \int_{x=o}^{a} \frac{\partial f_{uk}}{\partial x} \cos(\frac{\alpha_i x}{a}) \cos(\frac{\beta_r x}{a}) dx \int_{y=o}^{b} g_{u\ell} \sin(\frac{\alpha_j y}{b}) \times$$

$$\sin(\frac{\beta_s y}{b}) dy + \nu (\frac{\alpha_j \beta_s}{b^2}) \int_{x=o}^{a} \frac{\partial f_{uk}}{\partial x} \sin(\frac{\alpha_i x}{a}) \sin(\frac{\beta_r x}{a}) dx \times$$

$$\int_{y=o}^{b} g_{u\ell} \cos(\frac{\alpha_j y}{b}) \cos(\frac{\beta_s y}{b}) dy \ . \qquad (3.2.37a)$$

$$G_8 = (\frac{1-\nu}{2}) \frac{\partial}{\partial Z_{i,j}} \int_{x=o}^{a} \int_{y=o}^{b} \frac{\partial u_s}{\partial y} \frac{\partial z}{\partial x} \frac{\partial z}{\partial y} dx\ dy$$

$$= (\frac{1-\nu}{2}) \int_{x=o}^{a} \int_{y=o}^{b} [\frac{\partial u_s}{\partial y} \frac{\partial z}{\partial y} \frac{\partial}{\partial Z_{i,j}} (\frac{\partial z}{\partial x}) + \frac{\partial u_s}{\partial y} \frac{\partial z}{\partial x} \frac{\partial}{\partial Z_{i,j}} (\frac{\partial z}{\partial y})] \times$$

$$dx\ dy,$$

but, $\frac{\partial u_s}{\partial y} = \sum_{I=1}^{N_u} C(I)\ f_{uk} \frac{\partial g_{u\ell}}{\partial y}$, where $I = \ell + (k-1)\, N_{uy}$

therefore, $G_8 = (\frac{1-\nu}{2}) \sum_r \sum_s \sum_{I=1}^{N_u} Z_{r,s} \times C(I) \times Q_6$, (3.2.38)

where

$$Q_6 = \frac{\alpha_i \beta_s}{ab} \int_{x=o}^{a} f_{uk} \cos(\frac{\alpha_i x}{a}) \sin(\frac{\beta_r x}{a}) dx \int_{y=o}^{b} \frac{\partial g_{u\ell}}{\partial y} \sin(\frac{\alpha_j y}{b}) \times$$

$$\cos(\frac{\beta_s y}{b}) dy + \frac{\alpha_j \beta_r}{ab} \int_{x=o}^{a} f_{uk} \sin(\frac{\alpha_i x}{a}) \cos(\frac{\beta_r x}{a}) dx$$

$$\int_{y=o}^{b} \frac{\partial g_{u\ell}}{\partial y} \cos(\frac{\alpha_j y}{b}) \sin(\frac{\beta_s y}{b}) dy \ . \qquad (3.2.38a)$$

$$G_9 = \frac{1}{2} \frac{\partial}{\partial Z_{i,j}} \int_{x=o}^{a} \int_{y=o}^{b} \frac{\partial v_s}{\partial y} [(\frac{\partial z}{\partial y})^2 + \nu (\frac{\partial z}{\partial x})^2] dx\, dy \ .$$

By analogy with G_7 it can be shown that,

$$G_9 = \sum_r \sum_s \sum_{I=N_u+1}^{N_n} Z_{r,s} \times C(I) \times Q_7 , \qquad (3.2.39)$$

where $Q_7 = \frac{\alpha_j \beta_s}{b^2} \int_{x=o}^{a} f_{vm} \sin(\frac{\alpha_i x}{a}) \sin(\frac{\beta_r x}{a}) dx \times$

$$\int_{y=o}^{b} \frac{\partial g_{vn}}{\partial y} \cos(\frac{\alpha_j y}{b}) \cos(\frac{\beta_s y}{b}) dy$$

$$+ \nu \frac{\alpha_i \beta_r}{a^2} \int_{x=o}^{a} f_{vm} \cos(\frac{\alpha_i x}{a}) \cos(\frac{\beta_r x}{a}) dx \times$$

$$\int_{y=o}^{b} \frac{\partial g_{vn}}{\partial b} \sin(\frac{\alpha_j y}{b}) \sin(\frac{\beta_s y}{b}) dy, \qquad (3.2.39a)$$

in which $I = N_u = n + (m-1)\, N_{vy}$. (3.2.39b)

$$G_{10} = \left(\frac{1-\nu}{2}\right)\frac{\partial}{\partial Z_{i,j}}\int_{x=o}^{a}\int_{y=o}^{b}\frac{\partial v_s}{\partial x}\frac{\partial z}{\partial x}\frac{\partial z}{\partial y}\,dx\,dy\ .$$

By analogy with G_8 it can be shown that

$$G_{10} = \left(\frac{1-\nu}{2}\right)\sum_r \sum_s \sum_{I=N_u+1}^{N_n} Z_{r,s} \times C(I) \times Q_8, \qquad (3.2.40)$$

where

$$Q_8 = \frac{\alpha_i \beta_s}{ab}\int_{x=o}^{a}\frac{\partial f_{vm}}{\partial x}\cos\left(\frac{\alpha_i x}{a}\right)\sin\left(\frac{\beta_r x}{a}\right)dx \times$$

$$\int_{y=o}^{b} g_{vn}\ \sin\left(\frac{\alpha_j y}{b}\right)\cos\left(\frac{\beta_s y}{b}\right)dy$$

$$+ \frac{\alpha_j \beta_r}{ab}\int_{x=o}^{a}\frac{\partial f_{vm}}{\partial x}\sin\left(\frac{\alpha_i x}{a}\right)\cos\left(\frac{\beta_r x}{a}\right)dx \times$$

$$\int_{y=o}^{b} g_{vn}\ \cos\left(\frac{\alpha_j y}{b}\right)\sin\left(\frac{\beta_s y}{b}\right)dy\ . \qquad (3.2.40a)$$

From equations (3.2.29), (3.2.30) and (3.2.31),

$$\frac{\partial \bar{V}_T}{\partial Z_{i,j}} = \frac{Eh^3}{24(1-\nu^2)} G_1 + \frac{Eh}{(1-\nu^2)}\sum_{m=2}^{10} G_m\ . \qquad (3.2.41)$$

For each value of i,j, this gives a value for $\frac{\partial \bar{V}_T}{\partial Z_{i,j}}$. This can be expressed in matrix form as

$$\{R\}\ ,\ \text{where}\quad R(J) = \frac{\partial \bar{V}_T}{\partial Z_{i,j}}\ ,$$

in which $\quad J = j + (i-1)q_m\ .$

- {R} is the R.H.S. of equation (3.2.28a)

The terms in the L.H.S. of equation (3.2.28a) can be calculated as follows:

$$T_1 = \frac{\partial^2 \bar{V}_T}{\partial Z_{r,s} \partial Z_{i,j}} = \frac{Eh^3}{24(1-\nu^2)} \frac{\partial}{\partial Z_{r,s}} G_1 + \frac{Eh}{(1-\nu^2)} \sum_{m=2}^{10} \frac{\partial G_m}{\partial Z_{r,s}} . \tag{3.2.42}$$

The terms $\partial G_m / \partial Z_{r,s}$ are given as follows.

$$\left.\begin{aligned} \frac{\partial G_1}{\partial Z_{r,s}} &= [(\frac{\alpha_i}{a})^2 + (\frac{\alpha_j}{b})^2]^2 \frac{ab}{4} \text{ if } i=r \text{ and } j=s \\ &= 0 \text{ if } i \neq r \text{ or } j \neq s . \end{aligned}\right\} \tag{3.2.42a}$$

$$\frac{\partial G_2}{\partial Z_{r,s}} = \frac{1}{8} \int_{x=o}^{a} \int_{y=o}^{b} [12(\frac{\partial z}{\partial x})^2 \frac{\partial}{\partial Z_{r,s}}(\frac{\partial z}{\partial x}) \frac{\partial}{\partial Z_{i,j}}(\frac{\partial x}{\partial x})$$

$$+ 12(\frac{\partial z}{\partial y}) \frac{\partial}{\partial Z_{r,s}}(\frac{\partial z}{\partial y}) \frac{\partial}{\partial Z_{i,j}}(\frac{\partial z}{\partial y})] dx\, dy$$

$$= \frac{3}{2} \sum_p \sum_q \sum_k \sum_\ell (Z_{p,q} \; Z_{k,\ell}) \times Q_2 . \tag{3.2.42b}$$

$$\frac{\partial G_3}{\partial Z_{r,s}} = \frac{1}{2} \{ \int_{x=o}^{a} \int_{y=o}^{b} (\frac{\partial z}{\partial y})^2 \frac{\partial}{\partial Z_{r,s}}(\frac{\partial z}{\partial x}) \frac{\partial}{\partial Z_{i,j}}(\frac{\partial z}{\partial x}) dx\, dy$$

$$+ \int_{x=o}^{a} \int_{y=o}^{b} 2(\frac{\partial z}{\partial x})(\frac{\partial z}{\partial y}) \frac{\partial}{\partial Z_{r,s}}(\frac{\partial z}{\partial y}) \frac{\partial}{\partial Z_{i,j}}(\frac{\partial z}{\partial x}) dx\, dy$$

$$+ \int_{x=o}^{a} \int_{y=o}^{b} (\frac{\partial z}{\partial x})^2 \frac{\partial}{\partial Z_{r,s}}(\frac{\partial z}{\partial y}) \frac{\partial}{\partial Z_{i,j}}(\frac{\partial z}{\partial y}) dx\, dy$$

$$+ \int_{x=o}^{a} \int_{y=o}^{b} 2(\frac{\partial z}{\partial x})(\frac{\partial z}{\partial y}) \frac{\partial}{\partial Z_{r,s}}(\frac{\partial z}{\partial x}) \frac{\partial}{\partial Z_{i,j}}(\frac{\partial z}{\partial y}) dx\, dy \}$$

$$= \frac{1}{2} \sum_p \sum_q \sum_k \sum_\ell (Z_{p,q} Z_{k,\ell}) \times (Q_3 + Q_9 + Q_{10}) , \tag{3.2.42c}$$

where

$$Q_9 = 2\frac{\alpha_i \beta_s \gamma_p}{a^2 b^2} \phi_\ell \int_{x=o}^{a} \cos(\frac{\alpha_i x}{a}) \sin(\frac{\beta_r x}{a}) \cos(\frac{\gamma_p x}{a}) \sin(\frac{\phi_k x}{a}) dx$$

$$\times \int_{y=o}^{b} \sin(\frac{\alpha_j y}{b}) \cos(\frac{\beta_s y}{b}) \sin(\frac{\gamma_q y}{b}) \cos(\frac{\phi_\ell y}{b}) dy$$

and $$Q_{10} = 2\frac{\alpha_j \beta_r \gamma_q}{a^2 b^2} \phi_k \int_{x=o}^{a} \sin(\frac{\alpha_i x}{a}) \cos(\frac{\beta_r x}{a}) \sin(\frac{\gamma_p x}{a}) \cos(\frac{\phi_\ell x}{a}) dx$$

$$\times \int_{y=o}^{b} \cos(\frac{\alpha_j y}{b}) \sin(\frac{\beta_s y}{b}) \cos(\frac{\gamma_q y}{b}) \sin(\frac{\phi_\ell y}{b}) dy \; .$$

$$\frac{\partial G_4}{\partial Z_{r,s}} = -\frac{1}{2} \sum_p \sum_q \sum_k \sum_\ell (Zo_{p,q} \; Zo_{k,\ell}) \cdot Q_2 \; . \qquad (3.2.42d)$$

$$\frac{\partial G_5}{\partial Z_{r,s}} = \frac{-\nu}{2} \sum_p \sum_q \sum_k \sum_\ell (Zo_{p,q} \; Zo_{k,\ell}) \cdot Q_3 \; . \qquad (3.2.42e)$$

$$\frac{\partial G_6}{\partial Z_{r,s}} = \frac{-(1-\nu)}{2} \sum_p \sum_q \sum_k \sum_\ell (Zo_{p,q} \; Zo_{k,\ell}) \cdot Q_4 \; . \qquad (3.2.42f)$$

$$\frac{\partial G_7}{\partial Z_{r,s}} = \sum_{I=1}^{N_u} C(I) \cdot Q_5 \; . \qquad (3.2.42g)$$

$$\frac{\partial G_8}{\partial Z_{r,s}} = \sum_{I=1}^{N_u} C(I) \cdot Q_6 \cdot \frac{(1-\nu)}{2} \; . \qquad (3.2.42h)$$

$$\frac{\partial G_9}{\partial Z_{r,s}} = \sum_{I=N_u+1}^{N_n} C(I) \cdot Q_7 \; . \qquad (3.2.42i)$$

$$\frac{\partial G_{10}}{\partial Z_{r,s}} = \sum_{I=N_u+1}^{N_n} C(I) \times Q_8 \cdot \frac{(1-\nu)}{2} \qquad (3.2.42j)$$

Now the terms in the L.H.S. of equation (3.2.28a) resulting from

$$\{\frac{\partial^2 \bar{V}_T}{\partial C(I)\,\partial Z_{i,j}}\}^T \quad \{\frac{dC(I)}{dZ_{r,s}}\}$$

can be evaluated as follows:

By definition, $C(I) = H(I,1) \times P_x + \sum_L H(I,L)(Z_{p,q}\, Z_{r,s} - Z_{op,q}\, Z_{or,s})$ and

$$\frac{dC(I)}{dZ_{r,s}} = \sum_{L_1}^{L_2} H(I,L) \times Z_{p,q} \times F_2 \,, \qquad (3.2.43)$$

where $L_1 = 1 + I_r$

$L_2 = 1 = I_r + (I_{pq}-1)\,I_{pq}/2$

$F_2 = 1.0$ if $p \neq r$ or $q \neq s$ (3.2.43a)

$F_2 = 2.0$ if $p=r$ and $q=s$.

$$\frac{\partial^2 \bar{V}_T}{\partial C(I)\,\partial Z_{i,j}} = \frac{Eh}{(1-\nu^2)} \frac{\partial}{\partial C(I)} [G_7 + G_8 + G_9 + G_{10}]$$

$$= \frac{Eh}{(1-\nu^2)} \sum_r \sum_s Z_{r,s}(Q_5 + Q_6\frac{(1-\nu)}{2} + Q_7 + Q_8\,\frac{(1-\nu)}{2}) . \qquad (3.2.44)$$

From equations (3.2.43), (3.2.43a) and (3.2.44),

$$\left\{\frac{\partial^2 \overline{V}_T}{\partial C(I)\,\partial Z_{i,j}}\right\}^T \left\{\frac{dC(I)}{dZ_{r,s}}\right\} = \frac{Eh}{(1-\nu^2)}\, Z_{r,s} \times Z_{p,q} \times$$

$$. F_2 [Q_5 + Q_6 \frac{(1-\nu)}{2} + Q_7 + Q_8 \frac{(1-\nu)}{2}] \times \sum_{L_1}^{L_2} H(I,L) = T_2 \;. \quad (3.2.45)$$

Hence, the L.H.S. of equation (3.2.28a) can be written in matrix form as,

$$[S_\ell]\{\Delta Z\} = \text{L.H.S. of equation (3.2.28a)}, \quad (3.2.46)$$

where $S_\ell(I,J) = T_1 + T_2$. (3.2.46a)

From equations (3.2.28a) and (3.2.41),

$$[S_\ell]\{\Delta Z\} = -\{R\} \;. \quad (3.2.47)$$

This set of equations can be solved using Gaussian elimination until $\{\Delta Z\}$ becomes sufficiently small. Before each iteration, the coefficients of the matrix $[S_\ell]$ and the vector $\{R\}$ must be calculated using the latest value of $Z_{i,j}$.

The strains and stresses at a particular point $\overline{x}$, $\overline{y}$ are found by using the following formulae:

From equations (3.2.1), (3.2.2), (3.2.3), (3.2.4) and (3.2.5c),

$$\varepsilon_x = \sum_i \sum_j A_{i,j} \frac{\partial f_{ui}}{\partial x}(\overline{x}) g_{uj}(\overline{y}) + \frac{1}{2} \sum_p \sum_q \sum_r \sum_s (Z_{p,q} Z_{r,s} -$$

$$Z_{op,q} Z_{or,s}) \times (\frac{\alpha_p \beta_r}{a^2}) \cos(\frac{\alpha_p \overline{x}}{a}) \cos(\frac{\beta_r \overline{x}}{a}) \sin(\frac{\alpha_q \overline{y}}{b})$$

$$\sin(\frac{\beta_s \overline{y}}{b}), \quad (3.2.48)$$

$$\varepsilon_y = \sum_i \sum_j B_{i,j}\, f_{vi}(\bar{x}) \frac{\partial g_{vj}}{\partial y}(\bar{y}) + \frac{1}{2} \sum_p \sum_q \sum_r \sum_s (Z_{p,q}\, Z_{r,s}$$

$$- Z_{op,q}\, Z_{or,s}) \left(\frac{\alpha_q \beta_s}{b^2}\right) \sin\left(\frac{\alpha_p \bar{x}}{a}\right) \sin\left(\frac{\beta_r \bar{x}}{a}\right) \cos\left(\frac{\alpha_q \bar{y}}{b}\right) \cos\left(\frac{\beta_s \bar{y}}{b}\right), \qquad (3.2.49)$$

and
$$\gamma_{xy} = \sum_i \sum_j A_{i,j}\, f_{ui}(\bar{x}) \frac{\partial g_{uj}}{\partial y}(\bar{y}) + \sum_i \sum_j B_{i,j} \frac{\partial f_{vi}}{\partial x}(\bar{x})\, g_{vj}(\bar{y})$$

$$+ \sum_p \sum_q \sum_r \sum_s (Z_{p,q}\, Z_{r,s} - Z_{op,q}\, Z_{or,s}) \times$$

$$\left[\left(\frac{\alpha_p \beta_s}{ab}\right) \cos\left(\frac{\alpha_p \bar{x}}{a}\right) \sin\left(\frac{\beta_r \bar{x}}{a}\right) \sin\left(\frac{\alpha_q \bar{y}}{b}\right) \cos\left(\frac{\beta_s \bar{y}}{b}\right) + \right.$$

$$\left.\left(\frac{\alpha_q \beta_r}{ab}\right) \sin\left(\frac{\alpha_p \bar{x}}{a}\right) \cos\left(\frac{\beta_r \bar{x}}{a}\right) \cos\left(\frac{\alpha_q \bar{y}}{b}\right) \sin\left(\frac{\beta_s \bar{y}}{b}\right)\right], \qquad (3.2.50)$$

where

$$\left.\begin{aligned} \alpha_p &= (2p-1)\pi, & \beta_r &= (2r-1)\pi \\ \alpha_q &= (2q-1)\pi, & \beta_s &= (2s-1)\pi. \end{aligned}\right\} \qquad (3.2.51)$$

The in-plane stresses at point $(\bar{x}, \bar{y})$ are calculated using the following stress-strain relationships and equations (3.2.48), (3.2.49), and (3.2.50).

$$\left.\begin{aligned} \sigma_x &= \frac{E}{(1-\nu^2)} (\varepsilon_x + \nu\, \varepsilon_y), \\ \sigma_y &= \frac{E}{(1-\nu^2)} (\varepsilon_y + \nu\, \varepsilon_x), \\ \text{and } \tau_{xy} &= \frac{E}{2(1+\nu)}\, \gamma_{xy}. \end{aligned}\right\} \qquad (3.2.52)$$

3.3 APPLICATION OF THE RAYLEIGH-RITZ METHOD TO THE FREE VIBRATION ANALYSIS OF SIMPLY SUPPORTED RECTANGULAR CURVED PLATES SUBJECT TO IN-PLANE STRESSES

Consider the vibration of the rectangular plate treated in section 3.2. Figure 3.3.1 shows a section of the plate at the time of maximum positive excursion.

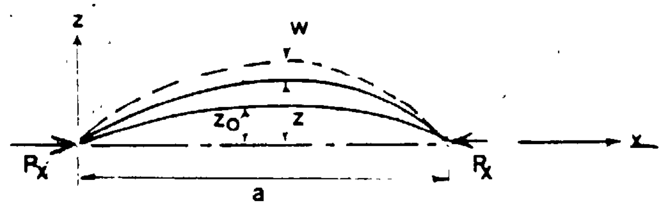

Figure 3.3.1

Assuming the motion to be simple harmonic, the dynamic displacement (w') of the plate from the equilibrium configuration (z) is given by

$$w' = \sum_i \sum_j H_{i,j} \; \text{Sin}\left(\frac{\alpha_i x}{a}\right) \text{Sin}\left(\frac{\alpha_j y}{b}\right) \text{Sin}(\omega t) \qquad (3.3.1)$$

$$i, j = 1, 2, 3 \ldots$$

where for symmetrical modes of vibration,

$$\alpha_i = (2i-1)\pi$$

At the time of maximum positive excursion,

$$w' = w = \sum_i \sum_j H_{i,j} \; \text{Sin}\left(\frac{\alpha_i x}{a}\right) \text{Sin}\left(\frac{\alpha_j y}{b}\right) . \qquad (3.3.1a)$$

$$i, j = 1, 2, 3 \ldots .$$

Let the maximum dynamic in-plane displacement in x,y directions be u_d, v_d,

where $$u_d = \sum_i \sum_j \bar{A}_{i,j}\, \bar{f}_{ui}(x)\, \bar{g}_{uj}(y), \tag{3.3.2}$$

$$v_d = \sum_i \sum_j \bar{B}_{i,j}\, \bar{f}_{vi}(x)\, \bar{g}_{vj}(y) \tag{3.3.3}$$

The total potential energy of the plate and the supporting frame consists of the following:

(a) Strain energy due to dynamic bending of the plate given by

$$\hat{U}_{be} = \frac{Eh^3}{24(1-\nu^2)} \int_{x=0}^{a} \int_{y=0}^{b} [(\frac{\partial^2 w}{\partial x^2} + \frac{\partial^2 w}{\partial y^2})^2 - 2(1-\nu)(\frac{\partial^2 w}{\partial x^2}\frac{\partial^2 w}{\partial y^2} - (\frac{\partial^2 w}{\partial x \partial y})^2)]dx\, dy\ , \tag{3.3.4}$$

(b) Strain energy due to the dynamic stretching of the middle surface given by

$$\hat{U}_{str} = \frac{Eh}{2(1-\nu^2)} \int_{x=0}^{a} \int_{y=0}^{b} [\bar{\varepsilon}_x^2 + \bar{\varepsilon}_y^2 + 2\nu\bar{\varepsilon}_x\bar{\varepsilon}_y + (\frac{1-\nu}{2})\bar{\gamma}_{xy}^2]dx\, dy\ , \tag{3.3.5a}$$

where the middle surface dynamic strains are related to the derivatives of the displacements as follows:

$$\left.\begin{aligned} \bar{\varepsilon}_x &= \frac{\partial u_d}{\partial x} + \frac{\partial w}{\partial x}\frac{\partial z}{\partial x} + \frac{1}{2}(\frac{\partial w}{\partial x})^2\ , \\ \bar{\varepsilon}_y &= \frac{\partial v_d}{\partial y} + \frac{\partial w}{\partial y}\frac{\partial z}{\partial y} + \frac{1}{2}(\frac{\partial w}{\partial y})^2\ , \\ \bar{\gamma}_{xy} &= \frac{\partial u_d}{\partial y} + \frac{\partial v_d}{\partial x} + \frac{\partial w}{\partial x}\frac{\partial z}{\partial y} + \frac{\partial z}{\partial x}\frac{\partial w}{\partial y} + \frac{\partial w}{\partial x}\frac{\partial w}{\partial y}\ . \end{aligned}\right\} \tag{3.3.5b}$$

Substituting equations (3.3.5b) into equation (3.3.5a) and neglecting the non-linear terms, as explained in Appendix F,

$$\hat{U}_{str} = \frac{Eh}{2(1-\nu^2)} \int_{x=0}^{a} \int_{y=0}^{b} \{ [\frac{\partial u_d}{\partial x} + \frac{\partial w}{\partial x}\frac{\partial z}{\partial x}]^2 + [\frac{\partial v_d}{\partial y} + \frac{\partial w}{\partial y}\frac{\partial z}{\partial y}]^2$$

$$+ 2\nu [\frac{\partial u_d}{\partial x} + \frac{\partial w}{\partial x}\frac{\partial z}{\partial x}][\frac{\partial v_d}{\partial y} + \frac{\partial w}{\partial y}\frac{\partial z}{\partial y}] + (\frac{1-\nu}{2})[\frac{\partial u_d}{\partial y} + \frac{\partial v_d}{\partial x}$$

$$+ \frac{\partial w}{\partial x}\frac{\partial z}{\partial y} + \frac{\partial w}{\partial y}\frac{\partial z}{\partial x}]^2 \} dx\, dy \ . \qquad (3.3.5c)$$

(c) Potential energy due to the change in the position of the static in-plane stress distribution is given by

$$\hat{V}_{str} = \int_{x=0}^{a} \int_{y=0}^{b} h(\sigma_x \bar{\varepsilon}_x + \sigma_y \bar{\varepsilon}_y + \tau_{xy}\bar{\gamma}_{xy})\, dx\, dy \ ,$$

where $\sigma_x, \sigma_y, \tau_{xy}$ are the static in-plane stresses. In terms of strains,

$$\hat{V}_{str} = \int_{x=0}^{a} \int_{y=0}^{b} \{ \frac{Eh}{(1-\nu^2)} [(\varepsilon_x + \nu\varepsilon_y)\bar{\varepsilon}_x + (\varepsilon_y + \nu\varepsilon_x)\bar{\varepsilon}_y]$$

$$+ Gh\, \gamma_{xy}\bar{\gamma}_{xy} \} dx\, dy \ .$$

Taking only the linear terms, as explained in Appendix F,

$$\hat{V}_{str} = \frac{Eh}{(1-\nu^2)} \int_{x=0}^{a} \int_{y=0}^{b} \{ [\frac{\partial u_s}{\partial x} + \frac{1}{2}(\frac{\partial z}{\partial x})^2 - \frac{1}{2}(\frac{\partial z_o}{\partial x})^2]$$

$$\frac{1}{2}[(\frac{\partial w}{\partial x})^2 + \nu(\frac{\partial w}{\partial y})^2] + [\frac{\partial v_s}{\partial y} + \frac{1}{2}(\frac{\partial z}{\partial y})^2 - \frac{1}{2}(\frac{\partial z_o}{\partial y})^2]$$

$$\frac{1}{2}[(\frac{\partial w}{\partial y})^2 + \nu(\frac{\partial w}{\partial x})^2] + (\frac{1-\nu}{2})[\frac{\partial u_s}{\partial y} + \frac{\partial v_s}{\partial x} + \frac{\partial z}{\partial x}\frac{\partial z}{\partial y}$$

$$- \frac{\partial z_o}{\partial x} \frac{\partial z_o}{\partial y}] [\frac{\partial w}{\partial x} \frac{\partial w}{\partial y}]\} \, dx \, dy. \qquad (3.3.6)$$

(d) Energy stored in working against partially restraining supports is given by

$$\hat{U}_{bound} = \frac{1}{2} \int_{y=0}^{b} k_x (u_d^2 \Big|_{x=0} + u_d^2 \Big|_{x=a}) \, dy$$

$$+ \frac{1}{2} \int_{x=0}^{a} k_y (v_d^2 \Big|_{y=0} + v_d^2 \Big|_{y=b}) \, dx \qquad (3.3.7)$$

where k_x, k_y are the boundary support stiffnesses in x,y directions respectively. (The calculation of the boundary stiffness for the test apparatus is explained in Appendix H.)

For a free boundary $k=0$ and for a fully restrained boundary $k \to \infty$.

Total potential energy due to vibration is given by

$$\hat{V}_T = \hat{U}_{be} + \hat{U}_{str} + \hat{V}_{str} + \hat{U}_{bound} \qquad (3.3.8)$$

Neglecting the in-plane inertia, maximum kinetic energy

$$\hat{T} = \frac{1}{2} \omega^2 \int_{x=0}^{a} \int_{y=0}^{b} \bar{m} \, w^2 \, dx \, dy \, , \qquad (3.3.9)$$

where ω is the frequency of vibration and

$\bar{m}$ is the mass density of the plate (mass/unit area).

Using the Rayleigh-Ritz method,

$$\{\frac{\partial \hat{V}_T}{\partial \bar{A}_{i,j}}\} = \underline{0} \, , \qquad (3.3.10)$$

$$\{\frac{\partial \hat{V}_T}{\partial \bar{B}_{i,j}}\} = \underline{0} \ , \tag{3.3.11}$$

and
$$\{\frac{\partial \hat{V}_t}{\partial H_{i,j}}\} - \{\frac{\partial \hat{T}}{\partial H_{i,j}}\} = \underline{0} \ . \tag{3.3.12}$$

<u>Calculation of the Dynamic Connection Coefficients</u>

Substituting equations (3.3.4), (3.3.5c), (3.3.6), (3.3.7) and (3.3.8) into equation (3.3.10) and noting that only terms associated with u_d will yield non-zero values in equation (3.3.10) gives

$$\frac{\partial}{\partial \bar{A}_{i,j}} \int_{x=0}^{a} \int_{y=0}^{b} \frac{Eh}{2(1-\nu^2)} \{(\frac{\partial u_d}{\partial x})^2 + 2\frac{\partial u_d}{\partial x}(\frac{\partial w}{\partial x}\frac{\partial z}{\partial x} + \nu\frac{\partial w}{\partial y}\frac{\partial z}{\partial y})$$
$$+ (\frac{1-\nu}{2})(\frac{\partial u_d}{\partial y})^2 + 2\nu\frac{\partial u_d}{\partial x}\frac{\partial v_d}{\partial y} + (1-\nu)\frac{\partial u_d}{\partial y}[\frac{\partial v_d}{\partial x} + \frac{\partial w}{\partial x}\frac{\partial z}{\partial y}$$
$$+ \frac{\partial w}{\partial y}\frac{\partial z}{\partial x}] \, dx \, dy + \frac{1}{2}\int_{x=0}^{a} k_x(u_d^2\Big|_{x=0} + u_d^2\Big|_{x=a}) dy\} = 0 . \tag{3.3.13}$$

This can be rearranged to give

$$\frac{\partial}{\partial \bar{A}_{i,j}} \{\frac{1}{2}\int_{x=0}^{a}\int_{y=0}^{b} [(\frac{\partial u_d}{\partial x})^2 + (1-\nu)(\frac{\partial u_d}{\partial y})^2 + 2\nu\frac{\partial u_d}{\partial x}\frac{\partial v_d}{\partial y}$$
$$+ (1-\nu)\frac{\partial u_d}{\partial y}\frac{\partial v_d}{\partial x}] \, dx \, dy + \int_{y=0}^{b} \frac{k_x(1-\nu^2)}{2Eh}(u_d^2\Big|_{x=0} + u_d^2\Big|_{x=a}) dy\}$$
$$= -\frac{\partial}{\partial \bar{A}_{i,j}} \int_{x=0}^{a}\int_{y=0}^{b} [\frac{\partial u_d}{\partial x}(\frac{\partial w}{\partial x}\frac{\partial z}{\partial x} + \nu\frac{\partial w}{\partial y}\frac{\partial z}{\partial y})$$
$$+ (1-\nu)\frac{\partial u_d}{\partial y}(\frac{\partial w}{\partial x}\frac{\partial z}{\partial y} + \frac{\partial w}{\partial y}\frac{\partial z}{\partial x})] \, dx \, dy . \tag{3.3.13a}$$

Let $\frac{\partial}{\partial \bar{A}_{i,j}} \int_{x=0}^{a} \int_{y=0}^{b} [\frac{1}{2}(\frac{\partial u_d}{\partial x})^2 + (\frac{1-\nu}{2})(\frac{\partial u_d}{\partial y})^2] dx\, dy$

$$= \sum_k \sum_\ell \bar{A}_{k,\ell} \cdot SU1_{i,j,k,\ell};$$

where $$SU1_{i,j,k,\ell} = (\int_{x=0}^{a} \frac{\partial \bar{f}_{ui}}{\partial x} \cdot \frac{\partial \bar{f}_{uk}}{\partial x} dx)(\int_{y=0}^{b} \bar{g}_{uj}\, \bar{g}_{u\ell} dy)$$

$$+ (1-\nu)(\int_{x=0}^{a} \bar{f}_{ui} \cdot \bar{f}_{uk} dx)(\int_{y=0}^{b} \frac{\partial \bar{g}_{uj}}{\partial y} \frac{\partial \bar{g}_{u\ell}}{\partial y} dy), \quad (3.3.13b)$$

$$\frac{\partial}{\partial \bar{A}_{i,j}} \int_{x=0}^{a} \int_{y=0}^{b} (\nu \frac{\partial u_d}{\partial x} \frac{\partial v_d}{\partial y} + \frac{1-\nu}{2} \frac{\partial u_d}{\partial y} \frac{\partial v_d}{\partial x}) dx\, dy$$

$$= \sum_m \sum_n \bar{B}_{m,n} \cdot SV2_{i,j,m,n},$$

where $$SV2_{i,j,m,n} = [\nu(\int_{x=0}^{a} \frac{\partial \bar{f}_{ui}}{\partial x} \bar{f}_{vm} dx) \int_{y=0}^{b} \bar{g}_{uj} \frac{\partial \bar{g}_{vn}}{\partial y} dy$$

$$+ (\frac{1-\nu}{2})(\int_{x=0}^{a} \bar{f}_{ui} \frac{\partial \bar{f}_{vm}}{\partial x} dx) \int_{y=0}^{b} \frac{\partial \bar{g}_{uj}}{\partial y} g_{vn} dy],$$

(3.3.13c)

$$\frac{\partial}{\partial \bar{A}_{i,j}} \int_{y=0}^{b} \frac{k_x(1-\nu^2)}{2Eh} (u_d^2\Big|_{x=0} + u_d^2\Big|_{x=a}) dy = \sum_k \sum_\ell SU3_{i,j,k,\ell} \cdot \bar{A}_{k,\ell},$$

where $$SU3_{i,j,k,\ell} = (\bar{f}_{ui}(o) \cdot \bar{f}_{uk}(o) + \bar{f}_{ui}(a) \cdot \bar{f}_{uk}(a))$$

$$\times \int_{y=0}^{b} \frac{k_x(1-\nu^2)}{Eh} \bar{g}_{uj}\, \bar{g}_{u\ell} dy. \quad (3.3.13d)$$

and

$$\frac{\partial}{\partial \bar{A}_{i,j}} \int_{x=0}^{a} \int_{y=0}^{b} \frac{\partial u_d}{\partial x} \left(\frac{\partial w}{\partial x} \frac{\partial z}{\partial x} + \nu \frac{\partial w}{\partial y} \frac{\partial z}{\partial y} \right)$$

$$= \sum_p \sum_q \sum_r \sum_s H_{p,q} \cdot Z_{r,s} \Big[\left(\frac{\alpha_p \beta_r}{a^2}\right) \left(\int_{x=0}^{a} \frac{\partial \bar{f}_{ui}}{\partial x} \text{Cos}\left(\frac{\alpha_p x}{a}\right) \text{Cos}\left(\frac{\beta_r x}{a}\right) dx \right)$$

$$\int_{y=0}^{b} \bar{g}_{uj} \text{ Sin}\left(\frac{\alpha_q y}{b}\right) \text{Sin}\left(\frac{\beta_s y}{b}\right) dy$$

$$+ \left(\nu \frac{\alpha_q \beta_s}{b^2}\right) \left(\int_{x=0}^{a} \frac{\partial \bar{f}_{ui}}{\partial x} \text{ Sin}\left(\frac{\alpha_p x}{a}\right) \text{Sin}\left(\frac{\beta_r x}{a}\right) dx \right)$$

$$\int_{y=0}^{b} \bar{g}_{uj} \text{ Cos}\left(\frac{\alpha_q y}{b}\right) \text{Cos}\left(\frac{\beta_s y}{b}\right) dy \quad ,$$

where $\alpha_p = (2p-1)\pi$, $\alpha_q = (2q-1)\pi$, $\beta_r = (2r-1)\pi$, $\beta_s = (2s-1)\pi$.

This leads to

$$\int_{x=0}^{a} \int_{y=0}^{b} \frac{\partial u_d}{\partial x} \left(\frac{\partial w}{\partial x} \frac{\partial z}{\partial x} + \nu \frac{\partial w}{\partial y} \frac{\partial z}{\partial y} \right) dx \, dy$$

$$= \sum_p \sum_q H_{p,q} \cdot ZD1_{i,j,p,q} \qquad (3.3.13e)$$

where $ZD1_{i,j,p,q} = \sum_r \sum_s Z_{r,s} \Big[\left(\frac{\alpha_p \beta_r}{a^2}\right) \int_{x=0}^{a} \frac{\partial \bar{f}_{ui}}{\partial x} \text{ Cos}\left(\frac{\alpha_p x}{a}\right) \text{Cos}\left(\frac{\beta_r x}{a}\right) dx$

$$\int_{y=0}^{b} \bar{g}_{uj} \cdot \text{Sin}\left(\frac{\alpha_q y}{b}\right) \text{Sin}\left(\frac{\beta_s y}{b}\right) dy + \left(\nu \frac{\alpha_q \beta_s}{b^2}\right) \int_{x=0}^{a} \frac{\partial \bar{f}_{ui}}{\partial x}$$

$$\text{Sin}\left(\frac{\alpha_p x}{a}\right) \text{Sin}\left(\frac{\beta_r x}{a}\right) dx \int_{y=0}^{b} \bar{g}_{uj} \cdot \text{Cos}\left(\frac{\alpha_q y}{b}\right) \text{Cos}\left(\frac{\beta_s y}{b}\right) dy \Big]$$

(3.3.13f)

Similarly,

$$\frac{\partial}{\partial \bar{A}_{i,j}} \int_{x=0}^{a} \int_{y=0}^{b} \left(\frac{1-\nu}{2}\right) \frac{\partial u_d}{\partial y} \left(\frac{\partial w}{\partial x}\frac{\partial z}{\partial y} + \frac{\partial w}{\partial y}\frac{\partial z}{\partial x}\right) dx\, dy$$

$$= \sum_p \sum_q H_{p,q} \cdot ZD2_{i,j,p,q}\ , \qquad (3.3.13g)$$

where

$$ZD2_{i,j,p,q} = \left(\frac{1-\nu}{2}\right) \sum_r \sum_s Z_{r,s} \Big[\left(\frac{\alpha_p \beta_s}{ab}\right) \int_{x=0}^{a} \bar{f}_{ui} \mathrm{Cos}\left(\frac{\alpha_p x}{a}\right) \mathrm{Sin}\left(\frac{\beta_r x}{a}\right) dx \cdot$$

$$\int_{y=0}^{b} \frac{\partial \bar{g}_{uj}}{\partial y} \cdot \mathrm{Sin}\left(\frac{\alpha_q y}{b}\right) \mathrm{Cos}\left(\frac{\beta_s y}{b}\right) dy + \left(\frac{\alpha_q \beta_r}{ab}\right) \int_{x=0}^{a} \bar{f}_{ui} \cdot$$

$$\mathrm{Sin}\left(\frac{\alpha_p x}{a}\right) \mathrm{Cos}\left(\frac{\beta_r x}{a}\right) dx \int_{y=0}^{b} \frac{\partial \bar{g}_{uj}}{\partial y} \cdot \mathrm{Cos}\left(\frac{\alpha_q y}{b}\right) \mathrm{Sin}\left(\frac{\beta_s y}{b}\right) dy \Big] .$$

$$(3.3.13h)$$

Substituting equations (3.3.13b) to (3.3.13h) into equation (3.3.13a) yields

$$\sum_k \sum_\ell (SU1_{i,j,k,\ell} + SU3_{i,j,k,\ell}) \bar{A}_{k,\ell} + \sum_m \sum_n \bar{B}_{m,n} \cdot SV2_{i,j,m,n}$$

$$= - \sum_p \sum_q H_{p,q} (ZD1_{i,j,p,q} + ZD2_{i,j,p,q}) .$$

$$(3.3.14)$$

This is the result of minimizing $\hat{V}_T$ with respect to $\bar{A}_{i,j}$. The following equation can be obtained by minimizing $\hat{V}_T$ with respect to $\bar{B}_{m,n}$:

$$\sum_k \sum_\ell (SU2_{i,j,k,\ell}) \bar{A}_{k,\ell} + \sum_m \sum_n (SV1_{i,j,m,n} + SV3_{i,j,m,n}) \cdot \bar{B}_{m,n}$$

$$= - \sum_p \sum_q H_{p,q} (ZD3_{i,j,p,q} + ZD4_{i,j,p,q}) , \qquad (3.3.15)$$

where,

$$SU2_{i,j,k,\ell} = [\nu \int_{x=0}^{a} \bar{f}_{vi} \frac{\partial \bar{f}_{uk}}{\partial x} dx \cdot \int_{y=0}^{b} \frac{\partial g_{vj}}{\partial y} \cdot g_{u\ell} dy$$

$$+ (\frac{1-\nu}{2}) \int_{x=0}^{a} \frac{\partial \bar{f}_{vi}}{\partial x} \bar{f}_{uk} dx \cdot \int_{y=0}^{b} g_{vj} \frac{\partial g_{u\ell}}{\partial y} dy] , \quad (3.3.15a)$$

$$SV1_{i,j,m,n} = (\int_{x=0}^{a} \bar{f}_{vi} \cdot \bar{f}_{vm} dx) (\int_{y=0}^{b} \frac{\partial \bar{g}_{vj}}{\partial y} \cdot \frac{\partial \bar{g}_{vn}}{\partial y} dy)$$

$$+ (1-\nu) (\int_{x=0}^{a} \frac{\partial \bar{f}_{vi}}{\partial x} \cdot \frac{\partial \bar{f}_{vm}}{\partial x} dx) (\int_{y=0}^{b} \bar{g}_{vj} \cdot \bar{g}_{vn} dy) , \quad (3.3.15b)$$

$$SV3_{i,j,m,n} = (\bar{g}_{vj}(o) \cdot \bar{g}_{vn}(o) + \bar{g}_{vj}(b) \cdot \bar{g}_{vn}(b))$$

$$\int_{x=0}^{a} \frac{k_y (1-\nu^2)}{Eh} \bar{f}_{vi} \cdot \bar{f}_{vm} dx , \quad (3.3.15c)$$

$$ZD3_{i,j,p,q} = \sum_r \sum_s Z_{r,s} [(\frac{\alpha_q \beta_s}{b^2}) (\int_{x=0}^{a} \bar{f}_{vi} \cdot Sin(\frac{\alpha_p x}{a}) Sin(\frac{\beta_r x}{a}) dx)$$

$$(\int_{y=0}^{b} \frac{\partial \bar{g}_{vj}}{\partial y} \cdot Cos(\frac{\alpha_q y}{b}) Cos(\frac{\beta_s y}{b}) dy)$$

$$+ (\nu \frac{\alpha_p \beta_r}{a^2}) (\int_{x=0}^{a} \bar{f}_{vi} \cdot Cos(\frac{\alpha_p x}{a}) Cos(\frac{\beta_r x}{a}) dx)$$

$$(\int_{y=0}^{b} \frac{\partial \bar{g}_{vj}}{\partial y} \cdot Sin(\frac{\alpha_q y}{b}) Sin(\frac{\beta_s y}{b}) dy) , \quad (3.3.15d)$$

and

$$ZD4_{i,j,p,q} = (\frac{1-\nu}{2}) \sum_r \sum_s Z_{r,s} [(\frac{\alpha_p \beta_s}{ab}) (\int_{x=0}^{a} \frac{\partial \bar{f}_{vi}}{\partial x} \cdot Cos(\frac{\alpha_p x}{a}) Sin(\frac{\beta_r x}{a}) dx)$$

$$(\int_{y=0}^{b} \bar{g}_{vj} \cdot Sin(\frac{\alpha_q y}{b}) Cos(\frac{\beta_s y}{b}) dy) + (\frac{\alpha_q \beta_r}{ab}) (\int_{x=0}^{a} \frac{\partial \bar{f}_{vi}}{\partial x}$$

$$Sin(\frac{\alpha_p x}{a}) Cos(\frac{\beta_r x}{a}) dx) \cdot (\int_{y=0}^{b} \bar{g}_{vj} \cdot Cos(\frac{\alpha_q y}{b}) Sin(\frac{\beta_s y}{b}) dy)] .$$

(3.3.15e)

Equations (3.3.14) and (3.3.15) will result in NN equations where NN is the total number of in-plane displacement coefficients. These equations can be written in matrix form as follows:

$$[SX]\{\bar{C}\} = [ZD]\{H\} \qquad (3.3.16)$$

where $I = j+(i-1) \times N_{uy}$ for $I \leq N_u$,

$I = N_u+j+(i-1) \times N_{vy}$ for $I > N_u$,

$J = \ell+(k-1) \times N_{uy}$ for $J \leq N_u$,

$J = N_u+n+(m-1) \times N_{vy}$ for $J > N_u$,

and

$SX(I,J) = (SU1_{i,j,k,\ell}+SU3_{i,j,k,\ell})$ for $I \leq N_u$ and $J \leq N_u$,

$SX(I,J) = SV2_{i,j,m,n}$ for $I \leq N_u$ and $J > N_u$,

$SX(I,J) = SU2_{i,j,k,\ell}$ for $I > N_u$ and $J \leq N_u$,

$SX(I,J) = (SV1_{i,j,m,n}+SV3_{i,j,m,n})$ for $I > N_u$ and $J > N_u$,

$\bar{C}(I) = \bar{A}_{i,j}$ for $I \leq N_u$,

$\bar{C}(I) = \bar{B}_{i,j}$ for $I > N_u$.

Also;

$H(L) = H_{p,q}$, where $L = q+(p-1) \times q_m$,

$ZD(I,L) = ZD1_{i,j,p,q} + ZD2_{i,j,p,q}$ if $I \leq N_u$,

and $ZD(I,L) = ZD3_{i,j,p,q} + ZD4_{i,j,p,q}$ if $I > N_u$.

Equation (3.3.16) is linear in $\bar{C}$ and therefore $\bar{C}$ can be calculated in the following manner:

If $G(I,L1) = \bar{C}(I)$ when $H(L) = 1.0$ for $L = L1$,

$H(L) = 0.0$ for $L \neq L1$,

then, $\bar{C}(I) = \sum_{L1} G(I,L1) \cdot H(L1)$, from linear algebra. $G(I,L1)$ can be defined as the 'connection coefficient' which gives the in-plane displacement coefficient $\bar{C}(I)$ for a unit out-of-plane displacement corresponding to the L1th mode.

As in the case of postbuckling analysis, [G] can be calculated by solving

$$[SX][G] = [ZD] \quad . \tag{3.3.17}$$

$\{\bar{C}\}$ is then given by

$$\{\bar{C}\} = [G]\{H\}. \tag{3.3.18}$$

Calculation of the Out-of-Plane Dynamic Displacement Coefficients

Consider equation (3.3.12).

From equation (3.3.8),

$$\frac{\partial \hat{V}_T}{\partial H_{i,j}} = \frac{\partial \hat{U}_{be}}{\partial H_{i,j}} + \frac{\partial \hat{U}_{str}}{\partial H_{i,j}} + \frac{\partial \hat{V}_{str}}{\partial H_{i,j}} + \frac{\partial \hat{U}_{bound}}{\partial H_{i,j}} \quad . \tag{3.3.19}$$

Since $\hat{U}_{bound}$ does not depend on w, $\frac{\partial \hat{U}_{bound}}{\partial H_{i,j}} = 0$ (3.3.20)

$$\frac{\partial \hat{U}_{be}}{\partial H_{i,j}} = \frac{Eh^3}{24(1-\nu^2)} \left[\left(\frac{\alpha_i}{a}\right)^2 + \left(\frac{\alpha_j}{b}\right)^2\right]^2 \left(\frac{ab}{4}\right) \cdot 2 \cdot H_{i,j} \quad , \tag{3.3.21}$$

where $\alpha_i = (2i-1)\pi$, $\alpha_j = (2j-1)\pi$ for symmetrical modes.

$$\frac{\partial \hat{U}_{str}}{\partial H_{i,j}} = \frac{Eh}{(1-\nu^2)} \sum_{r=1}^{8} \hat{X}_r , \tag{3.3.22}$$

where $\hat{X}_r$ can be found as follows:

Let $\beta_r=(2r-1)\pi$, $\gamma_p=(2p-1)\pi$, $\phi_k=(2k-1)\pi$, $\beta_s=(2s-1)\pi$,

$\gamma_q=(2q-1)\pi$, $\phi_\ell=(2\ell-1)\pi$.

$$\hat{X}_1 = \frac{\partial}{\partial H_{i,j}} \frac{1}{2} \int_{x=0}^{a} \int_{y=0}^{b} [(\frac{\partial w}{\partial x} \frac{\partial z}{\partial x})^2 + (\frac{\partial w}{\partial y} \frac{\partial z}{\partial y})^2] dx\, dy$$

$$= \int_{x=0}^{a} \int_{y=0}^{b} \frac{1}{2} [2 \frac{\partial w}{\partial x} \cdot \frac{\partial}{\partial H_{i,j}} (\frac{\partial w}{\partial x}) (\frac{\partial z}{\partial x})^2 + 2 \frac{\partial w}{\partial y} \cdot \frac{\partial}{\partial H_{i,j}} (\frac{\partial w}{\partial y}) (\frac{\partial z}{\partial y})^2] dx\, dy$$

$$= \sum_r \sum_s H_{r,s} \sum_p \sum_q \sum_k \sum_\ell (\frac{\alpha_i \beta_r \gamma_p \phi_k}{a^4} \cdot TX1 \cdot TY2$$

$$+ \frac{\alpha_j \beta_s \gamma_q \phi_\ell}{b^4} \cdot TX2 \cdot TY1) Z_{p,q} \cdot Z_{k,\ell} , \tag{3.3.23a}$$

where

$$TX1 = \int_{x=0}^{a} \text{Cos}(\frac{\alpha_i x}{a}) \text{Cos}(\frac{\beta_r x}{a}) \text{Cos}(\frac{\gamma_p x}{a}) \text{Cos}(\frac{\phi_k x}{a}) dx ,$$

$$TX2 = \int_{x=0}^{a} \text{Sin}(\frac{\alpha_i x}{a}) \text{Sin}(\frac{\beta_r x}{a}) \text{Sin}(\frac{\gamma_p x}{a}) \text{Sin}(\frac{\phi_k x}{a}) dx ,$$

$$TY1 = \int_{y=0}^{b} \text{Cos}(\frac{\alpha_j y}{b}) \text{Cos}(\frac{\beta_s y}{b}) \text{Cos}(\frac{\gamma_q y}{b}) \text{Cos}(\frac{\phi_\ell y}{b}) dy ,$$

and $$TY2 = \int_{y=0}^{b} \text{Sin}(\frac{\alpha_j y}{b}) \text{Sin}(\frac{\beta_s y}{b}) \text{Sin}(\frac{\gamma_q y}{b}) \text{Sin}(\frac{\phi_\ell y}{b}) dy .$$

$$\hat{X}_2 = \frac{\partial}{\partial H_{i,j}} \int_{x=0}^{a} \int_{y=0}^{b} \frac{\partial w}{\partial x} \cdot \frac{\partial z}{\partial x} \cdot \frac{\partial w}{\partial y} \cdot \frac{\partial z}{\partial y}\, dx\, dy$$

$$= \nu \int_{x=0}^{a} \int_{y=0}^{b} \frac{\partial z}{\partial x} \frac{\partial z}{\partial y} [\frac{\partial w}{\partial y} \frac{\partial}{\partial H_{i,j}} (\frac{\partial w}{\partial x}) + \frac{\partial w}{\partial x} \frac{\partial}{\partial H_{i,j}} (\frac{\partial w}{\partial y})] dx\, dy$$

$$= \nu \sum_r \sum_s H_{r,s} \sum_p \sum_q \sum_k \sum_\ell (Z_{p,q} \cdot Z_{k,\ell})$$

$$\left(\frac{\alpha_i \beta_s \gamma_p \phi_\ell}{a^2 b^2} \cdot TX3 \cdot TY4 + \left(\frac{\alpha_j \beta_r \gamma_q \phi_k}{a^2 b^2}\right) \cdot TX4 \cdot TY3\right), \quad (3.3.23b)$$

where

$$TX3 = \int_{x=0}^{a} \cos\left(\frac{\alpha_i x}{a}\right) \sin\left(\frac{\beta_r x}{a}\right) \cos\left(\frac{\gamma_p x}{a}\right) \sin\left(\frac{\phi_k x}{a}\right) dx ,$$

$$TX4 = \int_{x=0}^{a} \sin\left(\frac{\alpha_i x}{a}\right) \cos\left(\frac{\beta_r x}{a}\right) \sin\left(\frac{\gamma_p x}{a}\right) \cos\left(\frac{\phi_k x}{a}\right) dx ,$$

$$TY4 = \int_{y=0}^{b} \sin\left(\frac{\alpha_j y}{b}\right) \cos\left(\frac{\beta_s y}{b}\right) \sin\left(\frac{\gamma_q y}{b}\right) \cos\left(\frac{\phi_\ell y}{b}\right) dy ,$$

and $TY3 = \int_{y=0}^{b} \cos\left(\frac{\alpha_j y}{b}\right) \sin\left(\frac{\beta_s y}{b}\right) \cos\left(\frac{\gamma_q y}{b}\right) \sin\left(\frac{\phi_\ell y}{b}\right) dy .$

$$\hat{X}_3 = \frac{\partial}{\partial H_i} \left(\frac{1-\nu}{4}\right) \int_{x=0}^{a} \int_{y=0}^{b} \left[\left(\frac{\partial w}{\partial x}\right)^2 \left(\frac{\partial z}{\partial y}\right)^2 + \left(\frac{\partial w}{\partial y}\right)^2 \left(\frac{\partial z}{\partial x}\right)^2\right] dx\, dy$$

$$= \left(\frac{1-\nu}{2}\right) \int_{x=0}^{a} \int_{y=0}^{b} \left[\frac{\partial w}{\partial x} \left(\frac{\partial z}{\partial y}\right)^2 \frac{\partial}{\partial H_{i,j}} \left(\frac{\partial w}{\partial x}\right) + \frac{\partial w}{\partial y} \left(\frac{\partial z}{\partial x}\right)^2 \frac{\partial}{\partial H_{i,j}} \left(\frac{\partial w}{\partial y}\right)\right] dx\, dy$$

$$= \left(\frac{1-\nu}{2}\right) \sum_r \sum_s H_{r,s} \sum_p \sum_q \sum_k \sum_\ell \left[\frac{\alpha_i \beta_r \gamma_q \phi_\ell}{a^2 b^2} \cdot (TX5) \cdot (TY6)\right.$$

$$\left. + \frac{\alpha_j \beta_s \gamma_p \phi_k}{a^2 b^2} \cdot (TX6) \cdot (TY5)\right] Z_{p,q} \cdot Z_{k,\ell}, \quad (3.3.23c)$$

where

$$TX5 = \int_{x=0}^{a} \cos\left(\frac{\alpha_i x}{a}\right) \cos\left(\frac{\beta_r x}{a}\right) \sin\left(\frac{\gamma_p x}{a}\right) \sin\left(\frac{\phi_k x}{a}\right) dx ,$$

$$TX6 = \int_{x=0}^{a} \sin\left(\frac{\alpha_i x}{a}\right) \sin\left(\frac{\beta_r x}{a}\right) \cos\left(\frac{\gamma_p x}{a}\right) \cos\left(\frac{\phi_k x}{a}\right) dx ,$$

$$TY5 = \int_{y=0}^{b} \cos(\frac{\alpha_j y}{b}) \cos(\frac{\beta_s y}{b}) \sin(\frac{\gamma_q y}{b}) \sin(\frac{\phi_\ell y}{b})\, dy ,$$

and $$TY6 = \int_{y=0}^{b} \sin(\frac{\alpha_j y}{b}) \sin(\frac{\beta_s y}{b}) \cos(\frac{\gamma_q y}{b}) \cos(\frac{\phi_\ell y}{b})\, dy .$$

$$\hat{X}_4 = \frac{\partial}{\partial H_{i,j}} (\frac{1-\nu}{2}) \int_{x=0}^{a} \int_{y=0}^{b} \frac{\partial w}{\partial x} \cdot \frac{\partial w}{\partial y} \cdot \frac{\partial z}{\partial x} \cdot \frac{\partial z}{\partial y} \cdot dx\, dy$$

$$= (\frac{1-\nu}{2}) \int_{x=0}^{a} \int_{y=0}^{b} \frac{\partial z}{\partial x} \cdot \frac{\partial z}{\partial y} [\frac{\partial w}{\partial y} \cdot \frac{\partial}{\partial H_{i,j}} (\frac{\partial w}{\partial x}) + \frac{\partial w}{\partial x} \cdot \frac{\partial}{\partial H_{i,j}} (\frac{\partial w}{\partial y})] dx\, dy$$

$$= (\frac{1-\nu}{2}) \sum_r \sum_s H_{r,s} \sum_p \sum_q \sum_k \sum_\ell (\frac{\alpha_i \beta_s \gamma_p \phi_\ell}{a^2 b^2} \cdot TX3 \cdot TY4$$

$$+ \frac{\alpha_j \beta_r \gamma_q \phi_k}{a^2 b^2} \cdot TX4 \cdot TY3) Z_{p,q} \cdot Z_{k,\ell} . \qquad (3.3.23d)$$

$$\hat{X}_5 = \frac{\partial}{\partial H_{i,j}} \frac{1}{2} \int_{x=0}^{a} \int_{y=0}^{b} (2 \frac{\partial u_d}{\partial x} \cdot \frac{\partial w}{\partial x} \cdot \frac{\partial z}{\partial x} + 2\nu \frac{\partial u_d}{\partial x} \cdot \frac{\partial w}{\partial y} \cdot \frac{\partial z}{\partial y})\, dx\, dy$$

$$= \int_{x=0}^{a} \int_{y=0}^{b} [\frac{\partial u_d}{\partial x} \cdot \frac{\partial z}{\partial x} \frac{\partial}{\partial H_{i,j}} (\frac{\partial w}{\partial x}) + \nu \frac{\partial u_d}{\partial x} \cdot \frac{\partial z}{\partial y} \cdot \frac{\partial}{\partial H_{i,j}} (\frac{\partial w}{\partial y})]\, dx\, dy$$

$$= \sum_k \sum_\ell \bar{A}_{k,\ell} \sum_p \sum_q Z_{p,q} [(\frac{\alpha_i \gamma_p}{a^2}) (\int_{x=0}^{a} \frac{\partial \bar{f}_{uk}}{\partial x} \cdot \cos(\frac{\alpha_i x}{a}) \cos(\frac{\gamma_p x}{a})\, dx)$$

$$(\int_{y=0}^{b} \bar{g}_{u\ell} \cdot \sin(\frac{\alpha_j y}{b}) \sin(\frac{\gamma_q y}{b})\, dy)$$

$$+ \nu (\frac{\alpha_j \gamma_q}{b^2}) (\int_{x=0}^{a} \frac{\partial \bar{f}_{uk}}{\partial x} \sin(\frac{\alpha_i x}{a}) \sin(\frac{\gamma_p x}{a})\, dx)$$

$$(\int_{y=0}^{b} \bar{g}_{u\ell} \cdot \cos(\frac{\alpha_j y}{b}) \cos(\frac{\gamma_q y}{b})\, dy)] . \qquad (3.3.23e)$$

$$\hat{X}_6 = \frac{\partial}{\partial H_{i,j}} (\frac{1-\nu}{2}) \int_{x=0}^{a} \int_{y=0}^{b} \frac{\partial u_d}{\partial y} [\frac{\partial w}{\partial x} \cdot \frac{\partial z}{\partial y} + \frac{\partial w}{\partial y} \frac{\partial z}{\partial x}]\, dx\, dy$$

$$= (\frac{1-\nu}{2}) \sum_k \sum_\ell \bar{A}_{k,\ell} \sum_p \sum_q Z_{p,q} [(\frac{\alpha_i \gamma_q}{ab}) (\int_{x=0}^{a} \bar{f}_{uk} \cdot \cos(\frac{\alpha_i x}{a}) \sin(\frac{\gamma_p x}{a})\, dx)$$

$$\left(\int_{y=0}^{b} \frac{\partial \bar{g}_{u\ell}}{\partial y} \cdot \mathrm{Sin}\left(\frac{\alpha_j y}{b}\right) \mathrm{Cos}\left(\frac{\gamma_q y}{b}\right) dy\right)$$

$$+ \left(\frac{\alpha_j \gamma_p}{ab}\right) \left(\int_{x=0}^{a} \bar{f}_{uk} \cdot \mathrm{Sin}\left(\frac{\alpha_i x}{a}\right) \mathrm{Cos}\left(\frac{\gamma_p x}{a}\right) dx\right)$$

$$\left(\int_{y=0}^{b} \frac{\partial \bar{g}_{u\ell}}{\partial y} \cdot \mathrm{Cos}\left(\frac{\alpha_j y}{b}\right) \mathrm{Sin}\left(\frac{\gamma_q y}{b}\right) dy\right)\Big] \quad . \qquad (3.3.23f)$$

$$\hat{X}_7 = \frac{\partial}{\partial H_{i,j}} \frac{1}{2} \int_{x=0}^{a} \int_{y=0}^{b} \left(2 \frac{\partial v_d}{\partial y} \cdot \frac{\partial w}{\partial y} \cdot \frac{\partial z}{\partial y} + 2\nu \frac{\partial v_d}{\partial y} \cdot \frac{\partial w}{\partial x} \cdot \frac{\partial z}{\partial x}\right) dx \; dy$$

$$= \sum_m \sum_n \bar{B}_{m,n} \sum_p \sum_q Z_{p,q} \Big[\left(\int_{x=0}^{a} \bar{f}_{vm} \cdot \mathrm{Sin}\left(\frac{\alpha_i x}{a}\right) \mathrm{Sin}\left(\frac{\gamma_p x}{a}\right) dx\right)$$

$$\left(\int_{y=0}^{b} \frac{\partial \bar{g}_{vn}}{\partial y} \cdot \mathrm{Cos}\left(\frac{\alpha_j y}{b}\right) \mathrm{Cos}\left(\frac{\gamma_q y}{b}\right) dy\right) \left(\frac{\alpha_j \gamma_q}{b^2}\right) +$$

$$\left(\nu \frac{\alpha_i \gamma_p}{a^2}\right) \left(\int_{x=0}^{a} \bar{f}_{vm} \cdot \mathrm{Cos}\left(\frac{\alpha_i x}{a}\right) \mathrm{Cos}\left(\frac{\gamma_p x}{a}\right) dx\right)$$

$$\left(\int_{y=0}^{b} \frac{\partial \bar{g}_{vn}}{\partial y} \cdot \mathrm{Sin}\left(\frac{\alpha_j y}{b}\right) \mathrm{Sin}\left(\frac{\gamma_q y}{b}\right) dy\right)\Big] \quad . \qquad (3.3.23g)$$

$$\hat{X}_8 = \frac{\partial}{\partial H_{i,j}} \left(\frac{1-\nu}{2}\right) \int_{x=0}^{a} \int_{y=0}^{b} \frac{\partial v_d}{\partial x} \left[\frac{\partial w}{\partial x} \cdot \frac{\partial z}{\partial y} + \frac{\partial w}{\partial y} \frac{\partial z}{\partial x}\right] dx \cdot dy$$

$$= \left(\frac{1-\nu}{2}\right) \cdot \sum_m \sum_n \bar{B}_{m,n} \sum_p \sum_q Z_{p,q} \Big[\left(\frac{\alpha_i \gamma_q}{ab}\right)$$

$$\left(\int_{x=0}^{a} \frac{\partial \bar{f}_{vm}}{\partial x} \cdot \mathrm{Cos}\left(\frac{\alpha_i x}{a}\right) \mathrm{Sin}\left(\frac{\gamma_p x}{a}\right) dx\right)$$

$$\left(\int_{y=0}^{b} \bar{g}_{vn} \cdot \mathrm{Sin}\left(\frac{\alpha_j y}{b}\right) \mathrm{Cos}\left(\frac{\gamma_q y}{b}\right) dy\right) + \left(\frac{\alpha_j \gamma_p}{ab}\right)$$

$$\left(\int_{x=0}^{a} \frac{\partial \bar{f}_{vm}}{\partial x} \cdot \mathrm{Sin}\left(\frac{\alpha_i x}{a}\right) \mathrm{Cos}\left(\frac{\gamma_p x}{a}\right) dx\right)$$

$$\left(\int_{y=0}^{b} \bar{g}_{vn} \cdot \mathrm{Cos}\left(\frac{\alpha_j y}{b}\right) \mathrm{Sin}\left(\frac{\gamma_q y}{b}\right) dy\right)\Big] \quad . \qquad (3.3.23h)$$

$$\frac{\partial \hat{V}_{str}}{\partial H_{i,j}} = \frac{Eh}{(1-\nu^2)} \sum_{r=1}^{7} \hat{Y}_r \, , \qquad (3.3.24)$$

where $\hat{Y}_r$ can be found as follows:

$$\hat{Y}_1 = \frac{\partial}{\partial H_{i,j}} \int_{x=0}^{a} \int_{y=0}^{b} \frac{1}{2} \frac{\partial u_s}{\partial x} \left[\left(\frac{\partial w}{\partial x}\right)^2 + \nu \left(\frac{\partial w}{\partial y}\right)^2 \right] dx\, dy$$

$$= \sum_r \sum_s H_{r,s} \left[\left(\frac{\alpha_i \beta_r}{a^2}\right) \int_{x=0}^{a} \int_{y=0}^{b} \frac{\partial u_s}{\partial x} \cdot \cos\left(\frac{\alpha_i x}{a}\right) \cos\left(\frac{\beta_r x}{a}\right) \right.$$

$$\sin\left(\frac{\alpha_j y}{b}\right) \sin\left(\frac{\beta_s y}{b}\right) dx\, dy + \left(\nu \frac{\alpha_j \beta_s}{b^2}\right) \int_{x=0}^{a} \int_{y=0}^{b} \frac{\partial u_s}{\partial x} \cdot$$

$$\left. \sin\left(\frac{\alpha_i x}{a}\right) \sin\left(\frac{\beta_r x}{a}\right) \cos\left(\frac{\alpha_j y}{b}\right) \cos\left(\frac{\beta_s y}{b}\right) dx\, dy \right]$$

$$= \sum_r \sum_s H_{r,s} \sum_k \sum_\ell A_{k,\ell} \left[\left(\frac{\alpha_i \beta_r}{a^2}\right) \left(\int_{x=0}^{a} \frac{\partial f_{uk}}{\partial x} \cos\left(\frac{\alpha_i x}{a}\right) \cos\left(\frac{\beta_r x}{a}\right) dx \right) \right.$$

$$\left(\int_{y=0}^{b} g_{u\ell} \cdot \sin\left(\frac{\alpha_j y}{b}\right) \sin\left(\frac{\beta_s y}{b}\right) dy \right)$$

$$+ \left(\nu \frac{\alpha_j \beta_s}{b^2}\right) \left(\int_{x=0}^{a} \frac{\partial f_{uk}}{\partial x} \cdot \sin\left(\frac{\alpha_i x}{a}\right) \sin\left(\frac{\beta_r x}{a}\right) dx \right)$$

$$\left. \left(\int_{y=0}^{b} g_{u\ell} \cdot \cos\left(\frac{\alpha_j y}{b}\right) \cos\left(\frac{\beta_s y}{b}\right) dy \right) \right] . \qquad (3.3.25a)$$

$$\hat{Y}_2 = \frac{\partial}{\partial H_{i,j}} \int_{x=0}^{a} \int_{y=0}^{b} \left(\frac{1-\nu}{2}\right) \frac{\partial u_s}{\partial x} \frac{\partial w}{\partial x} \cdot \frac{\partial w}{\partial y} \, dx\, dy$$

$$= \left(\frac{1-\nu}{2}\right) \int_{x=0}^{a} \int_{y=0}^{b} \left[\frac{\partial u_s}{\partial y} \cdot \frac{\partial w}{\partial y} \frac{\partial}{\partial H_{i,j}} \left(\frac{\partial w}{\partial x}\right) + \frac{\partial u_s}{\partial y} \cdot \frac{\partial w}{\partial x} \cdot \frac{\partial}{\partial H_{i,j}} \left(\frac{\partial w}{\partial y}\right) \right] dx\, dy$$

$$= \left(\frac{1-\nu}{2}\right) \sum_r \sum_s H_{r,s} \sum_k \sum_\ell A_{k,\ell} \left[\left(\frac{\alpha_i \beta_s}{ab}\right) \left(\int_{x=0}^{a} f_{uk} \cdot \cos\left(\frac{\alpha_i x}{a}\right) \ldots \right. \right.$$

$$\mathrm{Sin}(\frac{\beta_r x}{a})dx)\,(\frac{\partial g_{u\ell}}{\partial y}\cdot \mathrm{Sin}(\frac{\alpha_j y}{b})\mathrm{Cos}(\frac{\beta_s y}{b})dy)+(\frac{\alpha_j\beta_r}{ab})$$

$$(\int_{x=0}^{a} f_{uk}\cdot \mathrm{Sin}(\frac{\alpha_i x}{a})\mathrm{Cos}(\frac{\beta_r x}{a})dx)\,(\frac{\partial g_{u\ell}}{\partial y}\cdot \mathrm{Cos}(\frac{\alpha_j y}{b})\mathrm{Sin}(\frac{\beta_s y}{b})dy)]. \quad (3.3.25b)$$

$$\hat{Y}_3 = \frac{\partial}{\partial H_{i,j}}\int_{x=0}^{a}\int_{y=0}^{b}\frac{\partial v_s}{\partial y}\,\frac{1}{2}[(\frac{\partial w}{\partial y})^2+\nu(\frac{\partial w}{\partial x})^2]\,dx\,dy$$

$$= \sum_r\sum_s H_{r,s}\sum_m\sum_n B_{m,n}[(\frac{\alpha_j\beta_s}{b^2})(f_{vm}\cdot \mathrm{Sin}(\frac{\alpha_i x}{a})\mathrm{Sin}(\frac{\beta_r x}{a})dx)$$

$$(\frac{\partial g_{vn}}{\partial y}\cdot \mathrm{Cos}(\frac{\alpha_j y}{b})\mathrm{Cos}(\frac{\beta_s y}{b})dy)+(\nu\frac{\alpha_i\beta_r}{a^2})(f_{vm}\cdot \mathrm{Cos}(\frac{\alpha_i x}{a})\mathrm{Cos}(\frac{\beta_r x}{a})dx)$$

$$(\frac{\partial g_{vn}}{\partial y}\cdot \mathrm{Sin}(\frac{\alpha_j y}{b})\mathrm{Sin}(\frac{\beta_s y}{b})dy)]. \quad (3.3.25c)$$

$$\hat{Y}_4 = \frac{\partial}{\partial H_{i,j}}\int_{x=0}^{a}\int_{y=0}^{b}(\frac{1-\nu}{2})\frac{\partial v_s}{\partial x}\cdot\frac{\partial w}{\partial x}\cdot\frac{\partial w}{\partial y}\,dx.dy$$

$$= (\frac{1-\nu}{2})\sum_r\sum_s H_{r,s}\sum_m\sum_n B_{m,n}\,[(\frac{\alpha_i\beta_s}{ab})(\int_{x=0}^{a}\frac{\partial f_{vm}}{\partial x}\cdot \mathrm{Cos}(\frac{\alpha_i x}{a})\mathrm{Sin}(\frac{\beta_r x}{a})$$

$$dx)(\int_{y=0}^{b} g_{vn}\cdot \mathrm{Sin}(\frac{\alpha_j y}{b})\mathrm{Cos}(\frac{\beta_s y}{b})dy)+(\frac{\alpha_j\beta_r}{ab})(\int_{x=0}^{a}\frac{\partial f_{vm}}{\partial x}\cdot$$

$$\mathrm{Sin}(\frac{\alpha_i x}{a})\mathrm{Cos}(\frac{\beta_r x}{a})dx)(\int_{y=0}^{b} g_{vn}\cdot \mathrm{Cos}(\frac{\alpha_j y}{b})\mathrm{Sin}(\frac{\beta_s y}{b})dy)]. \quad (3.3.25d)$$

$$\hat{Y}_5 = \frac{\partial}{\partial H_{i,j}}\int_{x=0}^{a}\int_{y=0}^{b}[\frac{1}{2}(\frac{\partial z}{\partial x})^2-\frac{1}{2}(\frac{\partial z_o}{\partial x})^2]\frac{1}{2}[(\frac{\partial w}{\partial x})^2+\nu(\frac{\partial w}{\partial y})^2]dx\,dy$$

$$= \frac{1}{2}\int_{x=0}^{a}\int_{y=0}^{b}[(\frac{\partial z}{\partial x})^2-(\frac{\partial z_o}{\partial x})^2][\frac{\partial w}{\partial x}\cdot\frac{\partial}{\partial H_{i,j}}(\frac{\partial w}{\partial x})+\nu\frac{\partial w}{\partial y}\,\frac{\partial}{\partial H_{i,j}}(\frac{\partial w}{\partial y})]dx\,dy$$

$$= \frac{1}{2} \sum_r \sum_s H_{r,s} \sum_p \sum_q \sum_k \sum_\ell (Z_{p,q} \cdot Z_{k,\ell} - Z_{o_{p,q}} \cdot Z_{o_{k,\ell}})$$

$$[(\frac{\alpha_i \beta_r \gamma_p \phi_k}{a^4}) \cdot TX1 \cdot TY2 + \nu (\frac{\alpha_j \beta_s \gamma_p \phi_k}{a^2 b^2}) \cdot TX6 \cdot TY5] \ . \quad (3.3.25e)$$

$$\hat{Y}_6 = \frac{\partial}{\partial H_{i,j}} \int_{x=0}^{a} \int_{y=0}^{b} [\frac{1}{2}(\frac{\partial z}{\partial y})^2 - \frac{1}{2}(\frac{\partial z_o}{\partial y})^2] \frac{1}{2}[(\frac{\partial w}{\partial y})^2 + \nu (\frac{\partial w}{\partial x})^2] dx\ dy$$

$$= \frac{1}{2} \sum_r \sum_s H_{r,s} \sum_p \sum_q \sum_k \sum_\ell (Z_{p,q} \cdot Z_{k,\ell} - Z_{o_{p,q}} \cdot Z_{o_{k,\ell}})$$

$$[(\frac{\alpha_j \beta_s \gamma_q \phi_\ell}{b^4}) \cdot TX2 \cdot TY1 + \nu (\frac{\alpha_i \beta_r \gamma_q \phi_\ell}{a^2 b^2}) \cdot TX5 \cdot TY6] \ . \quad (3.3.25f)$$

$$\hat{Y}_7 = \frac{\partial}{\partial H_{i,j}} (\frac{1-\nu}{2}) \int_{x=0}^{a} \int_{y=0}^{b} \frac{\partial w}{\partial x} \cdot \frac{\partial w}{\partial y} [\frac{\partial z}{\partial x} \cdot \frac{\partial z}{\partial y} - \frac{\partial z_o}{\partial x} \frac{\partial z_o}{\partial y}] dx\ dy$$

$$= (\frac{1-\nu}{2}) \sum_r \sum_s H_{r,s} \sum_p \sum_q \sum_k \sum_\ell (Z_{p,q} \cdot Z_{k,\ell} - Z_{o_{p,q}} \cdot Z_{o_{k,\ell}})$$

$$\cdot [(\frac{\alpha_i \beta_s \gamma_p \phi_\ell}{a^2 b^2}) \cdot TX3 \cdot TY4 + (\frac{\alpha_j \beta_r \gamma_q \phi_k}{a^2 b^2}) \cdot TX4 \cdot TY3] \ . \quad (3.3.25g)$$

From equations (3.3.19), (3.3.20), (3.3.21), (3.3.22) and (3.3.24),

$$\frac{\partial \hat{V}_T}{\partial H_{i,j}} = \frac{Eh^3}{24(1-\nu^2)} (\frac{ab}{4}) [(\frac{\alpha_i}{a})^2 + (\frac{\beta_j}{b})^2]^2 H_{i,j}$$

$$+ \sum_r \sum_s H_{r,s}\ C1 + \sum_k \sum_\ell \bar{A}_{k,\ell}\ C2 + \sum_m \sum_n \bar{B}_{m,n}\ C3 \ , \quad (3.3.26)$$

where C1, C2 and C3 can be found from equations (3.3.22) to (3.3.25g). Using the connection coefficients, equation (3.3.26) can be transformed into the following form:

$$\frac{\partial \hat{V}_T}{\partial H_{i,j}} = C4 \cdot H_{i,j} + \sum_r \sum_s H_{r,s}\ C5 \ , \quad (3.3.26a)$$

where the bending stiffness $C4 = \frac{Eh^3}{48(1-\nu^2)}((\frac{\alpha_i}{a})^2+(\frac{\alpha_j}{b^2}))^2 \cdot ab$.

C5 can be found by substituting equations (3.3.17) and (3.3.18) into equation (3.3.26).

From equation (3.3.9),

$$\frac{\partial \hat{T}}{\partial H_{i,j}} = \bar{m}\omega^2 (\frac{ab}{4}) H_{i,j} \qquad (3.3.27)$$

Substituting equations (3.3.26) and (3.3.27) in equation (3.3.12) gives $C_4 H_{i,j} + \sum_r \sum_s H_{r,s} C5 - \bar{m}\omega^2 (\frac{ab}{4}) H_{i,j} = 0$.
This can be expressed in matrix form as

$$[SK]\{H\} - \omega^2 [MASS]\{H\} = \underline{0} \qquad (3.3.28)$$

where [SK] is a dynamic stiffness matrix,
and [MASS] is a diagonal mass matrix.

This is a standard eigenvalue problem. Natural frequencies (ω) can be found by solving equation (3.3.28) in an iterative way.

3.4 SHAPE FUNCTIONS FOR IN-PLANE DISPLACEMENTS

The choice of shape functions depends on the in-plane boundary conditions. A study on the vibration of a curved beam indicates that the following shape functions are suitable for use in the Rayleigh-Ritz analysis for the symmetrical vibration modes.

2

MICROCOPY RESOLUTION TEST CHART
NBS 1010a
ANSI and ISO TEST CHART No. 2

(i) For normally fully restrained boundary conditions, $f_{ui}(x) = \sin(\frac{2i\pi x}{a})$ and $g_{vi}(y) = \sin(\frac{2i\pi y}{b})$ are satisfactory since these will give zero values at the restrained edges and the centrelines of the plate (axes of symmetry), as shown in Figure 3.4.1.

Figure 3.4.1

(ii) For normally free or partially restrained boundaries, in addition to the above functions, the following functions are also used to allow for the displacement at the edges:

$$f_{uo}(x) = (\frac{x}{a} - \frac{1}{2}) \quad , \quad g_{vo}(y) = (\frac{y}{b} - \frac{1}{2}) .$$

The shape of these functions is shown in Figure 3.4.2.

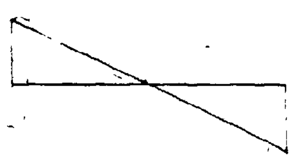

Figure 3.4.2

(iii) For tangentially fully restrained boundary conditions the following shapes (shown in Figure 3.4.3) are satisfactory:

$$f_{vi}(x) = \text{Sin}\left(\frac{(2i-1)\pi x}{a}\right),$$

$$g_{ui}(y) = \text{Sin}\left(\frac{(2i-1)\pi y}{b}\right).$$

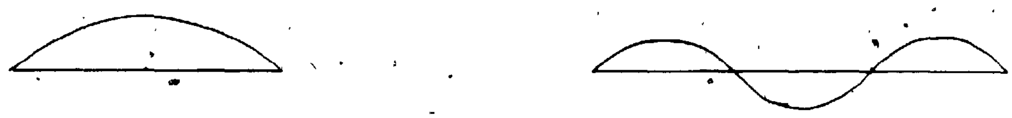

Figure 3.4.3

(iv) For tangentially free or partially restrained boundaries, the following functions are used, in addition to the above functions, to allow for the edge displacements (see Figure 3.4.4):

$$f_{vo}(x) = 1.0 \;, \; g_{vo}(y) = 1.0$$

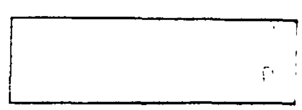

Figure 3.4.4

The same shape functions may be used in the static displacement calculation and vibration analysis if the boundary conditions remain unchanged. For a partially restrained edge, the shape functions are the same as that for an in-plane free edge. The effect of restraining stiffness is taken into account by adding the extra energy spent in working against the restraining boundary forces as in equation 3.3.7. Numerical results indicate that if the restraining stiffness is very high, the displacement coefficients which contribute to the work of restraint at the boundary approach zero. This results in shapes that approach the shapes for the fully restrained boundaries.

3.5 GENERAL OUTLINES OF A COMPUTER PROGRAM TO SOLVE THE RAYLEIGH-RITZ MINIMIZATION EQUATION FOR THE POST BUCKLING AND VIBRATION ANALYSIS

A Fortran program has been developed to solve the equations derived in sections 3.2 and 3.3. Some features and limitations of this program are outlined in the following paragraphs.

The static displacements and in-plane stress (and strain) distribution due to the applied load are calculated in the first part of the program. Using these calculated values, the natural frequencies and mode shapes are calculated in the second part.

Computation of Static Displacements

The in-plane displacement shape functions are set up using the subroutine SETUP. The program and all the integral subroutines are capable of generating and analytically integrating the products of, any combination of the following shapes:

f_1 = Constant

$f_2 = \mathrm{Sin}(\frac{\alpha x}{a})$

$f_3 = \mathrm{Cos}(\frac{\alpha x}{a})$

It is possible to approximately derive the function

$$f_4 = (\frac{x}{a} - \frac{1}{2}) \approx a_1 \mathrm{Sin}(\frac{\varepsilon x}{a}) - a_2 \mathrm{Cos}(\frac{\varepsilon x}{a})$$

where $a_1 = \frac{1}{2}\mathrm{Cos}(\frac{\varepsilon}{2})$, $a_2 = \frac{1}{2}\mathrm{Sin}(\frac{\varepsilon}{2})$

in which $\varepsilon \to 0$.

The computation of the coefficients of [SZ] and [ZB] in the equation (3.2.25) requires several subroutines of the integral of products such as,

$$\int_{x=0}^{a} f(x)\mathrm{Cos}(\frac{\alpha x}{a})\mathrm{Cos}(\frac{\beta x}{a})\,dx$$

$$\int_{x=0}^{a} f'(x)\mathrm{Cos}(\frac{\alpha x}{a})\mathrm{Cos}(\frac{\beta x}{a})\,dx$$

$$\int_{x=0}^{a} \mathrm{Cos}(\frac{\alpha x}{a})\mathrm{Cos}(\frac{\beta x}{a})\mathrm{Cos}(\frac{\gamma x}{a})\mathrm{Cos}(\frac{\delta x}{a})\,dx .$$

The computation of these integrals is carried out in the subroutines analytically based on the following five relationships.

(1) $$\int_0^a \mathrm{Cos}(\frac{\alpha x}{a}) = \frac{a}{\alpha}\mathrm{Sin}(\alpha) \quad \text{if } \alpha \neq 0$$
$$= a \quad \text{if } \alpha = 0$$

(2) $$\int_0^a \mathrm{Sin}(\frac{\alpha x}{a}) = \frac{a}{\alpha}[1-\mathrm{Cos}(\alpha)]$$

(3) $\sin(\frac{\alpha x}{a})\sin(\frac{\beta x}{a}) = \frac{1}{2}\cos[\frac{(\alpha-\beta)x}{a}] - \frac{1}{2}\cos[\frac{(\alpha+\beta)x}{a}]$

(4) $\cos(\frac{\alpha x}{a})\cos(\frac{\beta x}{a}) = \frac{1}{2}\cos[\frac{(\alpha-\beta)x}{a}] + \frac{1}{2}\cos[\frac{(\alpha+\beta)x}{a}]$

(5) $\cos(\frac{\alpha x}{a})\sin(\frac{\beta x}{a}) = \frac{1}{2}\sin[\frac{(\alpha+\beta)x}{a} - \frac{1}{2}\sin[\frac{(\alpha-\beta)x}{a}]$

Repeated application of the last three relationships gives the integrals of multiple products of trigonometric functions. This is done in the program using simple subroutines.

The out-of-plane and in-plane displacement functions used in the program are correct for symmetric out-of-plane displacements. To include anti-symmetrical terms, the set up of out-of-plane shape angles (α_x, β_x etc.) that are currently set to take only odd multiples of π must be altered. The set up of in-plane shape functions must also be corrected accordingly. The integral in equation (3.3.13d) involves the calculation of the stiffness of the supporting frame. This integration has been done numerically using a computer program STIFCAL which is attached in Appendix G. Analytical derivations associated with this, based on the slope deflection analysis of the frame is attached in Appendix H.

The effect of the mass of the loading head is introduced as a spring stiffness. The justification for this is explained in Appendix I.

The listing of the program and a typical output are attached in Appendix J for completeness.

CHAPTER 4

EXPERIMENTAL PROCEDURES

4.1 INTRODUCTION TO THE EXPERIMENTS

The object of the experiments conducted was to measure the first few natural frequencies and the out-of-plane deflection profiles of thin rectangular plates under various in-plane loadings and prescribed boundary conditions.

Providing the boundary conditions that can be accurately and conveniently modelled in the theoretical analysis was a difficult task. In the theoretical analysis, out-of-plane simply supported boundaries can be treated more conveniently than any other type of boundaries. For this reason, it was decided to design the experimental apparatus to provide simply supported boundaries along all four edges.

A Denison loading machine was used to apply the in-plane loading for most of the plates tested as shown in Figure 4.1.1. In one case, however, 'weights' were used to apply the load as shown in Figure 4.1.2 because, for the test plate used in that experiment, the buckling load was too small for the efficient use of the Denison machine. Tests were carried out at loads that were higher than the lowest buckling load in most cases and in one case (a 0.86 mm thick plate) the plate was loaded up to more than four times the lowest

Figure 4.1.1 Testing Rig in the Loading Machine

Figure 4.1.2 An Experimental Setup for a thin Plate

buckling load.

Non contacting, electro-magnetic transducers were used to excite the plates in vibration and to pick up the response which was then transmitted to an oscilloscope for visual observation as explained in section 4.3. A capacitance displacement transducer was used to measure the out-of-plane static displacements. In one case, the static strain distribution was measured. Details of the methods of measurement are given in section 4.3.

4.2 DESIGN OF THE TESTING RIG

The design of the testing rig was governed by the following requirements:

(1) to hold the plate in a suitable position with respect to the loading machine and to transfer the load smoothly to the plate;

(2) to provide the necessary boundary conditions at the edges of the plate;

(3) to allow the attachment of a displacement measuring device.

The rig (Figure 4.2.1) was made of four (76.2 x 31.75 x 6.35 mm) channel sections welded together to form a rectangular frame. A detachable circular loading head with two stout circular bars which could slide through two collars

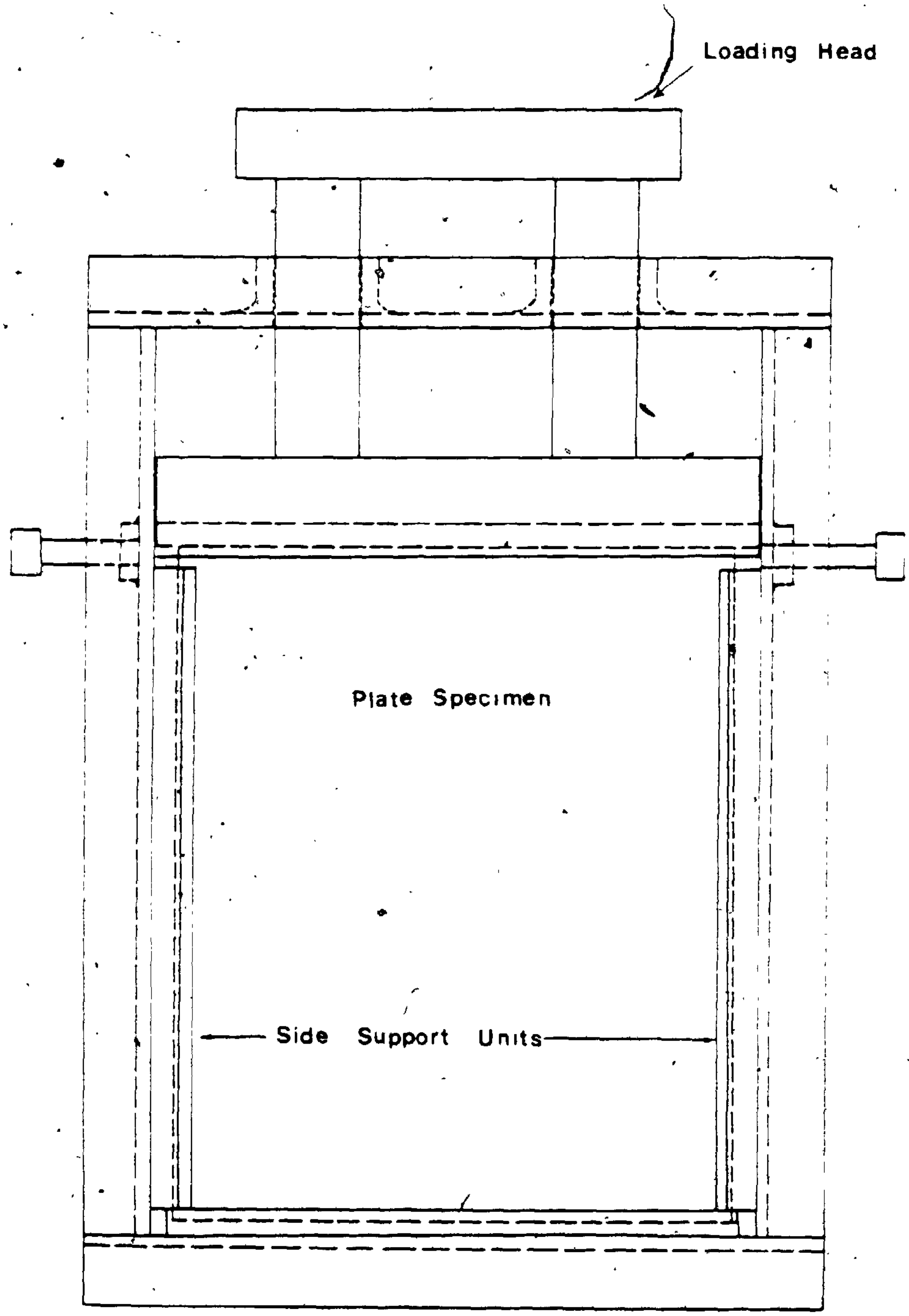

Figure 4.2.1 The Testing Rig

mounted on top of the channel was provided for transferring the load. The rods rested on top of a 'V' groove support, as shown in Figure 4.2.2. The bottom support was also a 'V' groove which was firmly attached to the channel base. The top and bottom edges of most of the test plates were machined to form knife edges which allowed rotation to take place. This arrangement closely satisfied the requirements for simply supported boundaries.

The top and bottom supports were very rigid. This setup was expected to constrain the normal in-plane displacements to be constant during loading. However, the flexibility of the supports was considered in the theory in an approximate manner. (The results obtained were very close to the results for a plate with absolutely constant edge displacements.)

To isolate the machine vibration, three layers of rubber were used between the loading machine and the loading head. One piece of rubber was 12.7 mm thick and the other two were somewhat thinner. The rubber, while transmitting the static force supplied by the loading machine, essentially eliminated any contribution from the machine to the in-plane constraint normal to the top edge of the plate during vibration. Initially, it had been intended that the top edge should have been considered as essentially in-plane clamped both experimentally and theoretically. However, the effect of the isolation was to cause the in-plane boundary condition along

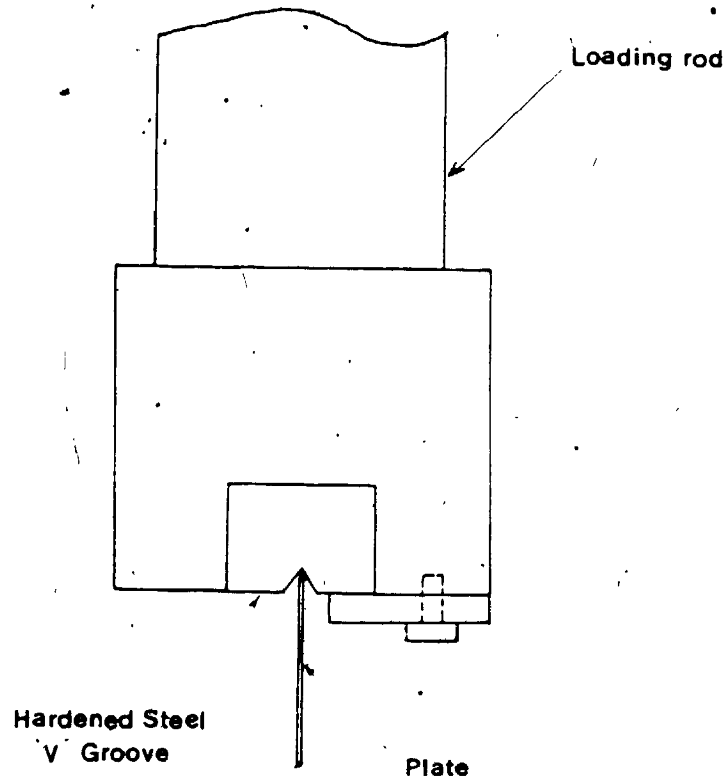

Figure 4-2-2 · Supporting Arrangment at the Top Edge the top edge to become one of constant in-plane motion normal to the edge. The tangential restraint was preserved, however. The vibration of the mass of the loading head provided some restraint which was calculated in an approximate manner, as explained in Appendix I and is included in the analysis.

The supporting arrangement for the sides consisted of two rows of ball bearings on 'V' grooves holding the plate on each side of both vertical edges as shown in Figure 4.2.3. By carefully adjusting the side screws, the contact force between the plate and the ball bearings could be minimized so that the plate could move freely in its plane and could rotate without significant restraint. However, the frictional restraint was not completely avoidable as the side screws had to be sufficiently tightened to straighten the plate edges and to hold the plate in the correct position. This was evident from the load-deflection graphs in Chapter 5, where a hysteresis can be observed. Under static loading, additional contact forces might have been induced as the ball bearings restrained the bending of the plate. It is believed that the frictional resistance generated by this increase in the contact force, was likely to be substantially smaller than the forces that were required to prevent static in-plane displacements normal to the plate edge. Therefore, the ball bearings did not prevent the slippage of the plate during loading. Tangential in-plane displacements could easily take place, since the balls could roll along the 'V' grooves.

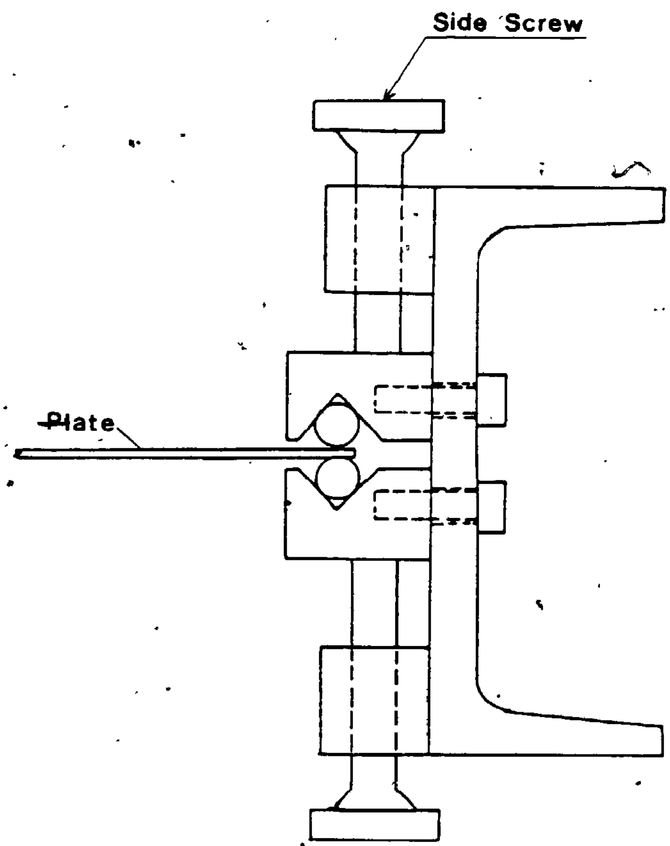

Figure 4.2.3 Side Support

Some grease was applied to the ball bearings to minimize the friction. This arrangement was expected to minimize the loss of applied load through friction at the sides.

In-plane boundary conditions for the vibration were different. Since the amplitude of vibration was very small compared to the amplitude of the static displacement, the forces that were necessary to prevent slippage of the plate at the ball bearings were also small. The contact forces which were induced during the static loading, were likely to have provided sufficient frictional restraint against normal slippage. This however, does not mean that the ball bearings provided a fully normally restrained boundary, since the supporting frame has some flexibility. An equivalent boundary stiffness calculation is explained in Appendix H, to model this partial restraint. In this calculation, the inertia of the frame has been neglected. To simplify the analysis, the 'V' groove supports are considered to run over the full length of the frame (in calculating the second moment of area of the section), although in the experiment the 'V' grooves terminated just below the top support. The effect of making these simplifications is expected to be negligible.

Some experiments were carried out with another type of side support, where the ball bearings were placed on two channel grooves instead of 'V' grooves as shown in Figure 4.2.4. In this arrangement, rolling of the ball bearings

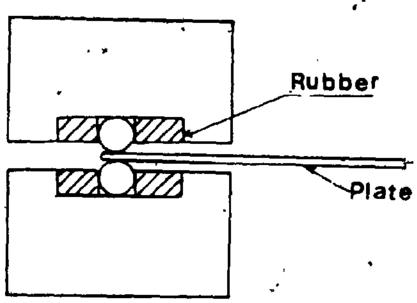

Figure 4.2.4 Channel Groove

across the groove was allowed by placing these between two strips of rubber. It was expected that this would reduce the resistance to in-plane displacement normal to the edges. However, it was found that the natural frequencies were significantly higher than the predicted values even at zero loading in some cases. The discrepancy was found to be random in nature and seemed to change each time the side supports were reset. It is thought that a misalignment of the ball bearings may have resulted in non-straight supports which would effectively apply some rotational restraint. Use of firm rubber strips, precisely cut to fill the gap between the ball bearings and the sides of the channel groove, may help to overcome this problem.

4.3 METHODS OF MEASUREMENTS

Natural Frequencies

A power signal generator (Brüel & Kjaer signal generator, type 1024) and an electro magnetic transducer were used to excite the plates. Another magnetic transducer picked up the response signal, that was observed using an oscilloscope (Phillips PM3232). Both transducers were mounted on an adjustable stand with a clamping arrangement (Retort stand and clamp). These probes were placed near different points on the plate to observe various modes of vibration. Figure 4.1.2 shows this setup. In some of the experiments, the output signal from the transducer was sent to the oscilloscope through a frequency filter (KROHN-HITE, Model 3500 filter). The frequencies of the input signal were measured using a Hewlett Packard 3734 electronic counter.

Deflection Profile

A capacitance probe was connected to a digital display unit (Hitec Proximic 3101-SP), which indicated the distance between the probe and the plate in units of 0.0254 mm (1/10,000 of an inch) directly. The deflection was measured at each point of intersection of the grid lines marked on the plates, and at a number of points as close to the edges as possible. Figure 4.3.1 shows the points on the plates, where the deflections were measured. Figure 4.3.2 illustrates this experimental setup.

The capacitance probe was mounted on an aluminum block holder. This holder could move along a horizontal bar which could be slid vertically on two parallel circular bars. These bars were attached to the channel frame by adjustable screws. The screws were adjusted to set the orientation of the vertical bars so that they were parallel. A machined angle block was used as the reference surface for the initial setting up.

Strain Distribution

One plate specimen was fitted with 27 strain gauges on

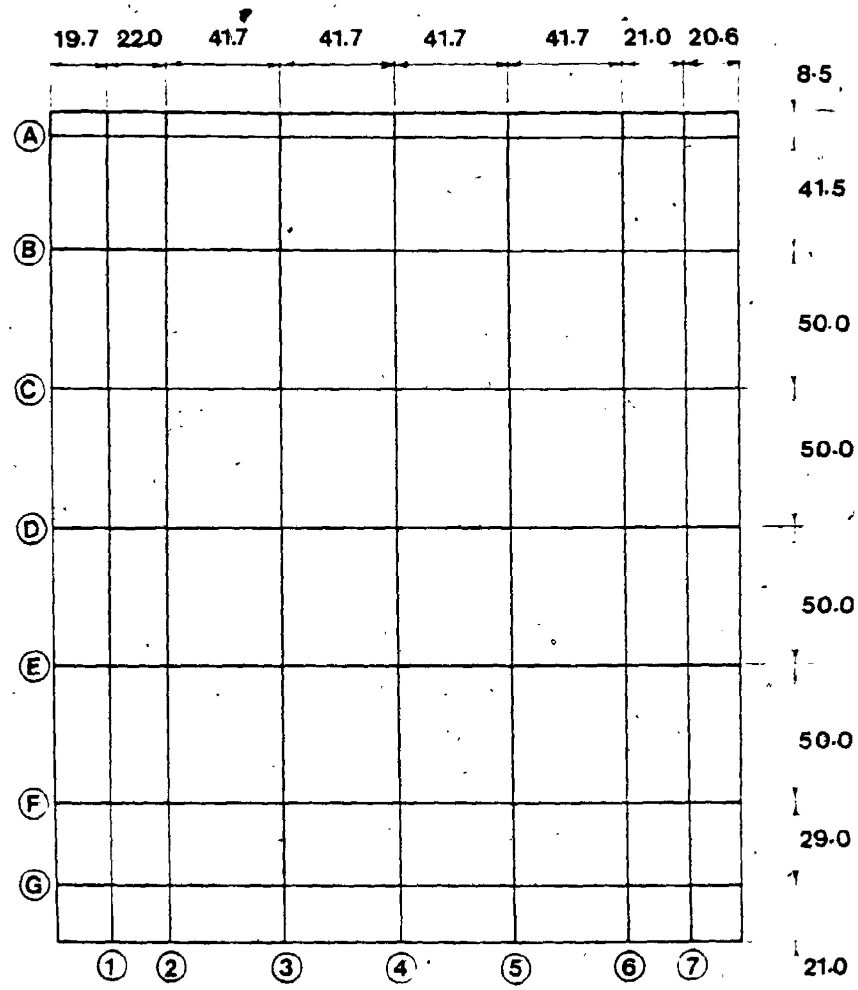

Figure 4.3.1 Grid lines for Deflection Measurements

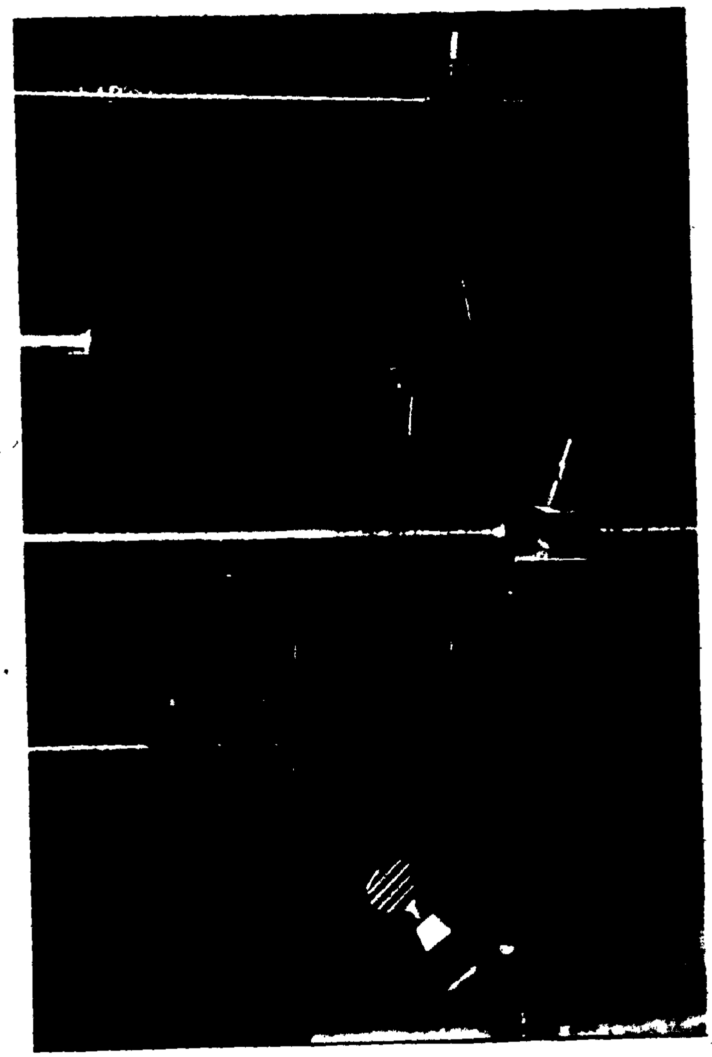

Figure 4.3.2 Deflection Measurement

each side at corresponding points to measure the strains. 6.35 mm (1/4 inch) strain gauges with a gauge factor of 2.1 were used. The gauges were connected to a balancing unit with digital display through six multi-channel switching units. Strain readings were taken at various loads. The average value of strains on both sides of the plate at a point gives the in-plane strain. The difference between the two gives twice the value of the maximum bending strain at the surface. The detailed results of the strain measurements are given in Appendix B. The measured in-plane strain variation at each point is compared with the theoretical values in Chapter 5. Figure 4.3.3 shows the plate with strain gauges. The locations of these gauges are shown in Figure 4.3.4.

Loading

The load was measured using the dial on the Denison machine (except for the 0.56 mm plate which was loaded using weights). The accuracy of this scale was first verified using a load cell (for up to 800 lbs).

4.4 PLATE SPECIMENS

Six mild steel rectangular plates with thickness ranging from 0.56 mm to 1.15 mm were tested. The properties of the mild steel were taken as follows:

Figure 4.3.3 Plate with Strain Gauges

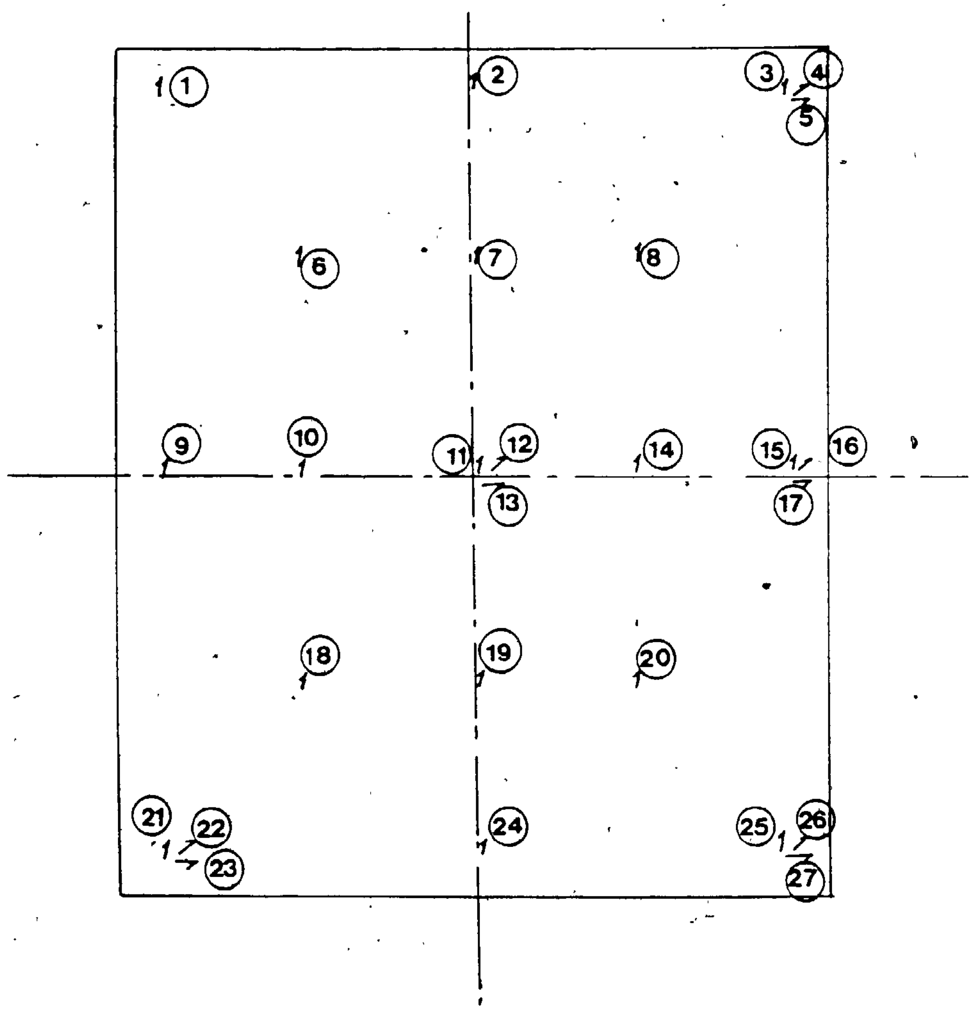

Figure 4.3.4 Locations of Strain Gauges

Young's modulus E = 207 MPa

Poisson's ratio ν = 0.3

Density = 7.738 kg/m^3

The density was taken from the measurements of weight and area. The Young's modulus and Poisson's ratio were assumed to be the normal values which are given in standard specifications.

All plates had overall dimensions of 0.3 m x 0.256 m. The distance between the centreline of the vertical rows of ball bearings was 0.25 m. The extra 6 mm in the width of the plates were allowed for placing in the rig.

The thicknesses of the plates are listed in the table below with identification numbers which will be used from hereonwards.

Plate Identification Number	Thickness (mm)
1 (fitted with strain gauges)	1.0
2	1.0
3	1.0
4	0.86
5	1.15
6	0.56

Plate 1 was fitted with strain gauges after the completion of the frequency measurement, so that the mass of the wires would not influence the natural frequencies.

CHAPTER 5

RESULTS AND DISCUSSION

5.1 THEORETICAL RESULTS

Comparison With Existing Results

Before comparing the experimental and theoretical results, it is necessary to study the accuracy of the theoretical results. Unfortunately, the theoretical results which exist in the literature can not be compared directly with the experimental results, since their applicability is limited to certain standard boundary conditions. To establish confidence in the theoretical approach used in this thesis, results obtained for some simple cases are compared with existing theoretical results or results generated using a package finite element program.

The static displacement values computed by using the Rayleigh-Ritz analysis will be compared with the results published by Yamaki [26] for simply supported out-of-plane boundary conditions and the following in-plane boundary conditions:

(i) Loaded edges free to slide tangentially (no shear) and having constant normal displacement.

(ii) Sides free in both directions (normally and tangentially).

Yamaki's results were obtained for a square plate with Poisson's ratio (ν) of 1/3. Results from the Rayleigh-Ritz analysis for the same plate with zero initial imperfection are compared with Yamaki's results in Table 5.1.1. In the table, the actual deflection of the plate is given by

$$z(x,y) = Z_{1,1} \operatorname{Sin}(\frac{\pi x}{a}) \operatorname{Sin}(\frac{\pi y}{b}) + Z_{3,1} \operatorname{Sin}(\frac{3\pi x}{a}) \operatorname{Sin}(\frac{\pi y}{b}) + Z_{1,3} \operatorname{Sin}(\frac{\pi x}{a}) \operatorname{Sin}(\frac{3\pi y}{b}) + Z_{3,3} \operatorname{Sin}(\frac{3\pi x}{a}) \operatorname{Sin}(\frac{3\pi y}{b}).$$

TABLE 5.1.1 Comparison of Theoretical Values of Static Displacements

	LOAD RATIO	CENTRAL* DEFLECTION	DEFLECTION COEFFICIENTS			
			$Z_{1,1}$	$Z_{3,1}$	$Z_{1,3}$	$Z_{3,3}$
Rayleigh-Ritz	1.456	3.850	4.419	0.385	0.338	0.154
Yamaki's	1.456	3.905	4.500	0.423	0.345	0.172

The agreement between the two results is good. The discrepancy in the central deflection is only about 1.4%. The Rayleigh-Ritz solution was obtained with four symmetrical out-of-plane displacement coefficients and twenty-five in-plane displacement coefficients. The Rayleigh-Ritz method usually gives a lower bound solution for the displacement. This was verified in a convergence study for the case of an experimental plate discussed later in this chapter.

The natural frequencies calculated by using the Rayleigh-Ritz method were to be compared with results from a finite element package program [35] which was applicable to analyze unstressed shells. A preliminary analysis using this program illustrated the significance of in-plane boundary conditions. The results for the fundamental natural frequencies of plate 1, under simply supported out-of-plane boundary conditions and various in-plane boundary conditions without any in-plane stress are given in Table 5.1.2. It can be observed that the frequency increases with restraining the boundaries.

In the finite element program, making use of symmetry, a quarter of the plate was divided into fifty triangular elements. The static shape of the plate was taken as

$$z = 0.8 \, \mathrm{Sin}\left(\frac{\pi x}{a}\right) \mathrm{Sin}\left(\frac{\pi y}{b}\right) \text{ mm.}$$

TABLE 5.1.2 Finite Element Results for Plate 1

In-plane Boundary Conditions	Fundamental Natural Frequency (Hz)
All edges in-plane free (normally and tangentially).	73.12
All edges tangentially free, normally constrained to move with constant displacement.	79.84
All edges normally free, tangentially restrained (Shear Diaphragm).	80.37
All edges normally restrained, tangentially free.	109.19
All edges normally and tangentially restrained.	109.30
Long edges free, short edges normally and tangentially restrained.	83.69
Long edges free, short edges normally restrained.	82.18
Flat Plate	66.71

The analytically calculated value of the fundamental frequency of the flat plate was 66.65 Hz. This agrees well with the finite element result of 66.71 Hz.

The curvature has increased the frequency for all in-plane boundary conditions. From Table 5.1.2, it is clear that any restraint at the boundary increases the frequency of a curved plate. It can also be observed that for a plate with normally restrained edges, tangential restraining does not change the frequency significantly.

The frequencies for various magnitudes of curvature for a plate with short edges normally restrained and long edges in-plane free are tabulated along with the amplitude of static deflection in Table 5.1.3. The deflection parameter μ, is given by μ = deflection at the centre/plate thickness h. The shape of the plate is $z = \mu \cdot h \cdot \mathrm{Sin}(\frac{\pi x}{a}) \cdot \mathrm{Sin}(\frac{\pi y}{b})$.

TABLE 5.1.3 Variation of Frequency With Curvature Using Finite Element Package Program

μ	0.2	0.475	0.588	0.80	0.95
Fundamental Frequency $\omega_{1,1}$ (Hz)	67.79	72.57	75.49	82.18	87.67

It is useful at this stage to introduce a frequency parameter λ^2 which is defined by $\lambda^2 = (\omega_{1,1}/\Omega_{1,1})^2$,

where $\omega_{1,1}$ and $\Omega_{1,1}$ are the theoretical values of the fundamental natural frequencies of a curved plate and the corresponding flat plate respectively.

λ^2 is plotted against μ^2 (which will be called the deflection parameter from hereonwards) in Figure 5.1.1. It

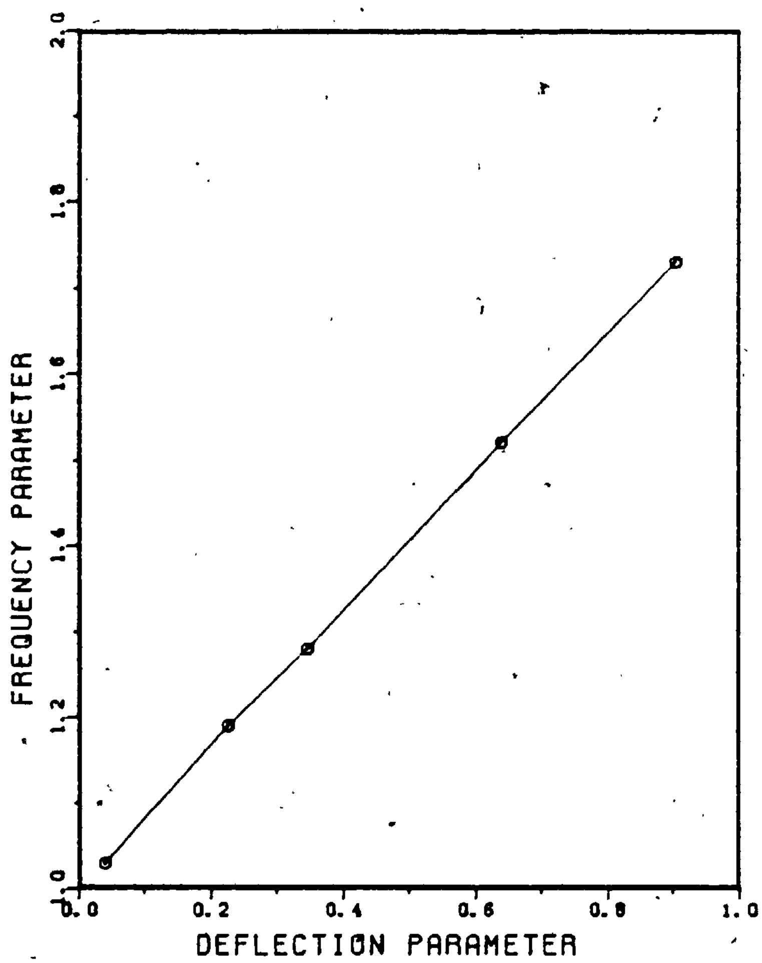

Figure 5.1.1 Finite Elements Result for Plate 1

is clear that the frequency parameter varies approximately linearly with the deflection parameter.

i.e. $\lambda^2 = 1 + k\mu^2$,

where k is the gradient of the straight line in Figure 5.1.1. The corresponding numerical values are given in Table 5.1.3a.

TABLE 5.1.3a Variation of λ^2 vs μ^2 Using Finite Element Program for In-Plane Free Short Edges and Normally Restrained Long Edges

μ^2	0.040	0.226	0.346	0.640	0.903
λ^2	1.03	1.19	1.28	1.52	1.73

As mentioned earlier, the use of Galerkin's method was explored for calculating the frequencies to be compared with the experimental results. However, due to difficulties encountered in modelling the experimental boundary conditions in the stress formulation, this approach was abandoned in favour of the Rayleigh-Ritz method. Nevertheless, certain results are included here for completeness.

The finite element results for the in-plane boundary conditions listed below are compared with results obtained using Galerkin's method (described in Appendix A) in Table 5.1.4, for $\mu = 0.8$.

The in-plane boundary conditions:

case (i) - All edges in-plane free.

case (ii) - All edges normally free, tangentially restrained.

TABLE 5.1.4 Comparison of Fundamental Natural Frequencies Obtained by Using Galerkin's Method and Finite Element Program

In-Plane Boundary Condition	Case (i)	Case (ii)
Finite Element Result	73.12 Hz	80.37 Hz
Galerkin's Method Result	73.16 Hz	81.67 Hz

In both cases, the agreement between the results is reasonably good. Galerkin's method was used with one out-of-plane displacement term only. A multi-term result may improve the agreement. Results for higher values of curvature were not calculated since the single term solution was not expected to give good results at high curvatures.

The results from the Rayleigh-Ritz method with undetermined displacement coefficients are compared with the corresponding finite element results for a stress free curved plate in Table 5.1.5. The Rayleigh-Ritz results were obtained using seventeen in-plane displacement shapes with one or four fully symmetric out-of-plane displacement shapes. The following in-plane boundary conditions were treated:

case (iii) - All edges fully restrained in-plane,

case (iv) - Short edges fully restrained, long edges in-plane free.

TABLE 5.1.5 Comparison of Fundamental Natural Frequencies Obtained By Using the Rayleigh-Ritz Method and Finite Element Method

μ		0.8		5.0	
In-Plane Boundary Condition		Case (iii)	Case (iv)	Case (iii)	Case (iv)
Finite Element Result		109.3	83.69	439.73	288.02
Result Using the Rayleigh-Ritz Method	one out-of-plane term	110.01	83.81	510.16	324.45
	four out-of-plane terms	109.88	83.62	434.03	287.10

The agreement between the results from both methods is good. The Rayleigh-Ritz method gives an upper bound for the frequencies. Non-conforming elements were used in the finite element method, thus it is not certain whether the frequencies determined are upper bounds or not.

This illustrates that the Rayleigh-Ritz method with undetermined displacement coefficients can be used satisfactorily for the calculation of the natural frequencies of curved plates.

A Note On the In-Plane Boundary Conditions At The Top And Bottom (Loaded) Edges of the Test Plates

In using the Rayleigh-Ritz method for the analysis of the experimental plates, the following simplification was made to reduce the computational effort, while taking into account the practical boundary conditions.

For static deflection calculations, the bending of the edge beams has been taken into account in an approximate manner. The beams at the top and bottom have different second moments of area, but the analysis is performed assuming symmetry about both axes through the centre of the plate. Therefore, a weighted average value of the stiffness is used. The bottom support is a part of the channel frame, but it has been taken as a simply supported beam. The load is applied at the top edge on two points as shown in Figure 5.1.2(a). The reactions at the bottom are at the edges of

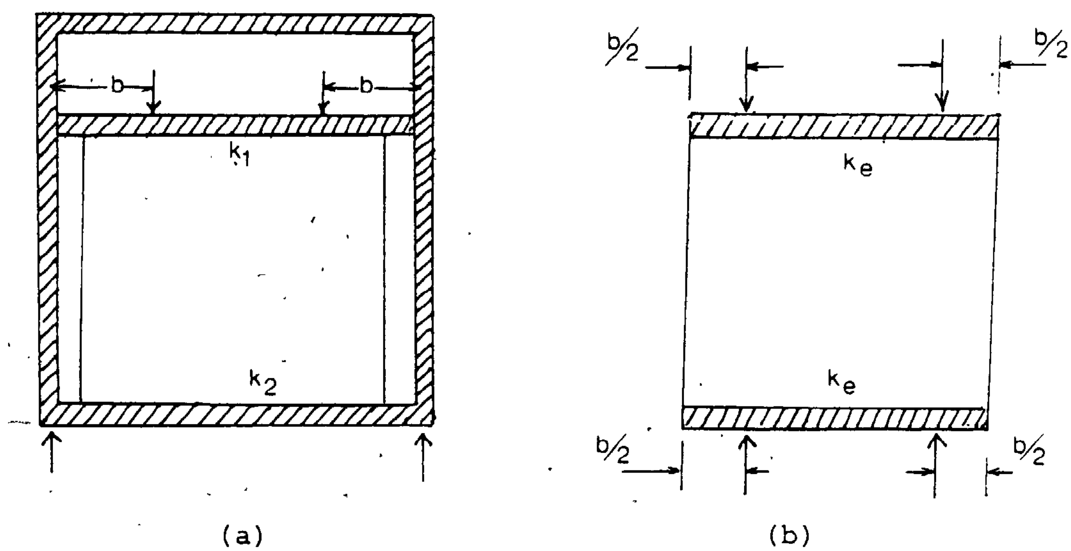

Figure 5.1.2

the beam which rests on two crossbars welded on the channel to keep the apparatus stable. In the analysis, the points of application of the load are taken as the midpoints between the bottom and top loading points. The approximate model is shown in Figure 5.1.2(b).

All these simplifications, however, are not likely to cause any significant error in the calculations, since the flexural rigidities of the edge beams are very high. This is illustrated in the following example. The results obtained using these simplifications (case (i)) are compared with those for a constant normal edge displacement (case (ii)) in Table 5.1.6, where it is seen that slightly lower deflections occur for the experimental condition than for the case of infinitely rigid supports. These results are given for plate 4, which had an initial imperfection μ_o of 0.47. The load ratio in Table 5.1.6 is defined as the in-plane load divided by the lowest buckling load (1967N in this case).

TABLE 5.1.6 Calculated Deflection Ratios For Plate 4

Load Ratio P/P_c	0.755	1.209	1.663	2.117	3.024	4.149
μ for case (i)	1.100	1.686	2.244	2.752	3.652	4.602
μ for case (ii)	1.109	1.708	2.270	2.781	3.676	4.620
Deviation (%)	0.8	1.3	1.2	1.1	0.7	0.4

5.2 COMPARISON OF EXPERIMENTAL AND THEORETICAL RESULTS

The experimental and theoretical results for plate 1 are compared graphically in Figure 5.2.1. The theoretical results were calculated using four fully symmetric out-of-plane displacement coefficients corresponding to the (1,1), (1,3), (3,1) and (3,3) modes, where the mode numbers (m,n) represent the number of half sine waves in x,y directions respectively. For in-plane displacement in x direction 3,4 terms were taken in x,y directions respectively. For in-plane displacement in y direction 3 terms in each direction were taken. (In the preliminary analysis, only three terms in each direction were taken for in-plane displacement in each direction. A fourth term for the constant displacement shape was included later to improve the accuracy of the solution.)

The variation of the measured and calculated values of the central deflection with load is illustrated in Figure 5.2.1a. The deflection parameter (μ^2) is defined as the square of the ratio of the central deflection to the thickness of the plate. The load ratio is the ratio of the in-plane load to the lowest critical load of the plate. The deflection measurement during unloading was generally higher than that during loading. This hysteresis is thought to be due to the friction at the ball bearings. The slippage at the ball bearings may have been prevented initially, until

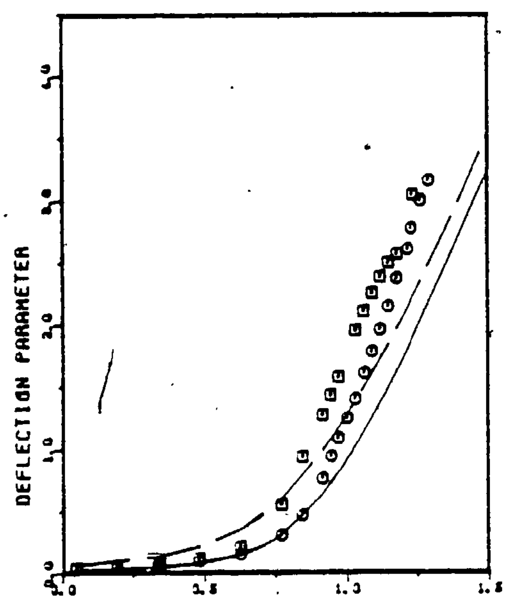

(a)

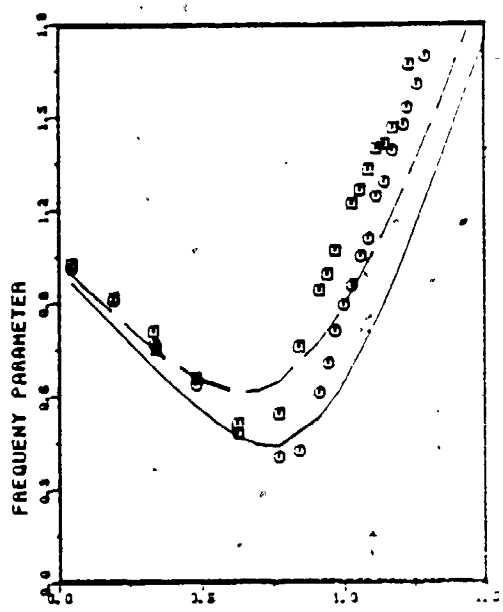

(b)

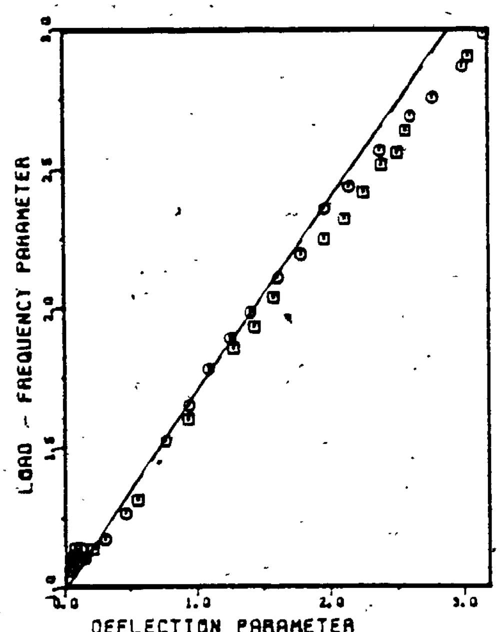

(c)

Legend for Figures 5.2.1 to 5.2.10

⊙- Experimental (loading)

⊡- Experimental (unloading)

— Theoretical

For Figures 5.2.1 to 5.2.3

— Theoretical for ω_o=0.15

— — Theoretical for ω_o=0.25

Figure 5.2.1 Results for Plate 1

sufficient in-plane forces developed to overcome the friction. The initial frictional forces that can be induced, depend on the tightening of the ball bearings. In later tests, grease was applied to the ball bearings which resulted in significant reduction in the hysteresis.

The theoretical values were calculated for initial imperfection amplitudes (μ_o) of 0.15 and 0.25. Southwell's method [33] was used to estimate the magnitude of the initial imperfection from the experimental data. The results from the data points for loading and unloading indicated initial imperfection magnitudes of 0.19 and 0.25 times the thickness respectively. (The data for the Southwell plots are given in Appendix B.) The magnitude of initial central deflection was also calculated by subtracting the displacement reading at the centre from the average of the displacement readings near the four corners of the plate prior to loading. This was found to be about 0.12 times the plate thickness. The discrepancy between this value and that indicated by Southwell's plot (0.19) may be due to the following factors:

(a) The bending of the plate may have resulted in some displacements near the corners where it was assumed to be zero.

(b) Although care was taken to set the side supports so that they were parallel, in most of the tests a small skew was present. This skew was calculated by taking the difference between the sums of the displacement readings near the corners on each diagonal. In most cases this skew was found to be less than 0.06 mm.

(c) Imperfections in the displacement measuring apparatus such as the bending of the guide frame on which the capacitance probe was mounted.

(d) In the theoretical analysis, all the initial imperfections are assumed to be of the form $z_o=\mu_o \cdot h \cdot \mathrm{Sin}(\frac{x}{a}) \cdot \mathrm{Sin}(\frac{y}{b})$. (It can also be expressed as a Fourier series. The first coefficients of this series were computed using the deflection measurements at all the grid points. These agreed very well with the magnitude of initial imperfection at the centre as shown in Table B.27.) The presence of other shapes of imperfection can influence the measurement of initial imperfection amplitude as well as the estimation of μ_o using Southwell's method. This is, however, not likely to change the results significantly at high loadings, since the effect of the actual magnitude of initial imperfection is not very significant at high loadings.

(e) Measurement of small values of displacement is less accurate than larger values. Southwell's method makes use of measured values of larger displacements, and therefore is considered to give a better estimation of the initial imperfection.

For the above listed reasons, the initial imperfection was estimated using Southwell's plot method whenever possible. For plate 4 and plate 6 however, this was not possible, because these plates had large initial imperfections.

Southwell's method is not applicable for plates with large initial imperfections since the membrane stretching affects the linearity of Southwell's plot. (It is not possible to draw a straight line through the data points.)

Figure 5.2.1b, shows the variation of the square of the non-dimensional natural frequency defined as the frequency parameter λ^2, where $\lambda^2 = \omega_{1,1}^2/\Omega_{1,1}^2$, in which $\omega_{1,1}$ is the measured fundamental natural frequency and $\Omega_{1,1}$ is the theoretical value of the fundamental natural frequency of the corresponding flat plate. The effect of friction can be seen on this plot also. The measured frequencies were higher than the calculated values generally. This is primarily due to the discrepancy between the calculated and measured values of the deflections. The calculated values of the deflections are smaller, thus causing smaller membrane stretching effect and hence lower frequencies.

Figure 5.2.1c shows the variation of the load-frequency parameter with deflection parameter. The load-frequency parameter is given by the summation of the load ratio and the frequency parameter ($P/P_c + \lambda^2$). It is interesting to notice that the experimental and theoretical results lie approximately on a straight line. Another interesting point is that the theoretical lines for μ_o=0.15 and μ_o=0.25 almost coincide with each other. The hysteresis in the experimental results has almost disappeared. This indicates that the discrepancy between the experimental and the theoretical results for the frequency is mainly due to the discrepancy in the deflections.

The results for plates 2 and 3 which had the same overall dimensions are shown in Figures 5.2.2 and 5.2.3 respectively. The measured imperfection in these cases varied between 0.14 and 0.25 times the plate thickness as indicated by Southwell's plot.

Tests were carried out on a thinner plate (plate 4 having 0.86 mm thickness) up to about three times the lowest critical load. The results are shown in Figure 5.2.4. Further tests with the same specimen were carried out for loads of up to 4.15 times the lowest critical load. The results are illustrated in Figure 5.2.5. For this plate, the initial imperfection was calculated using the displacement readings at the centre and at the corners, because it was not possible to draw a straight line in Southwell's format. The measured imperfection ratio was 0.47.

In Figures 5.2.4c and 5.2.5c, the end points of the theoretical results are connected to show the deviation of the results from a straight line. The slope of the theoretical curve increases with deflection. This increase may be attributed to the contribution from the vibration of the loading head. Since this plate is thinner than the previous ones, the restraint provided by the loading head, which

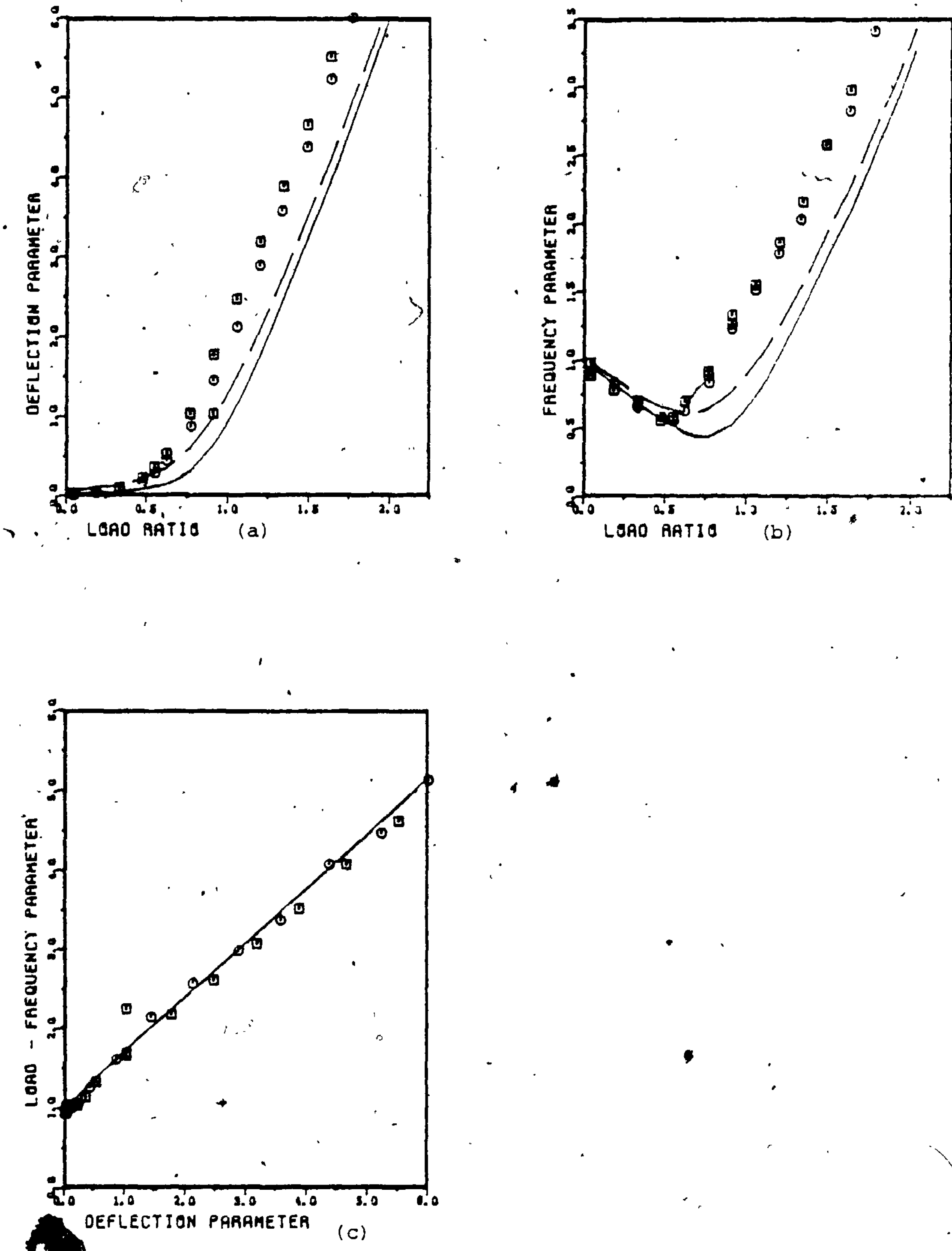

Figure 5.2.2 Results for Plate 2

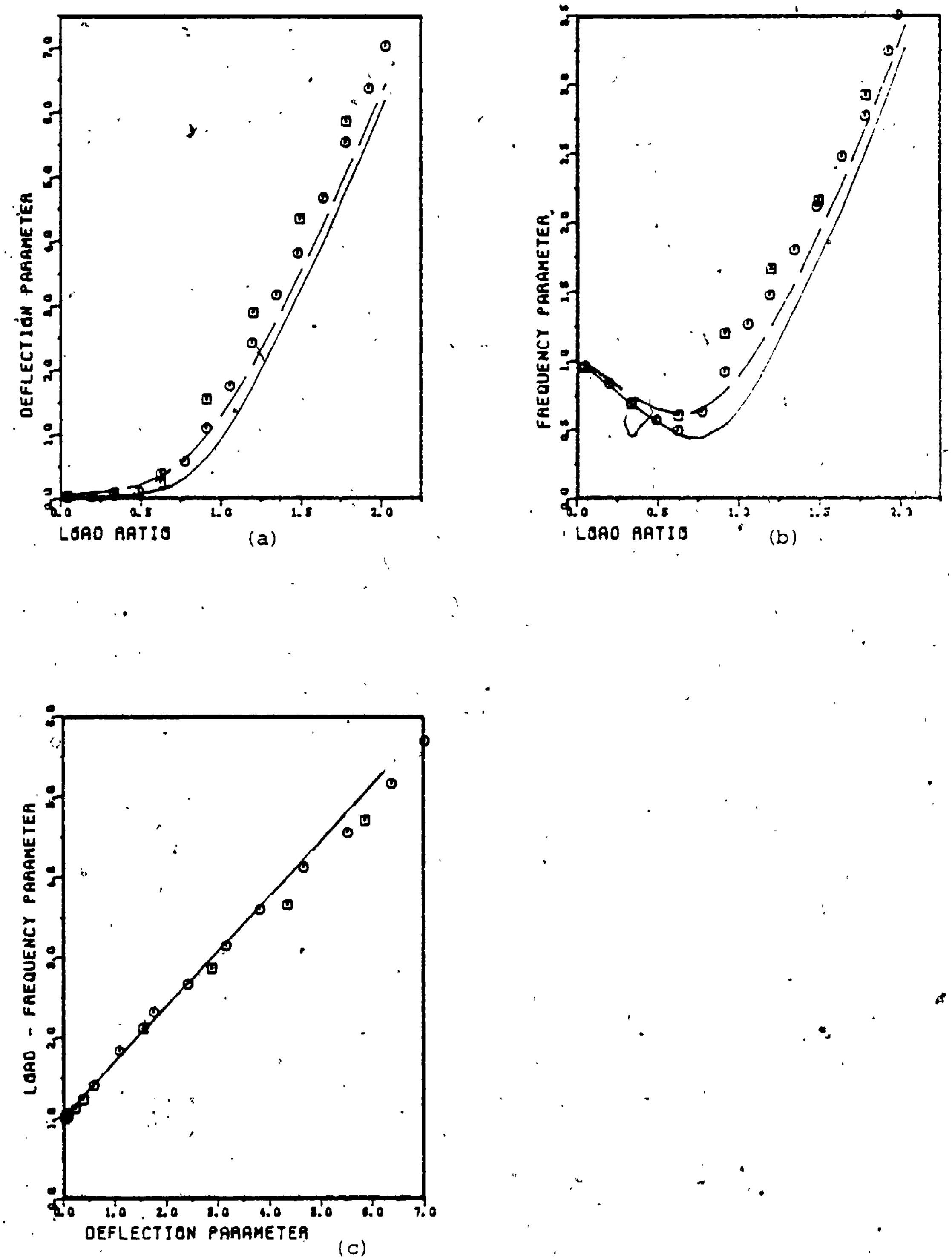

Figure 5.2.3 Results for Plate 3

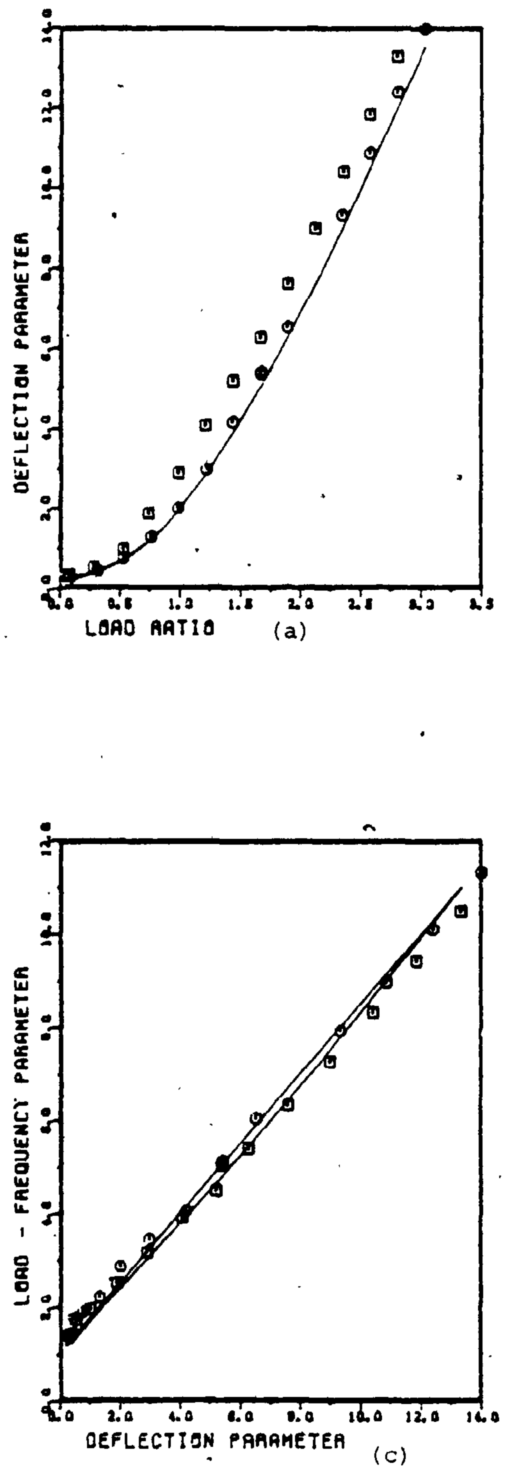

Figure 5.2.4 Results for Plate 4 (Test 1)

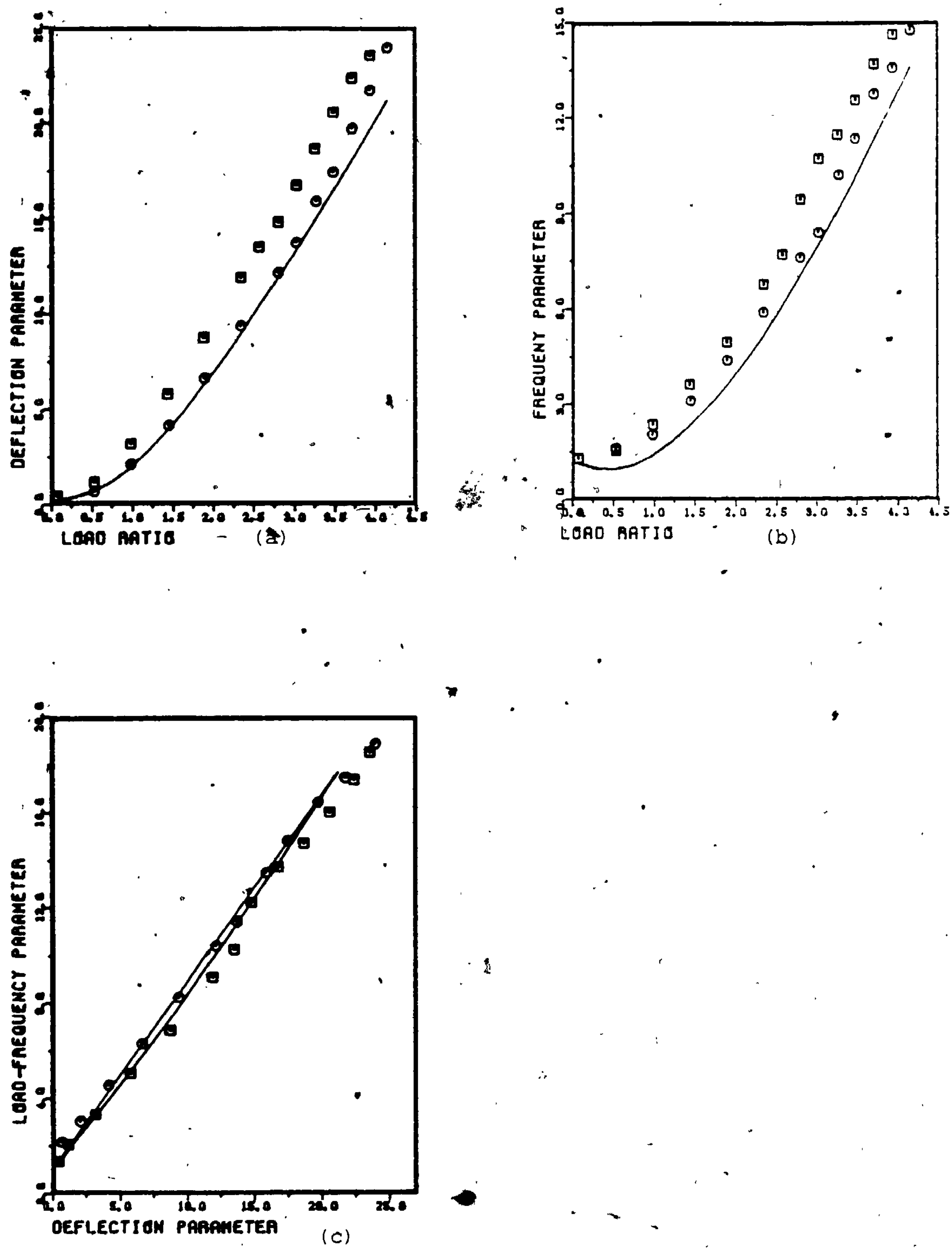

Figure 5.2.5 Further Results for Plate 4 (Test 2)

increases with the frequency, is higher than those for plates 1, 2 and 3. For plate 4, the agreement between the experimental and theoretical results is excellent. A further improvement in the agreement was observed when nine out-of-plane displacement coefficients and thirty-two in-plane displacement coefficients were included in the analysis as shown in Table 5.2.1.

TABLE 5.2.1 Theoretical and Experimental Results for Plate 4 At a Load Ratio of 4.15

	μ	$\omega_{1,1}$ (Hz)
Theoretical - 4 term	4.60	211.16
Theoretical - 9 term	4.79	215.49
Experimental	4.89	220.0

The deviation in the central deflection reduced from 6% to 2% and the deviation in the frequency reduced from 4% to 2% when the number of out-of-plane displacement coefficients was increased from four to nine.

Test results for plate 5 are shown in Figures 5.2.6 to 5.2.8. The thickness of the plate was 1.15 mm. After the first two tests were carried out, it was found that there was some gap between the plate and the ball bearings at the bottom on one side. (This was found as rattling was observed when the amplitude of excitation was increased which resulted in some disturbance on the oscilloscope

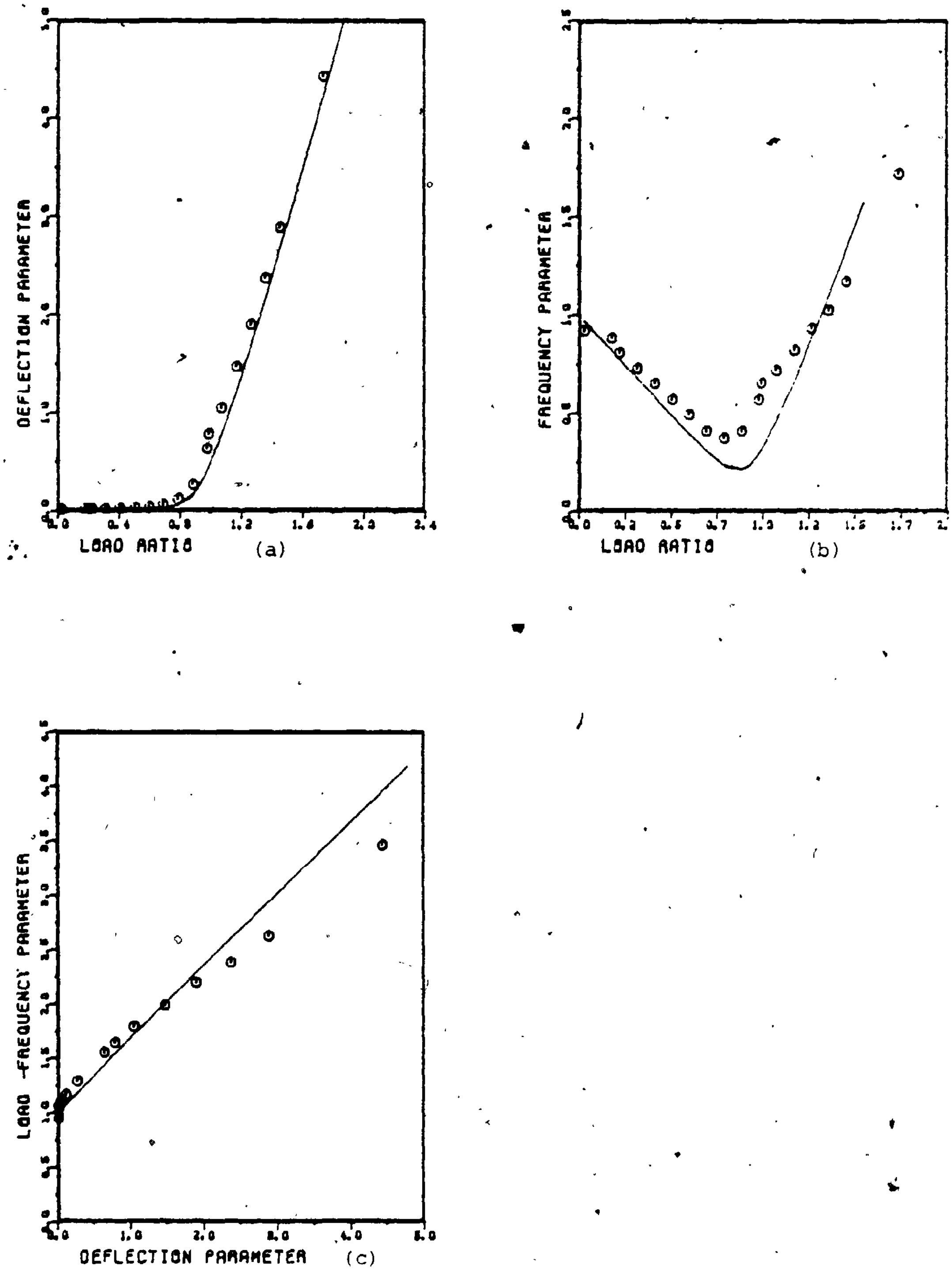

Figure 5.2.6 Results for Plate 5 (Test 1)

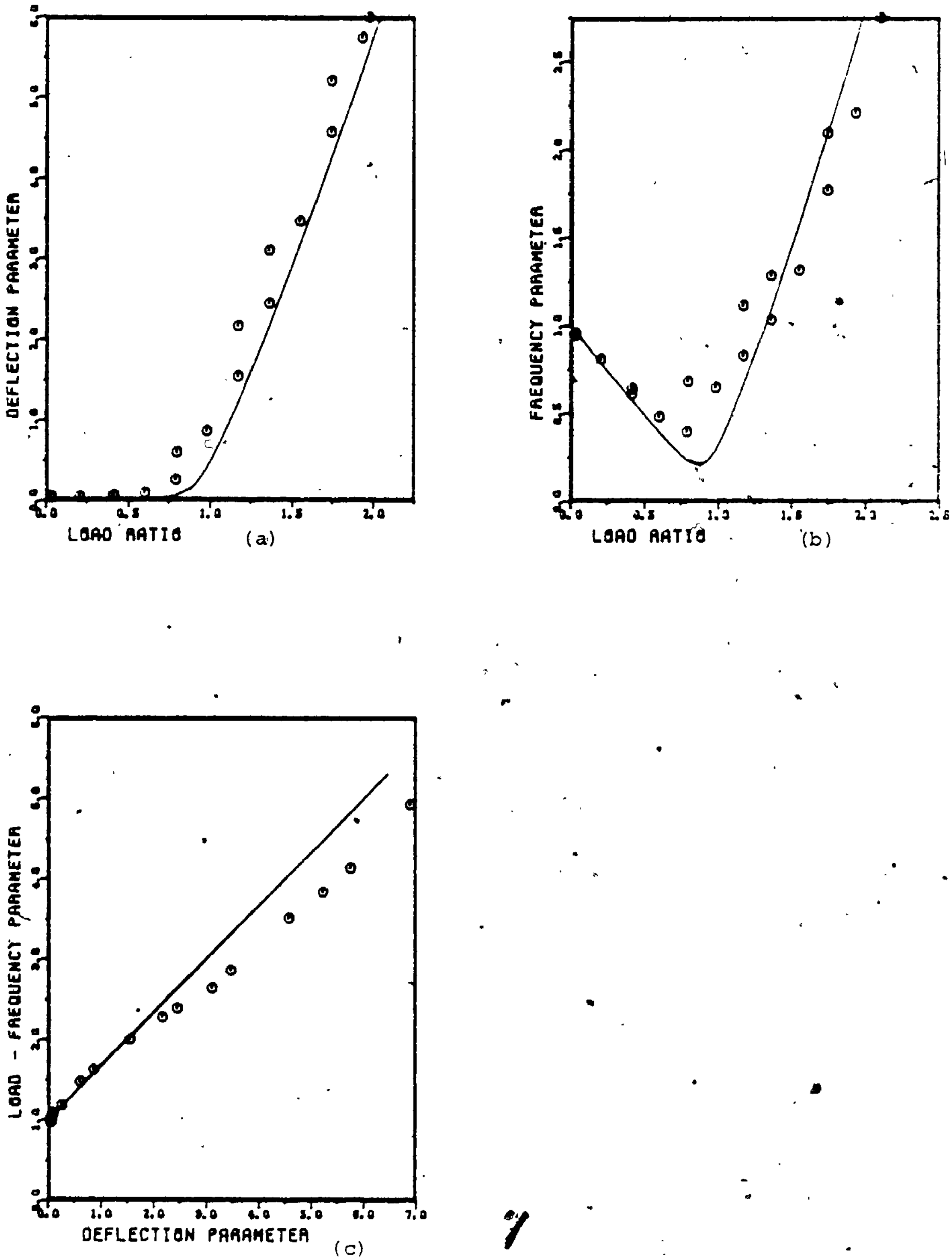

Figure 5.2.7 Further Results for Plate 5 (Test 2)

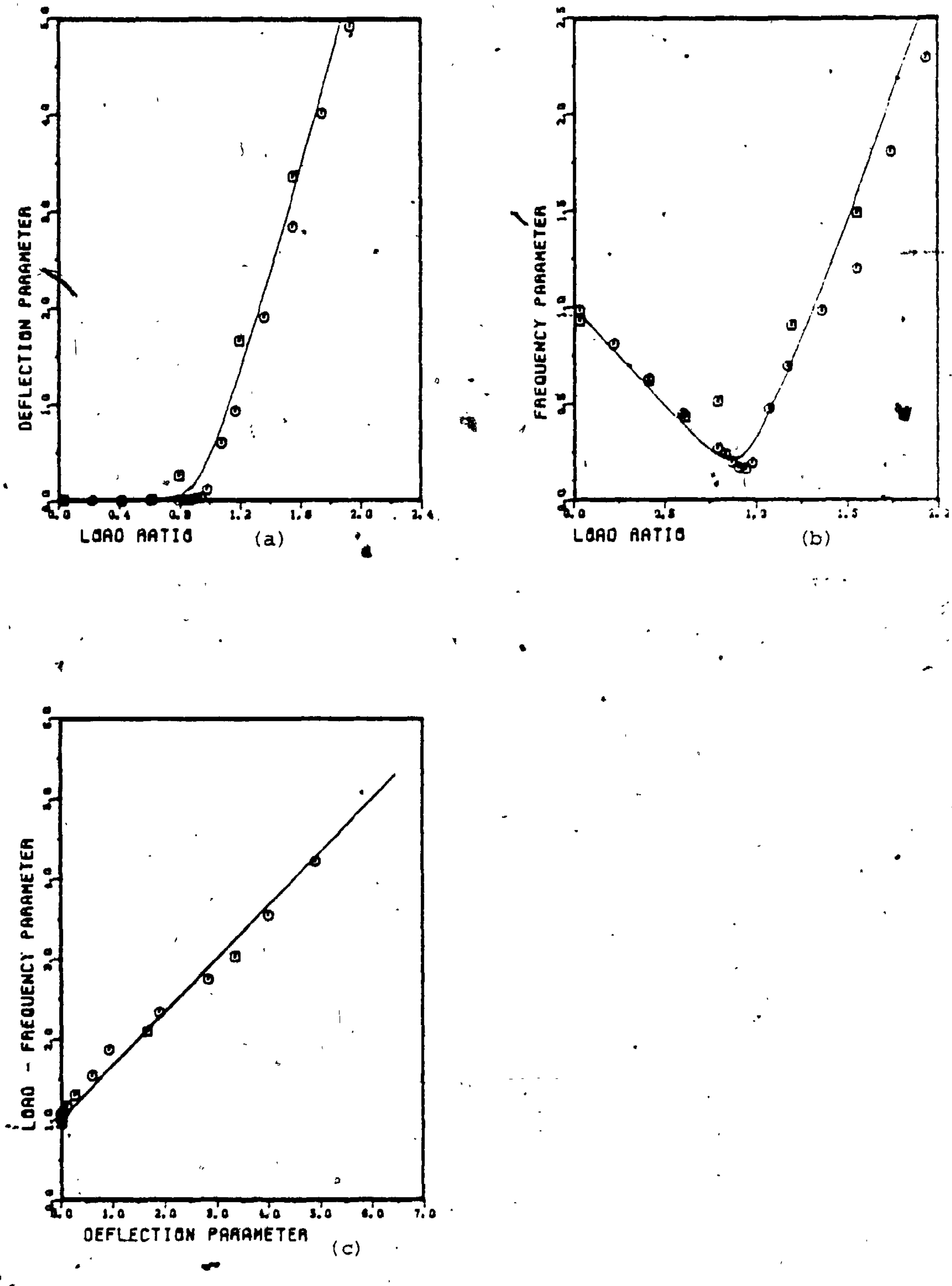

Figure 5.2.8 Further Results for Plate 5 (Test 3)

screen.) The bottom screws on the side support units were readjusted and the test was repeated. The final test results are shown in Figure 5.2.8. The upward curving of the load-frequency parameter vs deflection parameter plot is not noticeable for plate 5. This is because the effect of the inertia of the loading head is small. The agreement between the experimental and theoretical results is generally very good. The sharp change in the frequency parameter vs load ratio plot at the buckling load is because the plate is almost flat and a rapid change in displacement takes place near the buckling load.

The results for plate 6 (with an initial imperfection ratio μ_o=2.7) are shown in Figure 5.2.9. The experimental and theoretical values for the deflection and the frequency do not agree, but the trend in the variation of these parameters appears to be similar. The large discrepancies for this plate are thought to be due to the problems in the out-of-plane boundary conditions. The measured frequencies were lower than the calculated values. This may be due to a lack of fit at the top and bottom supports where the plate may have vibrated freely (flapping of the edges). The plate edges were straight (in-plane) when they were cut. When placing it in the rig, the sides which had some out-of-plane curvature, were straightened by 'clamping' between the side supports. This may have resulted in non-straight top and bottom edges. This problem may have occurred in other

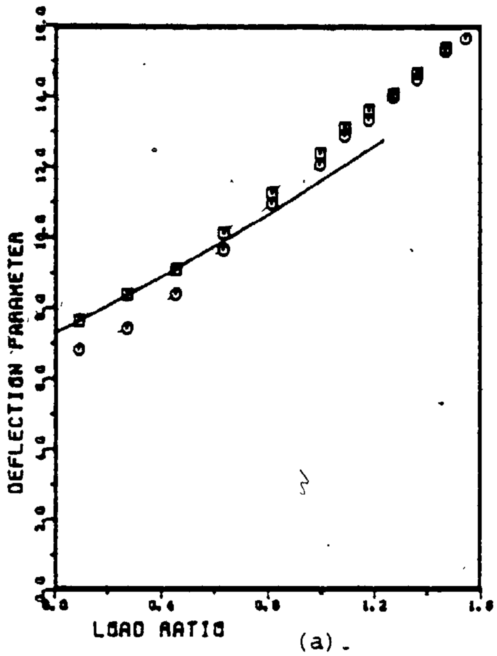

(a)

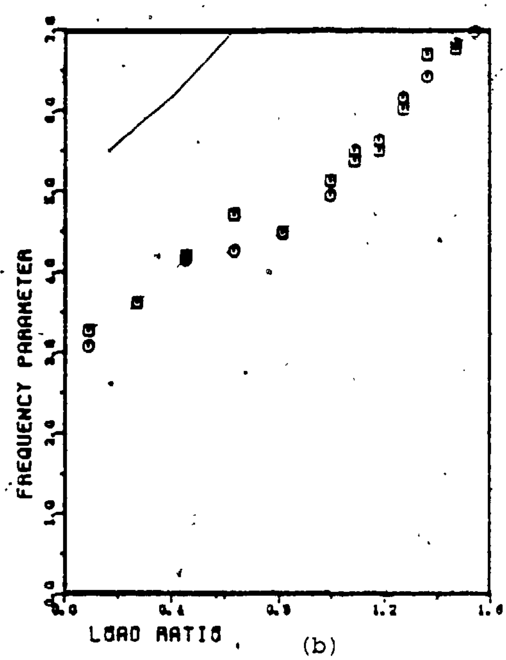

(b)

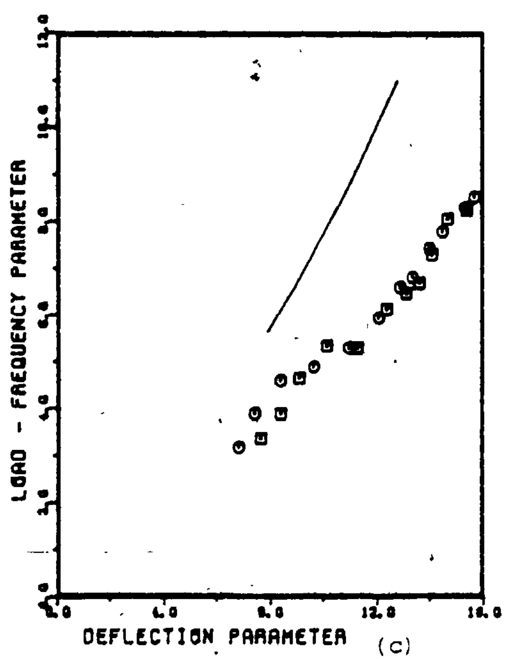

(c)

Figure 5.2.9 Results for Plate 6

plates too, but to a smaller degree, since the smaller imperfections would have caused smaller deviation from straightness at the top and bottom edges.

It is interesting to observe the results for another set of in-plane boundary conditions. The natural frequencies of plate 4 were calculated for in-plane normally constrained (constant motion) loaded edges and in-plane fully restrained sides. The variation of load-frequency parameter with the deflection parameter is shown in Figure 5.2.10 (dotted line) along with the theoretical results for the experimental boundary conditions (continuous line) and the points corresponding to the experimental results.

For plate 1 the strain values at twenty-seven points on each side of the plate were measured at various loads. These are compared with the corresponding theoretical values in Figures 5.2.11. The location and orientation of the gauges are given in Appendix B in tabular form and in Figure 4.3.4. The agreement in the overall pattern of the load-strain relationship is reasonably good for most of the gauge points. The discrepancy at some points indicates that there may have been some initial lack of fit at the top and bottom supports. At gauge locations 1 and 3, there was no change in the strain until about 0.3 times the buckling load was applied. This indicates that there was a small gap between the plate and the support near these points.

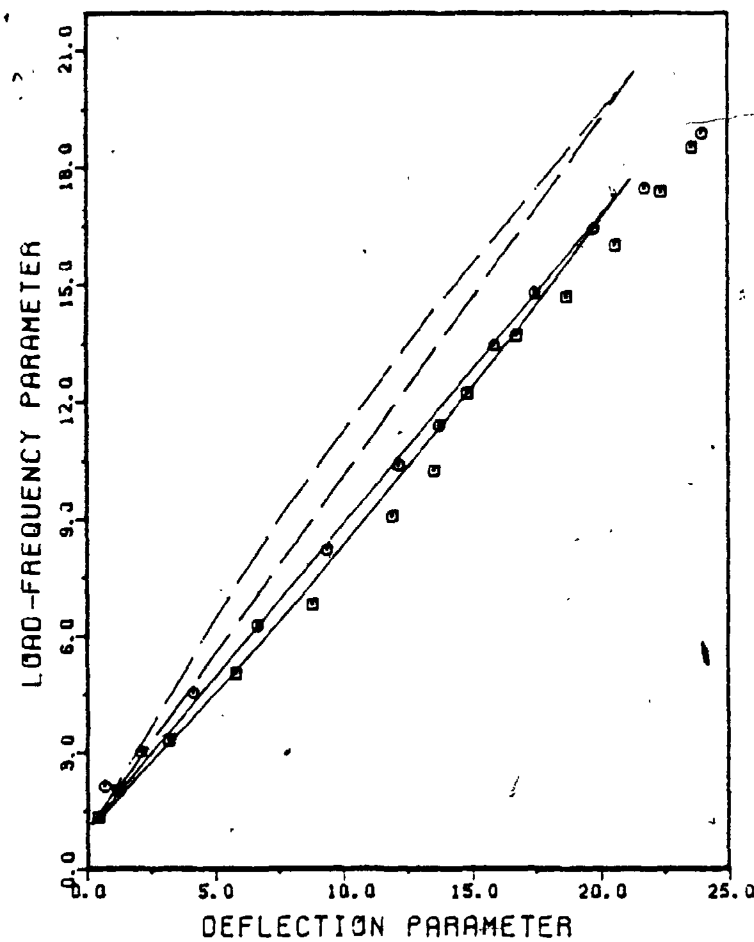

Figure 5.2.10 Results for Plate 1 Compared With the Results For a Plate With Standard Boundary Conditions

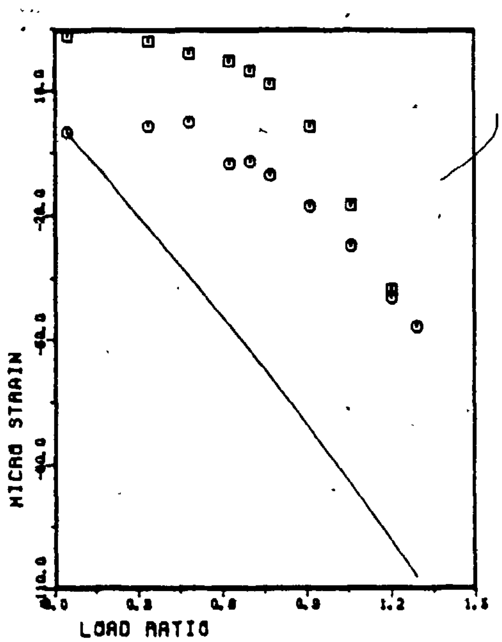

(Results for Gauge 1)

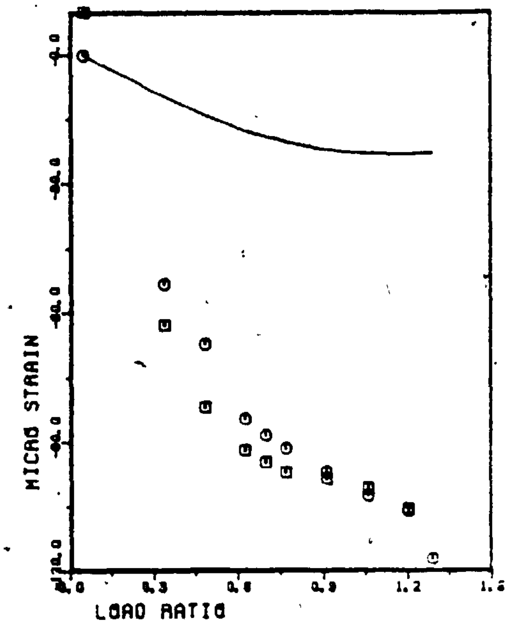

(Results for Gauge 2)

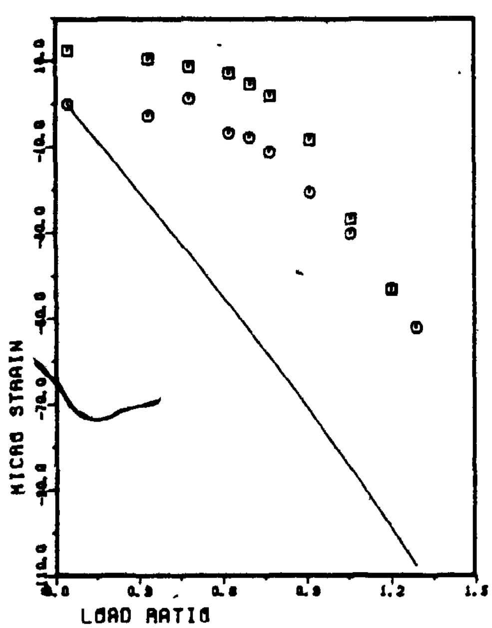

(Results for Gauge 3)

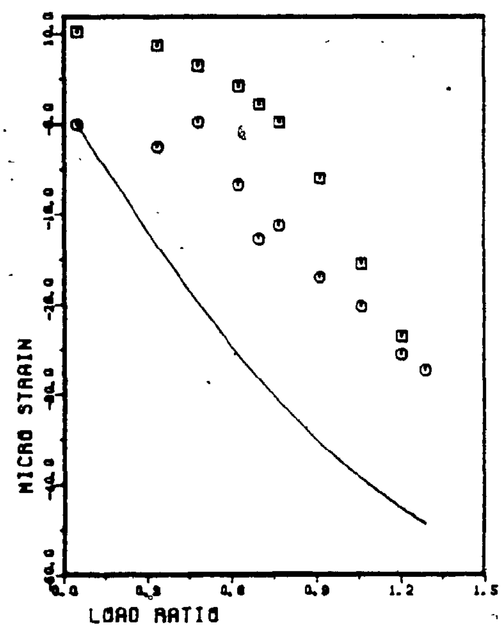

(Results for Gauge 4)

⊙ - Experimental (loading) , ⊡ - Experimental (unloading)

—— Theoretical

Figure 5.2.11 Load-Strain Relationship for Plate 1

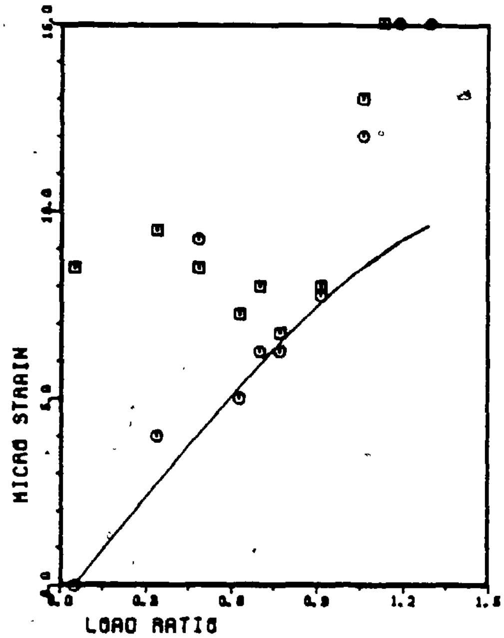

(Results for Gauge 5)

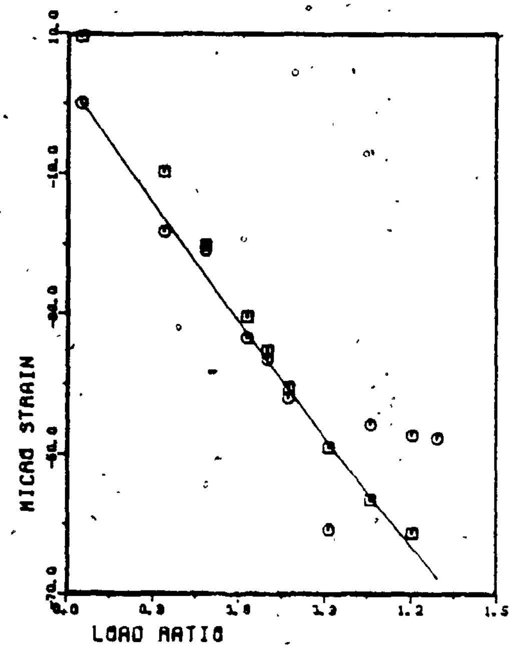

(Results for Gauge 6)

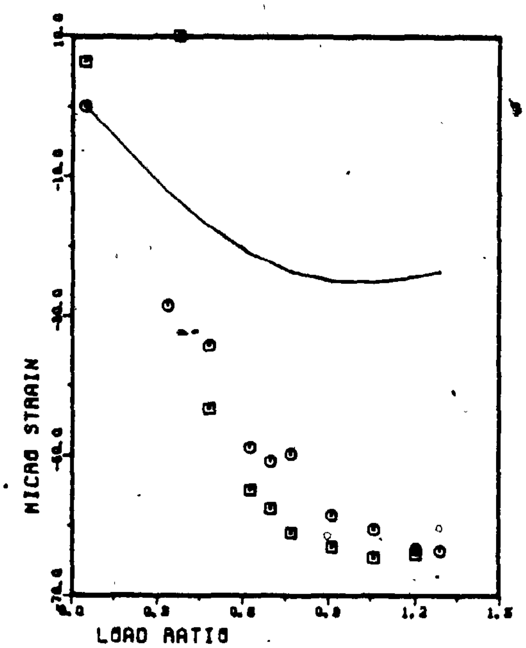

(Results for Gauge 7)

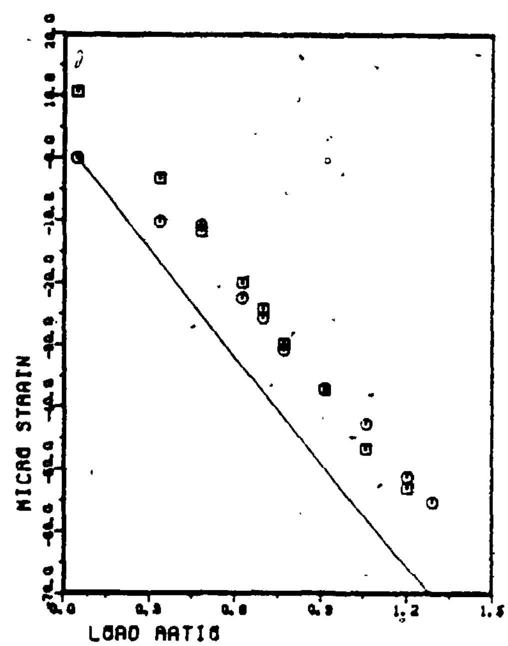

(Results for Gauge 8)

Figure 5.2.11 - continued

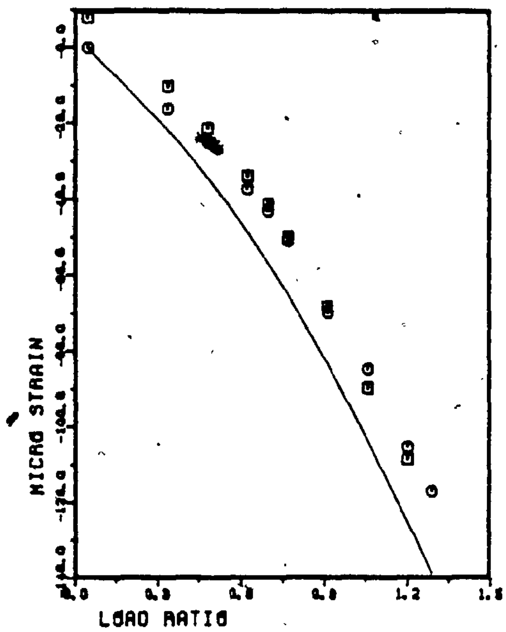

(Results for Gauge 9)

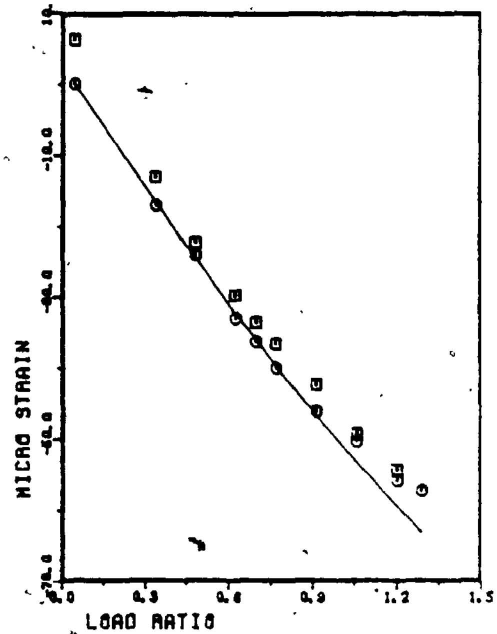

(Results for Gauge 10)

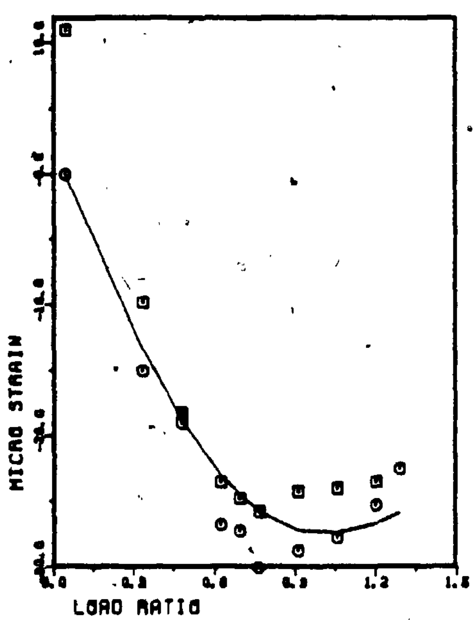

(Results for Gauge 11)

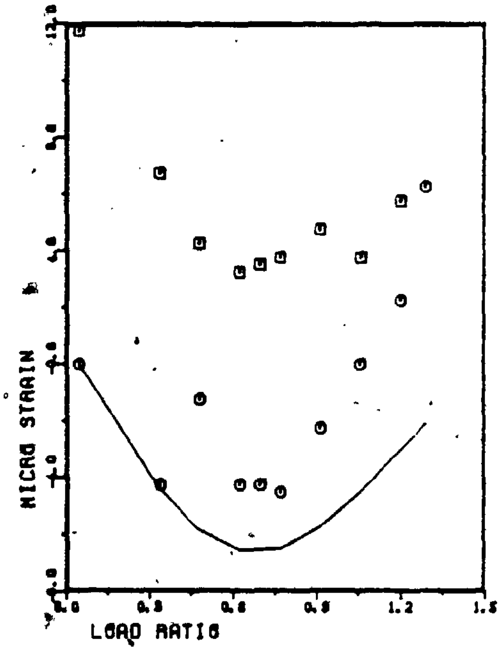

(Results for Gauge 12)

Figure 5.2.11 - Continued

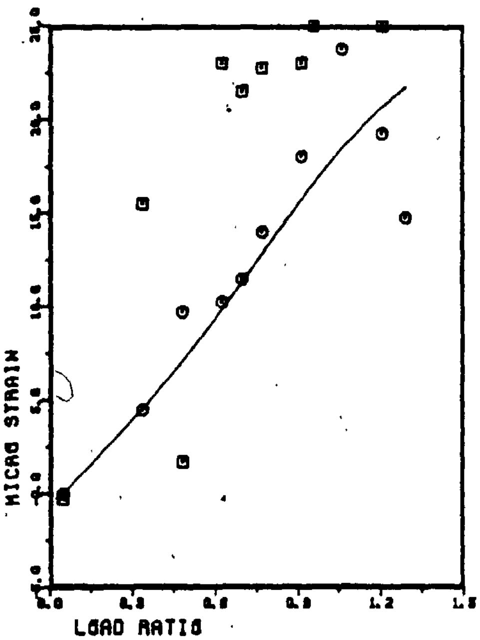

(Results for Gauge 13)

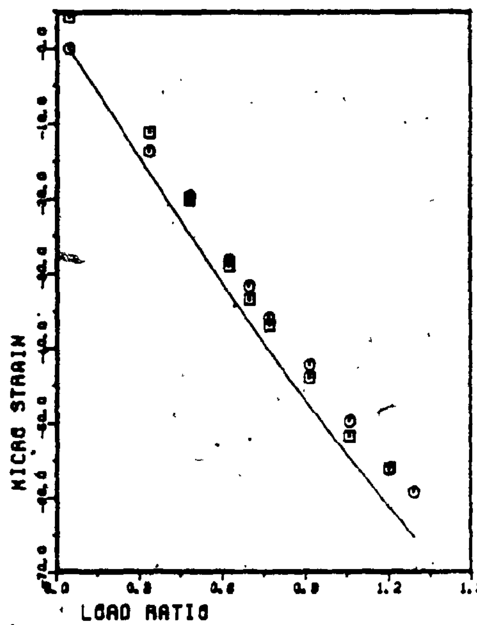

(Results for Gauge 14)

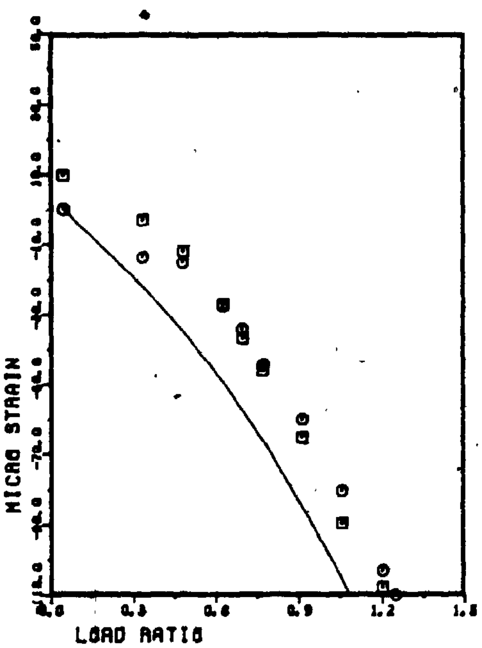

(Results for Gauge 15)

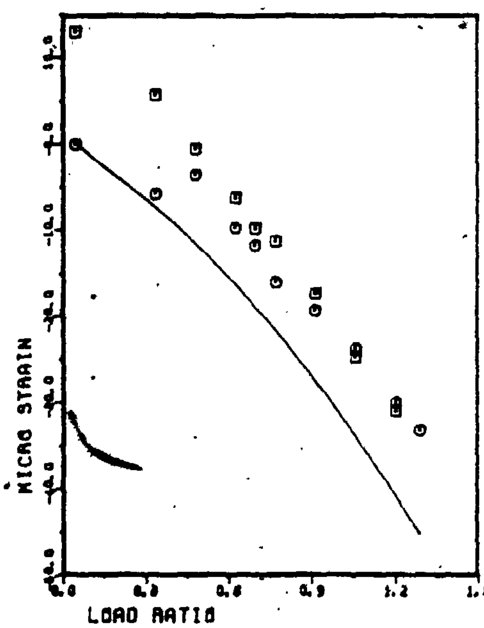

(Results for Gauge 16)

Figure 5.2.11 - Continued

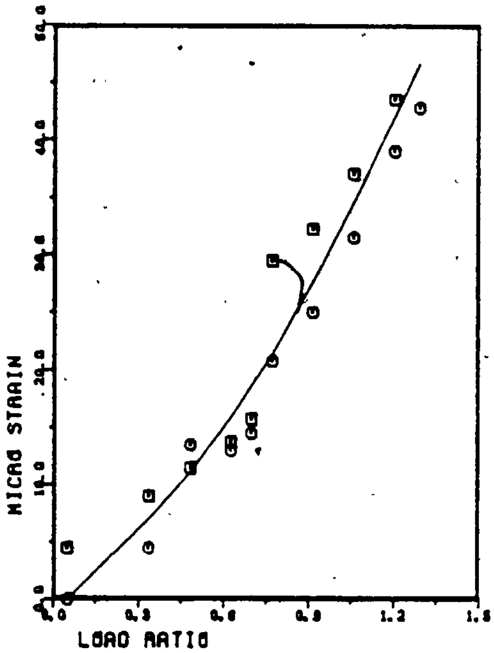

(Results for Gauge 17)

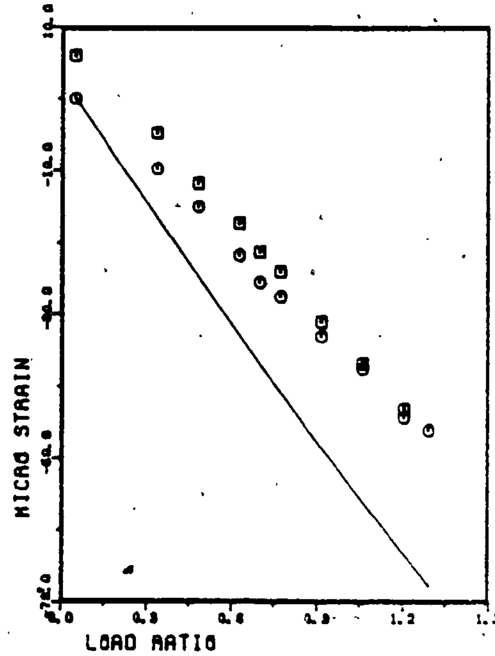

(Results for Gauge 18)

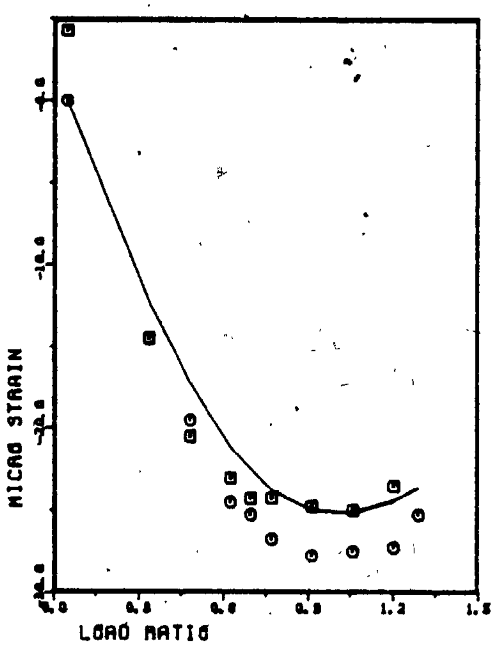

(Results for Gauge 19)

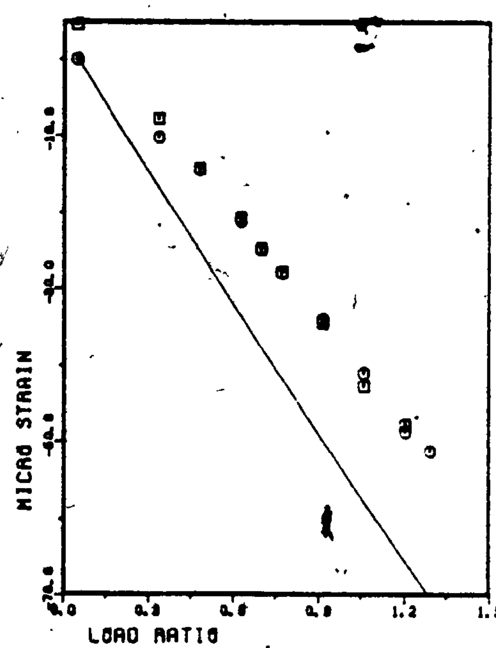

(Results for Gauge 20)

Figure 5.2.11 - Continued

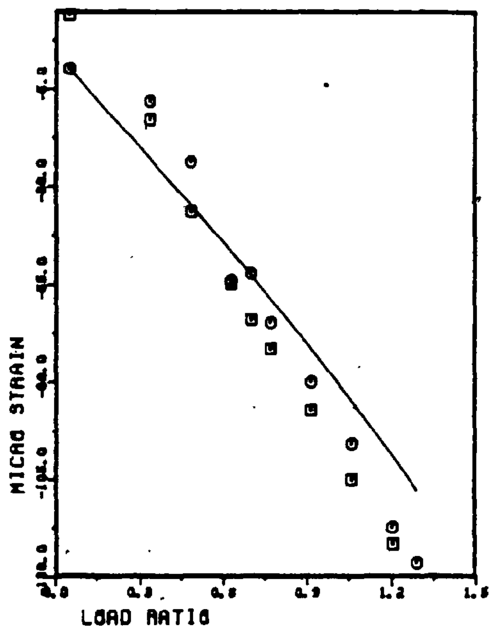

(Results for Gauge 21)

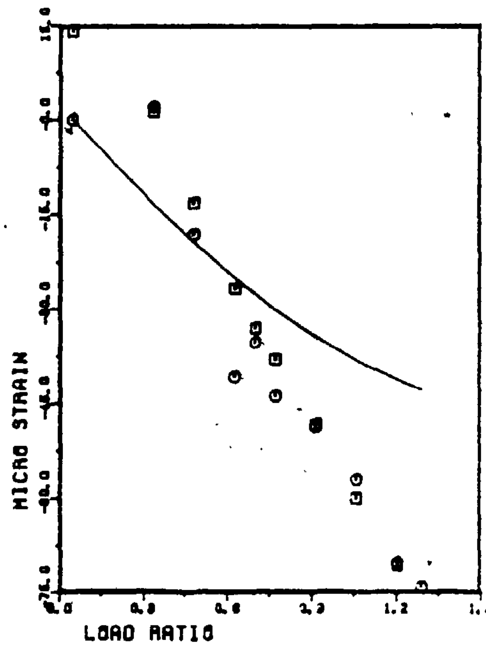

(Results for Gauge 22)

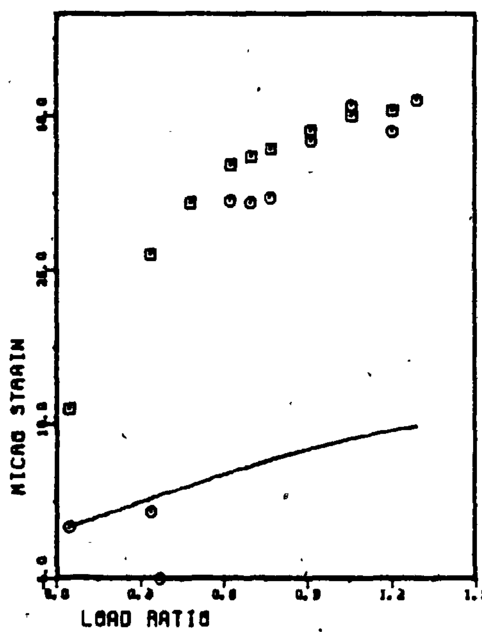

(Results for Gauge 23)

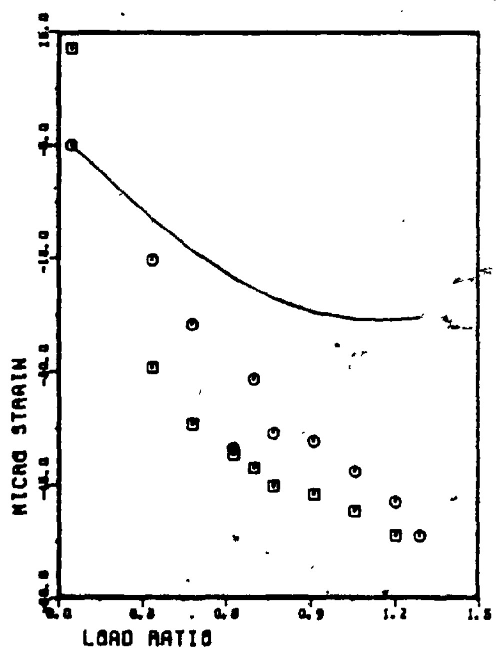

(Results for Gauge 24)

Figure 5.2.11 - Continued

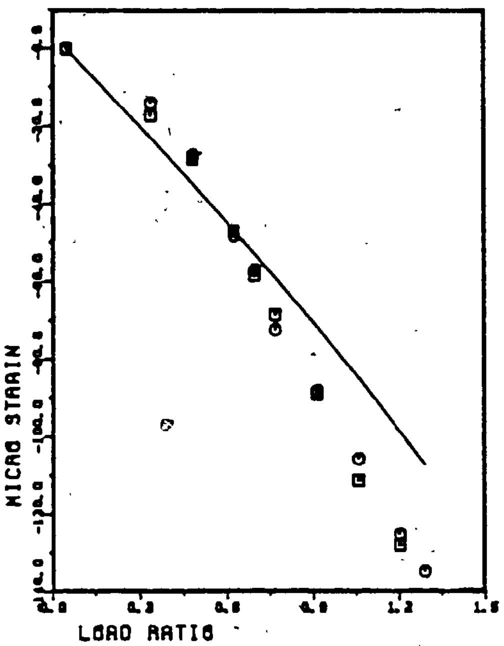

(Results for Gauge 25)

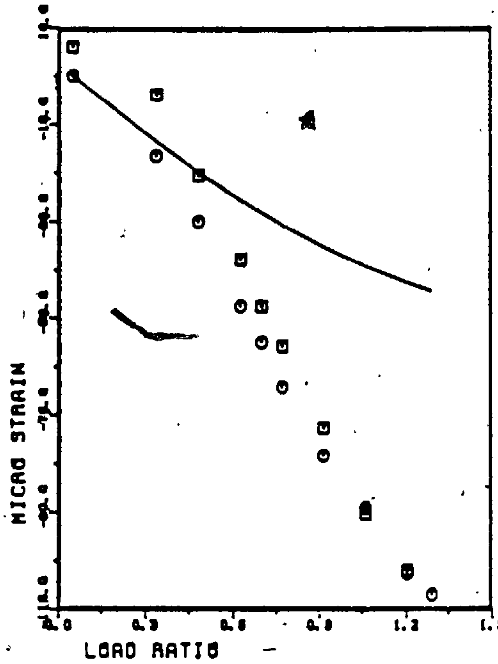

(Results for Gauge 26)

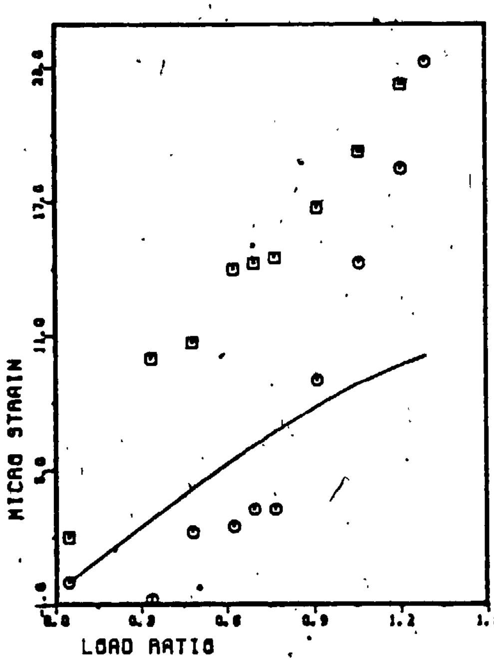

(Results for Gauge 27)

Figure 5.2.11 - Continued

At location 2 however, more strain was recorded experimentally than calculated. This indicates that more load was transferred to the plate near this point initially. From these observations it appears that the top edge of the plate was initially curved (in-plane) as shown in Figure 5.2.12.

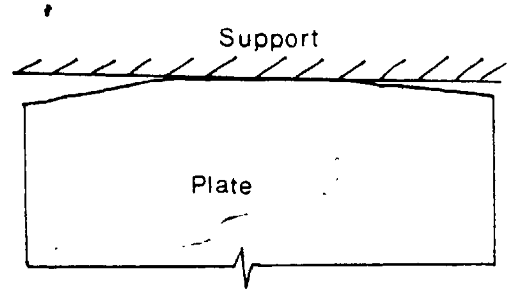

Figure 5.2.12

The agreement between the measured and calculated values of the strains in the direction of loading at the horizontal centreline of the plate is very good.

The discrepancy between the experimental and theoretical values of the deflections and in-plane strain distribution may be attributed to the following factors:

(1) The edges of the plate not being straight in their planes causing initial lack of fit at the loading edges.
(2) Presence of some restraint against rotation of the plate at the edges.
(3) Friction at the ball bearings when the load is not sufficiently large to produce in-plane forces which

can overcome the frictional resistance.

(4) Influence of anti-symmetric type of initial geometrical imperfections.

(5) Shape of the initial imperfection being different from the assumed shape.

(6) Initial setting errors causing skewness of the support.

(7) Presence of initial residual stresses since the plates were not stress relieved prior to testing.

(8) Induced initial stresses due to flattening of edges on set up.

(9) Measurement errors and errors due to simplifying assumptions made in modelling as explained in the previous sections. These are expected to be small as explained in Appendix K.

Since the agreement between the theoretical and experimental results are generally good (except for plate 6), it can be said that the above listed factors have not significantly influenced the results of the experiments on plates with small initial imperfections (less than 1/2 the plate thickness). With the exception of plate 6, the calculated and measured values of the fundamental natural frequencies agreed reasonably well for all the plates tested. The discrepancies are likely to be primarily due to the discrepancies in the calculated and measured values of the out-of-plane deflections and also due to the discrepancies in the calculated and measured values of in-plane stress distribution. Therefore, all the factors mentioned in the comparison of displacement results may have contributed to the discrepancies in the natural frequencies. This is clearly seen from the variation of load-frequency parameter with the deflection parameter, in which the theoretical and experimental results agree remarkably well.

If the approximately linear relationship between the load-frequency parameter and the deflection parameter which was exhibited for the plates tested can be established for slightly curved plates in general, the results may lead to some significant applications such as non-destructive testing of curved plates. If, for instance, the frequency and deflected shapes at various loads can be measured, the actual stress level in a curved plate may be estimated. This may be useful in the aircraft industry where thin curved panels are often used. It may lead to ways of optimizing the shape of curved panels.

CHAPTER 6

CONCLUSIONS AND RECOMMENDATIONS FOR FUTURE WORK

The following conclusions can be reached from the discussion in the previous chapter:

6.1 CONCLUDING REMARKS

1) The Rayleigh-Ritz method using undetermined in-plane and out-of-plane displacement coefficients has been successfully applied to calculate the static displacements, in-plane stress distributions and fundamental natural frequencies of simply supported rectangular plates subjected to static in-plane loadings varying from zero to well above the lowest buckling load.

2) Experiments have been conducted on several thin mild steel rectangular plates subject to uniaxial, in-plane loading, in which the static deflections, natural frequencies and, in one case, the static in-plane strain distribution were measured.

3) The calculated and measured values of the central deflections, strains and the fundamental natural frequencies agree very well for most of the plates tested.

4) It has been shown experimentally, as well as theoretically, that:

   a) The presence of initial imperfection influences the natural frequencies of rectangular plates. This effect increases with applied in-plane load due to the growth of deflection and change in stress distribution.

   b) The natural frequencies of curved plates depend on the in-plane boundary conditions; restraining in-plane displacement, generally increases the fundamental natural frequencies.

   c) The fundamental natural frequencies of curved plates are higher than those of the flat plates.

5) For the plates tested, there exists an approximate linear relationship between the square of the central deflection and a load-frequency parameter which can be defined as the summation of the square of the non-dimensional natural frequency and the in-plane load ratio.

6) This thesis represents the first successful attempt at comparing experimental and theoretical frequencies for geometrically imperfect rectangular plates subject to in-plane loads which are significantly larger than the lowest critical load.

6.2 RECOMMENDATIONS FOR FUTURE WORK

The work presented in this thesis can be extended in the following areas:

1) The theory for the vibration and postbuckling analysis using the Rayleigh-Ritz method with undetermined displacement coefficients may be extended for other out-of-plane boundary conditions.

2) Experimental work should be carried out for different in-plane and out-of-plane boundary conditions. Tests on plates with different aspect ratios should be carried out.

3) Theoretical and experimental investigation should be extended to include the higher modes of vibration and to include anti-symmetrical terms in the analysis.

4) A statistical study on practical plates may be carried out to verify the validity and limitation of the approximate linear relationship between the deflection parameter and the load-frequency parameter.

APPENDIX A

APPLICATION OF GALERKIN'S METHOD USING AIRY STRESS FUNCTIONS TO CALCULATE THE NATURAL FREQUENCIES AND DEFLECTIONS OF A SIMPLY SUPPORTED RECTANGULAR PLATE UNDER STATIC IN-PLANE LOADING

Von Kármán's non-linear large deflection equations and linear shell vibration equations in terms of the out-of-plane displacements and Airy stress functions have been solved by Hui and Leissa [25] for simply supported curved rectangular plates with the following boundary conditions using Galerkin's method: All edges free to move tangentially (shear free), but constrained to move with a constant displacement in the direction normal to the edges. The solution was based on the assumption that the out-of-plane buckling modes (and vibration modes) are decoupled. The stress functions were obtained by solving the compatibility equation exactly, for a particular buckling (or vibration) mode. In this appendix, a method to obtain the single term solution for other simple in-plane boundary conditions, in which the Airy stress functions are taken as the summation of a series of the products of beam functions and undetermined coefficients is described; the undetermined coefficients are found by solving the compatibility equations approximately, using Galerkin's method.

Calculation of the Static Displacements

The compatibility equation is [25],

$$\nabla^4 F = 2C_1 [(\frac{\partial^2 z}{\partial x \partial y})^2 - (\frac{\partial^2 z_o}{\partial x \partial y})^2 - \frac{\partial^2 z}{\partial x^2} \frac{\partial^2 z}{\partial y^2} + \frac{\partial^2 z_o}{\partial x^2} \frac{\partial^2 z_o}{\partial y^2}] \quad (A.1)$$

where

Initial Deflection, $z_o = Z_o \mathrm{Sin}(\frac{k\pi x}{a}) \mathrm{Sin}(\frac{\ell \pi y}{b})$ (A.1a)

Deflection under in-plane load, $z = Z \ \mathrm{Sin}(\frac{k\pi x}{a}) \cdot \mathrm{Sin}(\frac{\ell \pi y}{b})$ (A.1b)

and

$$C_1 = \frac{E \cdot h}{2} \quad (A.1c)$$

Airy stress function F can be expressed as a series of products of beam functions. This follows from an analogy between the Airy stress function and the out-of-plane displacement of a plate which is explained in a Thesis by Bassily [36].

i.e. $$F = \sum_{p}^{p_m} \sum_{q}^{q_m} \alpha_{p,q} \cdot \phi_p \cdot \psi_q , \quad (A.2)$$

for p,q = 1,2...

where

ϕ_p and ψ_q are the beam functions which satisfy the necessary boundary conditions for an analogous plate bending problem,

$\alpha_{p,q}$ are the undetermined weighting coefficients,

p_m, q_m are the maximum number of functions in x,y directions.

Equation (A.2) can be written in matrix form as,

$$F = \{\alpha\}^T\{(\phi\cdot\psi)\} \quad (A.3)$$

where

$$\alpha(J) = \alpha_{p,q}$$

in which $J = q + (p-1)\cdot q_m$

Let $\left(\frac{\pi^2 k\ell}{ab}\right)^2 = R$,

then, $$\left(\frac{\partial^2 z}{\partial x\partial y}\right)^2 - \left(\frac{\partial^2 z_o}{\partial x\partial y}\right)^2 = R\cdot(Z^2 - Z_o^2)\cos^2\left(\frac{k\pi x}{a}\right)\cos^2\left(\frac{\ell\pi y}{b}\right)$$

$$\frac{\partial^2 z}{\partial x^2}\cdot\frac{\partial^2 z}{\partial y^2} - \frac{\partial^2 z_o}{\partial x^2}\cdot\frac{\partial^2 z_o}{\partial y^2} = -R\cdot(Z^2 - Z_o^2)\sin^2\left(\frac{k\pi x}{a}\right)\sin^2\left(\frac{\ell\pi y}{b}\right)$$

Adding these two equations gives the R.H.S. of the compatibility equation as,

$$\text{R.H.S. of equation (A.1)} = 2R\cdot C_1(Z^2 - Z_o^2)\left[\cos^2\left(\frac{k\pi x}{a}\right)\cdot\cos^2\left(\frac{\ell\pi y}{b}\right) - \sin^2\left(\frac{k\pi x}{a}\right)\cdot\sin^2\left(\frac{\ell\pi y}{b}\right)\right]$$

$$= R\cdot C_1(Z^2 - Z_o^2)\left[\cos\left(\frac{2k\pi x}{a}\right) + \cos\left(\frac{2\ell\pi y}{b}\right)\right]$$

Now Galerkin's method can be applied to the compatibility equation. Let the weighting function be $(\phi_r\cdot\psi_s)$.

This gives,

$$\int_{x=0}^{a}\int_{y=0}^{b}(\phi_r\cdot\psi_s)\sum_p\sum_q\alpha_{p,q}\cdot\nabla^4(\phi_p\psi_q)\,dx\,dy$$

$$=\int_{x=0}^{a}\int_{y=0}^{b}C_1\cdot R(Z^2-Z_o^2)\left[\mathrm{Cos}\left(\frac{2k\pi x}{a}\right)+\mathrm{Cos}\left(\frac{2\ell\pi y}{b}\right)\right](\phi_r\psi_s)\,dx\,dy \tag{A.4}$$

This can be written in matrix form as

$$[SK]\{\alpha\} = (Z^2-Z_o^2)\{A\} \tag{A.5}$$

where,

$$SK(I,J) = \int_{x=0}^{a}\int_{y=0}^{b}(\phi_r\cdot\psi_s)\nabla^4(\phi_p\cdot\psi_q)\,dx\,dy \tag{A.5a}$$

and

$$A(I) = \int_{x=0}^{a}\int_{y=0}^{b}C_1\cdot R\left[\mathrm{Cos}\left(\frac{2k\pi x}{a}\right)+\mathrm{Cos}\left(\frac{2\ell\pi y}{b}\right)\right](\phi_r\psi_s)\,dx\,dy \tag{A.5b}$$

in which,

$I = s+(r-1)\cdot q_m$

and $J = q+(p-1)\cdot q_m$

$$\nabla^4(\phi_p\cdot\psi_q) = \phi_p^{IV}\cdot\psi_q + 2\phi_p^{II}\cdot\psi_q^{II} + \phi_p\cdot\psi_q^{IV}.$$

Using this, equation (A.5a) can be written as,

$$SK(I,J) = T_1S_3 + 2T_2S_2 + T_3S_3 \tag{A.6}$$

where

$$
\left.\begin{aligned}
T_1 &= \int_{x=0}^{a} \phi_r \phi_p^{IV} dx \; ; \; S_1 = \int_{y=0}^{b} \psi_s \psi_q^{IV} dy \; ; \\
T_2 &= \int_{x=0}^{a} \phi_r \phi_p'' \, dx \; ; \; S_2 = \int_{y=0}^{b} \psi_s \psi_q'' \, dy \; ; \\
T_3 &= \int_{x=0}^{a} \phi_r \phi_p \, dx \; ; \; S_3 = \int_{y=0}^{b} \psi_s \psi_q \, dy \; .
\end{aligned}\right\} \qquad \text{(A.6a)}
$$

Equation (A.5b) can be written as

$$A(I) = R \cdot C_1 (P_1 \cdot P_4 + P_2 \cdot P_3) , \qquad \text{(A.7)}$$

where

$$
\left.\begin{aligned}
P_1 &= \int_{x=0}^{a} \phi_r \cdot \mathrm{Cos}\left(\frac{2k\pi x}{a}\right) dx , \\
P_2 &= \int_{y=0}^{b} \psi_s \cdot \mathrm{Cos}\left(\frac{2\ell\pi y}{b}\right) dy , \\
P_3 &= \int_{x=0}^{a} \phi_r \, dx , \\
P_4 &= \int_{y=0}^{b} \psi_s \, dy .
\end{aligned}\right\} \qquad \text{(A.7a)}
$$

In equation (A.5), $\{\alpha\}$ and Z are unknowns. The solution of Z is a two step procedure. First, the solution of

$$[SK]\{\alpha'\} = \{A\} \qquad \text{(A.8)}$$

is found.

$$\{\alpha\} = (Z^2 - Z_o^2)\{\alpha'\} \qquad \text{(A.9)}$$

Having calculated $\{\alpha'\}$, equation (A.9) can be substituted in the equilibrium equation to evaluate Z in an iterative procedure.

The equation of static equilibrium is [25],

$$\nabla^4(z-z_o)+2C_1(\bar{\sigma}_x \frac{\partial^2 z}{\partial x^2} + \bar{\sigma}_y \frac{\partial^2 z}{\partial y^2}) = 2C_1(\frac{\partial^2 F}{\partial y^2} \cdot \frac{\partial^2 z}{\partial x^2}$$

$$+ \frac{\partial^2 F}{\partial x^2} \cdot \frac{\partial^2 z}{\partial y^2} - 2 \frac{\partial^2 F}{\partial x \partial y} \frac{\partial^2 z}{\partial x \partial y}) \qquad \text{(A.10)}$$

Differentiating equations (A.1a) and (A.1b) appropriately and substituting in equation (A.10) gives

$$\text{L.H.S. of equation (A.10)} = [\pi^4 \cdot Q_1 \cdot (Z-Z_o) - 2 \cdot C_1 \cdot \pi^2 \cdot Q_2 \cdot Z] \cdot$$

$$\sin(\frac{k\pi x}{a}) \sin(\frac{\ell \pi y}{b}) \qquad \text{(A.11)}$$

where,

$$Q_1 = (\frac{k^2}{a^2} + \frac{\ell^2}{b^2})^2 \qquad \text{(A.11a)}$$

and

$$Q_2 = (\frac{k^2 \bar{\sigma}_x}{a^2} + \frac{\ell^2 \bar{\sigma}_y}{b^2}) \qquad \text{(A.11b)}$$

Using equations (A.3) and (A.9), it can be shown that,

$$\text{R.H.S. of equation (A.10)} = -2C_1 \pi^2 Z(Z^2 - Z_o^2) \times$$

$$[T \sin(\frac{k\pi x}{a}) \sin(\frac{\ell \pi y}{b}) + U \cos(\frac{k\pi x}{a}) \cos(\frac{\ell \pi y}{b})] \qquad \text{(A.12)}$$

where,

$$T = \frac{k^2}{a^2}\{\alpha'\}^T\{(\phi\cdot\psi'')\} + \frac{\ell^2}{b^2}\{\alpha'\}^T\{(\phi''\cdot\psi)\} \qquad \text{(A.12a)}$$

and $$U = -\frac{2k\ell}{ab}\{\alpha'\}^T\{(\phi'\cdot\psi')\}. \qquad \text{(A.12b)}$$

Using $\text{Sin}(\frac{k\pi x}{a})\cdot\text{Sin}(\frac{\ell\pi y}{b})$ as the weighting function in Galerkin's method gives,

$$\int_{x=0}^{a}\int_{y=0}^{b}[\nabla^4(z-z_o)+2C_1(\bar{\sigma}_x\frac{\partial^2 z}{\partial x^2}+\bar{\sigma}_y\frac{\partial^2 z}{\partial y^2})]\text{Sin}(\frac{k\pi x}{a})\text{Sin}(\frac{\ell\pi y}{b})\,dx\,dy$$

$$= 2\cdot C_1\cdot(Z^2-Z_o^2)\cdot Z\cdot\pi^2\cdot Q_3, \qquad \text{(A.13)}$$

where

$$Q_3 = \int_{x=0}^{a}\int_{y=0}^{b}[T\ \text{Sin}^2(\frac{k\pi x}{a})\text{Sin}^2(\frac{\ell\pi y}{b}) + U\ \text{Cos}(\frac{k\pi x}{a})\text{Cos}(\frac{\ell\pi y}{b})$$

$$\cdot\ \text{Sin}(\frac{k\pi x}{a})\text{Sin}(\frac{\ell\pi y}{b})]\,dx\,dy. \qquad \text{(A.13a)}$$

And $$\int_{x=0}^{a}\text{Sin}^2(\frac{k\pi x}{a})\,dx = \frac{a}{2},$$

$$\int_{y=0}^{b}\text{Sin}^2(\frac{\ell\pi y}{b})\,dy = \frac{b}{2}.$$

Substituting these integrals and equation (A.11) in equation (A.13) gives,

$$\pi^4\cdot Q_1\cdot(Z-Z_o)-2\cdot C_1\cdot\pi^2\cdot Z - 2C_1(Z^2-Z_o^2)\cdot Z\cdot\pi^2\cdot Q_3\cdot(4/ab) = 0$$

(A.14)

This equation can be solved using an iterative procedure to compute Z.

Calculation of Natural Frequencies

Consider the vibration in (m,n) mode.

Let the displacement w, during vibration be given by,

$$w = H \cdot \text{Sin}(\frac{m\pi x}{a})\,\text{Sin}(\frac{n\pi y}{b})\,\text{Sin}(\omega t)$$

For the following analysis, H can be taken as unity, since for free vibration analysis the natural frequency does not depend on the amplitude (for small amplitude vibrations). For simplicity, the vibration at the time of maximum excursion ($\text{Sin}(\omega t)=1.0$) will be considered.

i.e. $$w = \text{Sin}(\frac{m\pi x}{a})\,\text{Sin}(\frac{n\pi y}{b}) \quad \text{(A.15)}$$

The compatibility equation is [25],

$$\nabla^4\overline{F} = 2C_1(\frac{\partial^2 z}{\partial x\partial y} \cdot \frac{\partial^2 w}{\partial x\partial y} - \frac{\partial^2 z}{\partial x^2} \cdot \frac{\partial^2 w}{\partial y^2} - \frac{\partial^2 z}{\partial y^2} \cdot \frac{\partial^2 w}{\partial x^2}) \quad \text{(A.16)}$$

The dynamic Airy stress function can be expressed as the summation of a series of the products of beam functions.

i.e. $$\overline{F} = \sum_{p}^{p_m} \sum_{q}^{q_m} \beta_{p,q}\,\phi_p\psi_q \quad \text{(A.17)}$$

$$= \{\beta\}^T\{(\phi\psi)\} \quad \text{(A.17a)}$$

By following the same procedure as in the static deflection calculation, it can be shown that the Galerkin's approximation to equation (A.16) is given by,

$$[SK]\{\beta\} = Z[B] \tag{A.18}$$

where,

$$\beta(I) = \beta_{p,q} \tag{A.18a}$$

$$B(I) = \frac{2C_1\pi^4}{a^2b^2}\,[2k\cdot\ell\cdot m\cdot n\;T_4\cdot S_4-(k^2n^2+m^2\ell^2)T_5S_5] \tag{A.18b}$$

in which,

$$T_4 = \int_{x=0}^{a} \mathrm{Cos}(\frac{k\pi x}{a})\cdot\mathrm{Cos}(\frac{m\pi x}{a})\cdot\phi_r\,dx$$

$$S_4 = \int_{y=0}^{b} \mathrm{Cos}(\frac{\ell\pi y}{b})\cdot\mathrm{Cos}(\frac{n\pi y}{b})\cdot\psi_s\,dy$$

$$T_5 = \int_{x=0}^{a} \mathrm{Sin}(\frac{k\pi x}{a})\cdot\mathrm{Sin}(\frac{m\pi x}{a})\cdot\phi_r\,dx \tag{A.18c}$$

$$S_5 = \int_{y=0}^{b} \mathrm{Sin}(\frac{\ell\pi y}{b})\cdot\mathrm{Sin}(\frac{n\pi y}{b})\cdot\psi_s\,dy$$

and $\quad I = s + (r-1)\cdot q_m\,.$ (A.18d)

[SK] is defined in equation (A.5a).

The equation of motion is [25],

$$\nabla^4 w - \lambda^2 w = 2C_1[(\frac{\partial^2F}{\partial y^2}-\bar{\sigma}_x)\cdot\frac{\partial^2w}{\partial x^2}+(\frac{\partial^2F}{\partial y^2}-\bar{\sigma}_y)\frac{\partial^2w}{\partial y^2}-2\frac{\partial^2F}{\partial x\partial y}\cdot\frac{\partial^2w}{\partial x\partial y}$$

$$+\frac{\partial^2z}{\partial x^2}\cdot\frac{\partial^2\bar{\bar{F}}}{\partial y^2}+\frac{\partial^2z}{\partial y^2}\cdot\frac{\partial^2\bar{\bar{F}}}{\partial x^2}-2\frac{\partial^2z}{\partial x\partial y}\cdot\frac{\partial^2\bar{\bar{F}}}{\partial x\partial y}] \tag{A.19}$$

where,

$$\lambda^2 = \frac{\rho\omega^2}{D} \tag{A.19a}$$

$$\frac{\partial^2 w}{\partial x^2} = -\frac{m^2\pi^2}{a^2} w ,$$

$$\frac{\partial^2 w}{\partial y^2} = -\frac{n^2\pi^2}{b^2} w ,$$

and $\nabla^4 w = (\frac{m^2}{a^2} + \frac{n^2}{b^2})^2 w.$

Substituting these in equation (A.19) gives,

$$\lambda^2 w = [\pi^4(\frac{m^2}{a^2} + \frac{n^2}{b^2})^2 - 2C_1\pi^2(\frac{m^2}{a^2}\bar{\sigma}_x + \frac{n^2}{b^2}\bar{\sigma}_y)]w$$

$$+ 2C_1\pi^2(\frac{m^2}{a^2} \cdot \frac{\partial^2 F}{\partial y^2} + \frac{n^2}{b^2} \cdot \frac{\partial^2 F}{\partial x^2})w$$

$$+ 4C_1 \frac{\partial^2 F}{\partial x\partial y} \cdot \frac{\partial^2 w}{\partial x\partial y}$$

$$+ 2C_1\{\frac{\partial^2 z}{\partial x^2} \cdot \frac{\partial^2 \bar{F}}{\partial y^2} + \frac{\partial^2 z}{\partial y^2} \cdot \frac{\partial^2 \bar{F}}{\partial x^2} - 2\frac{\partial^2 z}{\partial x\partial y} \cdot \frac{\partial^2 \bar{F}}{\partial x\partial y}\} \tag{A.20}$$

Using Galerkin's method (taking $\text{Sin}(\frac{m\pi x}{a}) \cdot \text{Sin}(\frac{n\pi y}{b})$ as the weighting function) gives,

$$\lambda^2(\frac{ab}{4}) = \{\pi^4(\frac{m^2}{a^2} + \frac{n^2}{b^2})^2 - 2C_1\pi^2(\frac{m^2\bar{\sigma}_x}{a^2} + \frac{n^2\bar{\sigma}_y}{b^2})\}(\frac{ab}{4})$$

$$+ R_1 + R_2 \tag{A.21}$$

where,

$$R_1 = 2C_1 \int_{x=0}^{a} \int_{y=0}^{b} \{\pi^2 (\frac{m^2}{a^2} \cdot \frac{\partial^2 F}{\partial y^2} + \frac{n^2}{b^2} \cdot \frac{\partial^2 F}{\partial x^2}) \cdot w^2$$

$$+ 2 \frac{\partial^2 F}{\partial x \partial y} \cdot \frac{\partial^2 w}{\partial x \partial y} \cdot w\} dx\ dy \qquad (A.21a)$$

and

$$R_2 = -2C_1 \int_{x=0}^{a} \int_{y=0}^{b} [\frac{\partial^2 z}{\partial x^2} \cdot \frac{\partial^2 \bar{F}}{\partial y^2} + \frac{\partial^2 z}{\partial y^2} \cdot \frac{\partial^2 \bar{F}}{\partial x^2}$$

$$- 2 \frac{\partial^2 z}{\partial x \partial y} \cdot \frac{\partial^2 \bar{F}}{\partial x \partial y}] \cdot W\ dx\ dy \qquad (A.21b)$$

Dividing equation (A.21) by $(\frac{ab}{4})$ gives,

$$\lambda^2 = \pi^4 (\frac{m^2}{a^2} + \frac{n^2}{b^2}) - 2C_1 \pi^2 (\frac{m^2}{a^2} \bar{\sigma}_x + \frac{n^2}{b^2} \bar{\sigma}_y) + \frac{4(R_1 + R_2)}{ab}$$

(A.22)

The natural frequency corresponding to the (m,n) mode is given by,

$$\omega_{m,n} = \lambda \sqrt{Eh^3/(12\rho(1-\nu^2))} \qquad (A.23)$$

R_1 and R_2 can be calculated as follows:

Substituting equation (A.3) in equation (A.21a) leads to,

$$R_1 = 2C_1 \pi^2 (Z^2 - Z_o^2) \int_{x=0}^{a} \int_{y=0}^{b} [[\frac{m^2}{a^2} \{\alpha'\}^T (\phi \cdot \psi'')\} + \frac{n^2}{b^2} \{\alpha'\}^T \{(\phi'' \cdot \psi)\}]$$

$$\mathrm{Sin}(\frac{m\pi x}{a}) \mathrm{Sin}(\frac{n\pi y}{b}) + 2 \frac{mn}{ab} \{\alpha'\}^T \{(\phi' \psi')\} \mathrm{Cos}(\frac{m\pi x}{a}) \mathrm{Cos}(\frac{n\pi y}{b})] dx\ dy$$

(A.24)

Substituting equation (A.17a) in equation (A.21b) leads to,

$$R_2 = 2C_1\pi^2 Z \int_{x=0} \int_{y=0} [[\frac{k^2}{a^2}\{\beta\}^T\{(\phi\cdot\psi'')\} + \frac{\ell^2}{b^2}\{\beta\}^T\{(\phi''\psi)\}] \times$$

$$\mathrm{Sin}(\frac{k\pi x}{a})\,\mathrm{Sin}(\frac{\ell\pi y}{b})$$

$$+ \frac{2k\ell}{ab}\{\beta\}^T\{(\phi'\cdot\psi')\}\mathrm{Cos}(\frac{k\pi x}{a})\,\mathrm{Cos}(\frac{\ell\pi y}{a})]\,dx\,dy \qquad (A.25)$$

Choice of Beam Functions

By analogy with plate bending problem, it can be shown [36] that in-plane shear diaphragm boundary conditions can be represented by simply supported out-of-plane boundary conditions, and in-plane free boundary conditions can be represented by out-of-plane clamped boundary condition. For example, $\phi(x) = \mathrm{Sin}(\frac{i\pi x}{a})$ can be used for shear diaphragm boundary conditions at x=0 and x=a.

APPENDIX B

NUMERICAL RESULTS

The numerical values for the theoretical and experimental results are given in this section. Tables B.1 to B.11 give the measured values of central displacements and the natural frequencies for the test plates. Two examples of the parameters required for the Southwell plot are given in tables B.12 and B.13. Calculation of the change in deflection due to the applied load (Δ) is simply done by subtracting the central deflection reading with the dead load (weight of the supporting beam and the loading head is 33 lbs) from the central deflection reading for a given load. Table B.12 and B.13 are derived from table B.1 and table B.3 respectively.

For example the deflection due to a load of 600 lbs.(actual load 633 lbs.) = 0.0542 - 0.0812 = -0.027 inches.

Theoretical results for the out-of-plane displacement coefficients ($Z_{1,1}$, $Z_{1,3}$, $Z_{3,1}$, $Z_{3,3}$), the central deflection parameter (μ) and the fundamental natural frequency (ω) are tabulated in tables B.14 to B.19. Table B.14 and table B.15 are for plate 1 with different initial imperfevtion (μ_0) as indicated. Table B.17 gives the theoretical results for plate 4 with the following in-plane boundary conditions: top and bottom edges normally constrained and sides fully restrained.

The deflection readings at various points on the plates (see Figure 4.3.1 for the identification of these points.) are given in table B.20 to table B.23.

The location of strain gauges are shown in table B.24, where the co-ordinate system used is defined in the figure. Table B.25 gives the strain readings on each side at all of the gauge points. The reduced values of these strains are compared with the theoretical results in table B.26.

LOAD (lbs)	Δ_c 10^{-3} inches	$\omega_{1,1}$ (Hz)
33.0	81.2	67.1
133.0	80.2	63.6
233.0	78.6	58.4
333.0	76.3	53.2
433.0	73.1	46.2
533.0	66.7	42.4
583.0	61.7	43.4
633.0	54.2	52.1
655.0	50.4	56.0
673.0	47.6	60.0
693.0	44.6	63.0
713.0	42.0	65.2
735.0	38.7	68.3
753.0	36.1	70.1
773.0	33.5	74.3
793.0	31.0	75.7
813.0	28.0	78.6
841.0	25.1	80.9
849.0	23.1	82.4
873.0	20.5	84.4
893.0	18.7	86.7

(a) Loading

LOAD (lbs)	Δ_c 10^{-3} inches	$\omega_{1,1}$ (Hz)
853.0	20.0	85.1
813.0	25.6	80.6
793.0	26.4	79.2
773.0	27.9	78.8
753.0	29.6	76.8
733.0	31.5	74.9
713.0	33.6	73.6
673.0	39.2	67.9
653.0	41.5	66.4
633.0	44.2	64.7
583.0	50.5	55.1
533.0	59.3	49.2
433.0	70.4	47.8
333.0	74.9	54.1
237.0	76.9	57.8
133.0	79.1	63.9
33.0	80.2	67.6

(b) Unloading

Initial Displacement Readings at the corners: 86.9, 85.3, 86.0, 85.4 milli inches

Δ_c = 81.2 milli inches

Amplitude of initial imperfection = (86.9 + 85.3 + 86.0 + 85.4)/4 − 81.2
= 4.7 milli inches.

Table B1 Experimental Results for Plate 1 – Test 1 (Fundamental Frequencies)

LOAD (lbs)	Δ_c 10^{-3} inches	$\omega_{1,2}$ (Hz)
33.0	80.2	145.2
133.0	79.3	136.9
233.0	77.5	123.5
337.0	74.8	111.5
433.0	71.2	101.6
533.0	63.9	92.5
583.0	57.9	92.0
635.0	49.7	97.4
653.0	47.2	99.8
673.0	44.4	105.4
693.0	41.3	108.9
712.0	38.5	118.0
733.0	36.1	122.8
755.0	33.3	128.7
771.0	31.4	133.8
793.0	28.9	137.3
815.0	26.5	142.8
833.0	25.0	146.0
849.0	23.1	149.6
873.0	20.5	155.5
893.0	18.7	158.4

(a) Loading

LOAD (lbs)	Δ_c 10^{-3} inches	$\omega_{1,2}$ (Hz)
853.0	20.0	155.8
793.0	23.8	149.6
753.0	28.7	140.8
713.0	32.5	132.9
673.0	38.0	123.4
633.0	41.9	116.7
583.0	49.4	100.8
533.0	57.0	95.1
433.0	67.9	100.7
333.0	73.3	111.4
233.0	76.3	124.0
133.0	78.7	135.7
33.0	80.2	139.7

(b) Unloading

Initial Displacement Readings at the corners: 86.9, 85.3, 86.0, 85.4 milli inches

Δ_c = 80.2 milli inches

Amplitude of initial imperfection = (86.9 + 85.3 + 86.0 + 85.4)/4 − 80.2
= 5.7 milli inches

Table B2 Experimental Results for Plate 1 Test 2
(Natural Frequencies – 2nd mode)

LOAD (lbs)	Δ_c 10^{-3} inches	ω_{13} (Hz)
33.0	80.6	273.9
233.0	77.7	249.9
333.0	74.4	237.1
433.0	70.3	225.6
483.0	67.1	222.1
533.0	62.3	216.9
583.0	55.8	214.9
653.0	45.0	218.9
673.0	42.5	220.7
693.0	39.7	224.8
713.0	37.1	226.3
733.0	34.1	229.8
773.0	29.6	237.5
833.0	23.2	251.1
893.0	17.3	262.3

(a) Loading

LOAD (lbs)	Δ_c 10^{-3} inches	ω_{13} (Hz)
833.0	19.7	256.0
793.0	23.0	249.9
733.0	29.1	239.7
633.0	41.0	225.3
583.0	49.2	219.6
533.0	57.5	219.7
433.0	69.4	226.3
333.0	73.5	237.9
233.0	76.8	247.7
133.0	79.2	267.5
33.0	80.1	273.7

(b) Unloading

Initial Displacement Readings 86.9, 85.3; 86.0, 85.4 } milli inches

Δ_c = 80.6 milli inches

Amplitude of initial imperfection = (86.9 + 85.3 + 86.0 + 85.4)/4 − 80.6 = 5.3 milli inches

Flapping of the top edge observed. When pressed with a finger at the top the frequency increased from 273.7 to 277.4 Hz at 33 lbs. After the application of load the frequency was not affected by touching at the top edge. Flapping ceased.

Table B3 Experimental Results for Plate 1 - 3rd Frequency (Test 3)

LOAD (lbs.)	Δ_c 10^{-3} inch	ω_{L1}	ω_{L2}
33.0	94.9	63.0-64.0	144.0
133.0	92.7	59.0-61.0	137.0-139.0
233.0	89.1	54.0-55.0	129.0-131.0
333.0	83.5	51.0	120.0
386.0	79.4	50.0	117.0
434.0	74.3	53.0	116.0
537.0	63.6	61.0	119.0
633.0	53.0	74.0	129.0
733.0	43.0	82.0	140.0
833.0	33.5	89.0	153.0
925.0	25.9	95.0	163.0
1033.0	18.1	107.0	176.0
1133.0	10.4	112.0	186.0
1233.0	3.5	123.0	194.0

(a). Loading

LOAD (lbs.)	Δ_c 10^{-3} inch	ω_{U1}	ω_{U2}
1133.0	8.0	115.0	197.0
1033.0	15.5	107.0	180.0
933.0	22.8	98.0	172.0
833.0	30.1	91.0	162.0
733.0	38.5	83.0	152.0
633.0	48.0	75.0-77.0	139.0
533.0	60.4	63.0-64.0	122.0
433.0	71.7	56.0	117.0
333.0	76.8	51.0	116.0
331.0	81.8	50.0	119.0
233.0	87.7	55.0-56.0	129.0
129.0	91.4	59.0	134.0
33.0	93.5	63.0-66.0	141.0-143.0

(b) Unloading

Table B4. Experimental Results for Plate 2.

LOAD (lbs.)	Δ_c 10^{-3} inch	$\omega_{1,1}$	$\omega_{1,2}$
33.0	99.6	65.5	143.0
135.0	98.3	61.0	137.0
233.0	96.2	55.5	127.0
338.0	92.5	50.5	118.0
433.0	86.1	47.0	110.0
537.0	75.7	53.0	107.0
633.0	64.7	64.0	115.0
733.0	53.8	75.0	128.5
827.0	44.7	81.0	144.0
933.0	35.9	89.5	158.0
1025.0	29.1	97.0	168.0
1135.0	20.9	105.0	181.0
1233.0	13.4	111.0	192.0
1333.0	6.6	120.0	198.0
1405.0	1.6	128.0	203.5

(a). Loading

LOAD (lbs.)	Δ_c 10^{-3} inch	$\omega_{1,1}$	$\omega_{1,2}$
1235.0	10.7	114.0	193.0
1033.0	23.9	98.0	180.0
833.0	39.0	86.0	157.0
633.0	57.0	73.0	132.0
433.0	81.2	52.0	113.0
233.0	93.2	55.5	127.5
33.0	97.7	65.0	143.0

(b) Unloading

Table B5. Experimental Results for Plate 3

LOAD (lbs.)	Δ_c ($\frac{1}{1000}$ inch)	$\omega_{1,1}$ (Hz)	$\omega_{1,2}$ (Hz)
33.0	77.1	66.0	134.0
138.0	71.8	69.0	128.0
233.0	64.9	67.0	122.0
333.0	55.7	69.5	120.0
433.0	46.3	79.0	124.0
535.0	35.8	86.0	134.0
633.0	25.2	93.0	149.0
733.0	16.0 ↓	105.5	163.5
	55.9		
833.0	47.7	117.0	176.0
933.0	38.5	MISSED	189.0
1033.0	30.8	135.5	199.0
1133.0	22.6	145.0	207.0
1233.0	15.0	155.0	212.0
1333.0	7.6	165.0	226.0

(a) LOADING

LOAD (lbs.)	Δ_c ($\frac{1}{1000}$ inch)	$\omega_{1,1}$ (Hz)	$\omega_{1,2}$ (Hz)
33.0	114.1	67.0	134.5
71.0	109.7	69.0	130.0
233.0	100.5	69.5	123.5
325.0	87.7	76.5	124.0
433.0	76.6	85.0	133.5
533.0	65.8	94.5	149.0
533.0	65.8	94.5	149.0
633.0	57.1	100.5	164.0
733.0	49.4	111.0	176.0
833.0	40.8	121.0	188.0
933.0	32.7	130.0	196.0
1037.0	25.0	140.0	204.0
1133.0	17.7	150.0	210.0
1233.0	10.8	159.0	MISSED

(b) UNLOADING

↓ - Capacitance probe was reset

Initial Displacement Readings (in mil inch) at the corners: 96.5, 93.0, 92.2, 95.9

Amplitude of initial imperfection = Δ_c - Average of the initial reading at the corners $= \left[77.1 - \left(\frac{96.5+93.0+92.2+95.9}{4}\right)\right] \times 10^{-3}$

$= -17.75 \times 10^{-3}$ inch

Table B6 Experimental Results for Plate 4 (Test 1)

LOAD (lbs.)	Δ_c 10^{-3} inch	$\omega_{1,1}$	$\omega_{1,2}$
33.0	116.5		
233.0	104.1	73.0	
433.0	83.3	82.0	
639.0	63.3	101.0	
837.0	45.1	120.0	
1033.0	28.7	139.0	
1233.0	14.2	158.0	
1333.0	6.8 ↓	166.0	
	19.7		
1441.0	10.8	183.0	
1533.0	4.4	193.0	
1547.0	2.3 ↓		
	46.5		
1635.0	39.6	204.5	
1733.0	32.1	211.0	
1829.0	24.2	220.0	

(a) Loading

LOAD (lbs.)	Δ_c 10^{-3} inch	$\omega_{1,1}$	$\omega_{1,2}$
1733.0	25.6	219.0	
1633.0	29.8	212.0	
1533.0	36.4	203.0	
1433.0	43.7	194.0	
1333.0	51.4	187.0	
1329.0	52.1 ↓		
	1.9		
1233.0	9.4	176.0	
1133.0	15.3	159.0	
1033.0	22.9	149.0	
833.0	39.6	126.0-129.0	
633.0	58.3	109.0	
433.0	79.3	88.0	
233.0	103.1	71.0	
33.0	117.3	65.0	

(b) Unloading

Table B.7 Experimental Results for Plate 4 (Test 2)

LOAD (lbs.)	Δ_c 10^{-3} inch	$\omega_{1,1}$	$\omega_{1,2}$
33.0	81.9	73.5	165.0
186.0	83.1	72.0	161.0
233.0	83.5	69.0	157.5
333.0	84.0	65.5	150.5
433.0	83.9	62.0	143.0
535.0	84.8	58.0	137.0
633.0	85.6	54.0	129.0
733.0	88.0	49.0	121.0
833.0	92.5	47.0	116.0
933.0	100.0	49.0	113.0
1033.0	112.6	58.0	—
1045.0	116.5	62.0	127.0
1133.0	122.8 ↓		
	76.2	65.0	132.0
1233.0	84.8	69.5	139.5
1333.0	92.2	74.0	149.0

LOAD (lbs.)	Δ_c 10^{-3} inch	$\omega_{1,1}$	$\omega_{1,2}$
1433.0	99.5	77.5	160.0
1533.0	106.7	83.0	—
1833.0	125.1	100.5	—

Initial Displacement Readings at the corners: 80.0, 80.0 ; 73.4, 72.0 } milli inches

Δ_c = 81.9 milli inches

Amplitude of initial imperfection = $\Delta_c - (80.0 + 80.0 + 73.4 + 72.0)/4$

= 5.5 milli inches

Table B8 Experimental Results for Plate 5 (Test 1)

LOAD (lbs.)	Δ_c 10^{-3} inch	$\omega_{1,1}$	$\omega_{1,2}$
33.0	35.7	74.5	166.5
217.0	36.3	69.0	157.0
433.0	37.7	60.0	142.0
633.0	40.3	53.5	128.0
833.0	49.2	48.5	117.0
1033.0	68.2	62.0	126.0
1233.0	82.4	70.0	143.5
1433.0	96.9	78.0	161.0
1633.0	110.4	88.0	179.0†
1833.0	122.9	102.0	193.5
1849.0	123.2 ↓ 95.7		
2033.0	107.1	114.0	206.0
2233.0	117.3	128.5	219.0

(a) Loading

† Not clear mode

LOAD (lbs.)	Δ_c 10^{-3} inch	$\omega_{1,1}$	$\omega_{1,2}$
1833.0	102.0	111.0	206.0
1433.0	79.5	87.0	185.0
††1461.0	79.6	87.0	185.0
1233.0	65.4	81.0	169.5
841.0	33.9	63.5	132.0
437.0	10.6	61.5	143.0
33.0	9.6	75.0	167.0

(b) Unloading

†† Load increased

Initial Displacement Readings at the corners : 37.0, 35.2, 28.1, 26.7 } milli inches

Δ_c = 35.7 milli inches

Amplitude of initial imperfection = $35.7 - \left(\frac{37.0+35.2+28.1+26.7}{4}\right)$ = 3.95 milli inches

Table B.9 Experimental Results for Plate 5 (Test 2)

LOAD (lbs.)	Δ_c 10^{-3} inch	$\omega_{1,1}$	$\omega_{1,2}$
33.0	32.2	76.0	165.5
233.0	33.2	69.0	156.0
433.0	33.7	61.0	142.5
633.0	33.0	51.5	126.5
833.0	33.5	40.0	110.0
879.0	34.2	37.5	105.5
917.0	34.9	34.0	102.0
953.0	35.9	31.5	98.5
993.0	37.7	30.0-32.0	95.5
1033.0	44.4	34.0	97.5
1133.0	63.9	53.0	110.0
1233.0	72.4	64.0	132.5
1433.0	91.1	76.0	155.0
1633.0	105.0	[illegible]4.0	175.5
1833.0	119.4	103.0	192.5
2033.0	129.0	116.0	206.0

(a) Loading.

LOAD (lbs.)	Δ_c 10^{-3} inch	$\omega_{1,1}$	$\omega_{1,2}$
1633.0	111.7	93.5	187.0
1257.0	87.0	73.0	159.5
833.0	52.0	55.0	124.0
645.0	34.9	50.5	125.0
433.0	31.2	60.5	14[illegible]5
33.0	32.7	74.0	164.5

(b) Unloading

Initial Displacement Readings at the corners: 32.8, 33.2, 24.7, 23.7 milli inches

Δ_c = 32.2 milli inches.

Amplitude of imperfection = 32.2 − (32.8 + 33.2 + 24.7 + 23.7)/4 = 3.6 milli inches

Table B.10. Experimental Results for Plate 5 (Test 3)

LOAD (kgf)	Δ_c 10^{-3} inch	$\omega_{1,1}$	$\omega_{1,2}$
5	82.7	65.5	104.5
15	85.2	71.0	107.5
25	89.0	76.0	118.0
35	93.6	77.0	118.5
45	98.1	79.0	119.5
55	101.7	83.0	135.5
60	104.2	87.5	138.0
65	105.6	88.5	138.0
70	107.5	92.5	139.5
75	109.0	94.5	140.5
81	111.3	97.5	142.5
85	112.3	98.5	143.5

(a) Loading

LOAD (kgf)	Δ_c 10^{-3} inch	$\omega_{1,1}$	$\omega_{1,2}$
81	111.5	97.0	143.0
75	109.5	96.5	140.5
70	107.8	91.5	140.5
65	106.4	87.5	140.5
60	104.9	86.5	140.5
55	102.7	84.5	137.5
45	99.1	79.0	134.5
35	95.3	81–86	126.0
25	91.6	76.5	118.0
15	89.0	71.0	109.0
5	86.1	68.0	106.5

(b) Unloading

Initial Displacement Readings at the corners 28.6, 12.2, 36.8, 23.7 } milli inches

Δ_c = 82.7 milli inches

Amplitude of initial imperfection = 82.7 − (28.6 + 12.2 + 36.8 + 23.7)/4
= 57.38 milli inches.

Loads given in kgf units

Table B21 Experimental Results for Plate 6 (Test 1)

LOAD (P) (lbs)	Δ (milli inches)	Δ/P ×10³
0	0	0/0
100	1.0	10.0
200	2.6	13.0
300	4.9	16.3
400	8.1	20.3
500	14.5	29.0
550	19.5	35.5
600	27.0	45.0
622	30.8	49.5
640	33.6	52.5
660	36.6	55.5
680	37.2	57.7
702	42.5	60.5
720	45.1	62.6
740	47.7	64.5
760	50.2	66.1
780	53.2	68.2
808	56.1	69.4

P	Δ	Δ/P
780	55.6	71.28
740	53.3	72.0
700	49.7	71.0
640	42.0	65.6
600	37.0	61.7
550	30.7	55.8
500	21.9	43.8
400	10.8	27.0
300	6.3	21.00
204	4.3	21.1
100	2.1	21.0

Table B12 Southwell's plot Data for Plate 1 — Test 1

LOAD (P) (lbs).	Δ (milli Inches)	Δ/P ×10^3
0	0	0/0
200	2.9	14.5
300	6.2	20.7
400	10.3	25.8
450	13.5	30.0
500	18.3	36.6
550	24.8	45.1
620	35.6	57.4
640	38.1	59.5
660	40.9	62.0
680	43.5	64.0
700	46.5	66.4
740	51.0	68.9
800	57.4	71.8
860	63.3	73.6

P	Δ	Δ/P ×10^3
800	60.9	76.1
760	57.6	75.8
700	51.5	73.6
600	39.6	66.0
550	31.4	57.1
500	23.1	46.2
400	12.2	30.5
300	7.1	23.7
200	3.8	19.0
100	1.4	14.0
0	0.5	0.0

Table B.13 Southwell's plot Data for Plate 1 – Test 3

LOAD (lbs)	$Z_{1,1}$	$Z_{1,3}$	$Z_{3,1}$	$Z_{3,3}$	μ	$\omega_{1,1}$ (Hz)
33	0.1576	0.0	0.0	0.0	0.1576	65.49
233	0.2268	-0.0002	-0.0005	-0.0002	0.2273	55.37
333					0.2880	50.16
433	0.3888	-0.0004	-0.0014	-0.0005	0.3901	45.70
483	0.462	0.00	-0.002	-0.001	0.463	44.35
533	0.556	0.00	-0.002	-0.001	0.557	44.19
633	0.800	0.0014	0.0006	-0.0011	0.7969	48.60
683	0.939	0.003	0.003	-0.001	0.932	52.56
733	1.0796	0.0056	0.0078	-0.0010	1.0652	57.41
783	1.22	0.009	0.014	-0.000	1.197	62.21
833	1.358	0.0126	0.0208	-0.0002	1.3244	67.51
933	1.6318	0.0225	0.0395	0.0019	1.5717	77.99
1135	2.1116	0.0476	0.0843	0.0099	1.9896	96.38
1333	2.5519	0.0789	0.1363	0.0235	2.3602	114.06
1405	2.7036	0.0913	0.1558	0.0297	2.4862	120.35

Table 8.4 Theoretical Results for 1 mm plate with

$z_0 = 0.15h \sin\left(\frac{\pi x}{a}\right) \sin\left(\frac{\pi y}{b}\right)$.

LOAD (lbs.)	$Z_{1,1}$	$Z_{1,3}$	$Z_{3,1}$	$Z_{3,3}$	μ	$\omega_{1,1}$ (Hz)
33	0·2625	0·0	0·0	0·0	0·2625	66·34
233	0·372	-0·0002	-0·0006	-0·0002	0·373	57·64
333	0·464	0·0	0·0	0·0	0·464	54·04
433	0·595	0·00	0·0	0·0	0·595	52·21
483	0·682	0·0	0·0	0·0	0·682	52·42
533	0·779	0·001	0·001	-0·001	0·776	53 59
633	1·0029	0·0043	0·0053	-0·0009	0·9924	58·63
683	1·124	0·007	0·009	0·0	1·108	62·11
733	1·2464	0·0094	0·0143	-0·0005	1·4938	66·13
783	1·369	0·0130	0·02	0·00	1·335	70·12
833	1·4895	0·0171	0·0278	0·0007	1·4453	74·42
933	1·7304	0·0268	0·0455	·0·0031	1·6612	83·12
1135	2·1913	0·0526	0·0903	0·0117	2·06	100·48
1333	2·6145	0·0837	0·1411	0·0254	2·4151	117·26
1405	2·7609	0·0961	0·1600	0·0317	2·5365	123·27

Table 8.15 Theoretical Results for 1 mm. plate with

$z_0 = 0.25h \sin(\frac{\pi x}{a}) \sin(\frac{\pi y}{b})$

LOAD (lbs)	$Z_{1,1}$	$Z_{1,3}$	$Z_{3,1}$	$Z_{3,3}$	μ	$\omega_{1,1}$ (Hz)
133	0·6444	0·0004	0·0002	-0·0003	0·6435	56·32
233	0·8459	0·0018	0·0020	-0·0005	0·8416	58·00
333	1·1140	0·0060	0·0080	0·00	1·1000	59·84
383	1·2660	0·0090	0·0140	0·00	1·2430	63·20
433	1·4260	0·0140	0·0220	0·0006	1·3900	67·28
533	1·754	0·027	0·044	0·003	1·686	76·67
633	2·081	0·045	0·074	0·009	1·971	86·87
733	2·402	0·066	0·109	0·017	2·244	97·41
833	2·715	0·091	0·148	0·028	2·504	108·27
933	3·016	0·118	0·188	0·042	2·752	119·14
1033	3·307	0·147	0·228	0·058	2·990	129·92
1333	4·113	0·236	0·338	0·113	3·652	162·06
1533	4·600	0·294	0·401	0·149	4·054	182·07
1829	5·257	0·374	0·482	0·201	4·602	211·16

Table B16 Theoretical Results for Plate 4 (with $\mu_0 = 0·47$)

LOAD (lbs.)	$Z_{1,1}$	$Z_{1,3}$	$Z_{3,1}$	$Z_{3,3}$	μ	$\omega_{1,1}$ (Hz)
0.0	0.47	—	—	—	0.47	62.78
333	1.130	0.007	0.014	0.000	1.109	70.59
533	1.791	0.029	0.060	0.0061	1.708	97.67
733	2.450	0.069	0.130	0.022	2.270	127.31
933	3.068	0.121	0.215	0.049	2.781	153.03
1333	4.156	0.237	0.362	0.119	3.676	193.02
1829	5.287	0.373	0.500	0.206	4.620	231.63

Table B17. Theoretical Results for Plate 4 with Standard Boundary Conditions.

3 OF/DE 3

MICROCOPY RESOLUTION TEST CHART
NBS 1010a
ANSI and ISO TEST CHART No. 2

1.0 1.1 1.25 1.4 1.6 1.8 2.0 2.2 2.5 2.8 3.2 3.6 4.0

LOAD (lbs.)	$Z_{1,1}$	$Z_{1,3}$	$Z_{3,1}$	$Z_{3,3}$	μ	$\omega_{1,1}$ (Hz)
33	0.0517	0.0	0.0	0.0	0.0517	75.47
533	0.1033	-0.0002	-0.0005	-0.0001	0.1039	53.64
733	0.1705	-0.0004	-0.0011	-0.0003	0.1717	42.62
833	0.2470	-0.0006	-0.002	-0.0006	0.249	37.23
933	0.3980	-0.0008	-0.0029	-0.0008	0.4009	35.31
950	0.4339	-0.0008	-0.0031	-0.0009	0.4369	35.76
975	0.4910	-0.0007	-0.0032	-0.0010	0.4939	36.98
983	0.5100				0.5130	37.42
1033	0.6359	-0.0001	-0.0028	-0.0012	0.6376	41.60
1083	0.7630	0.0010	-0.0010	-0.0013	0.7623	46.63
1133	0.8865	0.0022	0.0008	-0.0015	0.8820	52.07
1233	1.1154	0.0061	0.0078	-0.0014	1.1001	62.35
1433	1.5159	0.0178	0.0298	0.0005	1.4688	80.35
1633	1.8678	0.0336	0.0589	0.0047	1.7800	96.17
1933	2.3418	0.0630	0.1101	0.0160	2.1847	117.36
2033	2.4894	0.0740	0.1281	0.0210	2.3083	123.80
2233	2.7731	0.0975	0.1648	0.0326	2.5434	136.95

Table B.18. Theoretical Results for Plate 5 ($\mu_0 = 0.05$)

LOAD (Kgf)	$Z_{1,1}$	$Z_{1,3}$	$Z_{3,1}$	$Z_{3,3}$	μ	$\omega_{1,1}$ (Hz)
20	2.834	0.0105	0.0104	0.0013	2.8144	87.52
50	3.0398	0.0284	0.0286	0.0044	2.9872	92.86
100	3.3940	0.0638	0.0653	0.0128	3.2777	103.44
150	3.7590	0.1055	0.1090	0.0263	3.5708	116.38

Table B.19 Theoretical Results for Plate 6 with $\mu_0 = 27$

	Deflection Readings at Load = 33. lbs						
	1	2	3	4	5	6	7
A	869	854	845	881	827	857	853
B	920	896	862	828	799	799	79.9
C	914	893	859	821	78.4	79.7	800
D	887	872	845	809	793	807	815
E	862	857	845	815	799	822	830
F	842	854	861	834	827	838	842
G	860	887	895	876	847	858	854

	Deflection Readings at a load of 633 lbs						
	1	2	3	4	5	6	7
A	766	815	793	777	781	835	845
B	843	759	640	578	688	688	743
C	809	705	554	471	499	63.4	724
D	798	694	554	476	504	644	739
E	79.0	71.3	60.4	545	564	687	765
F	798	762	706	671	668	752	80.2
G	838	843	821	784	775	820	838

	Deflection Readings at a load of 733 lbs						
	1	2	3	4	·5	6	7
A	834	788	753	735	75.2	810	83.1
B	798	678	505	426	465	615	710
C	763	612	400	302	350	548	683
D	760	627	43.0	33.5	384	581	707
E	762	657	512	446	483	639	741
F	782	730	655	623	629	724	793
G	829	826	795	768	762	803	829

Table B.20 Deflection Readings for Plate 1

	Deflection Readings at a load of 793 lbs						
	1	2	3	4	5	6	7
A	827	776	745	73.5	749	810	832
B	778	639	441	362	412	585	673
C	739	574	327	217	271	513	663
D	741	590	371	276	330	546	690
E	747	623	466	392	433	603	727
F	773	716	623	58[illegible]	601	709	785
G	824	816	779	743	740	794	824

	Deflection Readings at a load of 33 lbs						
	1	2	3	4	5	6	7
A	867	855	848	836	826	857	854
B	921	898	865	833	799	793	793
C	910	890	857	817	770	776	[illegible]
D	885	870	845	817	801	807	815
E	859	854	843	824	814	821	830
F	844	854	859	843	826	836	84[illegible]
G	857	885	892	873	843	856	852

	Deflection Readings at a load of 793 lbs						
	1	2	3	4	5	6	7
A	827	77.7	745	733	746	807	831
B	77.8	637	439	366	414	581	693
C	74.1	575	330	229	283	515	663
D	743	593	372	276	334	547	691
E	747	63.1	465	392	442	617	726
F	773	714	625	583	599	709	730
G	825	818	779	74.9	74.3	795	826

Table B 20 — Continued.

	Deflection Readings at a load of 833 lbs						
	1	2	3	4	5	6	7
A	82 2	76 9	73 6	72 9	74 5	80 4	82 9
B	76 7	61 1	40 0	32 6	37 3	56 0	68 3
C	72 8	54 7	28 8	18 4	25 0	49 2	65 4
D	73 2	57 0	33 4	23 6	29 5	53 0	63 1
E	73 3	60 8	43 0	35 6	40 7	59 3	71 7
F	76 4	69 5	59 8	55 2	57 3	68 9	77 0
G	82 0	81 0	76 9	73 8	73 4	78 7	82 1

	Deflection Readings at a load of 393 lbs						
	1	2	3	4	5	6	7
A	81 2	75 1	71 4	70 9	72 1	79 3	82 4
B	74 4	57 5	34 0	26 1	32 1	52 9	66 6
C	70 7	50 3	22 0	10 6	19 0	44 8	63 4
D	71 4	54 2	27 5	16 2	23 7	49 4	66 3
E	72 2	57 8	37 5	29 2	34 8	56 1	70 2
F	75 5	67 7	56 8	51 6	54 1	67 2	76 3
G	81 4	79 8	75 1	71 8	71 3	77 7	81 4

	Deflection Readings at a load of 329 lbs						
	1	2	3	4	5	6	7
A	81·5	75 8	72 2	70 9	73 0	79 8	82 6
B	75 5	59 4	37 4	28 8	35 5	55 4	67 7
C	71·7	53 6	25 7	14 9	21 9	47 4	64 3
D	72 3	55 6	30 8	20 7	27 4	51 0	67 0
E	73 1	60 1	41 7	33 6	38 9	58 3	71 1
F	75 9	69 1	58·8	53 9	56 1	68 4	76 5
G	81 6	80 5	76 3	73 3	72 4	78 4	81 5

Table B20 – Continued

	Deflection Readings at a Load of 793 lbs						
	1	2	3	4	5	6	7
A	81 8	76 5	73 3	72 3	74 5	80 0	82 3
B	76 1	60 8	39 8	31 9	37 3	56 3	68 3
C	72 5	54 5	28 8	18 5	24 5	48 6	65 1
D	73 1	57 5	34 0	24 0	30 5	53 3	67 9
E	73 8	6 7	44 0	36 7	41 9	59 3	71 7
F	76 4	70 1	60 7	56 3	58 2	69 7	77
G	81 8	81 0	77 1	73 1	73 0	78 7	81 7

	Deflection Readings at a Load of 733 lbs						
	1	2	3	4	5	6	7
A	82 1	77 3	74 2	73 1	75 0	80 7	82 7
B	78 1	64 4	45 1	37 2	42 3	59 2	69 5
C	74 3	58 3	34 6	24 9	31 0	52 4	66 7
D	74 6	60 1	39 4	30 2	36 0	55 7	69 3
E	75 2	64 5	49 1	42 4	47 0	62 4	73 2
F	77 1	71 6	63 4	58 5	60 5	70 8	77 6
G	82 3	81 9	78 6	75 7	74 8	79 6	82 2

	Deflection Readings at a Load of 631 lbs						
	1	2	3	4	5	6	7
A	83 9	80 2	77 3	75 9	77 4	82 0	83 4
B	81 6	71 4	57 0	49 6	53 5	64 9	72 3
C	78.2	66 2	48 2	39 3	42 7	59 6	70 0
D	77 8	66 8	50 2	42 2	46 0	61 8	72.0
E	77 7	67 2	57 1	51 4	54 5	66 8	75 3
F	78 9	75 0	68 8	65 1	66 3	74 1	79 1
G	82 8	83 3	80 9	78 3	76 8	80 8	82 8

Table B 20-Continued

	Deflection Readings at a load of 533 lbs						
	1	2	3	4	5	6	7
A	850	824	803	799	791	835	840
B	856	791	697	650	646	713	754
C	826	745	631	562	581	671	736
D	812	734	623	563	579	682	75[illegible]
E	801	742	652	613	632	715	775
F	800	776	734	705	707	766	803
G	836	845	831	803	793	820	833

	Deflection Readings at a load of 433 lbs						
	1	2	3	4	5	6	7
A	860	841	825	823	817	844	842
B	886	847	78.9	750	730	758	775
C	862	818	748	697	688	73.5	766
D	842	795	72.3	681	679	738	777
E	822	784	730	69.0	696	756	794
F	817	806	781	755	749	792	816
G	83.9	856	849	824	80.8	830	833

	Deflection Readings at a load of 33 lbs						
	1	2	3	4	5	6	7
A	863	851	842	823	820	843	839
B	911	889	856	818	789	791	790
C	901	882	849	812	788	789	792
D	874	860	835	804	782	797	805
E	849	845	833	815	799	811	820
F	833	844	849	832	814	826	831
G	850	877	884	864	840	847	843

Table B.20 - Continued

	Deflection Readings at a load of 33 lbs						
	1	2	3	4	5	6	7
A	96 5	94 7	94 6	100 5	94 6	91 1	93 0
B	96 8	91 0	88 4	91 0	92 9	82 3	99 4
C	95 7	88 7	86 6	81 9	76 3	78 1	87 5
D	93 7	87 1	85 2	77 6	76 5	78 5	88 5
E	90 5	85 4	82 6	78 5	78 8	84 7	91 7
F	89 1	87 3	91 7	88 7	90 2	92 6	93 8
G	92 2	94 2	98 3	98 0	99 2	98 4	75 7

	Deflection Readings at a load of 733 lbs						
	1	2	3	4	5	6	7
A	94 2	88·6	35·8	90 7	88 6	91 5	94 7
B	81 8	63 4	45 4	45·9	44 1	56 1	73 4
C	79 0	56 3	31 0	19 0	20 8	42 7	66 4
D	78 3	58 5	31·7	15 7	20 8	42 4	66 2
E	75 7	57 9	35 6	24 7	29 0	50 6	69 3
F	72 6	67 1	58 3	51 3	54 9	65 6	74 4
G	85 5	82 2	78 7	75 4	76 6	79 0	80 0

	Deflection Readings at a load of 1323 lbs						
	1	2	3	4	5	6	7
A	129 6	122 6	121 5	125 2	123 7	123 1	131 0
B	107 7	70 9	41 1	42 4	44 0	68 4	101 1
C	109 7	71 5	21 9	5 9	14 1	55 8	96 6
D	110 5	73 4	25 5	3 9	14 6	56 7	97 2
E	106 6	74 1	31 0	16 7	24 6	62 6	98 7
F	109 2	85 4	65 3	57 8	60 4	80 0	103 6
G	122 8	114 0	106 9	103 7	103 5	108 7	116 3

Table B 21 Deflection Readings for Plate 4

	Deflection Readings at a load of 33 lbs						
	1	2	3	4	5	6	7
A	370	361	353	352	353	351	352
B	387	390	386	376	365	353	347
C	379	385	387	379	360	347	346
D	363	366	363	360	345	338	339
E	349	350	348	341	331	327	330
F	316	310	300	292	29.6	293	310
G	281	268	255	247	237	249	267

	Deflection Readings at a load of 1041 lbs						
	1	2	3	4	5	6	7
A	419	459	502	505	479	430	375
B	452	532	634	652	59.1	465	331
C	459	554	696	735	663	506	412
D	43.2	514	638	672	605	465	384
E	389	444	523	535	475	367	305
F	324	335	351	336	238	232	20
G	274	26.5	253	231	193	162	159

	Deflection Readings at a load of 2245 lbs						
	1	2	3	4	5	6	7
A	239	355	473	482	439	322	191
B	376	627	946	995	392	567	307
C	396	710	1139	1238	1100	664	349
D	36[illegible]	650	1059	1181	1034	610	313
E	30.3	539	872	959	313	462	229
F	168	29.7	462	481	374	161	35
G	5.7	105	160	154	31	*	*

* Probe on contact with the plate

Table B22 Deflection Readings for Plate 5

	Deflection Readings at a load 57.5 kgf						
	1	2	3	4	5	6	7
A	236	263	237	220	180	136	122
B	407	453	509	552	496	325	235
C	451	534	667	754	682	425	277
D	473	571	722	830	749	460	300
E	462	540	676	782	710	445	295
F	400	429	498	567	525	352	255
G	368	333	331	373	359	258	[illegible]

	Deflection Readings at a load of 55 kgf						
	1	2	3	4	5	6	7
A	219	191	197	209	198	161	137
B	471	570	651	675	639	421	292
C	509	651	845	951	867	547	343
D	525	668	856	1016	930	572	354
E	505	623	818	951	870	538	339
F	43.9	507	619	699	637	410	291
G	39.7	380	418	462	422	31.6	246

Table B.23 Deflection Readings for Plate 6

GAUGE LOCATION NO.	X-coordinate (mm)	Y-coordinate (mm)	Orientation θ (°)
1	15.0	19.0	0
2	15.0	128.5	0
3	19.0	238.0	0
4	17.0	237.0	+ 45
5	15.0	235.0	90
6	75.0	69.0	0
7	75.0	128.5	0
8	75.0	189.0	0
9	150.0	19.0	0
10	150.0	69.0	0
11	146.5	128.5	0
12	148.5	127.0	- 45
13	150.0	125.0	90
14	150.0	189.0	0
15	146.5	238.5	0
16	148.5	237.0	- 45
17	150.0	235.0	90

Table 8.24 LOCATION AND ORIENTATION OF THE STRAIN GAUGES

GAUGE LOCATION No	X COORDINATE (mm)	Y COORDINATE (mm)	ORIENTATION θ (°)
18	225.0	69.0	0
19	225.0	128.5	0
20	225.0	189.0	0
21	281.0	19.0	0
22	283.0	21.0	+ 45
23	284.5	23.0	90
24	284.5	128.5	0
25	281.0	239.0	0
26	283.0	237.5	- 45
27	284.5	236.0	90

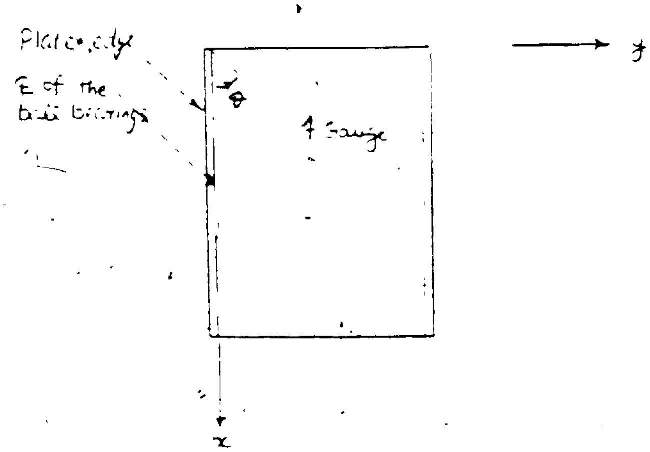

Table B 24 -- Continued

Gauge No →	Micro Strain Readings								Micro Strain Readings							
	1		2		3		4		5		6		7		8	
Load (lbs) / Side →	A	B	A	B	A	B	A	B	A	B	A	B	A	B	A	B
33	0.0	0.0	0.0	0.0	0.0	0.0	0.0	0.0	0.0	0.0	0.0	0.0	0.0	0.0	0.0	0.0
233	1.0	2.0	-60.5	-46.0	-2.5	-3.0	8.0	-12.0	3.5	4.5	-29.0	-7.5	-40.5	-16.5	-17.5	-3.0
333	-0.5	5.5	-74.5	-60.0	5.5	-3.0	24.0	-23.5	13.5	5.0	-36.5	-5.5	-51.5	-17.0	-19.5	-2.0
433	-24.0	9.0	-104.0	-65.0	-5.5	-8.0	30.5	-43.5	6.0	4.0	-67.0	0.0	-88.5	-9.0	-47.0	2.0
483	-24.5	10.5	-111.0	-65.6	-6.0	-9.5	39.5	-56.0	9.0	3.5	-77.5	4.6	-100.0	-1.5	-56.5	5.0
533	-35.5	15.0	-121.5	-61.6	-9.5	+13.0	50.0	-72.5	9.5	3.0	-93.6	9.5	-101.0	9.5	-70.5	9.0
633	-60.0	24.5	-144.5	-41.0	-20.6	-20.5	75.0	-107.0	13.0	2.5	-124.6	35.5	-152.5	35.5	-99.0	25.0
733	-89.5	35.0	-174.5	-30.5	-33.5	-27.0	103.0	-143.6	18.5	5.5	-157.0	65.5	-186.5	65.5	-137.5	42.0
833	-127.5	48.0	-207.0	-5.0	-53.0	-33.0	133.5	-184.5	23.5	7.5	-189.0	94.5	-221.0	94.5	-159.5	57.0
893	-149.5	56.0	-224.0	10.0	-65.5	-38.5	152.6	-207.0	28.0	10.0	-205.0	109.6	-236.5	109.5	-176.0	65.5
833	-138.0	62.5	-224.0	13.0	-57.0	-29.5	149.5	-196.6	25.5	9.0	-200.0	77.6	-233.5	105.5	-171.0	65.0
733	-104.6	69.5	-211.0	9.6	-38.0	-15.5	136.0	-167.0	22.0	4.0	-182.0	69.0	-211.5	90.5	-153.5	60.0
633	-69.0	72.0	-194.0	-3.0	-18.5	2.0	115.0	-127.0	15.0	1.0	-185.6	67.5	-194.0	68.0	-126.5	52.0
533	-39.5	63.0	-168.5	-25.5	-5.0	9.0	92.5	-91.5	11.5	2.0	-123.0	42.0	-163.5	41.5	-98.5	39.0
483	-28.0	58.0	-153.5	-35.5	-1.0	10.5	79.5	-75.0	13.5	2.6	-104.0	83.5	-142.5	27.5	-81.0	31.5
433	-16.5	51.0	-137.0	-46.5	3.0	11.5	65.0	-56.5	12.6	2.0	-84.0	23.0	-121.5	12.0	-64.0	24.0
333	3.0	35.0	-107.0	-56.5	6.5	11.0	41.5	-28.5	12.0	6.0	-48.6	8.0	-78.0	-8.5	-33.5	10.0
233	25.0	19.0	-76.0	-49.5	10.0	11.0	28.5	-11.0	12.0	7.0	-23.5	4.0	-46.5	-12.5	-12.0	5.5
33	42.6	4.0	14.0	6.0	12.0	18.0	14.0	6.5	12.0	5.0	10.0	9.0	7.0	5.5	11.5	8.0

Table B.25 Micro Strain Readings

Gauge No. →	9		10		11		12		13		14		15		16	
	MICRO STRAIN READINGS								MICRO STRAIN READINGS							
Load (lbs) / Side →	A	B	A	B	A	B	A	B	A	B	A	B	A	B	A	B
33	0.0	0.0	0.0	0.0	0.0	0.0	0.0	0.0	0.0	0.0	0.0	0.0	0.0	0.0	0.0	0.0
233	-18.5	-14.0	-22.0	-12.0	-21.0	-9.0	-13.5	5.0	-12.0	21.0	-18.5	-9.0	-17.5	-10.0	-6.0	-5.5
333	-26.0	-24.0	-31.5	-16.5	-27.0	-11.0	-18.5	11.0	-15.5	35.0	-28.0	-11.5	-15.5	-15.0	1.0	-8.0
433	-40.0	-34.5	-46.0	-20.0	-43.5	-10.0	-28.5	20.0	-31.5	52.0	-42.5	-14.0	-30.5	-24.5	-5.0	-14.5
483	-45.5	-40.5	-51.0	-21.5	-48.0	-6.5	-33.5	25.0	-38.5	61.5	-48.5	-15.0	-38.5	-30.0	-6.0	-17.5
533	-54.0	-47.5	-58.0	-22.0	-54.5	-6.0	-41.5	32.5	-45.0	73.0	-56.0	-16.0	-51.5	-37.0	-10.5	-21.5
633	-70.5	-61.0	-67.5	-24.5	-60.0	2.5	-50.5	46.0	-51.5	95.5	-68.0	-16.5	-67.5	-52.5	-10.0	-28.5
733	-89.0	-80.5	-75.0	-25.5	-62.0	6.5	-58.5	58.5	-70.0	117.5	-78.5	-21.0	-88.6	-72.0	-12.0	-35.5
833	-108.5	-102.0	-80.0	-31.5	-62.0	11.5	-66.5	71.0	-99.0	137.6	-86.6	-26.0	-111.0	-95.0	-19.0	-41.0
893	-121.0	-113.0	-82.0	-32.5	-60.0	15.0	-64.5	77.0	-110.5	149.6	-90.0	-28.6	-125.0	-106.5	-24.0	-42.5
833	-113.5	-103.6	-80.0	-28.6	-61.0	14.0	-65.5	77.0	-87.5	148.0	-85.6	-26.5	-116.0	-99.5	-28.5	-41.5
733	-95.5	-84.0	-73.0	-25.5	-57.0	9.0	-61.5	70.0	-76.0	136.5	-79.5	-24.0	-97.0	-82.0	-11.0	-38.5
633	-74.0	-62.5	-64.0	-20.5	-53.0	4.5	-51.0	60.5	-72.6	118.5	-68.0	-20.0	-70.5	-60.0	-1.0	-33.6
533	-54.0	-46.0	-56.0	-17.0	-60.0	-1.5	-42.5	50.0	-56.5	107.0	-58.0	-16.0	-49.5	-42.0	4.0	-24.6
483	-46.5	-36.0	-51.5	-15.6	-46.0	-3.5	-37.0	44.0	-48.0	91.0	-52.0	-16.0	-39.5	-34.0	3.0	-22.5
433	-37.5	-30.0	-46.0	-13.5	-42.5	-4.5	-30.0	36.5	-32.6	78.5	-45.0	-13.0	-28.0	-26.0	5.0	-17.5
333	-24.5	-18.0	-33.0	-11.5	-28.5	-8.0	-15.0	23.5	-49.0	52.5	-31.5	-9.0	-12.5	-11.5	7.0	-8.0
233	-13.0	-7.5	-20.0	-6.0	-14.0	-5.5	-2.5	16.0	-4.5	35.5	-17.5	-5.0	-0.5	-5.5	12.5	-1.0
33	7.5	8.5	6.0	6.6	16.5	5.6	16.5	7.0	-8.5	8.0	3.5	6.0	13.5	6.0	19.5	6.5

Table B25 - Continued

Gauge No. →	17		18		19		20	
Load (lbs) / Side →	A	B	A	B	A	B	A	B
33	0.0	0.0	0.0	0.0	0.0	0.0	0.0	0.0
233	2.5	6.5	-12.0	-7.5	-19.5	-1.5	-14.5	-6.0
333	15.0	12.0	-17.5	-12.5	-26.0	-13.0	-20.5	-8.5
433	7.0	17.0	-25.0	-18.5	-31.0	-16.0	-21.5	-14.0
483	8.5	20.5	-21.0	-22.0	-35.0	-16.5	-33.5	-16.5
533	16.5	25.0	-33.0	-22.0	-38.0	-15.5	-37.5	-18.5
633	13.5	36.5	-40.5	-25.5	-44.0	-11.5	-48.0	-20.0
733	12.5	50.5	-50.5	-24.5	-51.0	-3.0	-61.5	-20.5
833	11.5	66.5	-63.5	-23.0	-64.5	10.0	-77.5	-11.0
883	9.5	76.0	-74.5	-17.5	-72.5	22.0	-91.0	-11.5
833	15.0	72.0	-67.0	-17.0	-67.0	20.0	-84.5	-11.0
733	13.0	61.0	-53.0	-18.5	-57.0	7.0	-70.0	-15.5
633	17.5	47.0	-41.5	-20.5	-45.5	-4.0	-53.0	-16.0
533	23.0	36.0	-30.5	-17.5	-31.5	-10.0	-41.0	-14.5
483	0.5	31.0	-27.0	-15.5	-36.0	-13.5	-36.0	-13.5
433	1.5	26.0	-23.0	-11.5	-34.0	-12.0	-31.0	-10.5
333	4.0	19.0	-16.0	-7.5	-21.0	-12.0	-23.0	-5.5
233	4.0	14.0	-8.5	-1.0	-22.0	-7.0	-15.5	0.0
33	2.5	6.5	5.5	6.5	3.0	6.5	4.0	8.0

Gauge No. →	21		22		23		24	
Load (lbs) / Side →	A	B	A	B	A	B	A	B
33	0.0	0.0	0.0	0.0	0.0	0.0	0.0	0.0
233	-51.5	35.0	-20.0	24.0	23.0	-20.0	-47.5	12.0
333	-71.0	23.5	-27.0	-9.5	29.0	23.6	-50.0	2.5
433	-93.0	-15.0	-32.0	-47.5	31.0	30.5	-56.0	-24.5
483	-102.0	-2.5	-32.0	-31.5	33.5	29.5	-58.5	-3.5
533	-112.5	-17.0	-33.0	-54.5	35.0	21.0	-61.0	-15.5
633	-130.0	-30.0	-27.5	-70.0	41.0	34.0	-65.0	-13.5
733	-146.5	-45.0	-20.0	-94.0	44.0	38.0	-70.0	-16.5
833	-164.0	-70.5	-10.0	-130.5	41.0	28.0	-77.0	-17.5
883	-174.0	-71.5	-3.5	-144.5	52.0	31.0	-80.0	-23.5
833	-161.5	-73.5	-5.0	-136.5	51.0	29.0	-77.0	-26.5
733	-153.5	-56.5	-9.5	-110.5	50.0	30.0	-73.5	-23.5
633	-136.0	-39.5	-12.0	-84.5	49.0	28.5	-69.0	-21.5
533	-117.5	-25.5	-13.5	-62.5	48.5	25.0	-66.0	-24.5
483	-109.5	-18.5	-14.0	-52.0	48.0	24.0	-64.0	-21.5
433	-100.0	-9.5	-13.5	-40.0	48.0	22.5	-63.0	-20.0
333	-81.5	8.5	-11.0	-15.5	45.0	18.0	-58.0	-16.0
233	-55.5	29.5	-3.0	5.5	42.0	11.0	-49.0	-10.0
33	-14.0	42.0	5.5	22.5	21.0	2.0	4.5	21.0

Gauge No. →	25		26		27	
Load (lbs) / Side →	A	B	A	B	A	B
33	0.0	0.0	0.0	0.0	0.0	0.0
233	-40.0	11.5	-12.0	-21.0	1.0	-1.5
333	-65.5	0.5	-17.5	-42.5	15.0	-1.5
433	-77.5	-19.0	-25.5	-61.5	11.0	-6.0
483	-87.5	-24.5	-20.5	-81.5	12.5	-4.0
533	-100.0	-45.0	-31.5	-97.0	9.5	-3.0
633	-121.0	-55.5	-31.5	-125.0	15.0	3.0
733	-141.5	-70.8	-26.5	-151.5	11.0	9.5
833	-163.0	-87.5	-41.5	-185.5	21.0	14.0
883	-176.0	-93.5	-13.0	-201.0	25.5	11.0
833	-161.5	-86.5	-13.5	-190.5	25.5	19.0
733	-151.5	-70.0	-11.0	-162.5	22.5	16.0
633	-130.0	-41.0	-17.5	-127.5	17.5	14.0
533	-109.0	-28.0	-14.5	-97.0	18.5	10.5
483	-90.5	-18.5	-12.0	-83.0	15.0	10.5
433	-86.5	-7.5	-8.5	-67.0	17.5	8.5
333	-65.0	8.0	-2.5	-38.5	11.0	4.5
233	-44.5	10.0	5.5	-13.0	16.5	3.5
33	-12.5	12.0	5.5	6.5	4.0	0.0

MICRO STRAIN READINGS

Table B.25 - Continued

GAUGE LOCATION No. →		MICRO STRAIN AT MID PLANE							
		1		2		3		4	
LOAD (lbs)	LOAD RATIO	THEOR	EXP	THEOR	EXP	THEO	EXP.	THEO	EXP
33	0.048	0.00	0.00	0.00	0.00	0.00	0.00	0.00	0.00
233	0.336	-22.95	1.50	-9.75	-53.25	-23.03	-2.75	-13.54	-2.50
333	0.481	-34.61	2.50	-14.00	-67.25	-34.73	1.25	-19.84	2.30
433	0.625	-46.50	-7.50	-17.58	-84.50	-46.67	-6.75	-25.65	-6.15
483	0.697		-7.00		-88.25		-7.75		-12.75
533	0.769	-58.73	-10.25	-20.33	-91.50	-58.94	-11.25	-30.81	-11.25
633	0.913	-71.40	-17.75	-22.17	-96.75	-71.64	-20.50	-35.38	-11.60
733	1.058	-84.61	-27.25	-23.08	-102.50	-84.89	-30.25	-39.28	-20.25
833	1.202	-98.44	-39.75	-23.15	-106.00	-98.75	-43.00	-42.58	-25.50
893	1.289	-101.07	-46.75	-22.81	-117.00	-107.40	-52.00	-44.28	-27.25
833	1.202	-98.44	-37.75	-23.15	-105.60	-98.75	-43.25	-42.58	-23.50
733	1.058	-84.61	-17.50	-23.08	-100.75	-84.89	-26.75	-39.28	-15.50
633	0.913	-71.40	1.50	-22.17	-98.50	-71.64	-8.25	-35.38	-6.00
533	0.769	-58.73	11.75	-20.33	-97.00	-58.94	2.00	-30.84	0.25
483	0.697		15.00		-94.50		4.75		2.25
433	0.625	-46.50	17.25	-17.58	-91.75	-46.67	7.25	-25.45	4.26
333	0.481	-34.61	19.00	-14.00	-81.76	-34.73	8.75	-19.89	6.50
233	0.336	-22.95	22.00	-9.75	-62.75	-23.03	10.50	-13.54	8.75
33	0.048	0.00	23.25	0.00	10.00	0.00	12.50	0.00	10.25

GAUGE LOCATION No. →		MICRO STRAIN AT MID PLANE							
		5		6		7		8	
LOAD (lbs)	LOAD RATIO	THEOR	EXP	THEOR	EXP	THEO	EXP	THEO	EXP
33	0.048	0.00	0.00	0.00	0.00	0.00	0.00	0.00	0.00
233	0.336	2.72	4.00	-16.53	-18.25	-12.20	-28.50	-16.81	-10.25
333	0.481	4.04	9.25	-24.71	-21.00	-17.21	-34.25	-25.18	-10.75
433	0.625	5.30	5.00	-32.78	-33.50	-21.12	-41.75	-33.51	-22.50
483	0.697		6.26		-36.50		-50.75		-25.75
533	0.769	6.49	6.25	-40.72	-42.00	-2[illegible].10	-49.75	-41.75	-30.75
633	0.913	7.67	7.75	-48.48	-60.75	-24.98	-58.50	-49.90	-37.00
733	1.058	8.51	12.00	-56.03	-45.75	-25.12	-60.50	-57.90	-42.75
833	1.202	9.29	15.50	-63.35	-47.25	-24.39	-63.25	-65.72	-51.25
893	1.289	9.64	19.00	-67.62	-47.75	-23.61	-63.50	-70.30	-55.25
833	1.202	9.28	17.25	-63.36	-61.25	-24.39	-64.00	-65.72	-53.00
733	1.058	8.51	13.00	-56.03	-56.50	-25.12	-64.50	-57.90	-46.76
633	0.913	7.57	8.00	-46.48	-47.00	-24.98	-63.00	-49.90	-37.25
533	0.769	6.49	6.75	-40.72	-40.50	-23.70	-61.00	-41.75	-29.75
483	0.697		8.00		-35.25		-57.50		-24.25
433	0.625	5.30	7.25	-32.78	-30.50	-21.12	-54.75	-33.51	-20.00
333	0.481	4.04	8.50	-24.71	-20.25	-17.21	-43.25	-25.18	-11.75
233	0.336	2.72	9.50	-16.53	-9.75	-12.20	25.50	-16.81	-3.26
33	0.048	0.00	8.50	0.00	9.50	0.00	6.25	0.00	10.75

Table B26 Comparison of Theoretical and Experimental Values of Strains

Gauge Location No →		Micro Strain at Mid Plane							
		9		10		11		12	
Load (lbs)	Load Ratio	Theor	Exp	Theor	Exp	Theo	Exp	Theo	Exp
33	0.048	0.00	0.00	0.00	0.00	0.00	0.00	0.00	0.00
233	0.336	-21.69	-16.25	-16.49	-17.00	-13.31	-15.00	-4.39	-4.25
333	0.481	-34.26	-25.00	-24.51	-24.00	-18.77	-19.00	-5.83	-1.26
433	0.625	-48.59	-37.25	-32.26	-33.00	-22.99	-26.75	-6.55	-4.25
483	0.697		-43.00		-36.25		-27.25		-4.26
533	0.769	-64.97	-50.75	-39.65	-40.00	-25.79	-30.25	-6.46	-4.50
633	0.913	-83.38	-69.75	-46.64	-46.00	-27.19	-28.75	-5.69	-2.25
733	1.058	-103.56	-84.75	-53.22	-50.25	-27.38	-27.75	-4.45	0.00
833	1.202	-125.10	-105.25	-59.45	-55.75	-26.65	-25.25	-2.97	2.25
893	1.289	-138.56	-111.00	-63.04	-57.25	-25.16	-22.50	-2.05	6.26
833	1.202	-125.10	-108.50	-59.45	-54.25	-26.65	-23.50	-2.97	5.75
733	1.055	-103.56	-89.75	-53.22	-49.25	-27.38	-24.00	-4.45	3.75
633	0.913	-83.38	-68.25	-46.64	-42.25	-27.19	-24.25	-5.69	4.75
533	0.769	-64.97	-50.00	-39.65	-36.50	-25.79	-25.75	-6.46	3.75
483	0.697		-41.25		-33.50		-24.75		3.50
433	0.625	-48.59	-33.75	-32.26	-29.75	-22.99	-23.50	-6.55	3.25
333	0.481	-34.26	-21.25	-24.51	-22.25	-18.77	-18.25	-5.83	4.25
233	0.336	-21.69	-10.25	-16.49	-13.00	-13.31	-9.75	-4.39	6.75
33	0.048	0.00	8.00	0.00	6.25	0.00	11.00	0.00	11.75

Gauge Location No →		Micro Strain at Mid Plane							
		13		14		15		16	
Load (lbs)	Load Ratio	Theor	Exp	Theor	Exp	Theo	Exp	Theo	Exp
33	0.048	0.00	0.00	0.00	0.00	0.00	0.00	0.00	0.00
233	0.336	4.52	4.50	-16.66	-13.75	-21.90	-13.75	-7.31	-5.75
333	0.481	7.09	9.75	-24.81	-19.75	-34.64	-15.25	-6.48	-3.50
433	0.625	9.88	10.25	-32.76	-28.25	-49.21	-27.50	-16.19	-9.75
483	0.697		11.50		-31.75		-34.25		-11.75
533	0.769	12.84	14.00	-40.43	-36.00	-65.93	-44.25	-21.51	-16.00
633	0.913	15.77	11.00	-47.75	-42.25	-84.77	-60.00	-27.46	-19.25
733	1.058	18.45	23.75	-54.73	-49.75	-105.47	-80.25	-33.95	-23.75
833	1.202	20.66	19.25	-61.41	-56.25	-127.58	-103.00	-40.67	-30.00
893	1.289	21.71	14.75	-65.29	-57.26	-141.41	-115.15	-45.19	-33.25
833	1.202	20.66	30.25	-61.41	-56.00	-127.58	-107.75	-40.87	-31.00
733	1.055	18.45	29.75	-54.73	-51.75	-105.47	-89.50	-33.95	-24.75
633	0.913	15.77	23.00	-47.75	-44.00	-84.77	-65.25	-27.46	-17.25
533	0.769	12.64	22.75	-40.43	-37.00	-65.93	-45.75	-21.51	-11.25
483	0.697		21.50		-33.50		-36.75		-9.75
433	0.625	9.88	23.00	-32.76	-29.00	-49.21	-27.00	-16.16	-6.25
333	0.481	7.09	1.75	-24.81	-20.26	-34.64	-12.00	-11.48	-5.00
233	0.336	4.53	15.50	-16.66	-11.26	-21.90	-3.00	-7.39	5.75
33	0.048	0.00	-2.50	0.00	4.25	0.00	9.75	0.00	13.00

Table B26 - Continued

Gauge Location No		Micro Strain at Mid Plane							
		17		18		19		20	
Load (lbs)	Load Ratio	THEOR	EXP	THEOR	EXP	THEO	EXP.	THEO	EXP
33	0.048	0.00	0.00	0.00	0.00	0.00	0.00	0.00	0.00
233	0.336	6.98	4.50	-16.52	-9.75	-12.21	-14.50	-8.41	-10.88
333	0.481	11.10	13.50	-24.71	-15.00	-17.22	-19.50	-25.18	-14.50
433	0.625	15.86	13.00	-32.78	-21.75	-21.13	-24.50	-33.51	-21.25
483	0.697		14.50		-25.50		-25.25		-25.00
533	0.769	21.36	20.75	-40.72	-27.50	-23.71	-26.75	-41.75	-28.00
633	0.913	27.61	25.90	-48.47	-33.00	-24.99	-27.75	-49.90	-34.00
733	1.058	34.51	31.50	-56.03	-37.50	-25.14	-27.50	-57.50	-41.00
833	1.202	41.93	39.90	-63.35	-44.75	-24.40	-27.25	-65.72	-48.75
893	1.219	46.58	48.75	-67.62	-46.00	-23.61	-25.25	-70.30	-51.25
833	1.202	41.93	43.50	-63.35	-43.00	-24.40	-23.50	-65.72	-47.78
733	1.058	34.51	37.00	-56.03	-36.75	-25.14	-29.00	-57.90	-42.75
633	0.913	27.61	32.25	-48.47	-30.00	-24.99	-24.75	-49.90	-34.50
533	0.769	21.36	29.50	-40.72	-24.00	-23.71	-24.25	-41.75	-27.75
483	0.697		15.78		-21.25		-24.25		-24.75
433	0.625	15.86	13.75	-32.78	-17.25	-21.13	-23.00	-33.51	-26.75
333	0.481	11.10	11.50	-24.71	-11.75	-17.22	-20.50	-25.18	-14.25
233	0.336	6.98	9.00	-16.53	-4.75	-12.21	-14.50	-16.81	-7.75
33	0.048	0.00	4.50	0.00	6.00	0.00	4.25	0.00	-4.50

Gauge Location No		Micro Strain at Mid Plane							
		21		22		23		24	
Load (lbs)	Load Ratio	THEOR	EXP	THEOR	EXP	THEO	EXP	THEO	EXP
33	0.048	[illegible]	0.00	0.00	0.00	0.00	0.00	0.00	0.00
233	0.336	-22.85	-8.25	-13.24	2.00	2.73	1.50	-9.75	-15.25
333	0.481	-34.50	-23.75	-19.40	-18.25	4.06	-26.25	-14.08	-23.75
433	0.625	-46.42	-54.00	-25.05	-40.75	5.33	31.75	-17.53	-40.25
483	0.697		-57.25		-35.25		31.60		-31.00
533	0.769	-58.71	-64.75	-30.08	-43.75	6.53	32.00	-20.34	-38.25
633	0.913	-71.49	-80.00	-34.44	-48.75	7.64	37.50	-22.17	-39.25
733	1.058	-84.86	-95.75	-38.13	-57.00	8.61	41.00	-23.08	-43.25
833	1.202	-98.07	-117.25	-41.19	-70.25	9.42	38.80	-22.16	-47.25
893	1.219	-107.64	-126.25	-42.72	-74.00	9.81	41.50	-22.81	-51.75
833	1.202	-98.07	-123.50	-41.19	-70.78	9.42	40.80	-23.15	-61.78
733	1.058	-84.86	-105.00	-38.13	-60.00	8.61	40.00	-23.08	-48.50
633	0.913	-71.49	-81.25	-34.44	-48.25	7.64	38.60	-22.11	-46.35
533	0.769	-58.71	-71.60	-30.08	-38.00	6.53	36.76	-20.34	-45.25
483	0.697		-64.00		-33.00		36.00		-42.75
433	0.625	-46.42	-54.75	-25.05	-26.75	5.33	35.25	-17.59	-41.00
333	0.481	[illegible]	-36.50	-19.40	-12.25	4.05	31.50	-14.00	-31.00
233	0.336	[illegible]	-13.00	-13.24	1.25	2.73	26.50	-9.75	-29.50
33	0.048	[illegible]	14.00	0.00	14.00	0.00	11.50	0.00	12.75

Gauge Location No		Micro Strain at Mid Plane					
		25		26		27	
Load (lbs)	Load Ratio	THEOR	EXP.	THEOR	EXP	THEO	EXP
33	0.048	0.00	0.00	0.00	0.00	0.00	0.00
233	0.336	-23.11	-14.25	-11.53	-16.50	2.80	-0.75
333	0.481	-34.84	-27.50	-19.84	-30.00	4.17	2.25
433	0.625	-46.79	-49.25	-25.66	-47.50	5.48	2.50
483	0.697		-57.00		-55.00		3.25
533	0.769	-59.03	-72.50	-30.84	-64.25	6.72	3.25
633	0.913	-71.70	-88.25	-35.30	-78.25	7.86	7.00
733	1.058	-84.89	-105.75	-31.38	-59.00	8.87	14.25
833	1.202	-98.67	-125.25	-43.56	-102.60	9.70	18.50
893	1.219	-107.26	-134.75	-44.39	-107.00	10.10	23.25
833	1.202	-98.67	-128.00	-43.58	-163.00	9.70	22.25
733	1.058	-84.89	-111.25	-39.38	-90.25	8.87	19.25
633	0.913	-71.70	-89.00	-35.10	-72.50	7.86	16.75
533	0.769	-59.03	-68.50	-30.44	-58.75	6.72	14.50
483	0.697		-58.50		-41.50		14.25
433	0.625	-46.79	-47.00	-25.65	-37.75	5.48	14.00
333	0.481	-34.84	-28.50	-19.84	-20.50	4.17	10.75
233	0.336	-23.11	-17.28	-13.53	-3.75	2.80	10.00
33	0.048	0.00	-0.25	0.00	6.00	0.00	2.00

Table B26 - Continued

The first Fourier coefficients of the initial imperfection were calculated from the deflection readings at various points by using the following procedure:

$$z_{o_{1,1}} = \frac{4}{ab} \int_{x=0}^{a} \int_{y=0}^{b} z_o(x,y) \, \text{Sin}(\pi x/a) \, \text{Sin}(\pi y/b) \, dxdy \; .$$

The integration was carried out numerically using the measured values of $z_o(x,y)$ at the 49 grid points applying Simpson's rule.

The calculated values of $z_{o_{1,1}}$ are compared with the magnitudes of the initial imperfection at the centre in the following table. The deflection values for plates 2 and 3 were not measured at all the grid points.

Table B.27 First Fourier Coefficients of Initial Imperfection

Plate Number	Magnitude of Initial Imperfection at the Centre (1/1000 inches)	First Fourier Coefficient (1/1000 inches)
1	4.70	4.76
4 (Test 1)	17.22	17.75
5 (Test 1)	5.50	5.08
6	57.38	57.05

APPENDIX C

APPROXIMATE ANALYSIS OF THE POST BUCKLING AND VIBRATION BEHAVIOUR OF A SIMPLY SUPPORTED RECTANGULAR PLATE

The static displacements and natural frequencies of an imperfect plate subjected to uni-axial in-plane loading can be calculated in an approximate manner using the equilibrium approach. First, the deflections (static displacements) will be calculated. Having calculated the deflections and the static in-plane stresses, the same approach can be used for the calculation of natural frequencies.

Calculations of Deflections:

Consider the equilibrium of a simply supported rectangular plate subjected to uni-axial in-plane loading as shown in Figure C.1.

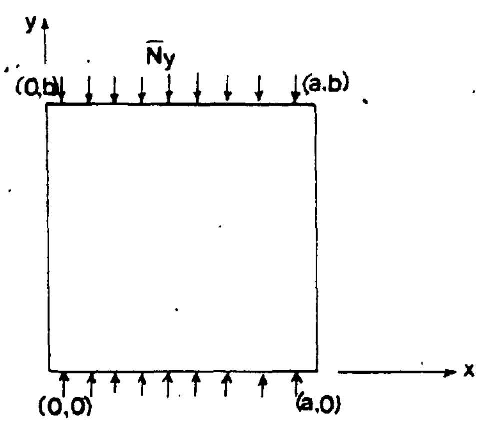

Figure C.1

Let the initial geometrical imperfection (distortion) of the plate be given by

$$z_o(x,y) = Z_o \sin(\frac{\pi x}{a}) \sin(\frac{\pi y}{b}) \quad (C.1)$$

The deflection at a load $\bar{N}_y$ (average in-plane load in y-direction per unit length) be expressed as

$$z(x,y) = \sum_{i=1,2..} \sum_{j=1,2..} Z_{i,j} \sin(\frac{i\pi x}{a}) \sin(\frac{j\pi y}{b}) \cdot \quad (C.2)$$

Consider the following in-plane boundary conditions:

(i) At sides x=o and x=a, the normal and tengential in-plane forces are zero (i.e. in-plane free).

(ii) At sides y=o and y=b, the normal displacements are constant (i.e. the load is applied via a rigid beam) and the tangential in-plane forces are zero (i.e. shear free).

The governing differential equation of equilibrium is

$$D\nabla^4(z-z_o) + N_x \frac{\partial^2 z}{\partial x^2} + N_y \frac{\partial^2 z}{\partial y^2} - 2 N_{xy} \frac{\partial^2 z}{\partial x \partial y} = 0, \quad (C.3)$$

where N_x, N_y and N_{xy} are the intensity of in-plane forces acting on the plate at a general point x,y, and D is the flexural rigidity of the plate.

The analysis can be simplified with the assumption that the in-plane shear force is negligible at all points on the plate

$$\text{i.e. } N_{xy} \doteq 0 \quad (C.4)$$

For equilibrium in the x-direction, $\frac{\partial N_x}{\partial x} + \frac{\partial N_{xy}}{\partial y} = 0$. (C.5)

From equation (C.4) and (C.5), $\frac{\partial N_x}{\partial x} = 0$.

But N_x = o at x=o and at x=a.

Therefore, $N_x = 0$ (C.5a)

at all points on the plate. Similarly equation of equilibrium in the y-direction gives,

$$\frac{\partial N_y}{\partial y} = 0$$

This means, N_{xy} is a function of x only. An expression for N_y may be formulated as follows:

Consider the displacement of a vertical strip of width δx at a distance x from the origin, as shown in Figure C.2.

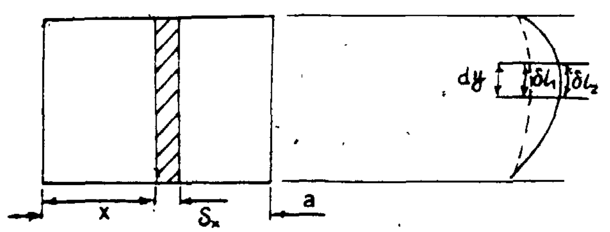

Figure C.2

If the plate was allowed to move freely at the top and bottom, the change in the curved length of the strip due to the loading is given by

$$\Delta \ell = \int_{y=o}^{b} (\delta \ell_2 - \delta \ell_1)\,dy = \frac{1}{2} \int_{y=o}^{b} [(\frac{\partial z}{\partial y})^2 - (\frac{\partial z_o}{\partial y})^2]\,dy .$$

Taking only the first term in the series for z from equation (C.2),

$$\Delta \ell = \frac{\pi^2}{2b^2} (Z^2_{1,1} - Z^2_o) \sin^2(\frac{\pi x}{a}) \int_{y=o}^{b} \cos^2(\frac{\pi y}{b}) dy$$

$$= \frac{\pi^2}{4b} (Z^2_{1,1} - Z^2_o) \sin^2(\frac{\pi x}{a}) \qquad (C.6)$$

In order to maintain a constant displacement at the top and bottom, this strip must be stretched back by a distance of $\Delta \ell$. The intensity of restraining stretching force required is given by:

$$R = -Eh(\frac{\Delta \ell}{b}) = -\frac{\pi^2 Eh}{4b^2} (Z^2_{1,1} - Z^2_o) \sin^2(\frac{\pi x}{a}) \qquad (C.7)$$

The resultant force from R is given by:

$$\bar{R} = \int_{x=o} R \, dx = -\frac{\pi^2 Eha}{8b^2} (Z^2_{1,1} - Z^2_o) \qquad (C.8)$$

The constant displacement condition at the top and bottom edges will not be violated if a constant uniform force intensity of $-\bar{R}/a$ is applied to maintain the equilibrium. Final distribution of net restraining force is then given by:

$$N_y = \bar{N}_y + R - \frac{\bar{R}}{a}$$

$$= \bar{N}_y - \frac{\pi^2 Eh}{4b^2}(Z^2_{1,1} - Z^2_o) \sin^2(\frac{\pi x}{a}) + \frac{\pi^2 Eh}{8b^2}(Z^2_{1,1} - Z^2_o)$$

$$= \bar{N}_y + \frac{\pi^2 Eh}{8b^2}(Z^2_{1,1} - Z^2_o) \cos(\frac{2\pi x}{a}) \qquad (C.9)$$

Substituting equations (C.4), (C.5a) and (C.9) into equation (C.3) yields the following equation:

$$\{D\pi^4(\frac{1}{a^2}+\frac{1}{b^2})^2(Z_{1,1}-Z_o) + [\bar{N}_y + \frac{-\pi^2 Eh}{8b^2}(Z_{1,1}^2-Z_o^2)\cos(\frac{2\pi x}{a})]$$

$$(\frac{-\pi^2 Z_{1,1}}{b^2})\} \cdot \sin(\frac{\pi x}{a})\sin(\frac{\pi y}{b}) = 0 \qquad \text{(C.10)}$$

Since the parameters within the square brackets are not functions of y,

$$\{D\pi^4(\frac{1}{a^2}+\frac{1}{b^2})^2(Z_{1,1}-Z_o)$$

$$+ [\bar{N}_y + \frac{\pi^2 Eh}{8b^2}(Z_{1,1}^2-Z_o^2)\cos(\frac{2\pi x}{a})](\frac{-\pi^2 Z_{1,1}}{b^2})\} \times$$

$$\sin(\frac{\pi x}{a}) = 0$$

Galerkin's method with the weighting function $\sin(\frac{\pi x}{a})$ gives

$$[D\pi^4(\frac{1}{a^2}+\frac{1}{b^2})^2(Z_{1,1}-Z_o)\frac{-\pi^2}{b^2} Z_{1,1} \bar{N}_y]\int_{x=o}^{a}\sin^2(\frac{\pi x}{a})dx$$

$$-\frac{\pi^4 Eh}{8b^4}Z_{1,1}(Z_{1,1}^2-Z_o^2)\int_{x=o}^{a}\cos(\frac{2\pi x}{a})\sin^2(\frac{\pi x}{a})dx = 0 \qquad \text{(C.11)}$$

but, $\displaystyle\int_{x=o}^{a}\sin^2(\frac{\pi x}{a})dx = \frac{a}{2}$ (C.11a)

and $\displaystyle\int_{x=o}^{a}\cos(\frac{2\pi x}{a})\sin^2(\frac{\pi x}{a})dx = -\frac{a}{4}$ (C.11b)

Substituting equations (C.11a) and (C.11b) in equation (C.11) gives:

$$[D\pi^4(\frac{1}{a^2}+\frac{1}{b^2})^2(Z_{1,1}-Z_o) - \frac{\pi^2}{b^2} Z_{1,1} \bar{N}_y]\frac{a}{2}$$

$$+ \pi^4 \frac{Eh}{8b^4} Z_{1,1}(Z_{1,1}^2-Z_o^2)\frac{a}{4} = 0 \qquad \text{(C.12)}$$

Let $\mu = \frac{Z_{1,1}}{h}$ and $\mu_o = \frac{Z_o}{h}$.

Dividing equation (C.12) by $D\pi^4(\frac{1}{a^2}+\frac{1}{b^2})^2 \frac{ah}{2}$

$$(\mu - \mu_o) - (\frac{\bar{N}_y}{\hat{N}_y})\mu + 1.5 \frac{(1-\nu^2)}{(1+\gamma^2)^2}\mu(\mu^2 - \mu_o^2) = 0 \qquad (C.13)$$

where γ is the aspect ratio given by $\gamma = b/a$, (C.13a)

and $\hat{N}_y$ is the critical force intensity given by

$$\hat{N}_y = \pi^2 D b^2 (\frac{1}{a^2}+\frac{1}{b^2})^2 \qquad (C.13b)$$

Let ρ be defined as a load ratio such that,

$$\rho = \frac{\bar{N}_y}{\hat{N}_y} \qquad (C.13c)$$

Equation (C.13) can be written as

$$(\mu - \mu_o) - \rho\mu + 1.5 \frac{(1-\nu^2)}{(1+\gamma^2)^2}\mu(\mu^2 - \mu_o^2) = 0$$

or $$[1 - \frac{\mu_o}{\mu} - \rho + C(\mu^2 - \mu_o^2)]\mu = 0 \qquad (C.14)$$

in which $C = 1.5 \frac{(1-\nu^2)}{(1+\gamma^2)^2}$ (C.14a)

for very small values of μ_o (i.e. if $\mu_o << \mu$),

$$[1 - \rho + C\mu^2]\mu = 0 \qquad (C.15)$$

This will be satisfied if $\mu = 0$ (C.15a),

or $\mu^2 = (\frac{1-\rho}{C})$ (C.15b).

Equations (C.15a) and (C.15b) represents the solution for the deflection of an initially flat plate. Figure C.3

illustrates the solution graphically

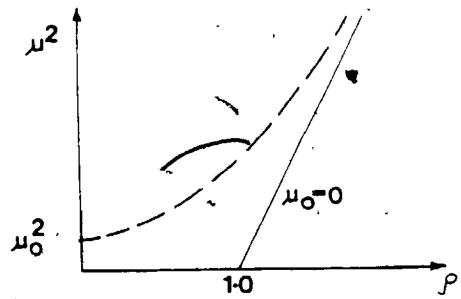

Figure C.3

For $\rho < 1.0$, $\mu = 0$ since the alternative solution $\mu^2 = \frac{1-\rho}{C}$ gives an imaginary value for μ.

Vibration Analysis

Neglecting the dynamic in-plane shear stresses in the plate, the plate vibration equation can be shown to be:

$$D\nabla^4 w + N_y \frac{\partial^2 w}{\partial y^2} + S_y \frac{\partial^2 z}{\partial x^2} - \bar{m}\,\omega^2 w = 0 \qquad (C.16)$$

where S_y is the dynamic in-plane force intensity in the y-direction

and w is the dynamic out-of-plane displacement given by

$$w(x,y,t) = H(t) \sin\left(\frac{\pi x}{a}\right) \sin\left(\frac{\pi y}{b}\right), \qquad (C.16a)$$

in which for simple harmonic motion,

$$H(t) = \hat{H} \sin(\omega t) \qquad (C.16b)$$

For dynamic analysis, the sides x = o and x = a can be taken as in-plane stress free (normal and shear). The top and bottom edges may be taken as being shear free (free to slide tangentially) and having constant normal displacements. Two simple cases are treated.

Case 1. Resultant Dynamic Forces at the Top and Bottom Edges are Zero

For this case S_y can be calculated as follows: Following the same procedure as in the case of deflection calculations, during vibration the change in length of a strip of plate at distance x from the origin is given by

$$\Delta\ell' = \frac{1}{2}\int_{y=o}^{b}[(\frac{\partial(z+w)}{\partial y})^2 - (\frac{\partial z}{\partial y})^2]dy$$

$$\approx \int_{y=o}^{b}\frac{\partial z}{\partial y}\frac{\partial w}{\partial y}dy \quad \text{for small amplitude vibrations}$$

$$\text{i.e. } \Delta\ell' = \frac{\pi^2 Z_{1,1}}{b^2} H \int_{y=o}^{b}\sin^2(\frac{\pi x}{a})\cos^2(\frac{\pi y}{b})dy$$

$$= \frac{\pi^2 Z_{1,1}}{b^2} H \ (\frac{b}{2}) \ \sin^2(\frac{\pi x}{a})$$

$$= \pi^2 \frac{\mu H h}{2b} \sin^2(\frac{\pi x}{a}) \qquad (C.17)$$

The corresponding intensity of stretching force is

$$S' = Eh\frac{\Delta\ell'}{b} = \pi^2\frac{Eh^2}{2b^2}\mu H \sin^2(\frac{\pi x}{a}) \qquad (C.18)$$

The resultant force $\bar{S}' = \int_{x=o}^{b} S'dx = \pi^2 Eh^2 \frac{\mu Ha}{4b^2}$ (C.19)

For equilibrium, the net force intensity $S_y = S' - \frac{\bar{S}'}{a}$

$$= -\pi^2 \frac{Eh^2}{4b^2} \mu H \cos(\frac{2\pi x}{a}) \quad (C.20)$$

Substuting equations (C.9) and (C.20) in equation (C.16) gives:

$$\{H D\pi^4 (\frac{1}{a^2} + \frac{1}{b^2})^2 - H \bar{N}_y \frac{\pi^2}{b^2} - [\pi^4 \frac{Eh^3}{8b^4} (\mu^2 - \mu_o^2)$$

$$+ \pi^4 \frac{Eh^3}{4b^4} \mu^2] H \cos(\frac{2\pi x}{a}) - \bar{m} \omega^2 H\} \sin(\frac{\pi x}{a}) \sin(\frac{\pi y}{b}) = 0$$

For non-trivial solution of H,

$$\{[D\pi^4 (\frac{1}{a^2} + \frac{1}{b^2})^2 - \bar{N}_y \frac{\pi^2}{b^2}] - [\pi^4 \frac{Eh^3}{8b^4} (\mu^2 - \mu_o^2)$$

$$+ \pi^4 \frac{Eh^3}{4b^4} \mu^2] \cos(\frac{2\pi x}{a}) - \bar{m} \omega^2\} \sin(\frac{\pi x}{a}) \sin(\frac{\pi y}{b}) = 0$$

Following the same procedure as in the deflection analysis, this can be transformed into:

$$\{1 - \rho + C[\mu^2 - \mu_o^2 + 2\mu^2] - \frac{\omega^2}{\Omega^2}\} = 0 \quad (C.21)$$

where $\Omega^2 = D \frac{\pi^4}{\bar{m}} (\frac{1}{a^2} + \frac{1}{b^2})^2$ (C.21a)

Ω can be recognized as the fundamental natural frequency of the unstressed plate.

Let $\lambda^2 = \frac{\omega^2}{\Omega^2}$ (C.22)

Then, $1 - \rho + C(\mu^2 - \mu_o^2) + 2C\mu^2 - \lambda^2 = 0$

or $\lambda^2 + \rho = 1 + 2C\mu^2 + C(\mu^2 - \mu_o^2)$ (C.23)

In equation (C.23), $2C\mu^2$ represents the effect of dynamic stretching of the plate (membrane stiffness on the frequency, and $C(\mu^2 - \mu_o^2)$ represents the effect of non-uniform static stress distribution on the frequency.

For $\mu_o << \mu$ (almost flat plate), the effect of membrane stretching is twice the effect of non-uniform stress distribution. Equation (C.23) is illustrated graphically in Figure C.4.

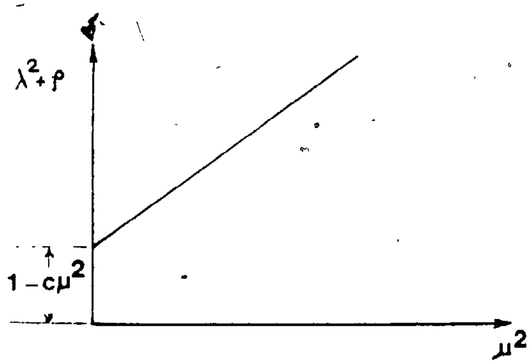

Figure C.4

Case 2 Top and Bottom Edges Fully Restrained Against Normal In-plane Movement

In this case, the analysis is similar to that for the previous case, except that no stress redistribution is required to maintain zero overall edge force.

$$\text{i.e. } S_y = S' = \pi^2 \frac{Eh^2}{2b^2} \mu H \sin^2(\frac{\pi x}{a}) \qquad (C.24)$$

The effect of S_y in the dynamic equilibrium equation can be determined by calculating the integral:

$$\int_{x=0}^{a} S_y\left(\frac{\partial^2 z}{\partial y^2}\right) \sin\left(\frac{\pi x}{a}\right) dx = 3\,\frac{\pi^4}{16b^4}\, Eh^3\, \mu^2 H$$

This leads to

$$1 - \rho + C(\mu^2 - \mu_o^2) + 6C\mu^2 - \lambda^2 = 0$$

$$\text{or } \lambda^2 + \rho = 1 + 6C\mu^2 + C(\mu^2 - \mu_o^2) \qquad \text{(C.25)}$$

The effect of dynamic membrane stretching is about six times as large as that of non-uniform stress distribution for an almost perfect plate ($\mu_o << \mu$).

From these relationships it can be observed that for a perfectly flat plate the following frequency load diagram is obtained.

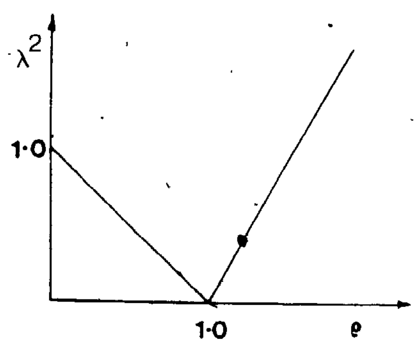

Figure C.5

The slope of the λ^2 vs ρ plot in the post buckling region is given by

$\theta = \tan^{-1}$ (3C) for case 1

and $\theta = \tan^{-1}$ (7C) for case 2.

From the above derivations it is clear that if the shear stress distribution is neglected and the static and dynamic out-of-plane displacements are assumed to take the shape of buckling and vibration of the corresponding flat plate, there exists a linear relationship between $(\lambda^2 + \rho)$ and μ^2. Such a relationship can also be derived for a spherically curved simply supported rectangular plate subjected to a constant uni-axial static in-plane stress distribution by adding the stress effect in the analysis published by Reissner [19].

APPENDIX D

DERIVATION OF THE EQUATION OF MOTION FOR A VIBRATING CURVED BEAM SUBJECTED TO STATIC AXIAL LOAD

The equation of motion for a curved beam subjected to static axial load can be derived using Newton's 2nd law of motion.

Consider the motion of the curved beam shown in Figure D.1, vibrating in its plane of curvature.

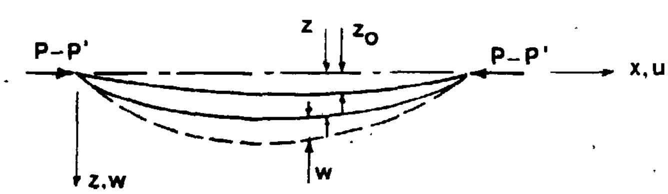

Figure D.1

Let z(x) be the transverse static displacement due to the applied compressive force P. Let u(x,t) and w(x,t) be the axial and transverse dynamic displacements (from the static equilibrium position) respectively. Let P' be the dynamic axial stretching force (tensile) induced on the beam during the vibration.

First consider the change in the transverse forces acting on a small element of length Δx.

The forces acting on the beam when it passes the static equilibrium position, and when it reaches the maximum positive excursion position are shown in Figure D.2 and Figure D.3 respectively.

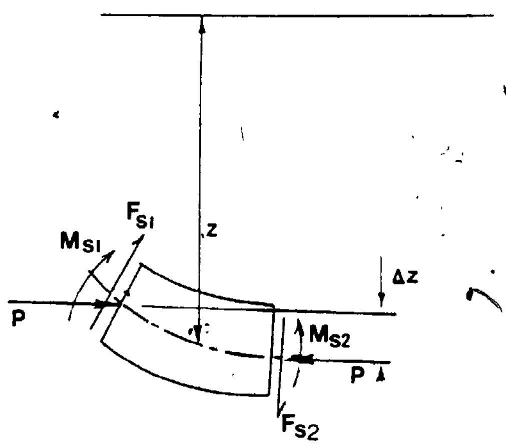

Figure D.2

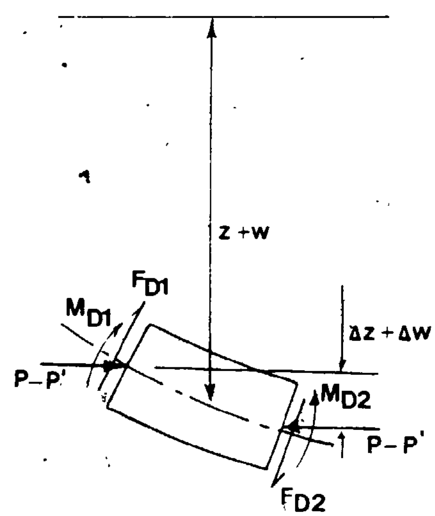

Figure D.3

For Figure D.2,

$$M_{s2}-M_{s1} = F_{s2}\cdot\Delta x + P\cdot\Delta z$$

As $\Delta x \to 0$,

$$= F_{s2}\cdot\Delta x + P\,\frac{\partial z}{\partial x}\cdot\Delta x$$

$$= (F_{s2} + P\,\frac{\partial z}{\partial x})\,\Delta x$$

or

$$\frac{\Delta M_s}{\Delta x} = F_{s2} + P\,\frac{\partial z}{\partial x}$$

as $\Delta x \to 0$, $$\frac{\partial M_s}{\partial x} = F_{s2} + P\frac{\partial z}{\partial x}.$$

$$F_{s2} = \frac{\partial M_s}{\partial x} - \frac{P\partial z}{\partial x}$$

$$F_{s2} - F_{s1} = \Delta F_s \simeq \frac{\partial F_{s2}}{\partial x} \cdot \Delta x$$

$$= \left(\frac{\partial^2 M_s}{\partial x^2} - P\cdot\frac{\partial^2 z}{\partial x^2}\right)\cdot \Delta x$$

But, using the Euler-Bernoulli's beam bending formula

$$\frac{\partial^2 M_s}{\partial x^2} = -EI\,\frac{\partial^4 z}{\partial x^4}$$

The net transverse force is,

$$\Delta F_s = \left(-EI\,\frac{\partial^4 z}{\partial x^4} - P\,\frac{\partial^2 z}{\partial x^2}\right)\Delta x$$

Similarly, by considering the equilibrium of forces shown in Figure D.3, it can be shown that

$$\Delta F_s + \Delta F_D = \left[-EI\,\frac{\partial^4 (z+w)}{\partial x^4} - P\,\frac{\partial^2 (z+w)}{\partial x^2} + P'\,\frac{\partial^2 (z+w)}{\partial x^2}\right]\Delta x$$

where P' is the axial force induced during vibration and can be calculated by considering the axial equilibrium.

The change in the transverse force during vibration is then given by

$$\Delta F_D = \left[-EI\,\frac{\partial^4 w}{\partial x^4} - P\,\frac{\partial^2 w}{\partial x^2} + P'\,\frac{\partial^2 (z+w)}{\partial x^2}\right]\ x$$

Using Newton's 2nd law of motion,

$$\Delta F_D = \bar{m}\ \Delta x\ \frac{\partial^2 w}{\partial t^2}$$

where, $\bar{m}$ is the mass per unit length.

This gives

$$-EI\ \frac{\partial^4 w}{\partial x^4} - P\ \frac{\partial^2 w}{\partial x^2} + P'\ \frac{\partial^2 z}{\partial x^2} + P'\ \frac{\partial^2 w}{\partial x^2} - \bar{m}\ \frac{\partial^2 w}{\partial t^2} = 0 \qquad \text{(D.1)}$$

P' is amplitude dependent and the product $P'\ \frac{\partial^2 w}{\partial x^2}$ can be neglected for small amplitude vibrations. For simple harmonic motion, $\frac{\partial^2 w}{\partial t^2} = -\omega^2 w$. Hence, equation (D.1) reduces to:-

$$EI\ \frac{\partial^4 w}{\partial x^4} + P\ \frac{\partial^2 w}{\partial x^2} - P'\ \frac{\partial^2 z}{\partial x^2} - \bar{m}\omega^2 w = 0 \qquad \text{(D.2)}$$

Neglecting the axial inertia $P' = EA\ \varepsilon'_x$

where ε'_x is the dynamic axial strain given by

$$\varepsilon'_x = \frac{\partial u}{\partial x} + \frac{1}{2}\left[\left(\frac{\partial(z+w)}{\partial x}\right)^2 - \left(\frac{\partial z}{\partial x}\right)^2\right]$$

$$\doteq \frac{\partial u}{\partial x} + \frac{\partial w}{\partial x} \cdot \frac{\partial z}{\partial x} + \frac{1}{2}\left(\frac{\partial w}{\partial x}\right)^2$$

$$\doteq \frac{\partial u}{\partial x} + \frac{\partial w}{\partial x} \cdot \frac{\partial z}{\partial x} \text{ (for small amplitude vibrations)}$$

or $$P' = EA\left(\frac{\partial u}{\partial x} + \frac{\partial w}{\partial x} \cdot \frac{\partial z}{\partial x}\right) \qquad \text{(D.3)}$$

The terms in equation (D.2) can be interpreted as follows:

Dynamic transverse force resisting the bending: $EI\ \frac{\partial^4 w}{\partial x^4}$

Dynamic transverse force resulting from the change in position of the applied axial force: $P\ \frac{\partial^2 w}{\partial x^2}$

Dynamic transverse resisting force due to the 'stretching' action of the beam: $P' \frac{\partial^2 z}{\partial x^2}$

The force resulting from the change in position of the stretching force $P' \frac{\partial^2 w}{\partial x^2}$ can be neglected for small amplitude vibrations.

Negative inertia force: $-m\omega^2 w$

All these forces maintain the dynamic equilibrium of the beam.

APPENDIX E

APPLICATION OF NEWTON-RAPHSON'S METHOD WITH A CONDITIONAL EQUATION

Consider the equations

$$A - uZ = 0 \tag{E.1}$$

and

$$u = Z^2 \tag{E.2}$$

where A is a constant.

Solving for Z using these two equations is equivalent to solving

$$A - Z^3 = 0 \tag{E.3}$$

Equation (E.3) can be solved using Newton-Raphson's method as follows:

Let $f(Z) = A - Z^3$.

$$\frac{\partial f}{\partial Z} = -3Z^2 .$$

$$\Delta f = \frac{\partial f}{\partial Z} \Delta Z = -3Z^2 (\Delta Z) \tag{E.4}$$

If equations (E.1) and (E.2) are treated separately,

i.e. $f = A - uZ \; ; \; u = Z^2$

$$\Delta f = \frac{\partial f}{\partial Z} \Delta Z + \frac{\partial f}{\partial u} \Delta u$$

$$= \frac{\partial f}{\partial Z} \Delta Z + \frac{\partial f}{\partial u} \cdot \frac{\partial u}{\partial Z} \Delta Z$$

$$= \left(\frac{\partial f}{\partial Z} + \frac{\partial f}{\partial u}\frac{\partial u}{\partial Z}\right)\Delta Z$$

$$= (-Z^2 - 2Z^2)\Delta Z = -3Z^2(\Delta Z)$$

This is the same as equation (E.4), and will lead to the iterative equation,

$$f_n = -3Z_n^2(Z_{n+1} - Z_n) \quad \text{(E.5)}$$

Hence, when using Newton-Raphson's method for a set of equations with several unknowns, if the relationship between some of the unknowns is known, then it is necessary to solve only some of the equations in terms of the independent unknowns - the relationship between which is not known. However, the effect of other unknowns is included by taking the total differential terms which contain the relationship between the independent and dependent unknowns.

In applying the Rayleigh-Ritz principle, first, all the displacement coefficients are treated as independent parameters when substituting in equations (3.2.7), (3.2.8) and (3.2.9). After this, the relationship between the in-plane and out-of-plane coefficients is established. Hereafter, the in-plane displacement coefficients are treated as dependent variables in solving the equation (3.2.9).

APPENDIX F

LINEARIZATION OF THE STRAIN ENERGY EXPRESSIONS FOR A VIBRATING CURVED BEAM UNDER AXIAL LOADING

Consider the free vibration of the beam shown in Figure F.1.

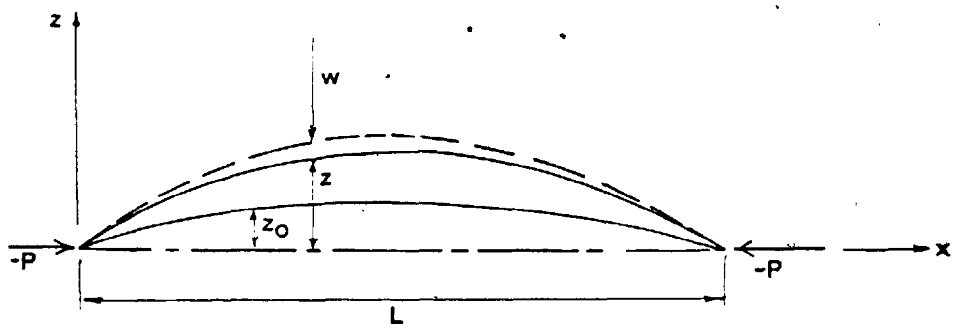

Figure F 1

Definitions

The static and dynamic displacements along x axis are given by u_s and u_d respectively.

The initial shape of the beam is given by z_o.

The transverse deflection of the beam under load P is z.

The transverse dynamic displacement from the equilibrium configuration is w.

z and w can be taken as a series with unknown coefficients i.e.

$$z = \sum_{\substack{i \\ i=1,2}} Z_i \phi_i \qquad (F.1)$$

$$w = \sum_{\substack{i \\ i=1,2}} H_i \psi_i \qquad (F.2)$$

where, ϕ_i and ψ_i are transverse shape functions that can represent the shape of the beam subject to boundary conditions.

Assuming that the beam is initially stress free, the static strain at a load P is given by,

$$\varepsilon = \frac{\partial u_s}{\partial x} + \frac{1}{2}\left(\frac{\partial z}{\partial x}\right)^2 - \frac{1}{2}\left(\frac{\partial z_o}{\partial x}\right)^2 \qquad (F.3)$$

The strain at the time of maximum positive excursion is given by,

$$\hat{\varepsilon} = \varepsilon + \varepsilon' \qquad (F.4)$$

where

$$\varepsilon' = \frac{\partial u_d}{\partial x} + \frac{1}{2}\left(\frac{\partial z}{\partial x} + \frac{\partial w}{\partial x}\right)^2 - \frac{1}{2}\left(\frac{\partial z}{\partial x}\right)^2$$

$$= \frac{\partial u}{\partial x} + \frac{\partial w}{\partial x} \cdot \frac{\partial z}{\partial x} + \frac{1}{2}\left(\frac{\partial w}{\partial x}\right)^2 \qquad (F.5)$$

The total potential energy of the beam at the time of maximum positive excursion is given by,

$$\hat{V} = \frac{1}{2}\int_{x=0}^{L} EI[\frac{\partial^2 z}{\partial x^2} + \frac{\partial^2 w}{\partial x^2} - \frac{\partial^2 z_o}{\partial x^2}]^2 dx + \frac{1}{2}\int_{x=0}^{L} EA(\varepsilon+\varepsilon')^2 dx$$

$$+ P[u_s+u_d]_{x=0}$$

$$- P[u_s+u_d]_{x=L}$$

$$= \frac{1}{2}\int_{x=0}^{L} EI[\frac{\partial^2 z}{\partial x^2} + \frac{\partial^2 w}{\partial x^2} - \frac{\partial^2 z_o}{\partial x^2}]^2 dx + \frac{1}{2}\int_{x=0}^{L} EA(\frac{\partial u_s}{\partial x} + \frac{\partial u_d}{\partial x}$$

$$+ \frac{1}{2}(\frac{\partial z}{\partial x})^2 - \frac{1}{2}(\frac{\partial z_o}{\partial x})^2 + \frac{\partial w}{\partial x} \cdot \frac{\partial z}{\partial x} + \frac{1}{2}(\frac{\partial w}{\partial x})^2]^2 dx$$

$$- P[u_s+u_d]_o^L \qquad (F.6)$$

This can be expressed as,

$$\hat{V} = \hat{U}_1 + \hat{U}_2 + \hat{U}_3 + \hat{U}_4 , \qquad (F.7)$$

where

$\hat{U}_1$ consists of static displacement terms only and is given by,

$$\hat{U}_1 = \frac{1}{2}\int_{x=0}^{L} EI(\frac{\partial^2 z}{\partial x^2} - \frac{\partial^2 z_o}{\partial x^2})^2 dx + \frac{1}{2}\int_{x=0}^{L} EA[\frac{\partial u_s}{\partial x}$$

$$+ \frac{1}{2}(\frac{\partial z}{\partial x})^2 - \frac{1}{2}(\frac{\partial z_o}{\partial x})^2]^2 dx - P[u_s]_o^L ; \qquad (F.7a)$$

$\hat{U}_2$ consists of first order dynamic terms, and is given by,

$$\hat{U}_2 = \int_{x=0}^{L} EI\left(\frac{\partial^2 z}{\partial x^2} - \frac{\partial^2 z_o}{\partial x^2}\right)\frac{\partial^2 w}{\partial x^2}dx + \int_{x=0}^{L} EA\left(\frac{\partial u_s}{\partial x}\right.$$

$$\left. + \frac{1}{2}\left(\left(\frac{\partial z}{\partial x}\right)^2 - \left(\frac{\partial z_o}{\partial x}\right)^2\right)\right)\left(\frac{\partial u_d}{\partial x} + \frac{\partial w}{\partial x}\cdot\frac{\partial z}{\partial x}\right)dx$$

$$- P[u_d]_{x=0}^{L} \qquad \text{(F.7b)}$$

$\hat{U}_3$ consists of second order dynamic terms, and is given by,

$$\hat{U}_3 = \frac{1}{2}\int_{x=0}^{L} EI\left(\frac{\partial^2 w}{\partial x^2}\right)^2 dx + \frac{1}{2}\int_{x=0}^{L} EA\left[\left(\frac{\partial u_d}{\partial x} + \frac{\partial w}{\partial x}\cdot\frac{\partial z}{\partial x}\right)^2\right.$$

$$\left. + \left(\frac{\partial u_s}{\partial x} + \frac{1}{2}\left(\frac{\partial z}{\partial x}\right)^2 - \frac{1}{2}\left(\frac{\partial z_o}{\partial x}\right)^2\right)\left(\frac{\partial w}{\partial x}\right)^2\right]dx \qquad \text{(F.7c)}$$

$\hat{U}_4$ consists of third and fourth order dynamic terms, and is given by,

$$\hat{U}_4 = \frac{1}{2}\int_{x=0}^{L} EA\left[\frac{1}{4}\left(\frac{\partial w}{\partial x}\right)^4 + \frac{\partial u_d}{\partial x}\left(\frac{\partial w}{\partial x}\right)^2 + \left(\frac{\partial w}{\partial x}\right)^3\left(\frac{\partial z}{\partial x}\right)\right]dx \qquad \text{(F.7d)}$$

When applying Rayleigh-Ritz method to the vibration analysis,

(i) $\hat{U}_1$ may be omitted since all terms in $\hat{U}_1$ are independent of dynamic displacements.

(ii) $\hat{U}_4$ consists of terms that are negligible compared to all other values ($\hat{U}_2$ and $\hat{U}_3$) for small amplitude vibrations.

(iii) It can be shown that although the individual terms in $\hat{U}_2$ are larger than those in $\hat{U}_3$, $\hat{U}_2$ must vanish by using the principle of virtual work as follows.

Let M be the bending moment induced at a section of the beam due to the applied load P

$$\text{i.e. } M = EI\left(\frac{\partial^2 z}{\partial x^2} - \frac{\partial^2 z_o}{\partial x^2}\right) \qquad \text{(F.8a)}$$

$$P = EA\varepsilon = EA\left[\frac{\partial u_s}{\partial x} + \frac{1}{2}\left(\frac{\partial z}{\partial x}\right)^2 - \frac{1}{2}\left(\frac{\partial z_o}{\partial x}\right)^2\right] \qquad \text{(F.8b)}$$

Substituting equations (F.8a) and (F.8b) in equation (F.7b) gives

$$\hat{U}_2 = \int_{x=0}^{L} \left[M \frac{\partial^2 w}{\partial x^2} + P\left(\frac{\partial u_d}{\partial x} + \frac{\partial w}{\partial x} \cdot \frac{\partial z}{\partial x}\right)\right] dx - P[u_d]_o^L \qquad \text{(F.9)}$$

For small amplitude vibrations, the dynamic axial strain ε' is given by,

$$\varepsilon' = \frac{\partial u_d}{\partial x} + \frac{\partial w}{\partial x} \cdot \frac{\partial z}{\partial x}$$

$$\text{Therefore } \hat{U}_2 = \int_{x=0}^{L} \left(M \frac{\partial^2 w}{\partial x^2} + P\,\varepsilon'\right) dx - P.\delta L \qquad \text{(F.10)}$$

where the elongation of the beam

$$\delta L = u_d(L) - u_d(O) \qquad \text{(F.10a)}$$

Since the dynamic displacement w is a geometrically compatible shape for the beam, it can be considered as a virtual displacement shape that induces a virtual strain ε' in the beam. $P.\delta L$ can be considered as the external virtual work due to the virtual displacement of the end forces (P). $\int_{x=0}^{L} (M \frac{\partial^2 w}{\partial x^2} + P\,\varepsilon')dx$ can be considered as the virtual internal work done on the beam. $\hat{U}_2$ then gives the net virtual work, which must be zero since M and P are the forces in equilibrium. This can be explicitly proven as follows.

Applying the Rayleigh-Ritz method for the static displacement analysis gives,

$$\frac{\partial \hat{U}_i}{\partial Z_i} = 0$$

$$\text{i.e. } \frac{\partial}{\partial Z_i} \{\frac{1}{2} \int_{x=0}^{L} EI(\frac{\partial^2 z}{\partial x^2} - \frac{\partial^2 z_o}{\partial x^2})^2 dx + \frac{1}{2} \int_{x=0}^{L} EA[\frac{\partial u_s}{\partial x}$$

$$+ \frac{1}{2}(\frac{\partial z}{\partial x})^2 - \frac{1}{2}(\frac{\partial z_o}{\partial x})^2]^2 dx - P[u_s]_o^L\} = 0$$

$$= \int_{x=0}^{L} EI(\frac{\partial^2 z}{\partial x^2} - \frac{\partial^2 z_o}{\partial x^2})\frac{\partial}{\partial Z_i}(\frac{\partial^2 z}{\partial x^2} - \frac{\partial^2 z_o}{\partial x^2})dx$$

$$+ \int_{x=0}^{L} EA[\frac{\partial u_s}{\partial x} + \frac{1}{2}(\frac{\partial z}{\partial x})^2 - \frac{1}{2}(\frac{\partial z_o}{\partial x})^2]\frac{\partial}{\partial Z_i}(\frac{1}{2}(\frac{\partial z}{\partial x})^2)dx = 0$$

$$= \int_{x=0}^{L} EI(\frac{\partial^2 z}{\partial x^2} - \frac{\partial^2 z_o}{\partial x^2})\frac{\partial^2 \phi_i}{\partial x^2} dx + \int_{x=0}^{L} EA[\frac{\partial u_s}{\partial x}$$

$$+ \frac{1}{2}(\frac{\partial z}{\partial x})^2 - \frac{1}{2}(\frac{\partial z_o}{\partial x})^2]\frac{\partial z}{\partial x} \cdot \frac{\partial \phi_i}{\partial x}$$

$$= \int_{x=0}^{L} (M \frac{\partial^2 \phi_i}{\partial x^2} + P \frac{\partial \phi_i}{\partial x} \cdot \frac{\partial z}{\partial x})dx \qquad (F.11)$$

Since ϕ_i is a valid shape function to be used in a virtual work concept, equation (F.11) can be considered as a statement of virtual work. If we replace ϕ_i by ψ_i, which is also a compatible displacement shape,

$$\int_{x=0}^{L} \left(M \frac{\partial^2 \psi_i}{\partial x^2} + P \frac{\partial \psi_i}{\partial x} \frac{\partial z}{\partial x}\right) dx = 0 \; .$$

Multiplying by H_i and summing gives

$$\sum_{i=1,2\ldots} \int_{x=0}^{L} \left(MH_i \frac{\partial^2 \psi_i}{\partial x^2} + P\, H_i \frac{\partial \psi_i}{\partial x} \frac{\partial z}{\partial x}\right) dx = 0 \; .$$

$$\text{i.e.} \quad \int_{x=0}^{L} \left\{M \sum_{i=1,2} H_i \frac{\partial^2 \psi_i}{\partial x^2} + P \frac{\partial z}{\partial x} \sum_{i=1,2,3} H_i \frac{\partial \psi_i}{\partial x}\right\} dx = 0 \, .$$

$$\int_{x=0}^{L} \left(M \frac{\partial^2 w}{\partial x^2} + P \frac{\partial w}{\partial x} \cdot \frac{\partial z}{\partial x}\right) dx = 0 \; . \qquad \text{(F.12)}$$

Equation (F.9) can be transformed as

$$\hat{U}_2 = \int_{x=0}^{L} \left(M \frac{\partial^2 w}{\partial x^2} + P \frac{\partial w}{\partial x} \cdot \frac{\partial z}{\partial x}\right) dx + \int_{x=0}^{L} P \frac{\partial u_d}{\partial x}\, dx - P[u_d]_o^L$$

$$= \int_{x=0}^{L} \left(M \frac{\partial^2 w}{\partial x^2} + P \frac{\partial w}{\partial x} \cdot \frac{\partial z}{\partial x}\right) dx + P[u_d]_o^L - P[u_d]_o^L$$

$$= 0 \quad \text{(using equation (F.12))} \qquad \text{(F.13)}$$

Hence, in the Rayleigh-Ritz analysis, it is only necessary to consider the terms associated with the second order dynamic displacement products for small amplitude vibrations. This results in linear minimization equations.

APPENDIX G

LISTING OF THE COMPUTER PROGRAM TO CALCULATE THE EFFECT OF THE FLEXIBILITY OF THE FRAME.

This program is used to calculate the terms associated with each deflection coefficient in the integral

$$\int_{x=0}^{a} k_y [v_d^2 \big|_{y=0} + v_d^2 \big|_{y=b}] dx,$$

where k_y is given by $k_y = 1/(f_{b1}+f_{b2}+f_{ax})$ as explained in Appendix H.

In the program f_{b1} is denoted as S1. S2 and S3 are the flexibilities due to the bending of the web of the channel and the axial straining respectively. The overall stiffness ST (k_y in Appendix H) is given by ST = 1/(S1+S2+S3).

The frame is subdivided into N elements and the integration is done numerically using trapezoidalmethod. JM and KM represent the mode numbers associated with the deflection coefficients. AX is the length of the plate and XL is the length of the vertical channels. XB is the length of channel near the top and bottom supports where the flexibility due to the bending of the web of the channel can be ignored. SK is the required integral. For a given IM,JM the calculated value of SK can be used in the main program given in Appendix J, for STIFM2(IM,JM).

The program listing is given below:

```
      PROGRAM ILA02(INPUT,OUTPUT,STIF,FLEX,TAPE5=STIF,TAPE6=FLEX)
      READ(5,*)N,JM,KM,AX,XL,XB
      PI=4.*ATAN(1.0)
      N1=N-1
      DO 30 J=1,JM
      DO 30 K=1,KM
      SUM=0.0
      X=0.0
      DX=AX/N1
      DO 15 I=1,N
      FAC=2.0
      IF((I.EQ.1).OR.(I.EQ.N))FAC=1.0
      X=X+DX
      X1=X/XL
      X2=X*PI/AX
      Y=1.0-X1
      Z=(X1-Y)*(X1-Y)/62.306
      S1=277.08*X1*X1*Y*Y*(0.229055-Z)
      IF(X.LT.XB)S2=0.0
      IF(X.GE.XB)S2=1.0/24.0
      IF(X.GE.(2.*XB))S2=1.0/16.9
      S3=(X1*X1+Y*Y)/7.89
      ST=1.0/(S1+S2+S3)
   15 SUM=SUM+FAC*ST*SIN(X2*J)*SIN(X2*K)
      SK=SUM/(2.0*N1)
      WRITE(6,25)J,K,N,SK,AX,XL,XB
   25 FORMAT(2X,3(I4,2X),4(E14.7,2X))
   30 CONTINUE
      STOP
      END
```

APPENDIX H

CALCULATIONS FOR THE FLEXIBILITY OF THE TEST RIG

The dynamic displacement of the ball bearings for 'no slippage' condition will be resisted by the testing rig. The rig can not provide a completely rigid support. The flexibility of the rig results from the bending of the channel frame, the bending of the web of the channel and the axial straining of the top and bottom channel beams. These effects can be estimated as follows:

(1) <u>Flexibility of the Support Due to Bending of the Frame</u>

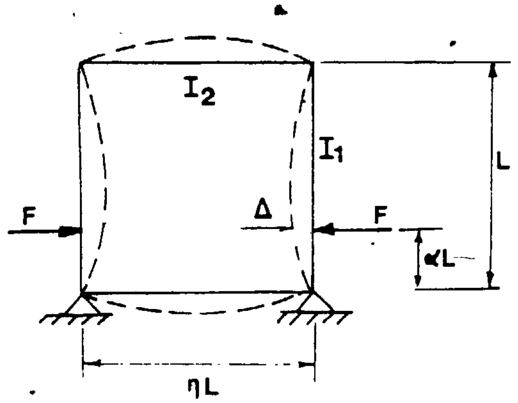

Figure H.1

Consider the rectangular frame shown in Figure H.1. When a force F is applied at a distance αL from the base of the rig symmetrically on both sides, the displacement Δ at these points can be shown to be given by,

$$\Delta = \frac{FL^3}{EI_1} \alpha^2(1-\alpha)^2 \{(1+n^1)c_1^2 + (\alpha-(1-\alpha))^2 \cdot c_2^2(n^1 + \frac{1}{3})$$

$$- (c_1 + \frac{(\alpha-(1-\alpha))^2}{3} c_2) + \frac{1}{3}\} \qquad (H.1)$$

where, $n^1 = n \cdot \frac{I_1}{I_2}$

$$c_1 = \frac{k_2}{2(k_1+k_2)}, \quad c_2 = \frac{k_2}{2(k_2+3k_1)x},$$

in which $k_1 = I_1/L$, $k_2 = I_2/(nL)$ and I_1, I_2 are second moments of area about the neutral axes of the frame.

The flexibility due to bending of the frame is then given by,

$$f_{b_1} = \frac{\Delta}{F} \qquad (H.2)$$

(2) <u>Flexibility Due to the Bending of the Web of the Channel</u>

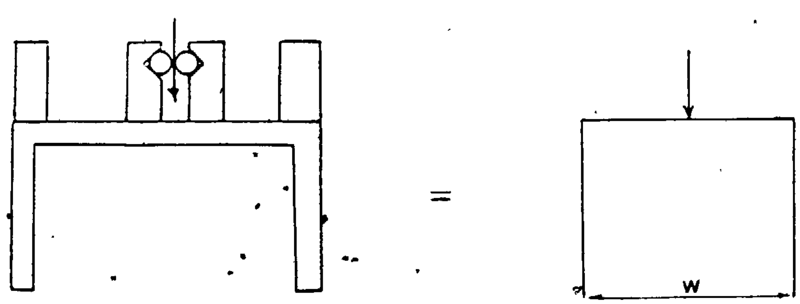

Figure H.2

The effect of the bending of the web is approximately estimated using an effective span of bending 'w' where w is the sum of all the clear space between the various edge beams attached to the channel. The table in Appendix B has been used to calculate the flexibility of the web (f_{b_2}) in three zones in the channel, two of which are near the joints and one in the middle; where the web can be taken as a one way spanning plate.

(3) <u>Flexibility Due to the Axial Straining of the Channel</u>

At the top and bottom edge of the channel, the only flexibility is due to the axial straining of the top and bottom channels. In order to improve the accuracy of the numerical integration of the effect of the overall flexibility, the axial straining is also considered as follows:

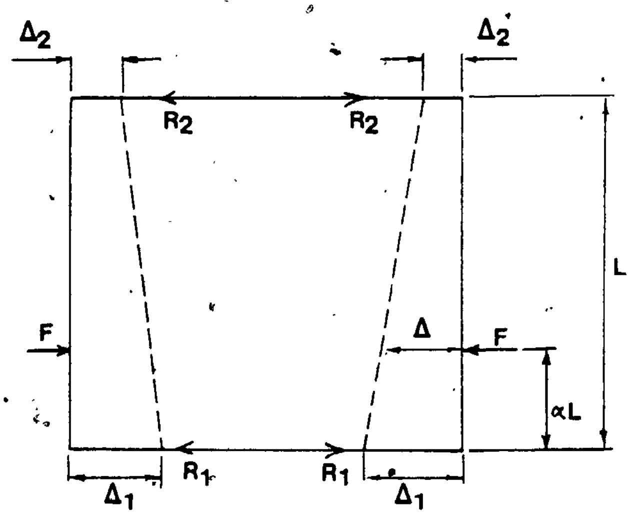

Figure H.3

The end forces R_1 and R_2 are given by

$$R_1 = F(1-\alpha), \quad R_2 = \alpha F$$

$$\Delta_1 = \frac{R_1}{K_{ax}} = \frac{F(1-\alpha)}{K_{ax}}$$

$$\Delta_2 = \frac{\alpha F}{K_{ax}}$$

where K_{ax} is the axial stiffness of the horizontal channel and other attached beams, and is given by

$$K_{ax} = \frac{EA_h}{\eta L}$$

in which A_h is the cross-sectional area of the horizontal channel and other attached beams. $\Delta = \Delta_1 + \alpha(\Delta_2 - \Delta_1)$. The axial flexibility

$$f_{ax} = \frac{\Delta}{F} = \frac{\eta L}{EA_h}\,(\alpha^2 + (1-\alpha)^2) \qquad \text{(H.3)}$$

The effect of all these flexibilities has been included in the evaluation of the frequencies for comparison with the experimental results. That is, the overall boundary stiffness $k_y = \frac{1}{f_{b_1} + f_{b_2} + f_{ax}}$ has been included in the minimization equation. The integral $\int_{x=0}^{a} k_y \left[V_d^2\Big|_{y=0} + V_d^2\Big|_{y=b}\right] dx$ has been calculated numerically and added in the main program appropriately in place of equation (3.3.15c).

APPENDIX I

EFFECT OF END MASSES ON THE VIBRATION OF A CURVED BEAM

Consider the vibration of a curved simply supported beam with two masses '$\bar{m}$' attached at the ends as shown in Figure I.1.

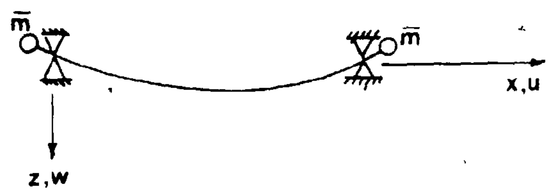

FIGURE I.1

For axial vibration of the mass at x = 0, the axial end force

$$F_e = \bar{m} \left. \frac{\partial^2 u}{\partial t^2} \right|_{x=0} = - \bar{m}\omega^2 u \Big|_{x=0} .$$

This has the same effect as that of a spring at the end with a stiffness $k = \bar{m}\omega^2$ (see Figure I.2).

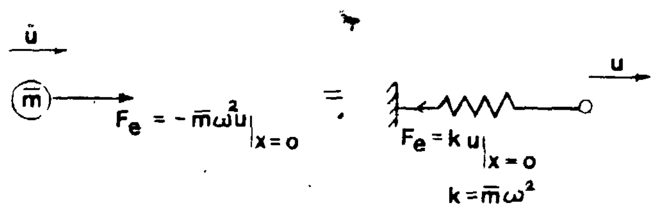

FIGURE I.2

Hence the end mass can be replaced by an equivalent spring with stiffness $k = \bar{m}\omega^2$.

This idea is used to calculate the effect of the mass of the loading head, which is isolated from the loading machine by three layers of rubber. The stiffnesses of some sample pieces of rubber that are similar to the ones that were used in the vibration experiment were found to be small compared to the effect of the mass of the loading head. Since the stiffness depends on the frequency, an estimate for $\hat{\omega}$ was used in the calculation of stiffness. It was found that the inaccuracy in the stiffness calculation did not change the natural frequency noticeably in the range of interest.

APPENDIX J

LISTING OF THE COMPUTER PROGRAM FOR THE POSTBUCKLING AND VIBRATION ANALYSIS

This program can be used to calculate the natural frequencies, displacements, in-plane stresses and strains for symmetrical modes of vibration of symmetrically curved plates. The modes and initial shapes must be symmetrical about both centrelines of the plate.

Input parameters that are required in this program are listed below in the order they appear on the program:

IFREQ - An integer flag number to indicate whether the natural frequency calculations are required or not. Any number other than zero will give frequency calculations. If only static deflections are required zero should be used.

IPR1 - A flag number to indicate whether the connection coefficients are to be printed or not. If these values are not required zero may be used. Any other input will result in printing all of the dynamic connection coefficients.

IPR2 - A flag number to indicate whether the static in-plane stress, strain results are required or not. If these are not required the input should be zero.

E - Young's modulus of the plate material.

PO - Poisson's ratio of the plate material.

RQ - Mass density of the plate.

XX - A test parameter used in a preliminary analysis. This should be set to 1.0 .

AX,AY - Dimensions of the plate in x,y directions.

T - Plate thickness.

NST,MST - Number of out-of-plane buckling mode shapes in x,y directions.

N,M - Number of out-of-plane vibration mode shapes in x,y directions.

IUSM - Number of mode shapes for u_s in x direction.

IUXM - Number of shapes for u_d in x direction.

IUYM - Number of shapes for u_s, u_d in y direction.

IVXM - Number of shapes for v_s, v_d in x direction.

IVYM - Number of shapes for v_s, v_d in y direction.

K,L - Integers used in a preliminary analysis. Not ued in this program.

NLO - Number of load cases to be treated.

DZI - A step parameter for Z used in a preliminary analysis. Not used in this program.

Z0 An initial imperfection parameter used in a preliminary analysis.

NSTF,MSTF - Same as nNST,MST.

NCOMP - A flag number to indicate whether the stress, strain calculations are required or not. If these calculatons are not required zero may be used. Any other value will result inthe calculation of stress and strain.

ITMAX - Maximum number of iterations in the static analysis

ZZ)(1) TO ZZ0(4) - Initial imperfection coefficients

$z_{0_{1,1}}$, $z_{0_{3,1}}$, $z_{0_{1,3}}$, $z_{0_{3,3}}$.

ZREAD - Initial trial value for $Z_{1,1}$.

FIN1,FIN2,CHEC1 to CHEC6 - Test parameters used in a preliminary analysis.

STIFM - Stiffness due to the vibration of the loading head but should be redefined for each frequency calculation as can be seen later.

STIFM3 - Stiffness parameter to allow for the flexibility of the top and bottom supports. A very high value for this will result in the solution for a plate with rigid supprts having absolutely constant movement,

STIFM2(I,J) - Stiffness factor to be calculated using the program in Appendix G.

POINT - Distance between the vertical centreline of the side support and the point of application of load as shown in the approximate model in Figure 5.1.2 .

NDP - Number of gauge points.

For each gauge,

NGAGE(I) - Type of strain required: 1- along x direction, 2- along y direction, 3 - at 45° to the x axis, 4 - at -45° to the x axis.

XCO(I) - x co-ordinate of the gauge.

YCO(I) - y co-ordinate of the gauge.

PX(I) - In-plane load.

For each loading case,

ZZC(1) to ZZC(4) - Initial trial values for $Z_{1,1}$, $Z_{1,3}$, $Z_{3,1}$, $Z_{3,3}$.

IPR1 - Defined earlier.

STIFM - Defined earlier.

The imprtant output parameters are as follows:

ZZC(1) to ZZC(4) - Out-of-plane displacement coefficients $Z_{1,1}$ to $Z_{3,3}$.

STRAIN - Strain at a point, the type of which is defined by NGAGE(I).

ALFR2(I) - Natural frequency of the curved plate.

```
      PROGRAM ILA01(INPUT,OUTPUT,HSY6,ZEF6,TAPE5=HSY6,TAPE6=ZEF6)
      DIMENSION H(21,11),ZD(21,11),SZ(21,21),ZC(2,2),ZZH(21),ZZG(21)
      DIMENSION ZZD(21),ZZE(21),SZZ(21,21)
      DIMENSION BUX5(3),BUY5(4),CUX5(3),CUY5(4),BVX5(3),BVY5(3),AUY5(4)
      DIMENSION C(21),CC(4),CAN(4,4),DELC(4),ZZ0(4),ZZC(4),AVX5(3)
      DIMENSION CVX5(3),CVY5(3)
      DIMENSION RUY1(11),RVX0(11),RVY0(11),RVX1(11),RVY1(11)
      DIMENSION U(11,11),V(11,11),W(11,11),FX(11,11),FY(11,11)
      DIMENSION RUX0(11),RUX1(11),RUY0(11)
      DIMENSION FXS(11,11),FYS(11,11),FXYS(11,11)
      DIMENSION EPX(11,11),EPY(11,11),EP45(11,11),EXY(25)
      DIMENSION FXY(11,11)
      DIMENSION ALGUX(3),ALGUY(4),ALGVX(3),ALGVY(3),DS(4),SG(4)
      DIMENSION ALFR1(4),ALFR2(4),ALFR3(4),ALFR4(4),DW(4)
      DIMENSION XK(4,4),XM(4,4),XLFI(4),XLFR(4),XH(4,4),XET(4)

      DIMENSION PX(10),SCH(10)
      DIMENSION G(21,4),ZB(21,4),SX(21,21)
      DIMENSION BUX(3),BUY(4),CUX(3),CUY(4),BVX(3),BVY(3),AUY(4)
      DIMENSION CVX(3),CVY(3),ALFUX(3),ALFUY(4),ALFVX(3),ALFVY(3)
      DIMENSION STIFM2(3,3)
      DIMENSION SQ(4),FR(4)
      DIMENSION SNX(11,11),SNY(11,11),SNXY(11,11)
      DIMENSION SRX(11,11),SRY(11,11),SRXY(11,11)
      DIMENSION EXST1(32),EXST2(32),EXST3(32),NGAGE(32),EXST4(32)
      DIMENSION SUX0(32),SUX1(32),SUY0(32),SUY1(32),SVX0(32)
      DIMENSION SVX1(32),SVY0(32),SVY1(32),XCO(32),YCO(32)
      READ(5,*)IFREQ,IPR1,IPR2
      READ(5,*)E,PO,RQ,XX
      READ(5,*)AX,AY,T
      READ(5,*)NST,MST,N,M,IUSM,IUXM,IUYM,IVXM,IVYM,K,L,NLO,DZI,Z0
      READ(5,*)MSTF,NSTF,NCOMP,ITMAX,ZZ0(1),ZZ0(2),ZZ0(3),ZZ0(4),ZREAD
      READ (5,*) STIFM,STIFM3
      DO 7777 IVX=1,IVXM
 7777 READ(5,*)(STIFM2(IVX,JVX),JVX=1,IVXM)
      WRITE(6,3020)MSTF,NSTF,NCOMP,ZZ0(1),ZZ0(2)
      NMSTF=NSTF*MSTF
 3020 FORMAT(3(2X,I3),3(2X,E14.7))
      WRITE(6,6)E,PO,RQ,AX,AY,T
      WRITE(6,7)NST,MST,N,M,IUSM,IUXM,IUYM,IVXM,IVYM,K,L,NLO
      Z0=ZZ0(1)
      WRITE(6,8)DZI,Z0
    6 FORMAT(6(2X,E14.7))
    7 FORMAT(12(2X,I3))
    8 FORMAT(2(2X,E14.7))
      READ(5,*)FIN,FIN1
      WRITE(6,8)FIN,FIN1
      READ(5,*)CHEC1,CHEC2,CHEC3,CHEC4,CHEC5,CHEC6
      WRITE(6,6)CHEC1,CHEC2,CHEC3,CHEC4,CHEC5,CHEC6
      PO2=PO*PO
      READ(5,*)POINT
      READ(5,*)NDP
      DO 7778 ID=1,NDP
      READ(5,*)NGAGE(ID),XCO(ID),YCO(ID)
      EXST1(ID)=0.0
      EXY(ID)=0.0
      EXST2(ID)=0.0
      EXST4(ID)=0.0
      EXST3(ID)=0.0
 7778 CONTINUE
      DO 5 I=1,NLO
      SCH(I)=0.0
    5 READ(5,*)PX(I)
      ZC(1,1)=Z0
```

```
      ZC(2,1)=0.0
      ZC(1,2)=0.0
      ZC(2,2)=0.0
      EM=E/(1.0-PO2)
      CF=1.0
      CALL MATSET(U,11,11)
      CALL MATSET(SNX,11,11)
      CALL MATSET(SRX,11,11)
      CALL MATSET(SNY,11,11)
      CALL MATSET(SNXY,11,11)
      CALL MATSET(SRXY,11,11)
      CALL MATSET(SRY,11,11)
      CALL MATSET(V,11,11)
      CALL MATSET(W,11,11)
      CALL MATSET(FX,11,11)
      CALL MATSET(FY,11,11)
      CALL MATSET(FXY,11,11)
      CALL MATSET(FXS,11,11)
      CALL MATSET(FYS,11,11)
      CALL MATSET(FXYS,11,11)
      CALL MATSET(EPX,11,11)
      CALL MATSET(EPY,11,11)
      CALL MATSET(EP45,11,11)

      D1=(1.0-PO)/2.0
      D2=(1.0+PO)/2.0
      D=E*T*T*T/(12.0*(1.0-PO2))
      PI=4.0*(ATAN(1.0E0))
      PI2=PI*PI
      PI3=PI2*PI
      PI4=PI3*PI
      IUMS=IUSM*IUYM
      IVM=IVXM*IVYM
      NMST=NST*MST
      NNST=IUMS+IVM
      AUX3=0.0
      AUY3=0.0
      AVX3=0.0
      AVX4=0.0
      AUX4=0.0
      AUY4=0.0

      AUY3=0.0
      AVY3=0.0
      AUY4=0.0
      AVY4=0.0

      CALL SETUP(IUSM,BUX5,CUX5,ALGUX,0.0E0,1.0E0,0.0E0,1.0E1,2)
      CALL SETUP(IUYM,BUY5,CUY5,ALGUY,1.0E0,0.0E0,0.0E0,0.0E0,2)
      CALL SETUP(IVXM,BVX5,CVX5,ALGVX,0.0E0,1.0E0,0.0E0,0.0E0,1)
      CALL SETUP(IVYM,BVY5,CVY5,ALGVY,1.0E0,0.0E0,0.0E0,0.0E0,1)
      DO 10 IG=1,IUYM
      AUY5(IG)=0.0
   10 CONTINUE
      DO  1010 IG=1,IVXM
 1010 AVX5(IG)=0.0
      AUY5(1)=1.0

      DO 45 IUX=1,IUSM
      ALUX3=ALGUX(IUX)
      BUX3=BUX5(IUX)
      CUX3=CUX5(IUX)

      IUY=1
   15 CONTINUE
```

```
      ALUY3=ALGUY(IUY)
      BUY3=BUY5(IUY)
      AUY3=AUY5(IUY)
      CUY3=CUY5(IUY)
      IU=(IUX-1)*IUYM+IUY

      II=1
      DO 25 IM=1,MSTF
      BEX=(IM*2-1)*PI

      DO 25 IN=1,NSTF
      BEY=(IN*2-1)*PI

      DO 25 IK=IM,MSTF
      GAX=(IK*2-1)*PI

      T2=DSSNRO(AX,BEX,GAX,0,AUX3,BUX3,CUX3,ALUX3)
      T3=DSSNRO(AX,GAX,BEX,0,AUX3,BUX3,CUX3,ALUX3)
      T6=CSCSRO(AX,BEX,GAX,1,AUX3,BUX3,CUX3,ALUX3)
      T7=SNSNRO(AX,BEX,GAX,1,AUX3,BUX3,CUX3,ALUX3)


      INO=1
      IF(IK.EQ.IM)INO=IN
      DO 25 IL=INO,NSTF
      GAY=(IL*2-1)*PI

      U1=CSCSRO(AY,BEY,GAY,0,AUY3,BUY3,CUY3,ALUY3)
      U4=SNSNRO(AY,BEY,GAY,0,AUY3,BUY3,CUY3,ALUY3)
      U6=DSSNRO(AY,GAY,BEY,1,AUY3,BUY3,CUY3,ALUY3)
      U7=DSSNRO(AY,BEY,GAY,1,AUY3,BUY3,CUY3,ALUY3)
      CMU=-1.0
      IF((IM.EQ.IK).AND.(IN.EQ.IL)) CMU=-0.5
      UV1=VALUE(AX,0.0,ALUX3,AUX3,BUX3,CUX3,0)
      UV2=VALUE(AX,AX,ALUX3,AUX3,BUX3,CUX3,0)

      S1=T6*U4*BEX*GAX/(AX*AX)
      S2=PO*T7*U1*GAY*BEY/(AY*AY)
      S3=D1*U6*T2*BEX*GAY/(AX*AY)
      S4=D1*U7*T3*BEY*GAX/(AX*AY)


      UUV1=VALUE(AY,POINT,ALUY3,AUY3,BUY3,CUY3,0)
      IF(II.EQ.1)ZD(IU,1)=UUV1*(UV1-UV2)/(2.688*D)
      II=II+1
      ZZH(IU)=ZD(IU,1)
      ZD(IU,II)=CMU*(S1+S2+S3+S4)
      IF(II.EQ.2)ZZD(IU)=ZD(IU,2)

   25 CONTINUE

      DO 35 JUX=1,IUSM
      ALUX4=ALGUX(JUX)
      BUX4=BUX5(JUX)
      CUX4=CUX5(JUX)

      TU1=PRIN(AX,AUX3,BUX3,CUX3,ALUX3,AUX4,BUX4,CUX4,ALUX4,1,1)
      TU2=PRIN(AX,AUX3,BUX3,CUX3,ALUX3,AUX4,BUX4,CUX4,ALUX4,0,0)

      JUY=1

   30 CONTINUE
      AUY4=AUY5(JUY)
      BUY4=BUY5(JUY)
      CUY4=CUY5(JUY)
```

```
      ALUY4=ALGUY(JUY)
      JU=(JUX-1)*IUYM+JUY

      SU1=PRIN(AY,AUY3,BUY3,CUY3,ALUY3,AUY4,BUY4,CUY4,ALUY4,1,1)
      SU2=PRIN(AY,AUY3,BUY3,CUY3,ALUY3,AUY4,BUY4,CUY4,ALUY4,0,0)
      UUV3=UUV1*VALUE(AY,POINT,ALUY4,AUY4,BUY4,CUY4,0)
      TPU1=PRIN(AY,AUY3,BUY3,CUY3,ALUY3,AUY4,BUY4,CUY4,ALUY4,2,2)
      TPU1=TPU1*STIFM3*VALUE(AX,0.0,ALUX3,AUX3,BUX3,CUX3,0)
      TPU1=TPU1*VALUE(AX,0.0,ALUX4,AUX4,BUX4,CUX4,0)
      JUY=JUY+1
      SZ(IU,JU)=(TPU1+TU1*SU2+D1*TU2*SU1)/(T*T)
      SZZ(IU,JU)=SZ(IU,JU)
      IF(JUY.LE.IUYM) GOTO 30
   35 CONTINUE

      DO 40 JVX=1,IVXM
      ALVX4=ALGVX(JVX)
      AVX4=AVX5(JVX)
      BVX4=BVX5(JVX)
      CVX4=CVX5(JVX)
      TU3=PRIN(AX,AUX3,BUX3,CUX3,ALUX3,AVX4,BVX4,CVX4,ALVX4,0,1)
      TU4=PRIN(AX,AUX3,BUX3,CUX3,ALUX3,AVX4,BVX4,CVX4,ALVX4,1,0)

      DO 40 JVY=1,IVYM
      ALVY4=ALGVY(JVY)
      BVY4=BVY5(JVY)
      CVY4=CVY5(JVY)
      JV=IUMS+JVY+(JVX-1)*IVYM
      SU3=PRIN(AY,AUY3,BUY3,CUY3,ALUY3,AVY4,BVY4,CVY4,ALVY4,0,1)
      SU4=PRIN(AY,AUY3,BUY3,CUY3,ALUY3,AVY4,BVY4,CVY4,ALVY4,1,0)

      SZ(IU,JV)=(PO*TU4*SU3+D1*TU3*SU4)/(T*T)
   40 SZZ(IU,JV)=SZ(IU,JV)
      IUY=IUY+1
      IF(IUY.LE.IUYM) GOTO 15
   45 CONTINUE

      DO 70 IVX=1,IVXM
      ALVX3=ALGVX(IVX)
      AVX3=AVX5(IVX)
      BVX3=BVX5(IVX)
      CVX3=CVX5(IVX)

      DO 70 IVY=1,IVYM
      ALVY3=ALGVY(IVY)
      BVY3=BVY5(IVY)
      CVY3=CVY5(IVY)
      IV=IUMS+IVY+(IVX-1)*IVYM

      II=1
      DO 55 IM=1,MSTF
      BEX=(IM*2-1)*PI

      DO 55 IN=1,NSTF
      BEY=(IN*2-1)*PI


      DO 55 IK=IM,MSTF
      GAX=(IK*2-1)*PI
      T1=CSCSRO(AX,BEX,GAX,0,AVX3,BVX3,CVX3,ALVX3)
      T4=SNSNRO(AX,BEX,GAX,0,AVX3,BVX3,CVX3,ALVX3)
      T8=DSSNRO(AX,BEX,GAX,1,AVX3,BVX3,CVX3,ALVX3)
      T9=DSSNRO(AX,GAX,BEX,1,AVX3,BVX3,CVX3,ALVX3)


      INO=1
```

```
      IF(IK.EQ.IM)INO=IN
      DO 55 IL=INO,NSTF
      GAY=(IL*2-1)*PI

      U2=DSSNRO(AY,BEY,GAY,0,AVY3,BVY3,CVY3,ALVY3)
      U3=DSSNRO(AY,GAY,BEY,0,AVY3,BVY3,CVY3,ALVY3)
      U8=CSCSRO(AY,BEY,GAY,1,AVY3,BVY3,CVY3,ALVY3)
      U9=SNSNRO(AY,BEY,GAY,1,AVY3,BVY3,CVY3,ALVY3)
      CMU=-1.0
      IF((IM.EQ.IK).AND.(IN.EQ.IL))CMU=-0.5

      S1=U8*T4*BEY*GAY/(AY*AY)
      S2=PO*U9*T1*BEX*GAX/(AX*AX)
      S3=D1*T8*U3*GAY*BEX/(AX*AY)
      S4=D1*T9*U2*GAX*BEY/(AX*AY)
      IF(II.EQ.1)ZD(IV,1)=0.0
      ZZH(IV)=0.0
      II=II+1
      ZD(IV,II)=CMU*(S1+S2+S3+S4)
      ZZD(IV)=ZD(IV,2)
      IIM=II

   55 CONTINUE

      DO 65 JUX=1,IUSM
      ALUX4=ALGUX(JUX)
      BUX4=BUX5(JUX)
      CUX4=CUX5(JUX)
      TV3=PRIN(AX,AVX3,BVX3,CVX3,ALVX3,AUX4,BUX4,CUX4,ALUX4,0,1)
      TV4=PRIN(AX,AVX3,BVX3,CVX3,ALVX3,AUX4,BUX4,CUX4,ALUX4,1,0)

      JUY=1
   60 CONTINUE
      ALUY4=ALGUY(JUY)
      BUY4=BUY5(JUY)
      AUY4=AUY5(JUY)
      CUY4=CUY5(JUY)
      JU=(JUX-1)*IUYM+JUY
      SV3=PRIN(AY,AVY3,BVY3,CVY3,ALVY3,AUY4,BUY4,CUY4,ALUY4,0,1)
      SV4=PRIN(AY,AVY3,BVY3,CVY3,ALVY3,AUY4,BUY4,CUY4,ALUY4,1,0)
      JUY=JUY+1
      SZ(IV,JU)=(PO*TV3*SV4+D1*TV4*SV3)/(T*T)
      SZZ(IV,JU)=SZ(IV,JU)
      IF(JUY.LE.IUYM) GOTO 60
   65 CONTINUE

      DO 70 JVX=1,IVXM
      ALVX4=ALGVX(JVX)
      AVX4=AVX5(JVX)
      BVX4=BVX5(JVX)
      CVX4=CVX5(JVX)

      TV1=PRIN(AX,AVX3,BVX3,CVX3,ALVX3,AVX4,BVX4,CVX4,ALVX4,1,1)
      TV2=PRIN(AX,AVX3,BVX3,CVX3,ALVX3,AVX4,BVX4,CVX4,ALVX4,0,0)

      DO 70 JVY=1,IVYM
      ALVY4=ALGVY(JVY)
      BVY4=BVY5(JVY)
      CVY4=CVY5(JVY)
      JV=IUMS+JVY+(JVX-1)*IVYM

      SV1=PRIN(AY,AVY3,BVY3,CVY3,ALVY3,AVY4,BVY4,CVY4,ALVY4,1,1)
      SV2=PRIN(AY,AVY3,BVY3,CVY3,ALVY3,AVY4,BVY4,CVY4,ALVY4,0,0)

      UQ1=VALUE(AY,0.0,ALVY3,AVY3,BVY3,CVY3,0)
```

```
      UQ2=VALUE(AY,0.0,ALVY4,AVY4,BVY4,CVY4,0)
      SZ(IV,JV)=(TV2*SV1+D1*TV1*SV2)/(T*T)
   70 SZZ(IV,JV)=SZ(IV,JV)
      WRITE(6,72)
   72 FORMAT(/////,2X,"CONNECTION STIFFNESS MATRIX",/)
      DO 74 IQ=1,NNST
      WRITE(6,73)(SZ(IQ,JQ),JQ=1,NNST)
   73 FORMAT(4(2X,E14.7))
   74 CONTINUE
      CALL GAUSEL(NNST,IIM,SZ,ZD,H)
      DO 4015 I=1,NNST
      SUM00=0.0
      SUM01=0.0
      DO 4010 J=1,NNST
      SUM01=SUM01+SZZ(I,J)*H(J,2)
 4010 SUM00=SZZ(I,J)*H(J,1)+SUM00
      ZZE(I)=ZZD(I)-SUM01
      ZZG(I)=ZZH(I)-SUM00
      WRITE(6,4013)I,ZZD(I),SUM01,ZZE(I),ZZH(I),SUM00,ZZG(I)
 4013 FORMAT(2X,I3,6(2X,E14.7))
 4015 CONTINUE
      WRITE(6,75)
   75 FORMAT(//,2X,"IN PLANE MODE INFLUENCE COEFFICIENTS",//)
      DO 82 IQ=1,NNST
      WRITE(6,80)ZD(IQ,1),H(IQ,1),ZD(IQ,2),H(IQ,2)
   80 FORMAT(4(2X,E14.7))
   82 CONTINUE
      DO 3995 ILO=2,NLO
      READ(5,*)ZZC(1),ZZC(2),ZZC(3),ZZC(4),IPR1,STIFM
      DO 7779 IW=1,NDP
       EXY(IW)=0.0
      EXST1(IW)=0.0
      EXST2(IW)=0.0
      EXST3(IW)=0.0
      EXST4(IW)=0.0
 7779 CONTINUE
      WRITE(6,8024)ZZC(1),ZZC(2),ZZC(3),ZZC(4),PX(ILO)
 8024 FORMAT(5(2X,E14.7))
      DO 8025 IG=1,NNST
      C(IG)=H(IG,1)*PX(ILO)
      II=1
      DO 8020 IH=1,NMSTF
      DO 8020 JH=IH,NMSTF
      II=II+1
      C(IG)=C(IG)+H(IG,II)*(ZZC(IH)*ZZC(JH)-ZZ0(IH)*ZZ0(JH))
 8020 CONTINUE
 8025 CONTINUE
      DO 3110 ITNOM=1,ITMAX
      DO 3100  IM=1,MSTF
      ALX=(IM*2-1)*PI
      DO 3100  IN=1,NSTF
      ALY=(IN*2-1)*PI
      I=(IM-1)*NSTF+IN
      DFAC=4.0
      ICO1=I
      ZUM1=0.0
      ZUM2=0.0
      ZUM3=0.0
      ZUM4=0.0
      ZUM6=0.0
      CC(ICO1)=0.0
```

```
      RR4=0.0
      RR6=0.0

      DO 3080 IR=1,MSTF
      BEX=(IR*2-1)*PI
      RC1=BEX*ALX/(AX*AX)
      DO 3080 IS=1,NSTF
      BEY=PI*(IS*2-1)
      J=(IR-1)*NSTF+IS
      DFAC2=3.0
      JCO1=J
      RC2=BEY*ALY/(AY*AY)
      RC3=0.5*(1.0-PO)*BEX*ALY/(AX*AY)
      RC4=0.5*(1.0-PO)*BEY*ALX/(AX*AY)
      RR3=0.0
      RR5=0.0
      ZUM5=0.0
      ZUM7=0.0

      DO 3065 JUX=1,IUSM
      ALUX3=ALGUX(JUX)
      BUX3=BUX5(JUX)
      CUX3=CUX5(JUX)
      JUY=1
 3071 CONTINUE
      ALUY3=ALGUY(JUY)
      BUY3=BUY5(JUY)
      CUY3=CUY5(JUY)
      AUY3=AUY5(JUY)
      JU=(JUX-1)*IUYM+JUY
      CCK=CSCSRO(AX,BEX,ALX,1,AUX3,BUX3,CUX3,ALUX3)
      CCK=CCK*SNSNRO(AY,BEY,ALY,0,AUY3,BUY3,CUY3,ALUY3)
      CCM=SNSNRO(AX,BEX,ALX,1,AUX3,BUX3,CUX3,ALUX3)
      CCM=CCM*CSCSRO(AY,BEY,ALY,0,AUY3,BUY3,CUY3,ALUY3)
      CCH=DSSNRO(AX,BEX,ALX,0,AUX3,BUX3,CUX3,ALUX3)
      CCH=CCH*DSSNRO(AY,ALY,BEY,1,AUY3,BUY3,CUY3,ALUY3)
      CCN=DSSNRO(AX,ALX,BEX,0,AUX3,BUX3,CUX3,ALUX3)
      CCN=CCN*DSSNRO(AY,BEY,ALY,1,AUY3,BUY3,CUY3,ALUY3)
      RR3=RR3+(CCK*RC1+PO*CCM*RC2+CCH*RC3+CCN*RC4)*C(JU)*T*T
      III=1
      DO 3063  IP=1,MSTF
      DO 3063  IQ=1,NSTF
      IPQ=IQ+(IP-1)*NSTF
      DO 3063  IK=IP,MSTF
      IQ0=1


      IF(IK.EQ.IP)IQ0=IQ
      DO 3063  IL=IQ0,NSTF
      IKL=IL+(IK-1)*NSTF
      III=III+1
      DIFC=1.0
      DIFC=DIFC*H(JU,III)
      RRR1=(CCK*RC1+PO*CCM*RC2+CCH*RC3+CCN*RC4)*T*T*ZZC(JCO1)
      CAN(ICO1,IPQ)=CAN(ICO1,IPQ)+RRR1*ZZC(IKL)*DIFC
      CAN(ICO1,IKL)=CAN(ICO1,IKL)+RRR1*ZZC(IPQ)*DIFC
 3063 CONTINUE
      JUY=JUY+1
      IF(JUY.LE.IUYM) GOTO 3071
 3065 CONTINUE
      CAN(JCO1,JCO1)=RR3+CAN(ICO1,JCO1)
      ZUM1=ZUM1-RR3*ZZC(JCO1)

      DO 3068 JVX=1,IVXM
```

```
      ALVX3=ALGVX(JVX)
      AVX3=AVX5(JVX)
      BVX3=BVX5(JVX)
      CVX3=CVX5(JVX)
      DO 3068 JVY=1,IVYM
      ALVY3=ALGVY(JVY)
      BVY3=BVY5(JVY)
      CVY3=CVY5(JVY)
      JV=(JVX-1)*IVYM+JVY+IUMS
      CCL=SNSNRO(AX,BEX,ALX,0,AVX3,BVX3,CVX3,ALVX3)
      CCL=CCL*CSCSRO(AY,BEY,ALY,1,AVY3,BVY3,CVY3,ALVY3)
      CCP=CSCSRO(AX,BEX,ALX,0,AVX3,BVX3,CVX3,ALVX3)
      CCP=CCP*SNSNRO(AY,BEY,ALY,1,AVY3,BVY3,CVY3,ALVY3)
      CCG=DSSNRO(AX,BEX,ALX,1,AVX3,BVX3,CVX3,ALVX3)
      CCG=CCG*DSSNRO(AY,ALY,BEY,0,AVY3,BVY3,CVY3,ALVY3)
      CCQ=DSSNRO(AX,ALX,BEX,1,AVX3,BVX3,CVX3,ALVX3)
      CCQ=CCQ*DSSNRO(AY,BEY,ALY,0,AVY3,BVY3,CVY3,ALVY3)

      RR5=RR5+(CCL*RC2+PO*RC1*CCP+RC3*CCG+RC4*CCQ)*C(JV)*T*T
      III=1
      DO 3069 IP=1,MSTF

      DO  3069 IQ=1,NSTF
      IPQ=IQ+(IP-1)*NSTF
      DO 3069 IK=IP,MSTF
      IQ0=1
      IF(IP.EQ.IK)IQ0=IQ
      DO 3069 IL=IQ0,NSTF
      IKL=IL+(IK-1)*NSTF
      III=III+1
      DIFC=1.0
      DIFC=DIFC*H(JV,III)
      RRR1=(CCL*RC2+PO*RC1*CCP+RC3*CCG+RC4*CCQ)*T*T*ZZC(JCO1)
      CAN(ICO1,IPQ)=CAN(ICO1,IPQ)+RRR1*ZZC(IKL)*DIFC
      CAN(ICO1,IKL)=CAN(ICO1,IKL)+RRR1*ZZC(IPQ)*DIFC
 3069 CONTINUE
 3068 CONTINUE
      CAN(ICO1,JCO1)=CAN(ICO1,JCO1)+RR5
      ZUM2=ZUM2-RR5*ZZC(JCO1)

      DO 3075 IP=1,MSTF
      GAX=PI*(IP*2-1)
      DO 3075 IQ=1,NSTF
      GAY=PI*(IQ*2-1)
      IPQ=IQ+(IP-1)*NSTF
      JCPQ=IPQ
      DO 3072 IK=1,MSTF
      PHIX=PI*(IK*2-1)
      DO 3072 IL=1,NSTF
      PHIY=(2*IL-1)*PI
      IKL=(IK-1)*NSTF+IL
      JCKL=IKL
      CCR=CCCCIN(AX,ALX,BEX,GAX,PHIX)*ALX*BEX*GAX*PHIX/(AX**4.0)
      CCR=CCR*SSSSIN(AY,ALY,BEY,GAY,PHIY)
      CCS=CCCCIN(AY,ALY,BEY,GAY,PHIY)*ALY*BEY*GAY*PHIY/(AY**4.0)
      CCS=CCS*SSSSIN(AX,ALX,BEX,GAX,PHIX)

      CCF1=.5*CCSSIN(AX,ALX,GAX,BEX,PHIX)*ALX*GAX/(AX*AX)
      CCG1=CCSSIN(AY,GAY,PHIY,ALY,BEY)*GAY*PHIY/(AY*AY)
      CCF2=0.5*CCSSIN(AX,GAX,PHIX,BEX,ALX)*GAX*PHIX/(AX*AX)
      CCG2=CCSSIN(AY,ALY,PHIY,BEY,GAY)*ALY*PHIY/(AY*AY)
      CCF3=0.5*CCSSIN(AX,ALX,BEX,GAX,PHIX)*ALX*BEX/(AX*AX)
      CCG3=CCG1
      CCF4=2.0*CCF1
      CCG4=CCSSIN(AY,BEY,PHIY,ALY,GAY)*BEY*PHIY/(AY*AY)
```

```
      CCF5=CCF2
      CCG5=CCSSIN(AY,ALY,BEY,GAY,PHIY)*ALY*BEY/(AY*AY)
      CCF6=0.5*CCSSIN(AX,GAX,BEX,ALX,PHIX)*GAX*BEX/(AX*AX)
      CCG6=CCG2
      CDIF1=(DFAC*(CCR+CCS)/8.0)+CCF3*CCG1+CCF2*CCG5
      CDIF1=CDIF1*ZZC(JCPQ)*ZZC(JCKL)*ZZC(JCO1)*T*T*T*T
      CDIF3=-PO*(CCF3*CCG1+CCG5*CCF2)-((CCR+CCS)/2.0)
      IF(ICO1.EQ.JCO1)CMUL=4.0
      IF(ICO1.NE.JCO1)CMUL=2.0
      CDIF3=CDIF3-D1*(CCF1*CCG4+CCF6*CCG2)*2.0
      ZUM4=ZUM4-CDIF1
      COMPUT=DFAC*DFAC2*(CCR+CCS)/8.0
      CDIF2=(COMPUT)+CCF3*CCG3+CCF4*CCG4+CCF5*CCG5+CCF6*CCG6
      CDIF2=CDIF2*ZZC(JCPQ)*ZZC(JCKL)*T*T*T*T
      ZUM5=ZUM5+CDIF2
      ZUM6=ZUM6-CDIF3*ZZC(JCO1)*ZZO(JCPQ)*ZZO(JCKL)*T*T*T*T*XX
      ZUM7=ZUM7+CDIF3*ZZO(JCKL)*ZZO(JCPQ)*T*T*T*T*XX
 3072 CONTINUE

 3075 CONTINUE
      IF(ICO1.EQ.JCO1) ZADD=(((ALX/AX)**2.+(ALY/AY)**2.)**2.0)*T*T*T*T
      ZADD=ZADD*AX*AY/48.0
      IF(ICO1.NE.JCO1) ZADD=0.0
      CAN(ICO1,JCO1)=CAN(ICO1,JCO1)+ZADD+ZUM5+ZUM7
      CC(ICO1)=CC(ICO1)-ZADD*(ZZC(ICO1)-ZZO(ICO1))
 3080 CONTINUE
      CC(ICO1)=CC(ICO1)+ZUM4+ZUM6+ZUM1+ZUM2
 3100 CONTINUE
      DO 3102  I=1,NMSTF
      WRITE(6,3101)CC(I),ZZC(I)
 3101 FORMAT(2(3X,E14.7),"***")
 3102 CONTINUE
      CALL MATPR(CAN,NMSTF,NMSTF)
      CALL GAUSI(NMSTF,CAN,CC,DELC)
      DO 3105 I=1,NMSTF
      ZZC(I)=ZZC(I)+DELC(I)
      WRITE(6,3103)CC(I),ZZC(I)
 3103 FORMAT(2(2X,E14.7))
 3105 CONTINUE
      WRITE(6,3106)
 3106 FORMAT("*************************+++++++*******")
      DO 4025 IG=1,NNST
      WRITE(6,4011)C(IG)
 4011 FORMAT(2X,"C(IG)=",E14.7,2X)
      C(IG)=H(IG,1)*PX(ILO)
      II=1
      DO 4020 IH=1,NMSTF
      DO 4020 JH=IH,NMSTF
      II=II+1
      C(IG)=C(IG)+H(IG,II)*(ZZC(IH)*ZZC(JH)-ZZO(IH)*ZZO(JH))
 4020 CONTINUE
 4025 CONTINUE
      CALL MATSET(CAN,NMSTF,NMSTF)
 3110 CONTINUE
      IF(NCOMP.EQ.0) GOTO 3995
      DO 3305 IUX=1,IUSM
      ALUX3=ALGUX(IUX)
      BUX3=BUX5(IUX)
      CUX3=CUX5(IUX)
      DO 3295 IX=1,11
      GX=(IX-1)*AX/10.0
      RUX0(IX)=VALUE(AX,GX,ALUX3,AUX3,BUX3,CUX3,0)
      RUX1(IX)=VALUE(AX,GX,ALUX3,AUX3,BUX3,CUX3,1)
 3295 CONTINUE
      DO 3297 ID=1,NDP
```

```
      GX=XCO(ID)
      SUX0(ID)=VALUE(AX,GX,ALUX3,AUX3,BUX3,CUX3,0)
      SUX1(ID)=VALUE(AX,GX,ALUX3,AUX3,BUX3,CUX3,1)
 3297 CONTINUE
      IUY=1
 3301 CONTINUE
      ALUY3=ALGUY(IUY)
      AUY3=AUY5(IUY)
      BUY3=BUY5(IUY)
      CUY3=CUY5(IUY)
      IU=(IUX-1)*IUYM+IUY
      DO 3300 IY=1,11
      Y=(IY-1)*AY/10.0
      RUY0(IY)=VALUE(AY,Y,ALUY3,AUY3,BUY3,CUY3,0)
      RUY1(IY)=VALUE(AY,Y,ALUY3,AUY3,BUY3,CUY3,1)
 3300 CONTINUE
      DO 3302 ID=1,NDP
      Y=YCO(ID)
      SUY0(ID)=VALUE(AY,Y,ALUY3,AUY3,BUY3,CUY3,0)
      SUY1(ID)=VALUE(AY,Y,ALUY3,AUY3,BUY3,CUY3,1)
 3302 CONTINUE
      DO 3303 IX=1,11
      DO 3303 IY=1,11
      SNX(IX,IY)=SNX(IX,IY)+C(IU)*RUX1(IX)*RUY0(IY)
      SNXY(IX,IY)=SNXY(IX,IY)+C(IU)*RUX0(IX)*RUY1(IY)
 3303 CONTINUE
      DO 3304 ID=1,NDP
      EXST1(ID)=EXST1(ID)+C(IU)*SUX1(ID)*SUY0(ID)
      EXY(ID)=EXY(ID)+C(IU)*SUX0(ID)*SUY1(ID)
 3304 CONTINUE
      IUY=IUY+1
      IF(IUY.LE.IUYM) GOTO 3301
 3305 CONTINUE

      DO 3322 IVX=1,IVXM
      ALVX3=ALGVX(IVX)
      AVX3=AVX5(IVX)
      BVX3=BVX5(IVX)
      CVX3=CVX5(IVX)

      DO 3310 IX=1,11
      GX=(IX-1)*AX/10.0
      RVX0(IX)=VALUE(AX,GX,ALVX3,AVX3,BVX3,CVX3,0)
      RVX1(IX)=VALUE(AX,GX,ALVX3,AVX3,BVX3,CVX3,1)
 3310 CONTINUE
      DO 3312 ID=1,NDP
      GX=XCO(ID)
      SVX0(ID)=VALUE(AX,GX,ALVX3,AVX3,BVX3,CVX3,0)
      SVX1(ID)=VALUE(AX,GX,ALVX3,AVX3,BVX3,CVX3,1)
 3312 CONTINUE

      DO 3322 IVY=1,IVYM
      IV=IUMS+(IVX-1)*IVYM+IVY
      ALVY3=ALGVY(IVY)
      BVY3=BVY5(IVY)
      CVY3=CVY5(IVY)
      DO 3315 IY=1,11
      Y=(IY-1)*AY/10.0
      RVY0(IY)=VALUE(AY,Y,ALVY3,AVY3,BVY3,CVY3,0)
      RVY1(IY)=VALUE(AY,Y,ALVY3,AVY3,BVY3,CVY3,1)
 3315 CONTINUE
      DO 3316 ID=1,NDP
      Y=YCO(ID)
      SVY0(ID)=VALUE(AY,Y,ALVY3,AVY3,BVY3,CVY3,0)
      SVY1(ID)=VALUE(AY,Y,ALVY3,AVY3,BVY3,CVY3,1)
```

```
 3316 CONTINUE
      DO 3320 IX=1,11
      DO 3320 IY=1,11
      SNY(IX,IY)=SNY(IX,IY)+C(IV)*RVX0(IX)*RVY1(IY)
 3320 SNXY(IX,IY)=SNXY(IX,IY)+C(IV)*RVX1(IX)*RVY0(IY)
      DO 3322 ID=1,NDP
      EXST2(ID)=EXST2(ID)+C(IV)*SVX0(ID)*SVY1(ID)
      EXY(ID)=EXY(ID)+C(IV)*SVX1(ID)*SVY0(ID)
 3322 CONTINUE

      DO 3340 IX=1,11
      GX=(IX-1)/10.0
      DO 3340 IY=1,11
      Y=(IY-1)/10.0
      DO 3340 IM=1,MSTF
      ALX=PI*(IM*2-1)
      RXW=GX*ALX
      DO 3340 IN=1,NSTF
      ALY=PI*(IN*2-1)
      IMN=IN+(IM-1)*NSTF
      RYW=Y*ALY
      DO 3340 IR=1,MSTF
      BEX=(IR*2-1)*PI
      SXW=BEX*GX
      DO 3340 IS=1,NSTF
      BEY=(2.0*IS-1)*PI
      SYW=BEY*Y
      IRS=IS+(IR-1)*NSTF
      ZZFU=(ZZC(IMN)*ZZC(IRS)-ZZ0(IMN)*ZZ0(IRS))*T*T
      VAL1=ALX*BEX*COS(RXW)*COS(SXW)*SIN(RYW)*SIN(SYW)/(AX*AX)
      VAL2=ALY*BEY*COS(RYW)*COS(SYW)*SIN(RXW)*SIN(SXW)/(AY*AY)
      VAL3=ALX*BEY*COS(RXW)*COS(SYW)*SIN(SXW)*SIN(RYW)/(AX*AY)
      VAL4=ALY*BEX*COS(RYW)*COS(SXW)*SIN(SYW)*SIN(RXW)/(AX*AY)
      SNX(IX,IY)=SNX(IX,IY)+0.5*ZZFU*VAL1
      SNY(IX,IY)=SNY(IX,IY)+0.5*ZZFU*VAL2
 3340 SNXY(IX,IY)=SNXY(IX,IY)+(VAL3+VAL4)*ZZFU

      DO 3342 ID=1,NDP
      GX=XCO(ID)
      Y=YCO(ID)
      DO 3342 IM=1,MSTF
      ALX=PI*(2*IM-1)
      RXW=ALX*GX/AX
      DO 3342 IN=1,NSTF
      ALY=PI*(IN*2-1)
      RYW=Y*ALY/AY
      IMN=IN+(IM-1)*NSTF
      DO 3342 IR=1,MSTF
      BEX=PI*(IR*2-1)
      SXW=BEX*GX/AX
      DO 3342 IS=1,NSTF
      BEY=PI*(IS*2-1)
      SYW=BEY*Y/AY
      IRS=IS+(IR-1)*NSTF
      ZZFU=(ZZC(IMN)*ZZC(IRS)-ZZ0(IMN)*ZZ0(IRS))*T*T
      VAL1=ALX*BEX*COS(RXW)*COS(SXW)*SIN(RYW)*SIN(SYW)/(AX*AX)
      VAL2=ALY*BEY*COS(RYW)*COS(SYW)*SIN(RXW)*SIN(SXW)/(AY*AY)
      VAL3=ALX*BEY*COS(RXW)*COS(SYW)*SIN(SXW)*SIN(RYW)/(AX*AY)
      VAL4=ALY*BEX*COS(SXW)*COS(RYW)*SIN(RXW)*SIN(SYW)/(AX*AY)
      EXST1(ID)=EXST1(ID)+0.5*ZZFU*VAL1
      EXST2(ID)=EXST2(ID)+0.5*ZZFU*VAL2
      EXY(ID)=EXY(ID)+(VAL3+VAL4)*ZZFU
 3342 CONTINUE
      DO 3345 IX=1,11
      DO 3345 IY=1,11
```

```
      SRX(IX,IY)=(SNX(IX,IY)+PO*SNY(IX,IY))*E/(1.-PO*PO)
      SRY(IX,IY)=(SNY(IX,IY)+PO*SNX(IX,IY))*E/(1.-PO*PO)
 3345 SRXY(IX,IY)=SNXY(IX,IY)*E/(2.0*(1.0+PO))
      IF(IPR2.EQ.0) GOTO 1192
      CALL MATPR(SNX,11,11)
      CALL MATPR(SNY,11,11)
      CALL MATPR(SNXY,11,11)
      CALL MATPR(SRX,11,11)
      CALL MATPR(SRY,11,11)
      CALL MATPR(SRXY,11,11)
 1192 CONTINUE
      IF(IFREQ.EQ.0)GOTO 371
      IUM=IUXM*IUYM
      IVM=IVXM*IVYM
      NM=N*M
      NN=IUM+IVM
      AUX1=0.0
      AVX1=0.0
      AUX2=0.0
      AVX2=0.0

      AUY1=0.0
      AVY1=0.0
      AUY2=0.0
      AVY2=0.0

      CALL SETUP(IUSM,BUX,CUX,ALFUX,0.0E0,1.0E0,0.0E0,1.0E1,2)
      CALL SETUP(IUYM,BUY,CUY,ALFUY,1.0E0,0.0E0,0.0E0,0.0E0,2)
      CALL SETUP(IVXM,BVX,CVX,ALFVX,0.0E0,1.0E0,0.0E0,0.0E0,1)
      CALL SETUP(IVYM,BVY,CVY,ALFVY,1.0E0,0.0E0,0.0E0,0.0E0,1)
      DO 155 IG=1,IUYM
      AUY(IG)=0.0
  155 CONTINUE
      AUY(1)=1.0

      DO 1175 IUX=1,IUXM
      ALUX1=ALFUX(IUX)
      BUX1=BUX(IUX)
      CUX1=CUX(IUX)

      IUY=1
  156 CONTINUE
      ALUY1=ALFUY(IUY)
      AUY1=AUY(IUY)
      BUY1=BUY(IUY)
      CUY1=CUY(IUY)
      IU=(IUX-1)*IUYM+IUY

      DO 170 IM=1,M
      BEX=(IM*2-1)*PI

      DO 170 IN=1,N
      BEY=(IN*2-1)*PI
      II=(IM-1)*N+IN
      S1=0.0
      S2=0.0
      S3=0.0
      S4=0.0

      DO 160 IK=1,MSTF
      GAX=(IK*2-1)*PI

      T2=DSSNRO(AX,BEX,GAX,0,AUX1,BUX1,CUX1,ALUX1)
      T3=DSSNRO(AX,GAX,BEX,0,AUX1,BUX1,CUX1,ALUX1)
      T6=CSCSRO(AX,BEX,GAX,1,AUX1,BUX1,CUX1,ALUX1)
```

```
      T7=SNSNRO(AX,BEX,GAX,1,AUX1,BUX1,CUX1,ALUX1)


      DO 160 IL=1,NSTF
      GAY=(IL*2-1)*PI
      JJ=(IK-1)*L+IL

      U1=CSCSRO(AY,BEY,GAY,0,AUY1,BUY1,CUY1,ALUY1)
      U4=SNSNRO(AY,BEY,GAY,0,AUY1,BUY1,CUY1,ALUY1)
      U6=DSSNRO(AX,GAY,BEY,1,AUY1,BUY1,CUY1,ALUY1)
      U7=DSSNRO(AY,BEY,GAY,1,AUY1,BUY1,CUY1,ALUY1)

      S1=S1-ZZC(JJ)*T6*U4*BEX*GAX/(AX*AX)
      S2=S2-ZZC(JJ)*PO*T7*U1*GAY*BEY/(AY*AY)
      S3=S3-ZZC(JJ)*D1*U6*T2*BEX*GAY/(AX*AY)
      S4=S4-ZZC(JJ)*D1*U7*T3*BEY*GAX/(AX*AY)


  160 CONTINUE

      ZB(IU,II)=S1+S2+S3+S4

  170 CONTINUE

      DO 173 JUX=1,IUXM
      ALUX2=ALFUX(JUX)
      BUX2=BUX(JUX)
      CUX2=CUX(JUX)

      UV3=VALUE(AX,0.0,ALUX1,AUX1,BUX1,CUX1,0)
      UV4=VALUE(AX,0.0,ALUX2,AUX2,BUX2,CUX2,0)
      TU1=PRIN(AX,AUX1,BUX1,CUX1,ALUX1,AUX2,BUX2,CUX2,ALUX2,1,1)
      TU2=PRIN(AX,AUX1,BUX1,CUX1,ALUX1,AUX2,BUX2,CUX2,ALUX2,0,0)

      JUY=1
  171 CONTINUE
      ALUY2=ALFUY(JUY)
      BUY2=BUY(JUY)
      AUY2=AUY(JUY)
      CUY2=CUY(JUY)
      JU=(JUX-1)*IUYM+JUY

      SU1=PRIN(AY,AUY1,BUY1,CUY1,ALUY1,AUY2,BUY2,CUY2,ALUY2,1,1)
      SU2=PRIN(AY,AUY1,BUY1,CUY1,ALUY1,AUY2,BUY2,CUY2,ALUY2,0,0)
      UUV2=VALUE(AY,POINT,ALUY1,AUY1,BUY1,CUY1,0)
      UUV2=UUV2*VALUE(AY,POINT,ALUY2,AUY2,BUY2,CUY2,0)
      TPU2=PRIN(AY,AUY1,BUY1,CUY1,ALUY1,AUY2,BUY2,CUY2,ALUY2,2,2)
      TPU2=STIFM3*TPU2*VALUE(AX,0.0,ALUX1,AUX1,BUX1,CUX1,0)
      TPU2=TPU2*VALUE(AX,0.0,ALUX2,AUX2,BUX2,CUX2,0)
      SX(IU,JU)=TU1*SU2+D1*TU2*SU1+STIFM*UV3*UV4*UUV2+TPU2
      JUY=JUY+1
      IF(JUY.LE.IUYM) GOTO 171
  173 CONTINUE

      DO 175 JVX=1,IVXM
      ALVX2=ALFVX(JVX)
      BVX2=BVX(JVX)
      CVX2=CVX(JVX)
      TU3=PRIN(AX,AUX1,BUX1,CUX1,ALUX1,AVX2,BVX2,CVX2,ALVX2,0,1)
      TU4=PRIN(AX,AUX1,BUX1,CUX1,ALUX1,AVX2,BVX2,CVX2,ALVX2,1,0)

      DO 175 JVY=1,IVYM
      ALVY2=ALFVY(JVY)
      BVY2=BVY(JVY)
      CVY2=CVY(JVY)
```

```
      JV=IUM+JVY+(JVX-1)*IVYM
      SU3=PRIN(AY,AUY1,BUY1,CUY1,ALUY1,AVY2,BVY2,CVY2,ALVY2,0,1)
      SU4=PRIN(AY,AUY1,BUY1,CUY1,ALUY1,AVY2,BVY2,CVY2,ALVY2,1,0)

 175  SX(IU,JV)=PO*TU4*SU3+D1*TU3*SU4
      IUY=IUY+1
      IF(IUY.LE.IUYM) GOTO 156
1175  CONTINUE

      DO 185 IVX=1,IVXM
      ALVX1=ALFVX(IVX)
      BVX1=BVX(IVX)
      CVX1=CVX(IVX)

      DO 185 IVY=1,IVYM
      ALVY1=ALFVY(IVY)
      BVY1=BVY(IVY)
      CVY1=CVY(IVY)
      IV=IUM+IVY+(IVX-1)*IVYM

      DO 180 IM=1,M
      BEX=(IM*2-1)*PI

      DO 180 IN=1,N
      BEY=(IN*2-1)*PI
      II=(IM-1)*N+IN

      S1=0.0
      S2=0.0
      S3=0.0
      S4=0.0

      DO 179 IK=1,MSTF
      GAX=(IK*2-1)*PI
      T1=CSCSRO(AX,BEX,GAX,0,AVX1,BVX1,CVX1,ALVX1)
      T4=SNSNRO(AX,BEX,GAX,0,AVX1,BVX1,CVX1,ALVX1)
      T8=DSSNRO(AX,BEX,GAX,1,AVX1,BVX1,CVX1,ALVX1)
      T9=DSSNRO(AX,GAX,BEX,1,AVX1,BVX1,CVX1,ALVX1)


      DO 179 IL=1,NSTF
      GAY=(IL*2-1)*PI
      JJ=(IK-1)*L+IL

      U2=DSSNRO(AY,BEY,GAY,0,AVY1,BVY1,CVY1,ALVY1)
      U3=DSSNRO(AY,GAY,BEY,0,AVY1,BVY1,CVY1,ALVY1)
      U8=CSCSRO(AY,BEY,GAY,1,AVY1,BVY1,CVY1,ALVY1)
      U9=SNSNRO(AY,BEY,GAY,1,AVY1,BVY1,CVY1,ALVY1)

      S1=S1-ZZC(JJ)*U8*T4*BEY*GAY/(AY*AY)
      S2=S2-ZZC(JJ)*PO*U9*T1*BEX*GAX/(AX*AX)
      S3=S3-ZZC(JJ)*D1*T8*U3*GAY*BEX/(AX*AY)
      S4=S4-ZZC(JJ)*D1*T9*U2*GAX*BEY/(AX*AY)
 179  CONTINUE

      ZB(IV,II)=S1+S2+S3+S4

 180  CONTINUE

      DO 183 JUX=1,IUXM
      ALUX2=ALFUX(JUX)
      BUX2=BUX(JUX)
      CUX2=CUX(JUX)
      TV3=PRIN(AX,AVX1,BVX1,CVX1,ALVX1,AUX2,BUX2,CUX2,ALUX2,0,1)
      TV4=PRIN(AX,AVX1,BVX1,CVX1,ALVX1,AUX2,BUX2,CUX2,ALUX2,1,0)
```

```
      JUY=1
  182 CONTINUE
      ALUY2=ALFUY(JUY)
      BUY2=BUY(JUY)
      AUY2=AUY(JUY)
      CUY2=CUY(JUY)
      JU=(JUX-1)*IUYM+JUY
      SV3=PRIN(AY,AVY1,BVY1,CVY1,ALVY1,AUY2,BUY2,CUY2,ALUY2,0,1)
      SV4=PRIN(AY,AVY1,BVY1,CVY1,ALVY1,AUY2,BUY2,CUY2,ALUY2,1,0)
      SX(IV,JU)=PO*TV3*SV4+D1*TV4*SV3
      JUY=JUY+1
      IF(JUY.LE.IUYM)GOTO 182
  183 CONTINUE

      DO 185 JVX=1,IVXM
      ALVX2=ALFVX(JVX)
      BVX2=BVX(JVX)
      CVX2=CVX(JVX)

      TV1=PRIN(AX,AVX1,BVX1,CVX1,ALVX1,AVX2,BVX2,CVX2,ALVX2,1,1)
      TV2=PRIN(AX,AVX1,BVX1,CVX1,ALVX1,AVX2,BVX2,CVX2,ALVX2,0,0)

      DO 185 JVY=1,IVYM
      ALVY2=ALFVY(JVY)
      BVY2=BVY(JVY)
      CVY2=CVY(JVY)
      JV=IUM+JVY+(JVX-1)*IVYM

      SV1=PRIN(AY,AVY1,BVY1,CVY1,ALVY1,AVY2,BVY2,CVY2,ALVY2,1,1)
      SV2=PRIN(AY,AVY1,BVY1,CVY1,ALVY1,AVY2,BVY2,CVY2,ALVY2,0,0)

      UV8=VALUE(AY,0.0,ALVY2,AVY2,BVY2,CVY2,0)
      UV7=VALUE(AY,0.0,ALVY1,AVY1,BVY1,CVY1,0)
  185 SX(IV,JV)=TV2*SV1+D1*TV1*SV2+2.*STIFM2(IVX,JVX)*UV7*UV8

      IF(IPR1.EQ.0) GOTO 1190
      WRITE(6,190)
  190 FORMAT(/////,2X,"CONNECTION STIFFNESS MATRIX",/)
      DO 193 IQ=1,NN
      WRITE(6,192)(SX(IQ,JQ),JQ=1,NN)
  192 FORMAT(4(2X,E14.7))
  193 CONTINUE
 1190 CONTINUE

      CALL GAUSEL(NN,NM,SX,ZB,G)
      IF(IPR1.EQ.0) GOTO 1191
      WRITE(6,195)
  195 FORMAT(//,2X,"IN PLANE MODE INFLUENCE COEFFICIENTS",//)
      DO 198 IQ=1,NN
      WRITE(6,197)ZB(IQ,1),G(IQ,1)
  197 FORMAT(2(2X,E14.7))
  198 CONTINUE
 1191 CONTINUE

      DO 220 IR=1,M
      ALX=(IR*2-1)*PI

      DO 220 IS=1,N
      ALY=(IS*2-1)*PI
      I=(IR-1)*N+IS

      DO 220 IM=1,M
      BEX=(IM*2-1)*PI
```

```
      DO 220 IN=1,N
      BEY=PI*(IN*2-1)
      J=(IM-1)*N+IN
      IF(I.EQ.J)XM(I,J)=RQ*AX*AY/4.0
      IF(I.NE.J)XK(I,J)=0.0
      IF(I.NE.J)XM(I,J)=0.0

      RR1=0.0
      RR2=0.0
      RR3=0.0
      RS1=0.0
      RS2=0.0
      RS3=0.0
      RW=0.0
      RST=0.0
      RSV=0.0
      RWS=0.0
      DO 210 IK=1,MSTF
      GAX=(IK*2-1)*PI
      RC1=GAX*ALX/(AX*AX)

      DO 210 IL=1,NSTF
      JJ=IL+(IK-1)*L
      ZP=ZZC(JJ)*ZZC(JJ)-(ZZ0(JJ)*ZZ0(JJ))
      GAY=(IL*2-1)*PI
      RC2=GAY*ALY/(AY*AY)
      RC3=0.5*(1.0-PO)*GAX*ALY/(AX*AY)
      RC4=0.5*(1.0-PO)*GAY*ALX/(AX*AY)


      DO 200 IUX=1,IUXM
      ALUX1=ALFUX(IUX)

      BUX1=BUX(IUX)
      CUX1=CUX(IUX)

      IUY=1
  199 CONTINUE
      ALUY1=ALFUY(IUY)

      BUY1=BUY(IUY)
      AUY1=AUY(IUY)
      CUY1=CUY(IUY)
      IU=(IUX-1)*IUYM+IUY
      CCK=G(IU,J)*ZZC(JJ)*CSCSRO(AX,GAX,ALX,1,AUX1,BUX1,CUX1,ALUX1)
      CCK=CCK*SNSNRO(AY,GAY,ALY,0,AUY1,BUY1,CUY1,ALUY1)
      CCM=G(IU,J)*ZZC(JJ)*SNSNRO(AX,GAX,ALX,1,AUX1,BUX1,CUX1,ALUX1)
      CCM=CCM*CSCSRO(AY,GAY,ALY,0,AUY1,BUY1,CUY1,ALUY1)
      RR1=RR1+RC1*CCK
      RR2=RR2+PO*RC2*CCM
      CCH=ZZC(JJ)*G(IU,J)*DSSNRO(AX,GAX,ALX,0,AUX1,BUX1,CUX1,ALUX1)
      CCH=CCH*DSSNRO(AY,ALY,GAY,1,AUY1,BUY1,CUY1,ALUY1)
      CCN=G(IU,J)*ZZC(JJ)*DSSNRO(AX,ALX,GAX,0,AUX1,BUX1,CUX1,ALUX1)
      CCN=CCN*DSSNRO(AY,GAY,ALY,1,AUY1,BUY1,CUY1,ALUY1)
      RR3=RR3+RC3*CCH+RC4*CCN
      IUY=IUY+1
      IF(IUY.LE.IUYM)GOTO 199
  200 CONTINUE

      DO 205 IVX=1,IVXM
      ALVX1=ALFVX(IVX)
      BVX1=BVX(IVX)
      CVX1=CVX(IVX)

      DO 205 IVY=1,IVYM
```

```
      ALVY1=ALFVY(IVY)
      BVY1=BVY(IVY)
      CVY1=CVY(IVY)
      IV=IUM+(IVX-1)*IVYM+IVY
      CCL=G(IV,J)*ZZC(JJ)*SNSNRO(AX,GAX,ALX,0,AVX1,BVX1,CVX1,ALVX1)
      CCL=CCL*CSCSRO(AY,GAY,ALY,1,AVY1,BVY1,CVY1,ALVY1)
      CCP=G(IV,J)*ZZC(JJ)*CSCSRO(AX,GAX,ALX,0,AVX1,BVX1,CVX1,ALVX1)
      CCP=CCP*SNSNRO(AY,GAY,ALY,1,AVY1,BVY1,CVY1,ALVY1)
      RS1=RS1+PO*RC1*CCP
      RS2=RS2+RC2*CCL
      CCG=G(IV,J)*ZZC(JJ)*DSSNRO(AX,GAX,ALX,1,AVX1,BVX1,CVX1,ALVX1)
      CCG=CCG*DSSNRO(AY,ALY,GAY,0,AVY1,BVY1,CVY1,ALVY1)
      CCQ=G(IV,J)*ZZC(JJ)*DSSNRO(AX,ALX,GAX,1,AVX1,BVX1,CVX1,ALVX1)
      CCQ=CCQ*DSSNRO(AY,GAY,ALY,0,AVY1,BVY1,CVY1,ALVY1)
      RS3=RS3+CCG*RC3+CCQ*RC4
  205 CONTINUE

       ARAT=AX*AX*AY*AY
      DO 210 IP=1,MSTF
      PHIX=(IP*2-1)*PI
      DO 210 IQ=1,NSTF
      PHIY=(IQ*2-1)*PI
      IPQ=(IP-1)*NSTF+IQ
       RW1=GAX*BEX*ALX*PHIX/(AX**4.0)
      RW1=RW1*CCCCIN(AX,GAX,BEX,PHIX,ALX)
      RW1=RW1*SSSSIN(AY,GAY,PHIY,BEY,ALY)
      RW2=GAY*PHIY*ALY*BEY/(AY**4.0)
      RW2=RW2*SSSSIN(AX,GAX,PHIX,BEX,ALX)
      RW2=RW2*CCCCIN(AY,GAY,PHIY,BEY,ALY)
      RW3=GAX*PHIY*ALX*BEY*D2/ARAT
      RW3=RW3*CCSSIN(AX,GAX,ALX,BEX,PHIX)
      RW3=RW3*CCSSIN(AY,PHIY,BEY,GAY,ALY)
      RW4=GAX*PHIY*ALY*BEX*D2/ARAT
      RW4=RW4*CCSSIN(AX,GAX,BEX,PHIX,ALX)
      RW4=RW4*CCSSIN(AY,PHIY,ALY,GAY,BEY)
      RW5=GAY*PHIY*D1*ALX*BEX/ARAT
      RW5=RW5*CCSSIN(AX,ALX,BEX,GAX,PHIX)
      RW5=RW5*CCSSIN(AY,GAY,PHIY,ALY,BEY)
      RW6=GAX*PHIX*D1*ALY*BEY/ARAT
      RW6=RW6*CCSSIN(AX,GAX,PHIX,ALX,BEX)
      RW6=RW6*CCSSIN(AY,ALY,BEY,GAY,PHIY)
      RW=RW+ZZC(JJ)*ZZC(IPQ)*(RW1+RW2+RW3+RW4+RW5+RW6)
      FQ1=0.5*FIN*(ZZC(JJ)*ZZC(IPQ)-ZZ0(JJ)*ZZ0(IPQ))
      RWS=RWS+FQ1*(RW1+RW2+RW3+RW4+RW5+RW6)
  210 CONTINUE

      DO 212 KUX=1,IUSM
      ALUX3=ALGUX(KUX)
      BUX3=BUX5(KUX)
      CUX3=CUX5(KUX)
      KUY=1
  211 CONTINUE
      ALUY3=ALGUY(KUY)
      AUY3=AUY5(KUY)
      BUY3=BUY5(KUY)
      CUY3=CUY5(KUY)
      KU=(KUX-1)*IUYM+KUY
      TCK=CSCSRO(AX,ALX,BEX,1,AUX3,BUX3,CUX3,ALUX3)
      TCK=TCK*SNSNRO(AY,ALY,BEY,0,AUY3,BUY3,CUY3,ALUY3)
      TCK=TCK*ALX*BEX/(AX*AX)
      TCM=CSCSRO(AY,ALY,BEY,0,AUY3,BUY3,CUY3,ALUY3)
      TCM=TCM*SNSNRO(AX,ALX,BEX,1,AUX3,BUX3,CUX3,ALUX3)
      TCM=TCM*ALY*BEY*PO/(AY*AY)
      TCH=DSSNRO(AX,ALX,BEX,0,AUX3,BUX3,CUX3,ALUX3)
      TCH=TCH*DSSNRO(AY,BEY,ALY,1,AUY3,BUY3,CUY3,ALUY3)
```

```
      TCH=TCH*0.5*(1.0-PO)*ALX*BEY/(AX*AY)
      TCN=DSSNRO(AX,BEX,ALX,0,AUX3,BUX3,CUX3,ALUX3)
      TCN=TCN*DSSNRO(AY,ALY,BEY,1,AUY3,BUY3,CUY3,ALUY3)
      TCN=TCN*0.5*(1.0-PO)*ALY*BEX/(AX*AY)
      TCKMH=(TCK+TCM+TCH+TCN)/(T*T)
      RST=RST+C(KU)*TCKMH
      KUY=KUY+1
      IF(KUY.LE.IUYM) GOTO 211
  212 CONTINUE

      DO 215 KVX=1,IVXM
      ALVX3=ALGVX(KVX)
      AVX3=AVX5(KVX)
      BVX3=BVX5(KVX)
      CVX3=CVX5(KVX)
      DO 215 KVY=1,IVYM
      ALVY3=ALGVY(KVY)
      BVY3=BVY5(KVY)
      CVY3=CVY5(KVY)
      KV=IUMS+(KVX-1)*IVYM+KVY
      TCL=SNSNRO(AX,BEX,ALX,0,AVX3,BVX3,CVX3,ALVX3)
      TCL=TCL*CSCSRO(AY,BEY,ALY,1,AVY3,BVY3,CVY3,ALVY3)
      TCL=TCL*BEY*ALY/(AY*AY)
      TCP=CSCSRO(AX,BEX,ALX,0,AVX3,BVX3,CVX3,ALVX3)
      TCP=TCP*SNSNRO(AY,BEY,ALY,1,AVY3,BVY3,CVY3,ALVY3)
      TCP=TCP*PO*BEX*ALX/(AX*AX)
      TCG=DSSNRO(AX,BEX,ALX,1,AVX3,BVX3,CVX3,ALVX3)
      TCG=TCG*DSSNRO(AY,ALY,BEY,0,AVY3,BVY3,CVY3,ALVY3)
      TCG=TCG*0.5*(1.0-PO)*BEX*ALY/(AX*AY)
      TCQ=DSSNRO(AX,ALX,BEX,1,AVX3,BVX3,CVX3,ALVX3)
      TCQ=TCQ*DSSNRO(AY,BEY,ALY,0,AVY3,BVY3,CVY3,ALVY3)
      TCQ=TCQ*0.5*(1.0-PO)*ALX*BEY/(AX*AY)
      RSV=RSV+C(KV)*(TCL+TCP+TCG+TCQ)/(T*T)
  215 CONTINUE
      RWWS=RWS*CHEC2
      RSSV=RSV*CHEC2
      SS1=(RW+RWWS+RST*CHEC1+RSSV+RR1+RR2+RR3+RS1+RS2+RS3)
      FR(I)=D*((ALX/AX)**2.0+(ALY/AY)**2.0)**2.0
      IF(I.EQ.J)XK(I,J)=FR(I)*AX*AY/4.0
      XK(I,J)=XK(I,J)+(12.0*D*SS1)
      IF(I.EQ.J)SQ(I)=XK(I,I)*4.0/(AX*AY)
  220 CONTINUE

      WRITE(6,8)XK(1,1),XK(2,2)
      WRITE(6,8)XK(1,2),XK(2,1)
      WRITE(6,8)XM(1,1),XM(2,2)
      WRITE(6,8)XM(1,2),XM(2,1)
      CALL RGG(NM,NM,XK,XM,XLFR,XLFI,XET,1,XH,IERR)

      DO 225 J=1,NM
      ALFR1(J)=XLFR(J)*CF*CF/XET(J)
  225 CONTINUE
      KI1=NM-1
      DO 235 KF=1,KI1
      K1=KF+1
      DO 235 I=K1,NM
      IF(ABS(ALFR1(KF)).LT.ABS(ALFR1(I))) GO TO 235
      AI=ALFR1(KF)
      ALFR1(KF)=ALFR1(I)
      ALFR1(I)=AI
      DO 230 J=1,NM
      AI=XH(J,I)
      XH(J,I)=XH(J,KF)
      XH(J,KF)=AI
  230 CONTINUE
```

```
  235 CONTINUE
      DO 240 J=1,NM
      ALFR2(J)=ABS(ALFR1(J))
      ALFR2(J)=SQRT(ALFR2(J))/(PI+PI)
      SQ(J)=SQ(J)/RQ
      SQ(J)=SQRT(SQ(J))
  240 CONTINUE
      DO 275 I=1,NM
      WRITE(6,245)
  245 FORMAT(1X)
      AI=XH(1,I)
      KF=1
      DO 250 J=2,NM
      IF(ABS(AI).GT.ABS(XH(J,I))) GO TO 250
      KF=J
      AI=XH(J,I)
  250 CONTINUE
  255 IK=MOD(KF,N)
      JM=((KF-IK)/N)+1
      IF(IK.EQ.0)IK=N
      IF(IK.EQ.N)JM=KF/N
      IF(I.NE.1) GO TO 265
      WRITE(6;260)
  260 FORMAT(2X,"FREQY. SQUARED",7X,"FREQY.",7X,"FREQ2./FLAT",5X,"FREQ/F
     CLAT",7X,"CHANGE",9X,"I",2X,"J")
  265 CONTINUE
      ALFR3(I)=FR(KF)/RQ
      DS(I)=100.*((SQ(KF)*SQ(KF)-ALFR1(I))/(ALFR1(I)-ALFR3(I)))
      SG(I)=SQ(KF)/(PI+PI)
      DW(I)=100.*((ALFR1(I)/ALFR3(I))-1.0)
      ALFR4(I)=SQRT(ALFR3(I))/(PI+PI)
      WRITE(6,270)ALFR1(I),ALFR2(I),ALFR3(I),ALFR4(I),DW(I),IK,JM
  270 FORMAT(1X,5(E14.7,2X),I2,2X,I2)
  275 CONTINUE
      WRITE(6,280)
  280 FORMAT(//,2X,"1 TERM SOLN.",4X,"MULTI.TERM SOLN.",3X,"PCNTGE.ERROR",/
     C",/)
      DO 290 I=1,NM
      WRITE(6,285)SG(I),ALFR2(I),DS(I)
  285 FORMAT(2X,3(E14.7,3X))
  290 CONTINUE
  371 CONTINUE
      WRITE(6,7774)PX(ILO)
 7774 FORMAT(/,2X,"LOAD= ",E14.7,/)



      DO 7775 ID=1,NDP
      EXST3(ID)=(EXST1(ID)+EXST2(ID)-EXY(ID))/2.0
      EXST4(ID)=(EXST1(ID)+EXST2(ID)+EXY(ID))/2.0
      IF(NGAGE(ID).EQ.1)STRAIN=EXST1(ID)
      IF(NGAGE(ID).EQ.2)STRAIN=EXST2(ID)
      IF(NGAGE(ID).EQ.3)STRAIN=EXST3(ID)
      IF(NGAGE(ID).EQ.4)STRAIN=EXST4(ID)
      WRITE(6,7773)ID,NGAGE(ID),XCO(ID),YCO(ID),STRAIN
 7773 FORMAT(2(2X,I3),3(2X,E14.7))
 7775 CONTINUE
 3995 CONTINUE
      STOP
      END

      REAL FUNCTION CCSSIN(A,AL,BE,BS,SH)
      REAL A,AL,BE,PS,SH,E3,E4
      E3=AL+BE
      E4=AL-BE
```

```
      CCSSIN=(SNSNCS(A,PS,SH,E3)+SNSNCS(A,PS,SH,E4))/2.0
      RETURN
      END

      REAL FUNCTION CCCCIN(A,AL,BE,PS,SH)
      REAL A,AL,BE,PS,SH,E3,E4
      E3=AL+BE
      E4=AL-BE
      CCCCIN=(CSCSCS(A,PS,SH,E3)+CSCSCS(A,PS,SH,E4))/2.0
      RETURN
      END


      REAL FUNCTION SSSSIN(A,AL,BE,PS,SH)
      REAL A,AL,BE,PS,SH,E3,E4
      E3=AL+BE
      E4=AL-BE
      SSSSIN=(SNSNCS(A,PS,SH,E4)-SNSNCS(A,PS,SH,E3))/2.0
      RETURN
      END


      REAL FUNCTION CSCSSN(A,AL1,AL2,AL3)
      REAL A,AL1,AL2,AL3,E5,E6
      E5=AL1+AL2
      E6=AL1-AL2
      CSCSSN=(CSSN(A,E5,AL3)+CSSN(A,E6,AL3))/2.0
      RETURN
      END


      REAL FUNCTION SNSNSN(A,AL1,AL2,AL3)
      REAL A,AL1,AL2,AL3,E5,E6
      E5=AL1+AL2
      E6=AL1-AL2
      SNSNSN=(CSSN(A,E6,AL3)-CSSN(A,E5,AL3))/2.0
      RETURN
      END


      REAL FUNCTION SNSNCS(A,AL1,AL2,AL3)
      REAL A,AL1,AL2,AL3,E5,E6
      E5=AL1+AL2
      E6=AL1-AL2
      SNSNCS=(CSCS(A,E6,AL3)-CSCS(A,E5,AL3))/2.0
      RETURN
      END


      REAL FUNCTION CSCSCS(A,AL1,AL2,AL3)
      REAL A,AL1,AL2,AL3,E5,E6
      E5=AL1+AL2
      E6=AL1-AL2
      CSCSCS=(CSCS(A,E5,AL3)+CSCS(A,E6,AL3))/2.0
      RETURN
      END


      REAL FUNCTION CSCSRO(A,BE2,BE3,N,A1,B1,C1,BE1)
      REAL A,BE1,BE2,BE3,A1,B1,C1,R1,AA1,BB1,CC1
      AA1=A1
      BB1=B1
      CC1=C1
      IF(N.NE.1)GOTO 530
      AA1=0.0
```

```
      BB1=C1*BE1/A
      CC1=-B1*BE1/A
  530 IF(N.NE.2)GOTO 535
      AA1=0.0
      BB1=-B1*BE1*BE1/(A*A)
      CC1=-C1*BE1*BE1/(A*A)
  535 R1=AA1*CSCS(A,BE2,BE3)
      R1=R1+BB1*CSCSCS(A,BE1,BE2,BE3)
      R1=R1+CC1*CSCSSN(A,BE2,BE3,BE1)
      CSCSRO=R1
      RETURN
      END


      REAL FUNCTION DSSNRO(A,BE2,BE3,N,A1,B1,C1,BE1)
      REAL A,BE1,BE2,BE3,A1,B1,C1,R1,AA1,BB1,CC1
      AA1=A1
      BB1=B1
      CC1=C1
      IF(N.NE.1)GOTO 540
      AA1=0.0
      BB1=C1*BE1/A
      CC1=-B1*BE1/A
  540 IF(N.NE.2)GOTO 545
      AA1=0.0
      BB1=-B1*BE1*BE1/(A*A)
      CC1=-C1*BE1*BE1/(A*A)
  545 R1=AA1*CSSN(A,BE2,BE3)
      R1=R1+BB1*CSCSSN(A,BE1,BE2,BE3)+CC1*SNSNCS(A,BE1,BE3,BE2)
      DSSNRO=R1
      RETURN
      END


      REAL FUNCTION SNSNRO(A,BE2,BE3,N,A1,B1,C1,BE1)
      REAL A,BE1,BE2,BE3,A1,B1,C1,R1,AA1,BB1,CC1
      AA1=A1
      BB1=B1
      CC1=C1
      IF(N.NE.1)GOTO 550
      AA1=0.0
      BB1=C1*BE1/A
      CC1=-B1*BE1/A
  550 IF(N.NE.2)GOTO 555
      AA1=0.0
      BB1=-B1*BE1*BE1/(A*A)
      CC1=-C1*BE1*BE1/(A*A)
  555 R1=AA1*SNSN(A,BE2,BE3)
      R1=R1+BB1*SNSNCS(A,BE2,BE3,BE1)+CC1*SNSNSN(A,BE1,BE2,BE3)
      SNSNRO=R1
      RETURN
      END



      REAL FUNCTION CSCS(A,B,C)
      REAL A,B,C,F,FF
      F=B*SIN(B)*COS(C)-C*COS(B)*SIN(C)
      RZ=ABS(ABS(B)-ABS(C))
      EPS=0.00000001
      IF((ABS(B).LE.EPS).AND.(ABS(C).LE.EPS))GOTO 601
      IF(RZ.GT.EPS)FF=(A*F/(B*B-C*C))
      IF(RZ.LT.EPS)FF=(A*SIN(2.0*B)/(4.0*B))+(A/2.0)
  601 IF((ABS(B).LE.EPS).AND.(ABS(C).LE.EPS))FF=A
      CSCS=FF
```

```
      RETURN
      END


      REAL FUNCTION CSSN(A,B,C)
      REAL A,B,C,F,FF
      EPS=0.00000001
      F=B*SIN(B)*SIN(C)+C*COS(B)*COS(C)-C
      RZ=ABS(ABS(B)-ABS(C))
      IF((ABS(B).LE.EPS).AND.(ABS(C).LE.EPS))GOTO 602
      IF(RZ.GE.EPS)FF=A*F/(B*B-C*C)
      IF(RZ.LT.EPS)FF=A*(SIN(C))*SIN(C)/(2.0*C)
  602 IF((ABS(B).LE.EPS).AND.(ABS(C).LE.EPS))FF=0.0
      CSSN=FF
      RETURN
      END


      REAL FUNCTION SNSN(A,B,C)
      REAL A,B,C,F,FF
      F=C*SIN(B)*COS(C)-B*COS(B)*SIN(C)
      RZ=ABS(ABS(B)-ABS(C))
      EPS=0.00000001
      IF(RZ.GE.EPS)FF=A*F/(B*B-C*C)
      IF((ABS(B).LE.EPS).AND.(ABS(C).LE.EPS))GOTO 603
      IF(RZ.LT.EPS)FF=-A*SIN(2.0*B)/(4.0*B)
      IF(RZ.LT.EPS)FF=FF+(A/2.0)
      IF(ABS(B+C).LE.EPS)FF=-FF
  603 IF((ABS(B).LE.EPS).AND.(ABS(C).LE.EPS))FF=0.0
      SNSN=FF
      RETURN
      END



      REAL FUNCTION PRIN(A,A1,B1,C1,DE1,A2,B2,C2,DE2,I1,I2)
      REAL A,A1,B1,C1,A2,B2,C2,DE1,DE2,R1,R2,R3,AA1,BB1,CC1
      REAL UG,UH,VG,VH,AA2,BB2,CC2
      AA1=A1
      BB1=B1
      CC1=C1
      AA2=A2
      BB2=B2
      CC2=C2

      IF(I1.NE.1)GOTO 610
      AA1=0.0
      BB1=C1*DE1/A
      CC1=-B1*DE1/A
  610 IF(I1.NE.2)GOTO 615
      AA1=0.0
      BB1=-B1*DE1*DE1/(A*A)
      CC1=-C1*DE1*DE1/(A*A)

  615 IF(I2.NE.1)GOTO 620
      AA2=0.0
      BB2=C2*DE2/A
      CC2=-B2*DE2/A
  620 IF(I2.NE.2) GOTO 622
      AA2=0.0
      BB2=-B2*DE2*DE2/(A*A)
      CC2=-C2*DE2*DE2/(A*A)
  622 CONTINUE
      EPS=0.00000001
      IF(ABS(DE1).GT.EPS)UG=SIN(DE1)/DE1

```

```
      IF(ABS(DE1).LE.EPS)UG=1.0
      IF(ABS(DE2).GT.EPS)UH=SIN(DE2)/DE2
      IF(ABS(DE2).LE.EPS)UH=1.0
      IF(ABS(DE1).GT.EPS)VG=(1.0-COS(DE1))/DE1
      IF(ABS(DE1).LE.EPS)VG=0.0
      IF(ABS(DE2).GT.EPS)VH=(1.0-COS(DE2))/DE2
      IF(ABS(DE2).LE.EPS)VH=0.0
      R1=AA1*AA2*A+(AA2*BB1*UG*A)+(AA1*BB2*A*UH)
      R2=(AA2*CC1*A*VG)+(AA1*CC2*A*VH)
      R3=BB1*BB2*CSCS(A,DE1,DE2)+CC1*BB2*CSSN(A,DE2,DE1)
      R3=R3+BB1*CC2*CSSN(A,DE1,DE2)+CC1*CC2*SNSN(A,DE1,DE2)
      PRIN=R1+R2+R3
      RETURN
      END

      SUBROUTINE GAUSI(N,S,B,X)
      DIMENSION S(N,N),B(N),X(N)
      DO 3700 K=1,N
      K2=K+1
      IF(K2.GT.N) GOTO 3700
      DO 3685 I=K2,N
      IF(S(K,K).EQ.0.0)R=0.0
      IF(S(K,K).EQ.0.0)WRITE(6,4680)K
 4680 FORMAT(2X,"WARNING ** S(",I2,")=0")
      IF(S(K,K).NE.0.0)R=S(I,K)/S(K,K)
      DO 3680 J=K,N
 3680 S(I,J)=S(I,J)-R*S(K,J)
      B(I)=B(I)-R*B(K)
 3685 CONTINUE
 3700 CONTINUE
      IF(S(N,N).EQ.0.0)X(N)=0.0
      IF(S(N,N).EQ.0.0)WRITE(6,4681)
 4681 FORMAT(2X,"S(N,N)=0.0")
      IF(S(N,N).NE.0.0)X(N)=B(N)/S(N,N)
      NH=N-1
      DO 3900 KK=1,NH
      K=N-KK
      SM=B(K)
      DO 3800 JJ=1,KK
      J=N+1-JJ
 3800 SM=SM-S(K,J)*X(J)
      IF(ABS(S(K,K)).LT.(1./10.**18.))GOTO 3850
      X(K)=SM/S(K,K)
      GOTO 3875
 3850 X(K)=0.0
      WRITE(6,3860)K
 3860 FORMAT(2X,"EMPTY ROW NO.",I3)
 3875 CONTINUE
 3900 CONTINUE
      RETURN
      END

      SUBROUTINE GAUSEL(N,M,S,B,X)
      REAL SM,R
      DIMENSION X(N,M),B(N,M),S(N,N)
      DO 700 K=1,N
      K2=K+1
      IF(K2.GT.N)GOTO 700
      DO 685 I=K2,N
      IF(S(K,K).EQ.0.0)R=0.0
      IF(S(K,K).EQ.0.0)WRITE(6,5680)K
 5680 FORMAT(2X,"WARNING*** S(",I2,")=0.0")
      IF(S(K,K).NE.0.0)R=S(I,K)/S(K,K)
      DO 680 J=K,N
  680 S(I,J)=S(I,J)-R*S(K,J)
```

```
      DO 682 L=1,M
  682 B(I,L)=B(I,L)-R*B(K,L)
  685 CONTINUE
  700 CONTINUE
      DO 905 L=1,M
      IF(S(N,N).NE.0.0)X(N,L)=B(N,L)/S(N,N)
      IF(S(N,N).EQ.0.0)X(N,L)=0.0

      IF(S(N,N).EQ.0.0)WRITE(6,5681)
 5681 FORMAT(2X,"S(N,N)=0.0")
      NH=N-1
      DO 900  KK=1,NH
      K=N-KK
      SM=B(K,L)
      DO 800  JJ=1,KK
      J=N+1-JJ
  800 SM=SM-S(K,J)*X(J,L)
      IF(S(K,K).EQ.0.0)GOTO 850
      X(K,L)=SM/S(K,K)
      GOTO 875
  850 X(K,L)=0.0
      WRITE(6,860)K
  860 FORMAT(2X,"EMPTY ROW NO.",I3)
  875 CONTINUE
  900 CONTINUE
  905 CONTINUE
      RETURN
      END

      SUBROUTINE SETUP(N,B,C,ALP,Z1,Z2,Z3,Z4,IND)
      REAL Z1,Z2,Z3,Z4
      DIMENSION B(N),C(N),ALP(N)
      PI=4.0*ATAN(1.0E0)
      I=1
      IF(Z1.LT.0.01)GOTO 444
      IF(IND.EQ.2)GOTO 442
      ALP(1)=0.001
      B(1)=-SIN(0.0005)
      C(1)=COS(0.0005)
      ALP(2)=PI*2.
      B(2)=0.0
      C(2)=1.0
      ALP(3)=PI*4.
      B(3)=0.0
      C(3)=1.0
      GOTO 448
  442 IF(IND.EQ.1)GOTO 444
      ALP(2)=PI
      B(2)=0.0
      C(2)=-1.0
      B(1)=0.0
      C(1)=0.0
      ALP(1)=0.0
      ALP(3)=PI*3.
      C(3)=1.0
      B(3)=0.0
      ALP(4)=PI*5.
      C(4)=1.0
      B(4)=0.0
      GOTO 448
  444 CONTINUE
      K=1
  445 CONTINUE
      B(I)=Z1
      C(I)=Z2
```

```
      IF(IND.EQ.1)ALP(I)=PI*(2*K-1)
      IF(IND.EQ.2)ALP(I)=PI*2*K
      IF(IND.EQ.3)ALP(I)=PI*K
      K=K+1
      I=I+1
      IF(I.LE.N)GOTO 445
      IF(Z4.LE.0.5)GOTO 448
      ALP(N)=0.0001
      B(N)=-SIN(0.00005)
      C(N)=COS(0.00005)
  448 CONTINUE
      RETURN
      END

      REAL FUNCTION VALUE(A,X,AL,A1,A2,A3,N)
      REAL A,X,AL,A1,A2,A3,R
      R=X*AL/A
      IF(N.EQ.0)VALUE=A1+A2*COS(R)+A3*SIN(R)
      IF(N.EQ.1)VALUE=-A2*(AL/A)*SIN(R)+A3*(AL/A)*COS(R)
      IF(N.EQ.2)VALUE=-AL*AL*(A2*COS(R)+A3*SIN(R))/(A*A)
      RETURN
      END

      SUBROUTINE MATPR(S,N,M)
      DIMENSION S(N,M)
      DO 1000 I=1,N
      WRITE(6,999)(S(I,J),J=1,M)
  999 FORMAT(2X,4(E14.7,2X))
 1000 CONTINUE
      WRITE(6,1001)
 1001 FORMAT('  ****************************************  ')
      RETURN
      END

      SUBROUTINE MATSET(S,N,M)
      DIMENSION S(N,M)
      DO 1002 I=1,N
      DO 1002 J=1,M
      S(I,J)=0.0
 1002 CONTINUE
      RETURN
      END

      REAL FUNCTION DEFN(AX,AY,ZF,Z0,TEM1,TEM2)
      TFN=(9./(AX**4.0))+(9.0/(AY**4.0))+(2./(AX*AX*AY*AY))
      PI=4.0*ATAN(1.0)
      PI4=PI**4.0
      RN1=2.0*ZF*TEM2*(ZF*ZF-Z0*Z0)
      RN4=2.0*ZF*TEM1
      RN2=PI4*AX*AY*((1./(AX*AX))+(1./(AY*AY)))**2.0
      RN2=RN2*(ZF-Z0)/24.0
      RN3=TFN*AX*AY*PI4*((ZF*ZF*ZF)-(ZF*Z0*Z0))/64.0
      DEFN=RN1+RN2+RN3+RN4
      RETURN
      END

      INTEGER FUNCTION ICONX(N1,N2,NM)
      IF(N1.GT.N2)K=N2
      IF(N1.GT.N2)J=N1
      IF(N2.GE.N1)K=N1
      IF(N2.GE.N1)J=N2
      I1=(K-1)*NM+J
      ICONX=I1-((K*K-K)/2)+1
      RETURN
      END
```

APPENDIX K

ERRORS DUE TO MEASUREMENTS AND SIMPLIFYING ASSUMPTIONS

The accuracy of the calculated values of the frequencies depend on the accuracy of the input parameters. The maximum possible error in the fundamental frequency (calculated) of an unstressed flat plate due to the measurement errors is given by [23],

$$\frac{\delta\Omega}{\Omega} = \frac{2}{(1/a^2+1/b^2)} \left[\frac{1}{a^2} \cdot \left(\frac{\delta a}{a}\right) + \frac{1}{b^2} \cdot \left(\frac{\delta b}{b}\right)\right]$$

$$\pm \frac{1}{2}\left(\frac{\delta E}{E}\right) \pm \frac{3}{2}\left(\frac{\delta h}{h}\right) \pm \frac{1}{2}\left(\frac{\delta \bar{m}}{\bar{m}}\right) \pm \frac{\nu^2}{(1-\nu^2)}\left(\frac{\delta\nu}{\nu}\right) .$$

The maximum possible error in the fundamental frequency of a stressed plate can be estimated as follows:

$$\omega \approx \Omega\sqrt{\left(1 - \frac{P}{P_c} + k\mu^2\right)} .$$

$$\frac{\delta\omega}{\omega} = \frac{\delta\Omega}{\Omega} \pm \frac{1}{2}\left(\frac{\Omega}{\omega}\right)^2\left(\frac{P}{P_c}\right)\left(\frac{\delta P}{P}\right) \pm k\mu^2\left(\frac{\Omega}{\omega}\right)^2\left(\frac{\delta\mu}{\mu}\right) .$$

For plate 4 at a load ratio (P/P_c) of 4.15 the above equations give $\frac{\delta\omega}{\omega} = .00495$. (4.95%) This is based on the assumption that all possible errors occur in such a way that the error in the frequency accumulates, and that the errors in the input parameters are as listed below:

$\delta E/E = .01$
$\delta a/a = .004$ (1 mm for a = 250 mm)
$\delta b/b = .003$ (1 mm for b = 300 mm)

$\delta h/h = .003 \quad (10^{-4}$ inch for $h = .86$ mm)

$\delta \bar{m}/\bar{m} = .01$

$\delta \nu/\nu = .02$

$\delta P/P = .0022 \quad$ (4 lbs at 1829 lbs)

$\delta \mu/\mu = .013 \quad (2\times10^{-3}$ inch at 155×10^{-3} inch)

Errors caused by the simplifying assumptions, such as in the case of neglecting damping and neglecting the in-plane inertia, are expected to be very small. For example, it was assumed that the vibration takes place in a vacuum. The experiments were conducted in air. However, including the aerodynamic damping in the analysis (say for a damping ratio of 0.1%) does not change the resonance frequency significantly (order of .0002%).

REFERENCES

1. Rayleigh, J.W.S.B., Theory of Sound, MacMillan & Co., 1877.

2. Temple, G. and Bickley, W.G., Rayleigh's Principle and Its Applications to Engineering. New York: Dover Publications, 1956.

3. Timoshenko, S., Vibration Problems in Engineering, 3rd Edition. New York: Van Nostrand, 1955.

4. Leissa, A.W., Vibration of Plates, NASA Special Publication, NASA SP-160, 1969.

5. Dickinson, S.M., Lateral Vibration of Rectangular Plates Subject to In-Plane Forces, Journal of Sound and Vibration, Vol. 16, part 4, pp. 465-472, 1971.

6. Dickinson, S.M., The Flexural Vibration of Rectangular Orthotropic Plates Subject to In-Plane Forces, Journal of Applied Mechanics, Vol. 38, No. 3, pp. 699-700, 1971.

7. Bassily, S.F. and Dickinson, S.M., Buckling and Lateral Vibration of Rectangular Plates Subject to In-Plane Loads - A Ritz Approach, Journal of Sound and Vibration, Vol. 24, part 2, pp. 219-239, 1972.

8. Bassily, S.F. and Dickinson, S.M., Buckling and Vibration of In-Plane Loaded Plates Treated by a Unified Ritz Approach, Journal of Sound and Vibration, Vol. 59, part 1, pp. 1-14, 1978.

9. Dickinson, S.M., Bolotin's Method Applied to the Buckling and Lateral Vibration of Stressed Plates, AIAA Journal, Vol. 13, No. 1, pp. 109-110, 1975.

10. Kaldas, M.M. and Dickinson, S.M., Vibration and Buckling Calculations for Rectangular Plates Subject to Complicated In-Plane Stress Distributions by Using Numerical Integration in a Rayleigh-Ritz Analysis, Journal of Sound and Vibration, Vol. 75, part 2, pp. 151-162, 1981.

11. Kaldas, M.M. and Dickinson, S.M., The Flexural Vibration of Welded Rectangular Plates, Journal of Sound and Vibration, Vol. 75, part 2, pp. 163-178, 1981.

12. Wittrick, W.H. and Williams, F.W., Computational Procedures for a Matrix Analysis of the Stability and Vibration of Thin Flat Walled Structures in Compression, International Journal of Mechanical Sciences, Vol. 11, 1969.

13. Wittrick, W.H. and Williams, F.W., Buckling and Vibration of Anisotropic or Isotropic Plate Assemblies Under Combined Loadings, International Journal of Mechanical Sciences, Vol. 6, 1974.

14. Dawe, D.J. and Morris, I.R., Vibration of Curved Plate Assemblies Subjected to Membrane Stresses, Journal of Sound and Vibration, Vol. 81, part 2, pp. 229-237, 1982.

15. Laura, P.A.A. and Romanelli, E., Vibrations of Rectangular Plates Elastically Restrained Against Rotation Along All Edges and Subjected to a Biaxial State of Stress, Journal of Sound and Vibration, Vol. 37, part 3, pp. 367-377, 1974.

16. Leissa, A.W., Recent Research in Plate Vibrations 1973-1976: Complicating Effects, Shock and Vibration Digest, Vol. 10(12), pp. 21-35, 1978.

17. Leissa, A.W., Plate Vibration Research, 1976-1980: Complicating Effects, Shock and Vibration Digest, Vol. 13(10), pp. 19-36, 1981.

18. Phillips, I.G. and Jubb, J.E.M., The Effect of Distortion on the Lowest Natural Frequency of a Rectangular Steel Plate, Journal of Sound and Vibration, Vol. 33(1), pp. 41-48, 1974.

19. Reissner, E., On Transverse Vibrations of Thin, Shallow, Elastic Shells, Quarterly of Applied Mathematics, Vol. 13, pp. 169-176, 1955.

20. Lurie, H., Lateral Vibrations As Related to Structural Stability, Journal of Applied Mechanics, Vol. 19, pp. 196-204, 1952.

21. Massonnet, C.H., Le Voilement des Plaques Planes Sollicitees dans leur Plan, Final Report of the Third Congress of the International Association for Bridge and Structural Engineering, 1948.

22. Jubb, J.E.M. et al., Interrelation of Structural Stability, Stiffness, Residual Stress and Natural Frequency, Journal of Sound and Vibration, Vol. 39(1), pp. 121-134, 1975.

23. Ilanko, S., The Vibration Behaviour of In-Plane Loaded Rectangular Plates, M.Sc. Dissertation, University of Manchester, U.K., 1981.

24. Ilanko, S. and Tillman, S.C., The Natural Frequencies of In-Plane Stressed Rectangular Plates, Journal of Sound and Vibration, Vol. 98(1), pp. 25-34, 1985.

25. Hui, D. and Leissa, A.W., Effects of Geometric Imperfections on Vibrations of Biaxially Compressed Rectangular Plates, Journal of Applied Mechanics, Vol. 105, Trans. ASME, Vol. 50, Series E, pp. 750-756, 1983.

26. Yamaki, N., Postbuckling Behaviour of Rectangular Plates With Small Initial Curvature Loaded in Edge Compression, Journal of Applied Mechanics, Vol. 26, Trans. ASME, Vol. 81, Series E, pp. 407-414, Sept. 1959.

27. Yamaki, N., Postbuckling Behaviour of Rectangular Plates With Small Initial Curvature Loaded in Edge Compression - (Continued), Journal of Applied Mechanics, Vol. 27, Trans. ASME, Vol. 82, pp. 335-342, June 1960.

28. Yamaki, N., Experiments on the Postbuckling Behaviour of Square Plates Loaded in Edge Compression, Journal of Applied Mechanics, Vol. 28, Trans. ASME, Vol. 83, pp. 238-244, June 1961.

29. Coan, J.M., Large Deflection Theory for Plates With Small Initial Curvature Loaded in Edge Compression, Journal of Applied Mechanics, Vol. 18, Trans. ASME, Vol. 73, pp. 143-151, 1951.

30. Bhattacharya, A.P., Note on the Postbuckling Analysis of Cross-Ply Laminated Plates With Elastically Restrained Edges and Initial Curvatures, Journal of Structural Mechanics, Vol. 10(3), pp. 359-372, 1982-1983.

31. Chia, C.Y., Nonlinear Analysis of Plates, McGraw Hill, pp. 166, 1980.

32. Plaut, R.H. and Johnson, E.R., The Effect of Initial Thrust and Elastic Foundation on the Vibration Frequencies of a Shallow Arch, Journal of Sound and Vibration, Vol. 78(4), pp. 565-571, 1981.

33. Horne, M.R. and Merchant, W., The Stability of Frames. London: Pergamon Press Ltd., 1965.

34. Dickinson, S.M., Flexural Vibration of Rectangular Plates, Ph.D. Thesis, University of Nottingham, U.K. 1966.

35. PAFEC 75 Package Program, Pafec Ltd., Strelley, Nottingham, U.K.

36. Bassily, S.F., General Analytical Approaches Applied to Thin-Walled Structures, Ph.D. Thesis, The University of Western Ontario, Canada, 1974.

END

08 04 87

FIN